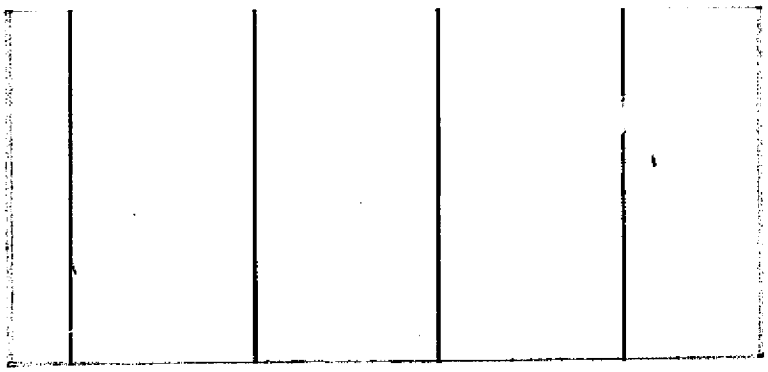

THE UNIVERSITY OF KANSAS CENTER FOR RESEARCH, INC.
2291 Irving Hill Rd.—Campus West Lawrence, Kansas 66044

A STUDY OF COMMUTER AIRPLANE DESIGN OPTIMIZATION

Third Status Report

KU-FRL 313-4

This work was performed under
NASA Grant NSG-2145

31 August 1977

Prepared by: R. David Wyatt
Douglas A. Griswold
James L. Hammer

Principal Investigator: J. Roskam,
Ackers Professor
of Engineering

Approved by: J. Roskam, Director
Flight Research Laboratory

TABLE OF CONTENTS

TABLE OF CONTENTS (CONT'D)

TABLE OF CONTENTS (CONT'D)

LIST OF ACRONYMS

Acronym	Definition
AFT	Available File Table
DOC	Direct Operating Costs
FAR	Federal Aviation Regulations
GASP	General Aviation Synthesis Program
KU-FRL	Kansas University Flight Research Lab
NASA	National Aeronautics and Space Administration
NCSU	North Carolina State University

LIST OF SYMBOLS

Symbol	Definition	Units
A	Area, Aspect ratio	ft^2, in^2
Aeff	Effective aspect ratio	
a	Constant in regression formula	
b	Constant in regression formula	
b_f	Maximum fuselage width	ft
b_H	Horizontal tail span	ft
b_v	Vertical tail span	ft
C_{D_0}	Zero-lift drag coefficient	
$C_{D_{O_B}}$	Fuselage zero-lift drag coefficient	
C_f	Skin friction drag coefficient	
C_{f_B}	Body skin friction drag coefficient	
$\overline{CL}$	Nose cone centerline	
C_{L_α}	Lift curve slope	$radians^{-1}$
C_{m_α}	Pitching moment due to angle of attack	$radians^{-1}$
C_{n_β}	Yawing moment derivative due to sideslip	$radians^{-1}$
$\overline{C}$	Mean geometric chord	ft, in
D	Cabin diameter	ft, in
D_{C_0}	Outside cabin diameter	ft, in

LIST OF SYMBOLS (CONT'D)

Symbol	Definition	Units
D_{FUS}	Fuselage	
D_p	Propeller diameter	ft, in
$\frac{dC_M}{dC_L}$	Variation of pitching moment coefficient with change in lift coefficient	
$\frac{dV}{dS}$		
$\frac{d\varepsilon}{d\alpha}$	Variation of downwash angle with change in angle of attack	
$\frac{d\sigma}{d\beta}$	Variation of sidewash angle with change in angle of side-slip	
$F=\frac{S_{wet_{actual}}}{S_{wet_{equiv}}}$	Tail cone wetted area correction factor	
F_H	Empennage weight factor	
F_V	Empennage weight factor	
H	Body height	ft
H	Total pressure increase	lb/ft^2
h	Height; Inside body height	ft, in
h_b	Inside body height	ft, in
h_{b_c}	Baggage compartment height, wall side	ft, in
h_c	Inside cabin height	ft, in
h_f	Floor height	ft, in

LIST OF SYMBOLS (CONT'D)

Symbol	Definition	Units
J_{eff}	Effective advance ratio for propellers in perturbed flow	
J_{is}	Advance ratio for isolated propellers	
K_A		
K_H	Empennage weight factor	
K_C		
K_N	Empirical factor for body + wing effects	
K_P	Surface area correction factor	
K_{R_ℓ}	Reynold's number factor for fuselage	
K_V	Empennage weight factor	
K_W	Wetted area correction factor	
K_{W_F}	Shell weight correction factor	
K	Empirical factor from Fig. 7.3, Ref. 14	
$K_{1\to4}$	Weight estimation factors	
L	Lift	lbs
ℓ	Length	ft, in
ℓ_B	Length of fuselage	ft
$\ell_{B/D}$	Fineness ratio	

LIST OF SYMBOLS (CONT'D)

Symbol	Definition	Units
ℓ_c	Tail cone length	ft
ℓ_h	Distance from wing quarter chord to horizontal tail quarter chord	ft
ℓ_S	Seat pitch	in
ℓ_u	Utility section (cabin) length	ft
$\ell_{u_{PAX}}$	Cabin length for passenger seating	ft
ℓ_V	Vertical tail moment arm	ft, in
M	Mach number	
M.A.C.	Mean aerodynamic chord	ft, in
m	Slope of line, number of radial segments	
N_A	Number of aisles	
N_S	Number of seats	
N_{Rows}	Number of rows of seats	
PAX	Number of passengers	
R.L.S.		
RN	Reynolds number	
r_{b1}	Cone N_1 radius, bottom	
r_{b2}	Cone N_2 radius, bottom	
r_{bc}	Cabin radius, bottom	

LIST OF SYMBOLS (CONT'D)

Symbol	Definition	Units
r_c	Cabin radius for circular cabin	ft, in
r_{bp}	Predicted outside body radius	in
r_{bt}	Tail cone radius, bottom	
r_{t1}	Cone N1 radius, top	
r_{t2}	Cone N2 radius, top	
r_{tc}	Cabin radius, top	
r_{tt}	Tail radius, top	
S_{B_s}	Body side area	ft^2
S_{EMP}	Empennage planform area	
S_G	Gross shell area	ft^2
S_H	Horizontal tail area	ft^2
S_V	Vertical tail area	ft^2
S_{WET_B}	Fuselage wetted area	ft^2
$(S_{WET})_{BODY}$	Fuselage wetted area	ft^2
$(S_{WET})_{Cabin}$	Cabin wetted area	ft^2
S_{WET_H}	Horizontal tail wetted area	ft^2
$(S_{WET})_{NOSE}$	Nose wetted area	ft^2

LIST OF SYMBOLS (CONT'D)

Symbol	Definition	Units
$(S_{WET})_{TAIL}$	Empennage wetted area	ft^2
S_{WET_V}	Vertical tail wetted area	ft^2
S_{Wing}	Wing area	
T_{C_q}	Apparent propeller thrust-loading coefficient	
t/c	Thickness ratio	
V_1	Velocity increase far behind propeller	ft/sec
V_R	Resultant velocity about a body	ft/sec
W_{EMP}	Empennage weight	lbs
W_F	Fuselage shell weight	
$(W_{GR})'$	Adjusted gross weight	lbs
W_H	Horizontal tail weight	lbs
$(W_{GROSS})_i$	Total gross weight for i'th tail cone/empennage configuration	lbs
W_V	Vertical tail weight	lbs
W	Unit seat width	
W_A	Aisle width	ft, in
w_c	Inside cabin width	ft, in
W_{cb}	Crewbox width	ft, in

LIST OF SYMBOLS (CONT'D)

Symbol	Definition	Units
X	Seats on one side of aisle	
$(X_{cg})_0$	Baseline c.g. location relative to nose	ft
$(X_{cg})_M$	Horizontal tail c.g. location relative to nose	ft
$X_{cg_{TAIL}}$	Tail cone c.g. location relative to nose	
$\bar{X}_{TAIL}$	Tail centroid	
$\bar{x}_{ac}$	Aerodynamic center location in terms of $\bar{c}$	
$\bar{x}_{ac_w}$	Wing aerodynamic center location in terms of $\bar{c}$	
Y	Seats on one side of aisle	
y_b	$r_{bc}(\frac{W}{2})$	
y_{sb}	Horizontal location of lower round-off radius	
y_{st}	Horizontal location of upper round-off radius	
y_t	$r_{tc}(\frac{W}{2})$	
Z	Vertical location of cabin center pt.	in
Z_b	$r_{bc}(\frac{H}{2})$	
Z_{mc}	Distance from tail cone centerline to upper surface	ft, in
Z_0	Cross-section center vertical offset	

LIST OF SYMBOLS (CONT'D)

Symbol	Definition	Units
Z_{sb}	Vertical location of lower round-off radius	
Z_{st}	Vertical location of upper round-off radius	
Z_t	$r_{tc}(\frac{H}{2})$	
β	Prandtl-Glauert transformation factor	
ϵ_{cg}	C.g. correction	
η	Propeller efficiency	
η_{EFF}	Effective propeller efficiency	
η_{ULT}	Ultimate airplane load factor	
Λ	Sweep angle	degrees
$\Lambda_{c/2}$	Sweep angle at the half-chord	degrees
ϕ_1	Cone taper parameter	
ϕ_2	Cone bluntness parameter	

LIST OF FIGURES

LIST OF FIGURES (CONT'D)

LIST OF FIGURES (CONT'D)

LIST OF FIGURES (CONT'D)

LIST OF FIGURES (CONT'D)

LIST OF FIGURES (CONT'D)

LIST OF TABLES

CHAPTER 1 INTRODUCTION

This report documents the research accomplished from May 16, 1976 through July 31, 1977 under the funding of NASA Grant NSG-2145. The research conducted was concerned with the design optimization of short haul and commuter airplanes as proposed in References 1 and 2. The intent of the research was to look at the problem of commuter airplane configuration design for the minimization of Direct Operating Costs (DOC). A more detailed explanation of the purpose and objectives of this project is provided in the following section. The status of the research and finances of the project are discussed in Section 1.2.

1.1 Purpose and Objectives

It was proposed to look at the problem of commuter airplane configuration design from the following view points:

- Assume that a specific cabin volume is needed to meet some mission criterion. This will be called a utility constraint. The investigation will focus on commuter type airplanes with a crew of two and a passenger load up to approximately thirty.

- Assume that specific stability and control requirements must be met. These will be called stability and control constraints.

- Assume that specific mission profiles must be flown. These will be called mission constraints.

- Assume that specific performance (for example, field length, minimum speed, single-engine climb, etc.) requirements must be met. These will be called performance constraints. Attention will be focussed on field lengths in the 2500 ft. to 4500 ft. range.

The problem then was to design an airplane configuration which would have the lowest DOC. Figure 1.1 illustrates the problem . The approach taken to the solution of this problem was along the following lines:

Given:

1)  Cabin-Utility Constraint

2)  Mission Constraint

3) Stability and Control Constraints

4) Performance Constraints

Find:

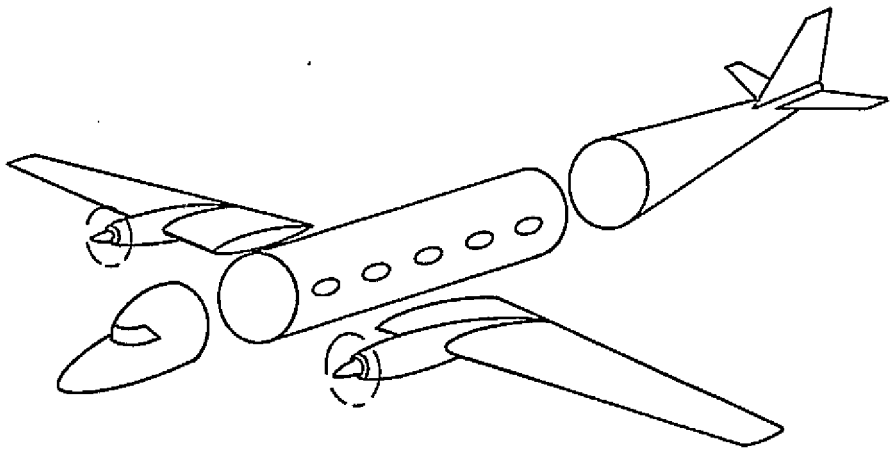

The Configuration Which Minimizes D.O.C.

Figure 1.1 Illustration of the Design Problem

a) Investigate methods for determining the fuselage shape and size which would yield minimum fuselage drag and weight. The fuselage was to be treated as three separate sections (the nose, the cabin, and the tail cone), and methods for the design of each section were to be considered. Chapter 2 discusses the configuration design approaches considered for the fuselage.

b) Determine how the methods of item a) might be integrated into the NASA-Ames General Aviation Synthesis Program (GASP). The GASP was chosen to be the most effective way to apply configuration design methods to the overall preliminary airplane design process. Chapter 3 discusses the ways in which the methods of item a) were to be integrated into the GASP.

c) Determine the critical stability and control constraints which needed to be integrated simultaneously into the GASP. Chapter 5 discusses the stability and control constraints that were considered and explains the ways in which they were to be integrated into the GASP.

d) Perform a short study of wing sizing methods to consider trade-offs in wing loading for effects on performance, ride qualities, etc. One method in particular that was to be considered for wing sizing was the method proposed in Reference 3. Also to be considered was a rational approach to wing placement, bearing in mind weight and balance, stability and control, passenger acceptability, and feasibility of associated structural arrangements. These studies are discussed in Chapter 3.

e) Consider the problem of estimating the drag of airplane components submerged in a propeller slipstream. This problem is discussed in Chapter 4.

As has been stated, the GASP was to be the medium through which all of the configuration design methodologies were to be applied. Unfortunately particular difficulty was encountered in getting a version of the GASP to run on the University of Kansas Honeywell 66/60 computer. For this reason it has not been possible to complete the integration of the design methodologies into GASP. A complete discussion of the transliteration process is presented in Chapter 5.

1.2 Research and Financial Status

1.2.1 Research Status

At the time of this report much of the work outlined in the objectives has been completed. The fact that the GASP is still inoperational has provided the greatest set-back. Revisions to the GASP to include the newly developed methods could not be made without first being assured that the GASP could be operated properly in its existing form. Also, more research needs to be conducted in the area of stability and control methods. Table 1.1 summarizes the status of each research area. Also, Table 1.1 refers to the chapters where each facet of the research will be discussed.

1.2.2 Financial Status

Tables 1.2 and 1.3 present the budgets for the two phases of the project as proposed in References 1 and 2. Together, they represent a total allocation of $50,590 through NASA Grant NSG-2145. Although a complete breakdown of expenses through July 31, 1977 was not available at the time of this report, it was possible to arrive at an estimate as to the remaining balance as of that date. It is estimated that as of July 31, 1977 the balance of funds remaining in NASA Grant NSG-2145 will be approximately $100.

TABLE 1.1 DESIGN OPTIMIZATION GRANT STATUS
31 JULY 77

ITEMS AND/OR OBJECTIVES PROPOSED		ITEMS ACCOMPLISHED	ITEMS PENDING	ITEMS TO BE PROPOSED
PROPOSAL I	PROPOSAL II			PROPOSAL III
1)Procedure to find fuselage/ empennage shape for min. drag				
a)Roskam/Fillman Method		1)KU-FRL 902; Program written and tested. Results questionable Chapter 2, this report	1)Test Roskam/Fillman Method with Wing Balance included in GASP	
b)Cabin Arrangement and Baggage Compartment Studies	1)Continued Cabin arra[illegible] & Baggage Compartment Studies	2)KU-FRL 901; Preliminary correlations Chapter 2, this report	2)Comparisons with McDonnell Douglas and Boeing Vertol Methods Chapter 2, this report	
c)Wetted Area Studies		3)KU-FRL 901; Preliminary correlations Chapter 4, this report	3)Correlation of Actual Wetted Areas with FUSE-computed Areas Chapter 4, this report	
2)Weight Estimation Methods				
a)Torenbeek's Method		4)KU-FRL 902; included in Roskam/Fillman Method Program Chapter 2, this report	4)Checking use of GASP Weight Estimation Methods	

TABLE I.1 DESIGN OPTIMIZATION GRANT STATUS (CONT'D)

ITEMS AND/OR OBJECTIVES PROPOSED		ITEMS ACCOMPLISHED	ITEMS PENDING	ITEMS TO BE PROPOSED
PROPOSAL I	PROPOSAL II			PROPOSAL III
3)Stability Constraints	2)Analysis of GASP designs	5)KU-FRL 902; Empennage Sizing by C_{m_α} & C_{n_β} in the Roskam/Fillman Method	5)Looking at ways to replace GASP V methods, to include inertia est. to enable dynamic stability analysis, and to locate wing	1)Chapter 6, this report
4)Slipstream Drag Analysis		6)KU-FRL 902 Chapter 4		
5)Include Methods into GASP		7)KU-FRL 902; Flowcharts	6)Updating Cessna version of GASP to NASA version Chapter 5, this report	
	3)Fuselage Config. Studies			
	a)Nose section model	8)KU-FRL 313-3; FUSE	7)Use of FUSE with NCSU BODY Program to Analyze Nose	
	b)Cabin sizing	9)Same as Above; Design Mode of FUSE Chapter 2, this report		

TABLE 1.1 DESIGN OPTIMIZATION GRANT STATUS (CONT'D)

ITEMS AND/OR OBJECTIVES PROPOSED		ITEMS ACCOMPLISHED	ITEMS PENDING	ITEMS TO BE PROPOSED
PROPOSAL I	PROPOSAL II			PROPOSAL III
	4)Wing Config.			
	a)Sizing	10)Chapter 3, this report	8)Loftin's Method to be Considered	
	b)Placement	11)Chapter 3, this report	9)Considering combination of GASP and Torenbeek's method	
	5)Develop algorithms for GASP	12)Chapter 3, this report	10)Finding that it is possible to simply amend GASP methods	2)Complete addition of developed algorithms into GASP and check them out

Table 1.2 Proposed Budget

May 16, 1976 - December 15, 1976

	NASA	KU	TOTAL
Salaries & Wages			
Principal Investigator (Roskam)			
20% for 4 mos. academic*	1,271	1,271	2,542
67% for 3 mos. summer	5,807	0	5,807
Research Assistants (3 1/2)			
50% for 7 months	9,800	0	9,800
Secretary			
2 man-months	1,000	0	1,000
Total Salaries & Wages	17,878	1,271	19,149
Fringe Benefits			
16% Faculty & Staff	1,293	203	1,496
7% Students	686	0	686
Computer	2,000	0	2,000
Supplies & Reproduction	200	0	200
Telephone	200	0	200
Travel (2 trips to Ames)	750	0	750
Total Direct Costs	23,007	1,474	24,481
Indirect Costs - 53.6% of Total S & W	9,583	681	10,264
Total Proposed Costs	32,590	2,155	34,745

*Principal Investigator's academic time cost shared by KU and NASA equally. Each paying only 10% for 4 mos. academic time = 20%.

Salary Schedule	FY76	FY77
Roskam	2,889/mo.	3,178/mo.
Research Assistant	800/mo.	NA
Secretary	500/mo.	NA

Table 1.3 PROPOSED BUDGET

January 1, 1977 - June 30, 1977

	NASA	KU	TOTAL
Direct Costs			
Salaries & Wages			
Principal Investigator - Roskam			
25% for 1 mo. academic FY 77	$ 416	$ 417	$ 833
75% for 1 mo. summer FY 77	2,500	0	2,500
Graduate Research Assistant			
75% for 4.5 mos. academic 77	3,038	0	3,038
100% for 1 mo. summer 77	900	0	900
75% for .5 mo. summer 77	337	0	337
Undergraduate Research Assistants			
75% for 5 mos. academic 77 (1 student)	2,625	0	2,625
100% for 1.5 mos. summer 77 (1 student)	1,050	0	1,050
100% for .5 mo. summer 77 (1 student)	350	0	350
Secretary			
2.33 man-months (student)	1,398	0	1,398
Total Salaries and Wages	12,614	417	13,031
Fringe Benefits			
17% staff	496	71	567
7% students	679	0	679
Other Direct Costs			
Computer	2,540	0	2,540
Supplies and Reproduction	400	0	400
Telephone	500	0	500
Travel	1,000	0	1,000
Total Direct Costs	18,229	488	18,717
Indirect Costs @ 53.6% of Salaries & Wages	6,761	224	6,985
Total Proposed Costs	$ 24,990	$ 712	$ 25,702
Less unexpended balance in NASA Grant NSG 2145	6,990		
TOTAL PROPOSED COSTS	$ 18,000		

CHAPTER 2 FUSELAGE CONFIGURATION STUDIES

As stated in Chapter 1 one of the objectives of the research program was to investigate methods for determining the fuselage shape and size which would yield minimum fuselage drag and weight. A two-phase approach was taken to meet this objective. The first phase consisted of evaluating existing methods for sizing the fuselage or, where the need arose, to develop new methods. Also included in this phase was an evaluation of existing methods for determining fuselage drag and weight. The second phase of this approach was to integrate the methods chosen as a result of the first phase into the GASP and to perform trade-offs in the fuselage configuration design to find trends from which optimum configurations might be determined. In this manner it was also hoped that it might become possible to locate critical configuration determining parameters, and eventually to develop routines to optimize the fuselage directly, for a given set of constraints. Unfortunately, because of the difficulties encountered in putting the GASP into an operational status, the second phase of the approach has not been completed at the time of this report. For this reason, this chapter is concerned primarily with the first phase - the evaluation and development of fuselage design and analysis methods.

To facilitate the fuselage design procedures, the fuselage was considered to be composed of three distinct sections - the nose cone, the cabin and the tail cone. This is illustrated in Figure 2.1. Design methods were considered for each section individually and then were integrated to provide a method to determine the overall fuselage shape and size. The methods considered for each section are discussed in the following sections of this chapter. Section 2.1 compares different methods for sizing the cabin given a specified number of passengers. Section 2.2 describes a method for sizing the nose cone and crew compartment. Section 2.3 discusses a method for determining the fuselage/empennage configuration to meet specified static stability

criteria. Section 2.4 presents the results of a study to determine baggage compartment requirements for commuter airplanes and the alternatives for satisfying those requirements. Finally a method for sizing the overall fuselage is discussed in Section 2.5.

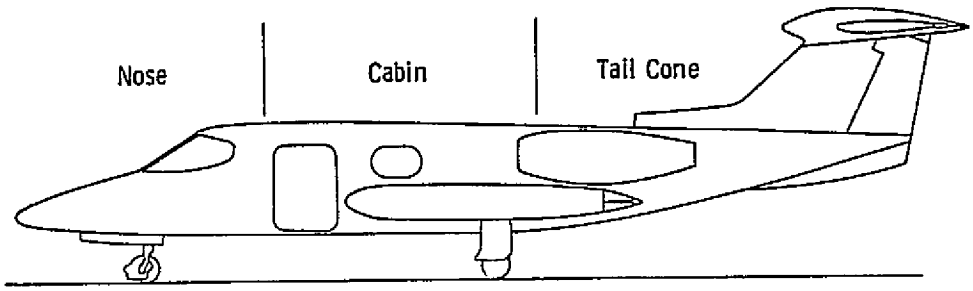

Figure 2.1 Definition of Fuselage Sections

2.1 Cabin Arrangement

The fuselage cabin design is primarily dependent upon the number and arrangement of passengers. However, possible use of the airplane for cargo payloads, the location of the wing carry-through structure, and location of main landing-gear storage can also enter into the cabin design. Although the main emphasis of this research was to determine and evaluate methods to size the cabin for utility (i.e. passengers) constraints, a conscious attempt was made to keep other factors in mind.

Before looking at existing sizing methods, or developing any new ones, a survey was conducted to examine the dimensions of existing commuter airplane cabins. The results of this survey are presented in Table 2.1. In Table 2.1 the seating configuration is indicated in an X/Y format where the values of X and Y indicate the number of seats abreast on either side of a single cabin aisle. The sole exception to this is the Britten-Norman Trislander which has no aisle.

Table 2.1 Cabin Dimensions of Existing Commuter Aircraft

No	Aircraft	Seating Config.	Passenger Seats	Cabin* Width (in.)	Cabin* Height (in.)	Cabin** Length (in.)
1	Beech 99	1/1	15	55	57	276
2	Cessna 402	1/1	7	56	51	174
3	Britten-Norman Islander	1/1	10	43	50	156
4	Swearingen Metro	1/1	19	62	57	306
5	Queen Air	1/1	7	52	57	108
6	GAF Nomad	1/1	15	51	62	331
7	Piper Navajo Chieftain	1/1	8	51	52	-
8	Saunders ST-27	1/1	22	54	69	336
9	Beriev Be-30	1/1	16	60	60	264
10	Pilatus Twin Porter	1/1	8	46	50	120
11	Mitsubishi MU-2L	1/1	11	59	51	-
12	Twin Otter	1/2	20	63	59	222
13	Short Skyliner SC-7	1/2	22	78	78	223
14	Falcon 30	1/2	30	96	73	445
15	Short SD3-30	1/2	30	78	78	372
16	YAK-40	1/2	33	80	62	336
17	Nord 262	1/2	29	84	70	300
18	Casa C.212	1/2	18	82	70	192
19	Handley Page Jetstream	1/2	18	73	71	288
20	Piper PA35	1/2	16	76	70	204
21	Omnipol L-410	1/2	14	69	65	216
22	Fokker-VFW 614	2/2	44	105	78	444
23	Antonov AN-24	2/2	50	109	75	444
24	Breguet 941c	2/2	56	102	88	432
25	deHavilland DHC-5	2/2	53	105	82	480
26	deHavilland DHC-7	2/2	48	103	77	444

* Inside Dimensions

** Approximate-varies with configuration

No	Aircraft	Seating Config.	Passenger Seats	Cabin* Width (in.)	Cabin* Height (in.)	Cabin** Length (in.)
27	Fokker F.27	2/2	52	88	79	-
28	GAC-100	2/2	32	98	75	372
29	Handley Page Herald	2/2	54	109	76	-
30	Canadair CL-215	2/2	30	94	75	360
31	Hawker Siddeley HS. 748	2/2	52	97	75	558
32	NAMC YS-11	2/2	60	106	78	528
33	IAI Arava	2/2	18	75	68	144

* Inside Dimensions

** Approximate-varies with configuration

Where the data were available seat, aisle and seat pitch dimensions were also examined, in addition to the inside cabin width and height dimensions. Figures 2.2 and 2.3 define the cabin and cabin seating dimensions that will be referred to throughout this section.

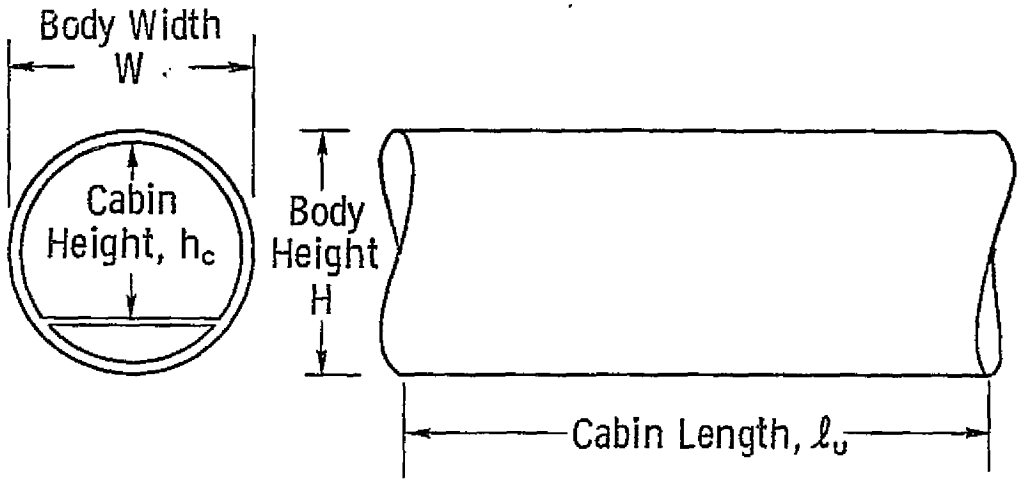

Figure 2.2 Definition of Cabin Dimensions

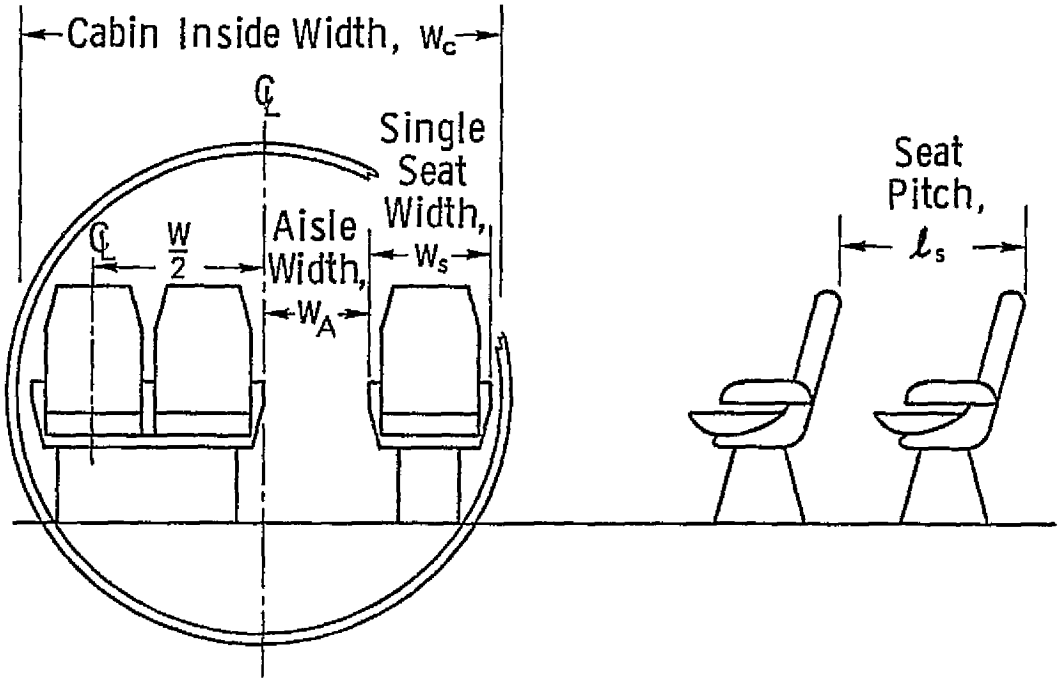

Figure 2.3 Definition of Seating Arrangement Dimensions

The cabin sizing problem is one of trading-off passenger comfort and seat-miles for drag and weight. Passenger comfort may be related to the spacing between seats. As spacing is increased, so is passenger comfort. However, as comfort, and for that matter the number of total passenger seats is increased so are the drag and the weight of the overall airplane, which tends to reduce cost-effectiveness. Although this section only deals with sizing the cabin for specified comfort levels and seating arrangements, the trade-offs will be considered to some extent in Chapter 4.

Comfort level is difficult to define. In lieu of trying to survey passengers as to what might be considered as 'comfortable' or not, and then having to extract the size-related factors from noise, vibration, ride quality, etc., it was decided to take what data were available for cabin seating arrangements and attempt to define general comfort levels. A letter from the project technical monitor at NASA-Ames, Tom Galloway (Reference 4), defined three comfort levels as shown in Table 2.2. For the most part the data available supported these values. The one exception was in the case of aisle width. A number of aircraft were found to have aisle widths lower than 16 inches. For this reason the comfort levels that will be used in this report are as presented in Table 2.3.

Table 2.2 Seating Arrangement

Comfort Level

(From Reference 4)

Dimension	Minimum	Adequate	Maximum
Single Seat Width	18"	20"	22"
Seat Pitch	28"	30"	32"
Aisle Width	16"	18"	20"
Standup Headroom	64"	70"	76"

Table 2.3 Revised Seating Arrangement Comfort Levels

Dimension	Minimum	Adequate	Maximum
Seat Width	18"	20"	22"
Seat Pitch	28"	30"	32"
Aisle Width	12"	18"	20"
Standup Headroom	64"	70"	76"

2.1.1 Determination of Cabin Cross-Section

As was stated in Chapter 1, the GASP was to be the medium of application for all design methods that were developed under this project. The GASP presently assumes that the cabin may be represented by a right circular cylinder of constant cross-section. For the purpose of this project the constant cross-section assumption was maintained. However, the cross-section was not limited to circular shapes. The smaller commuter airplanes frequently have cabin cross-sectional shapes which are far from being circular. For this reason, circular, elliptical, and what will be referred to as rounded-rectangular shapes were considered. This report will deal with the circular and round-rectangular shapes only. The elliptically shaped cross-sections are inherently covered by the methods that will be discussed here. The geometry for the rounded-rectangular cross-sectional shapes is presented in Figure 2.4. Note that the rounded-rectangular cross-section becomes an ellipse (or circle) for r_{tc} and $r_{bc} = 1$.

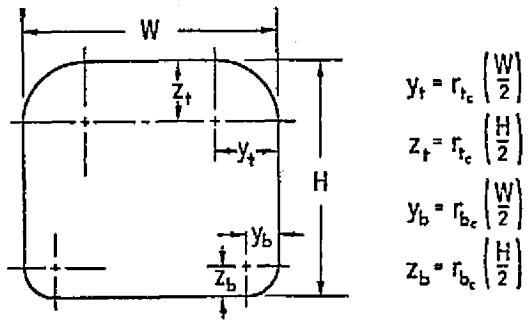

Figure 2.4 Geometric Definition of Rounded- Rectangular Cross-sections

For both circular and rounded-rectangular cross-sections the values for the inside cabin height and width were expected to be largely dependent on the seating arrangement selected and the comfort level. To help in finding the best methods for determining these two dimensions the data of Table 2.1 were plotted to correlate total passenger seats and seating arrangement with inside cabin width and height. These plots are presented as Figures 2.5 and 2.6.

From Figures 2.5 and 2.6 note first that for the range of airplanes considered there seemed to be more or less definite passenger capacities for which each seating configuration was used. Table 2.4 presents the apparent passenger capacity ranges for each seating configuration. Note also from Figure 2.5 that the cabin width ranges for each seating configuration are well defined. These are also presented in Table 2.4. The cabin heights for each seating configuration are not so well defined in Figure 2.6. This would seem to indicate that cabin height is not as dependent upon the seating arrangement as was originally expected. This will be discussed further at a later point in this section.

Table 2.4 Passenger Capacity and Cabin Width Ranges for Seating Configurations of Existing Commuter Aircraft

Seating Config.	Passenger Capacity Range	Cabin Width Range (in.)
1/1	0 - 22	43 - 62
1/2	15 - 33	62 - 96
2/2	30 - 60	88 - 109

It is interesting at this point to compare the cabin width ranges of Table 2.4 with the comfort levels of Table 2.3. Using values resulting from the sum of the seat widths and aisle width as as estimated cabin width Table 2.5 compares the values for minimum and maximum comfort levels with the observed cabin width ranges.

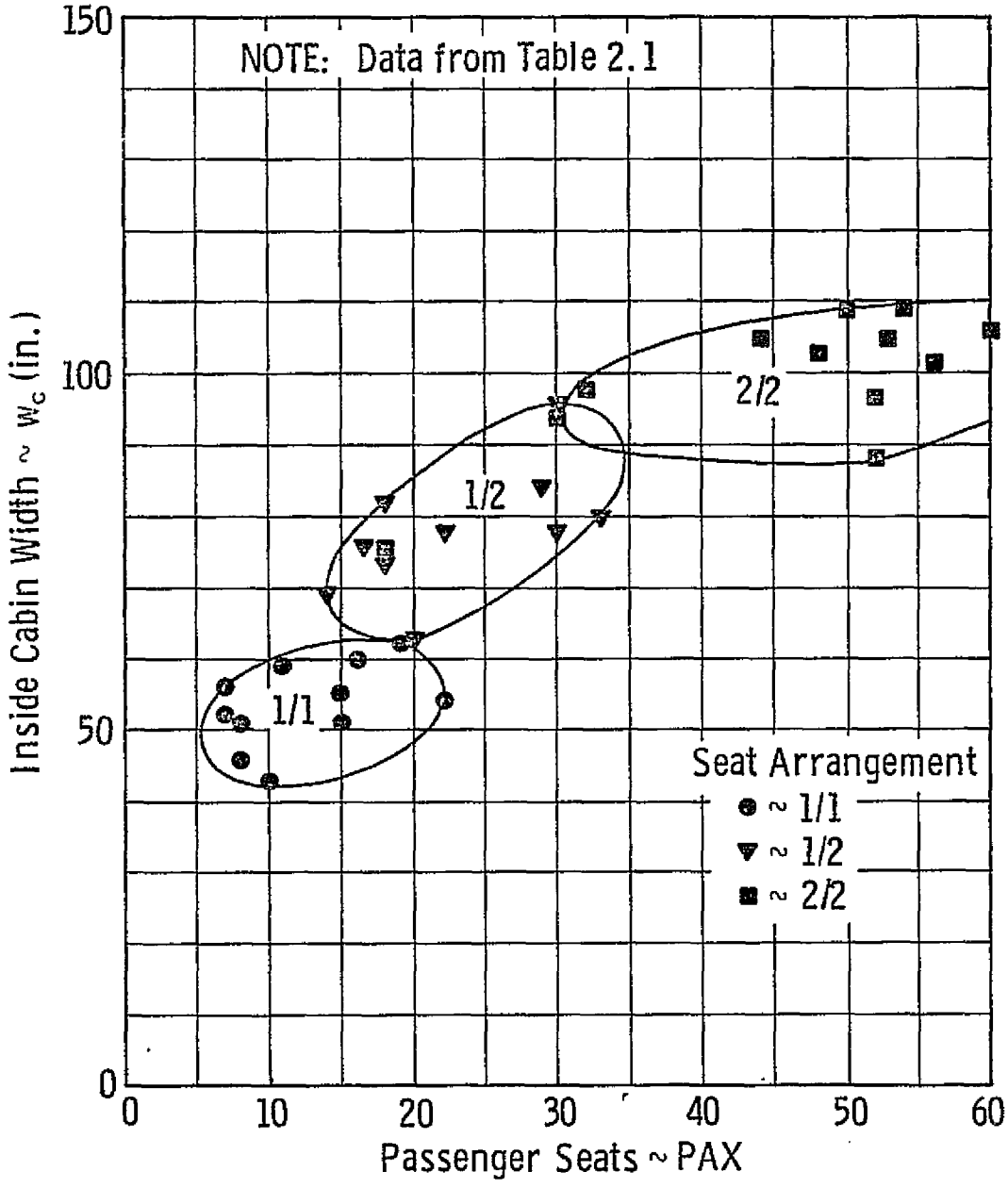

Figure 2.5 Correlation of Inside Cabin Width with Number of Passengers

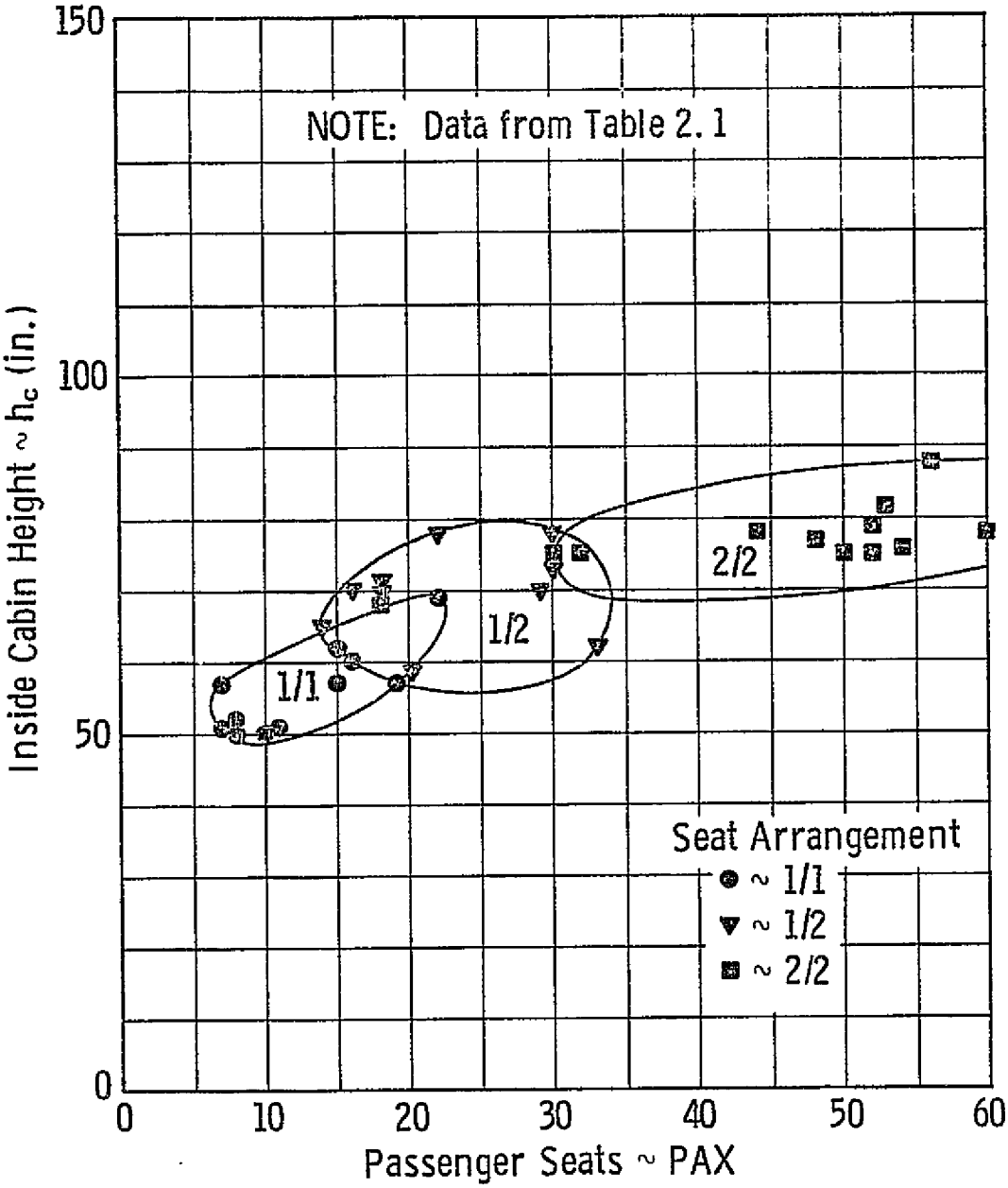

Figure 2.6 Correlation of Inside Cabin Height with Number of Passengers

Table 2.5 would seem to indicate that the comfort level criteria are reasonable. The minimum comfort level does indicate larger cabin widths for the 1/1 and 1/2 configurations, however in a number of cases aisle width values lower than 12 inches were observed. Also it should be noted that the 43 inch cabin width was the Britten-Norman Islander which has no aisle.

Table 2.5 Comparisons of Existing Cabin Widths with Comfort Level Cabin Widths

Seating Config.	Cabin Width Range (Table 2.4) (in.)	Minimum Comfort Level Cabin Width (in.)	Maximum Comfort Level Cabin Width (in.)
1/1	43 - 62	48	64
1/2	62 - 96	66	86
2/2	88 - 109	84	108

In an attempt to derive relationships for cabin width and cabin height as a function of passenger capacity and/or seating arrangement least-squares linear and logarithmic curve fits were applied to both Figures 2.5 and 2.6. The results of these curve fit applications are presented as Figures 2.7 through 2.9. Note that the cabin width data are only presented in the "thumbprint" form. This has been done purely to add clarity to the figures. All of the curve fit calculations are based on the data of Table 2.1. Note in Figure 2.7 that the 1/1 and 2/2 configuration lines are almost parallel and that the 1/2 configuration line seems to represent a transition between the two. A linear regression analysis was performed for each seating configuration for the cabin height case but the resulting relationship reinforced the conclusion made earlier that cabin height is not very dependent upon the seating arrangement. Both of the logarithmic curve fits (Figures 2.8 and 2.9) show that cabin width and cabin height may be

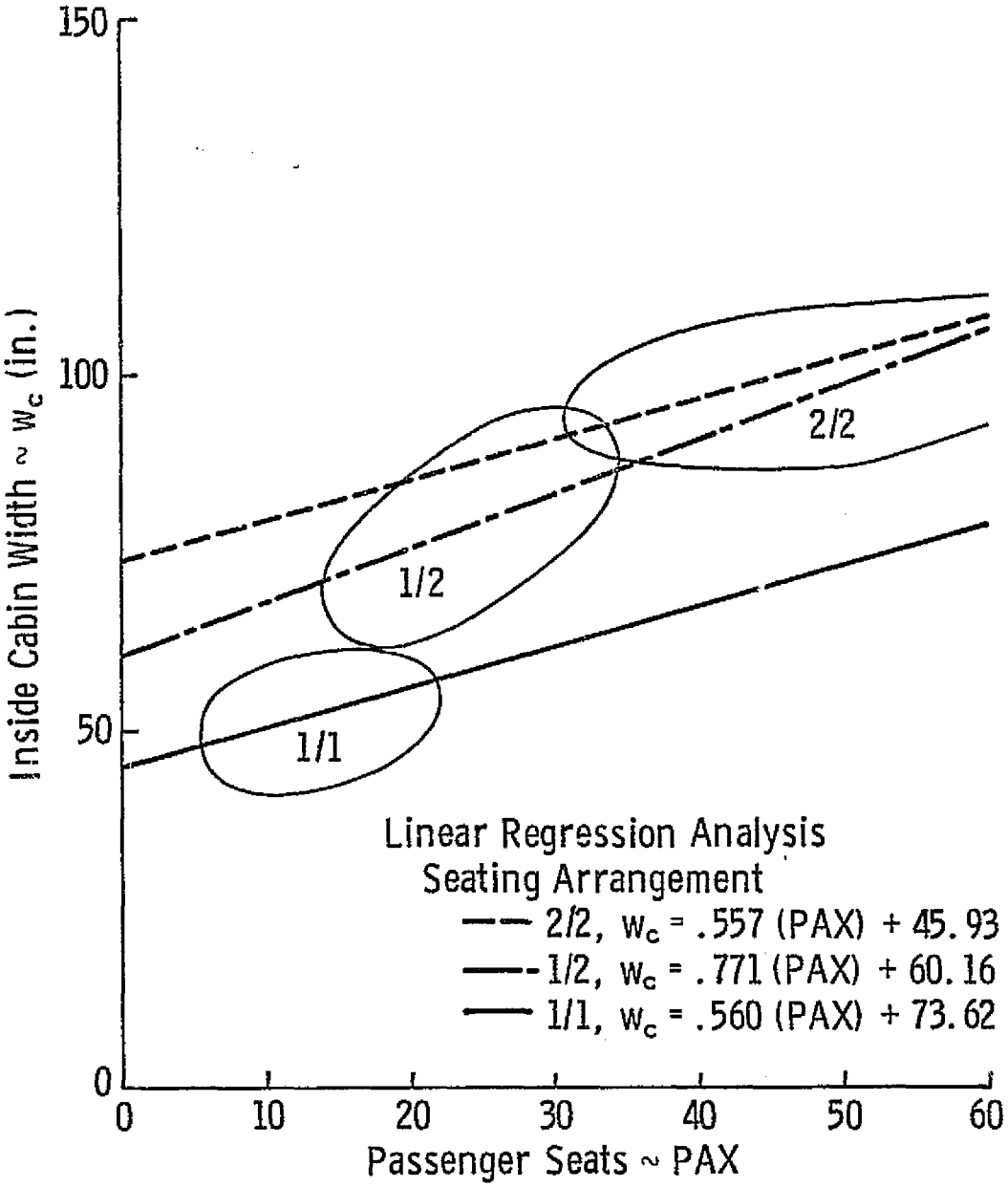

Figure 2.7 Linear Correlation of Inside Cabin Width with Number of Passengers

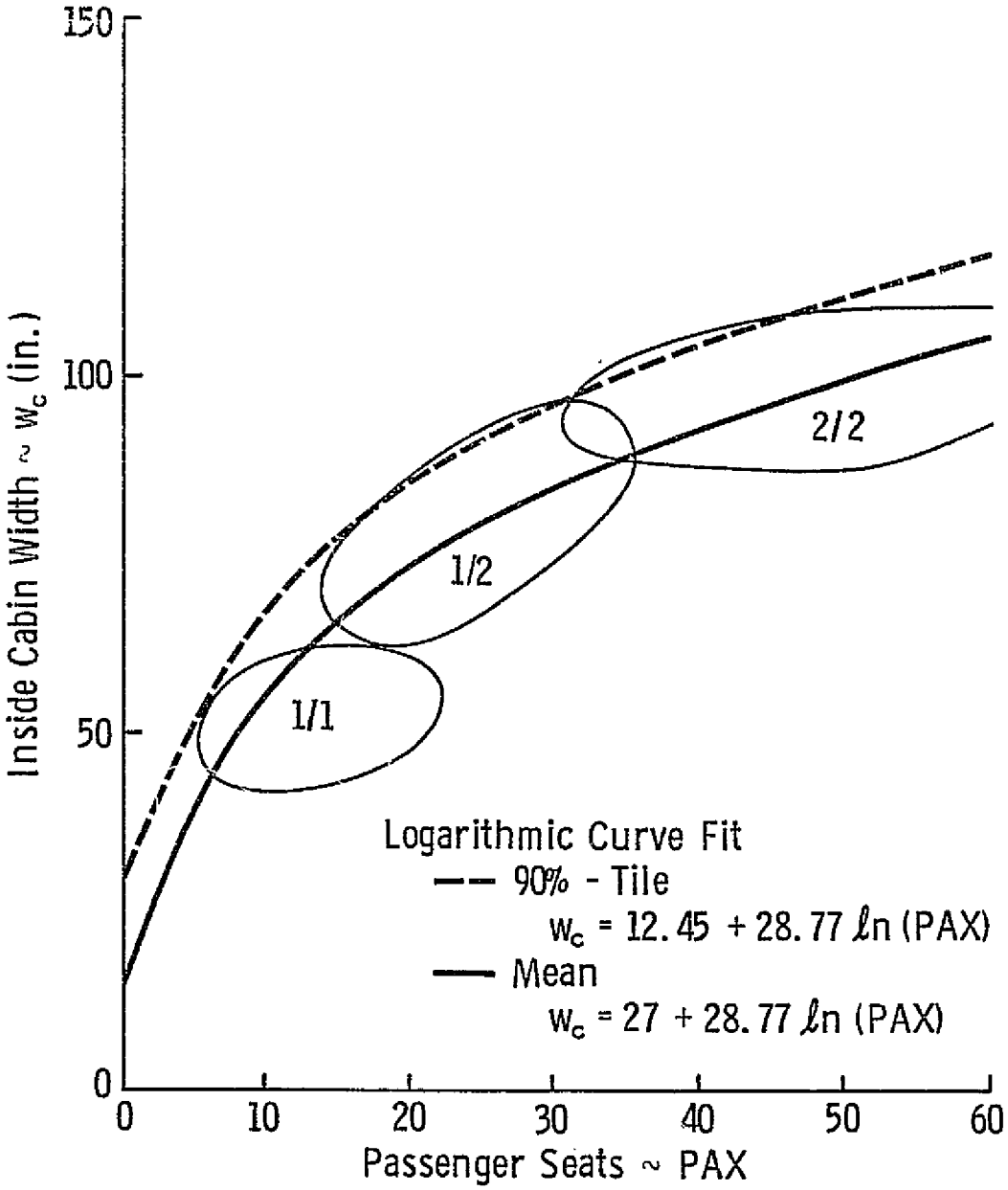

Figure 2.8 Logarithmic Correlation of Inside Cabin Width with Number of Passengers

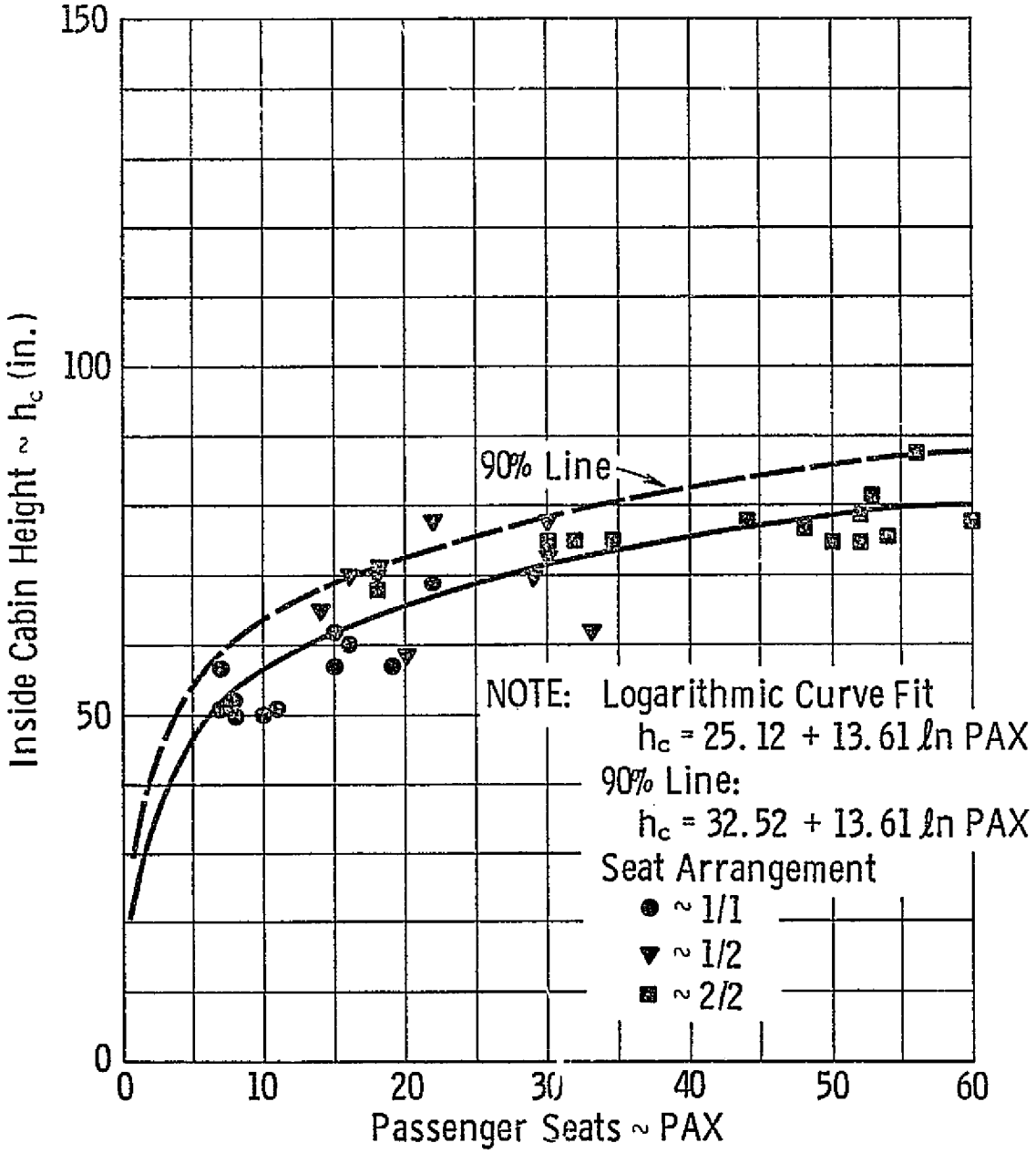

Figure 2.9 Logarithmic Correlation of Inside Cabin Height with Number of Passengers

related to total passenger capacity.

As both cabin width and cabin height may be related to total passenger capacity but only cabin width may be easily related to the number of seats abreast, then it was thought that perhaps cabin height could be related to the cabin's other primary dimension, length. It seems reasonable, at least from a comfort point of view, that the longer the cabin, the less passengers will like having to put up with a low ceiling aisle. Figure 2.10 relates cabin height with cabin length. Figure 2.10 does seem to indicate that there is some relationship but the correlation is not as good as was expected. No further research was pursued along this line.

2.1.1.1 Existing Cross-Section Sizing Methods

Only three existing cross-section sizing methods were available for evaluation - the Boeing Vertol Method (Reference 5), the McDonnell Douglas method (Reference 6), and the GASP method. Each of these methods assumes a circular cross-section.

The Boeing Vertol method is based on the assumption that a circular cabin cross-section can be designed for a particular seating arrangement that will clear certain body-seated control points. The method was developed in the following manner. Five control points were chosen to constrain the inner cabin wall about a seated passenger as shown in Figure 2.11. Using these control points layouts for different configuration layouts were made. An empirical relationship was developed based on the number of seats abreast, seat width, number of aisles, and aisle width using the data derived from the layouts. This relationship is presented in Figure 2.12. The outside body radius was then computed as a constant percentage of the inner radius. A comparison of actual outside body radii and computed outside body radii is presented in Figure 2.13.

Although reference will be made to the McDonnell Douglas method, no actual sizing method was available. Instead the results of a study of the operational requirements for medium density air transportation were available. These results are presented in References 6, 7 and 8.

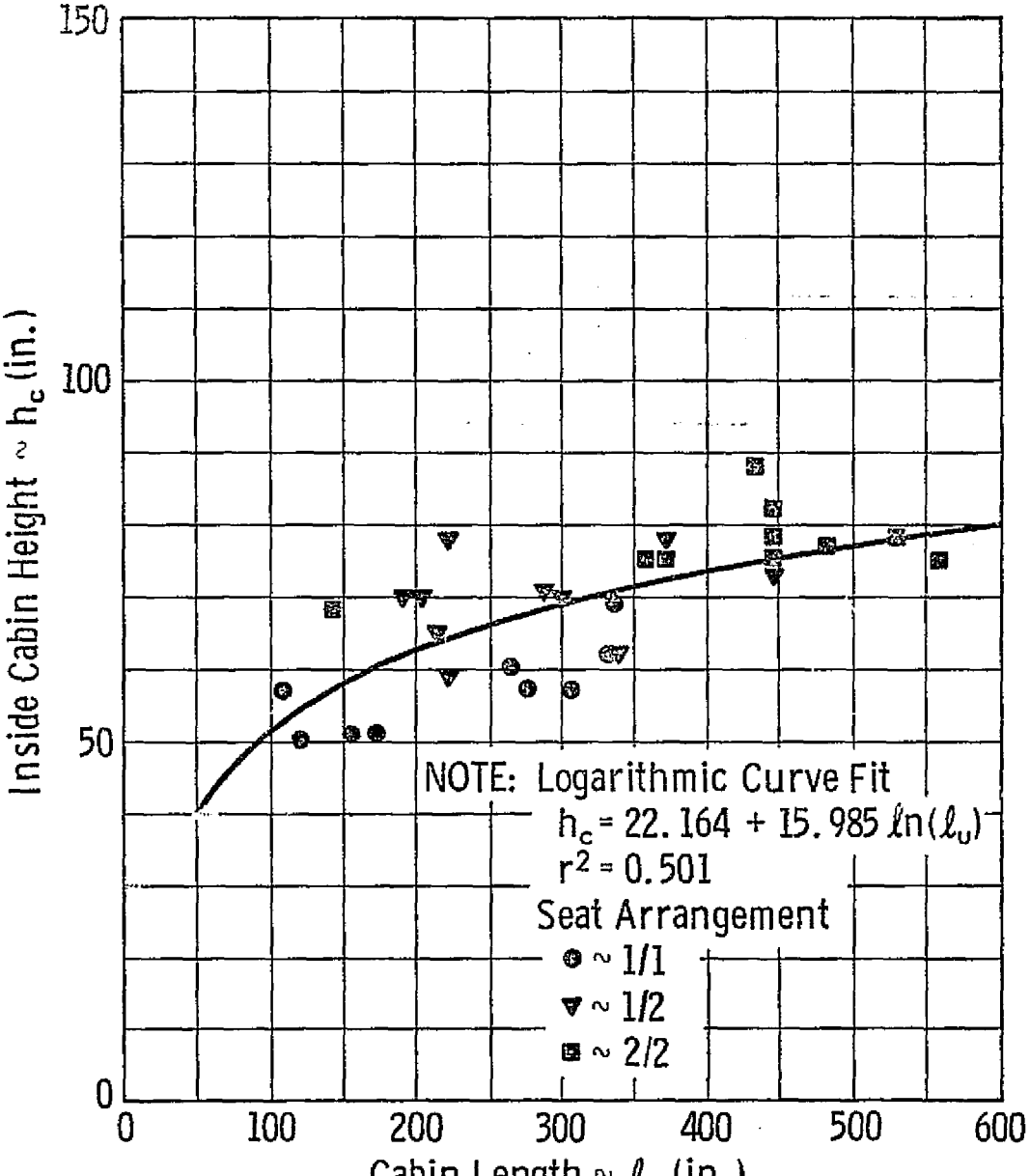

Figure 2.10 Logarithmic Correlation of Inside Cabin Height with Cabin Length

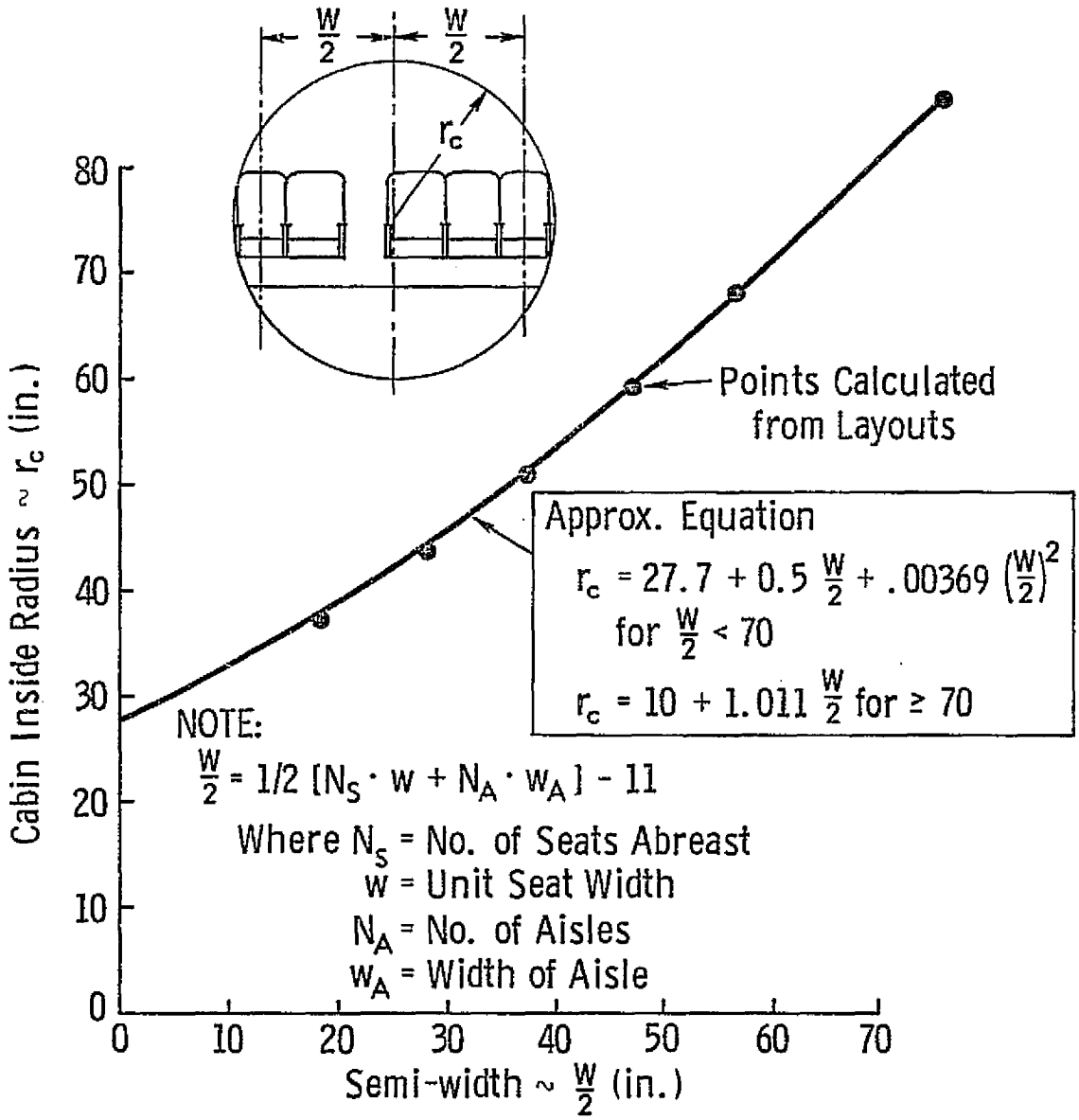

Figure 2.12 Empirical Relationship for Cabin Radius by the Boeing Vertol Method (Reproduced from Reference 5)

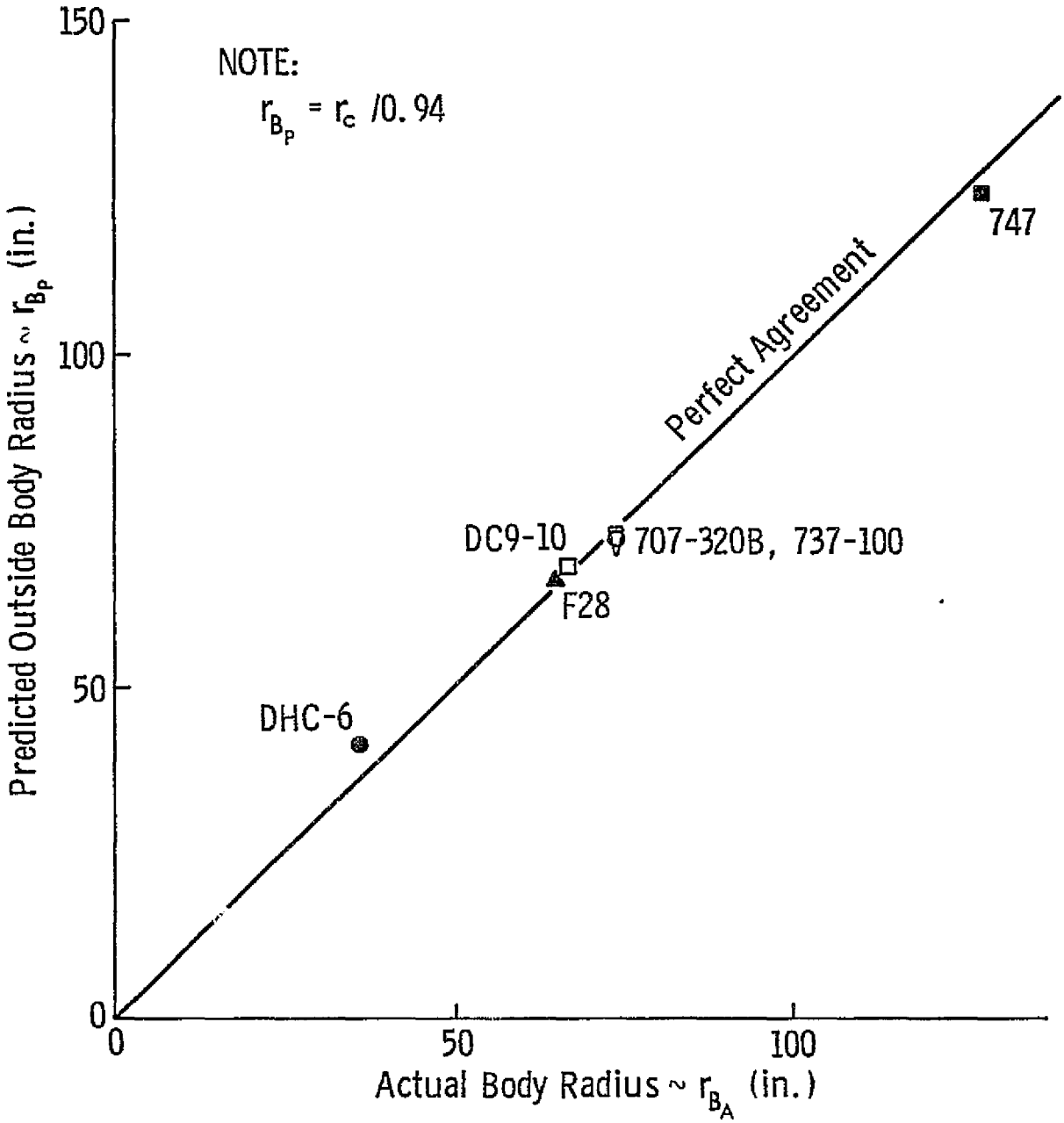

Figure 2.13 Comparison of Predicted Body Radius with Actual Body Radius for Six Commercial Aircraft (Reproduced from Reference 5)

Figure 2.14 is a reproduction from Reference 8 of the cross-section developed for the baseline feederliner of the McDonnell Douglas study. The cross-section was designed not only with passenger seating in mind, but also to accept palletized cargo. The only control points specified to constrain the shape for passenger seating were at the tangent to a seven inch circle drawn about the center of the head for a 95 percentile seated man and at the top-center of the cabin. A further control point was defined at the base of the outer seat leg, six inches from the seat center line. With the seat dimensions and aisle height (i.e. cabin inside height), these points could be located and the cross-section shape determined.

Having specified three control points on the inner wall of the cabin, and defining these points relative to the cabin center point, the cabin cross-section is over-constrained. Only two constraints are required, but by having three it is possible to choose which constraints are critical in the case being considered. Equations 2.1, 2.2 and 2.3 define the inside cabin radius from each control point in terms of the seating configuration and the cabin center point:

A. Ceiling Constraint (Control Point A):

$$r_c = h_c - z \tag{2.1}$$

B. Passenger Headroom Constraint (Control Point B):

$$r_c = \sqrt{[1/2((N_s - 1)w_s + N_A w_A)]^2 + (48 - z)^2} \tag{2.2}$$

C. Floor Constraint (Control Point C):

$$r_c = \sqrt{[1/2((N_s - 1)w_s + N_A w_A) + 6]^2 + z^2} \tag{2.3}$$

where, in the above equations,

N_s = number of seats abreast

w_s = single seat width (in.)

N_A = number of aisles

w_A = aisle width (in.)

z = vertical location of the cabin center point with respect to the floor (in.)

h_c = inside cabin height from the floor (in.)

It is assumed that the only unknowns in equations 2.1, 2.2, and 2.3 are r_c and z. The value of cabin height will be assumed to be a given comfort level value. To find the cabin radius any pair of constraints may be chosen. By then solving the resulting pair of equations for r_c the cabin is sized for those particular constraints. The third equation may then be solved to determine if the cabin radius is adequate for that constraint.

In most cases, constraints B and C will probably be critical. By solving equations 2.2 and 2.3 simultaneously for r_c these constraints can be met. However, in this case the cabin height must also become a variable. After determining the cabin radius and the center point locations, the cabin height may be checked. If the cabin height is inadequate the cabin may be sized for new constraints.

Equations 2.4, 2.5 and 2.6 provide the solutions for r_c for each constraint pair.

Constraints A and B :

$$r_c = \frac{\left(\frac{w}{2}\right)^2 + (48 - h_c)^2 - 49}{2(55 - h_c)} \qquad (2.4)$$

Constraints A and C :

$$r_c = \frac{\left[\left(\frac{w}{2}\right) + 6\right]^2 + h_c^2}{2h_c} \qquad (2.5)$$

Constraints B and C:

$$r_c = \frac{-B \pm \sqrt{B^2 - 4AC}}{2A} \qquad (2.6)$$

where

$$A = \frac{49}{2304} - 1$$

$$B = -\frac{98}{2304}\left[\frac{6}{7}\left(\frac{w}{2}\right) - \frac{2219}{14}\right]$$

$$C = \frac{49}{2304}\left[\frac{6}{7}\left(\frac{w}{2}\right) - \frac{2219}{14}\right]^2 + \left[\left(\frac{w}{2}\right) + 6\right]^2$$

For all of the above equations:

$$\left(\frac{w}{2}\right) = \frac{1}{2}\left[(N_s - 1)w_s + N_A w_A\right]$$

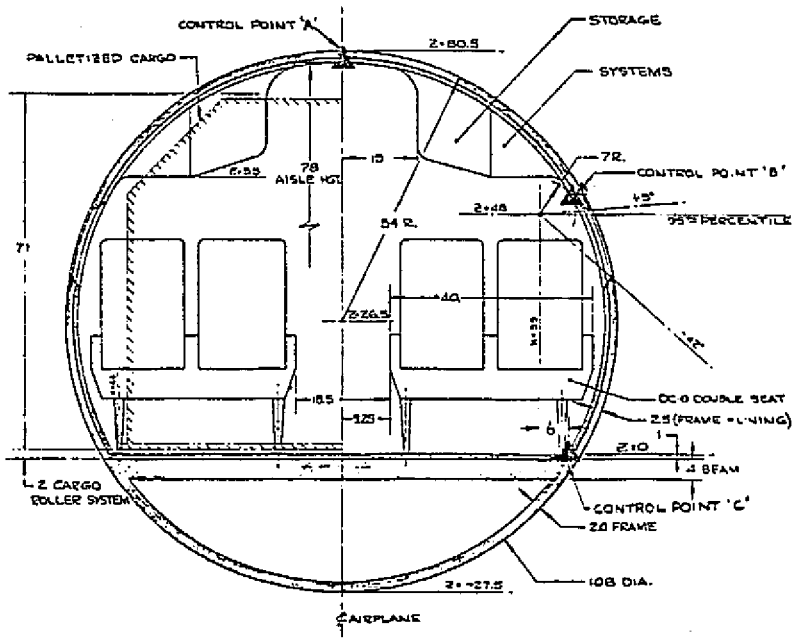

108 DIA. FUSELAGE CROSS-SECTION
SCALE 1/10 SIZE

Figure 2.14 McDonnell Douglas 30-Passenger Feederliner Cross-Section (Reproduced From Reference 8)

Table 2.6 Cabin Widths* for the Minimum Comfort Level

Seating Config.	Boeing Vertol Method	McDonnell Douglas Method	GASP Method (Outside)
1/1	69.65	67.04	60.00
1/2	80.97	79.26	78.00
2/2	93.49	93.53	96.00

Table 2.7 Cabin Widths* for the Adequate Comfort Level

Seating Config.	Boeing Vertol Method	McDonnell Douglas Method	GASP Method (Outside)
1/1	75.79	72.14	70.00
1/2	89.19	87.00	90.00
2/2	104.06	103.75	110.00

Table 2.8 Cabin Widths* for the Maximum Comfort Level

Seating Config.	Boeing Vertol Method	McDonnell Douglas Method	GASP Method (Outside)
1/1	79.66	74.90	76.00
1/2	94.96	91.88	98.00
2/2	112.05	110.77	120.00

* Cabin Width in inches

The GASP method only sizes for the outside dimension of the cabin. As with the other methods a circular cross-section is assumed with a diameter determined as in equation 2.7. The constant twelve inches are intended to account for clearances about the seats and for the structure.

$$D = N_s \cdot w_s + N_A \cdot w_A + 12 \qquad \text{(inches)} \qquad (2.7)$$

where: D_{c_o} = outside cabin diameter (inches)

N_s = number of seats abreast

N_A = number of aisles

w_s = seat width (inches)

w_A = aisle width (inches)

2.1.1.2 Evaluation of Cross-Section Sizing Methods

To evaluate the application of the cabin sizing methods described above to the design of short haul and commuter airplanes, it was decided to compare cabin widths computed by these methods for each comfort level with the data of Table 2.1 and Figure 2.5. As the cross-section is assumed to be circular at this point the inside cabin width, w_c, may be assumed to be equal to the inside cabin diameter. Tables 2.6, 2.7, and 2.8 present the results for the minimum, adequate, and maximum comfort levels respectively. Figures 2.15, 2.16, and 2.17 plot the results of each of these tables respectively on the seating arrangement thumbprints of Figure 2.5, for each sizing method and each seating arrangement.

From Figures 2.15 through 2.17 it is apparent that the methods generally size for cabins larger than those of existing aircraft. This is especially true for the 1/1 configurations. In this case the GASP method seems to do the best job when it is taken into consideration that the GASP sizings are for outside widths. The Boeing Vertol and McDonnell Douglas methods do fairly well for the 1/2 and 2/2 seating configurations however. It is also noted that the McDonnell

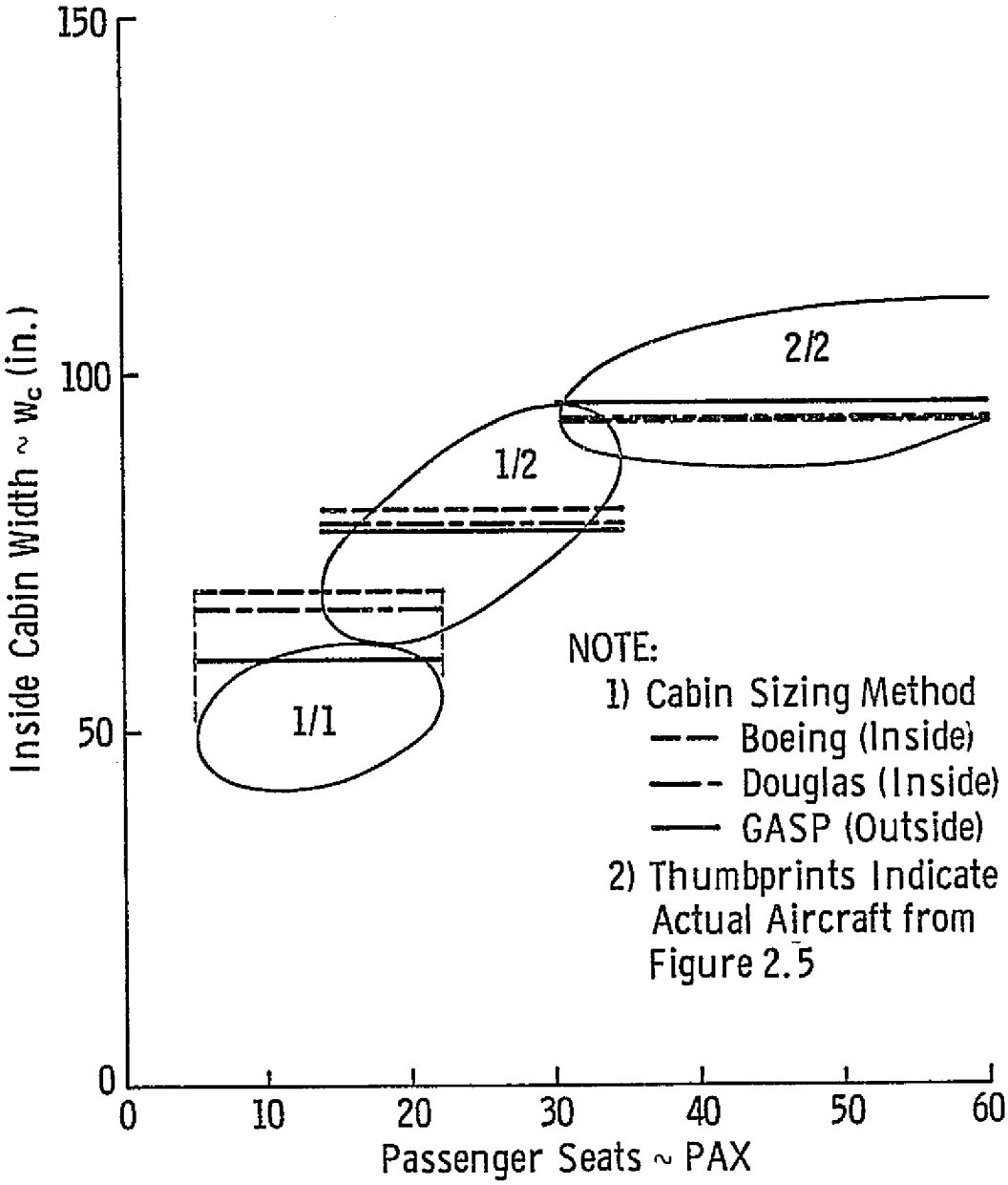

Figure 2.15 Comparison of Computed Minimum Comfort Level Cabin Widths with Existing Aircraft Data

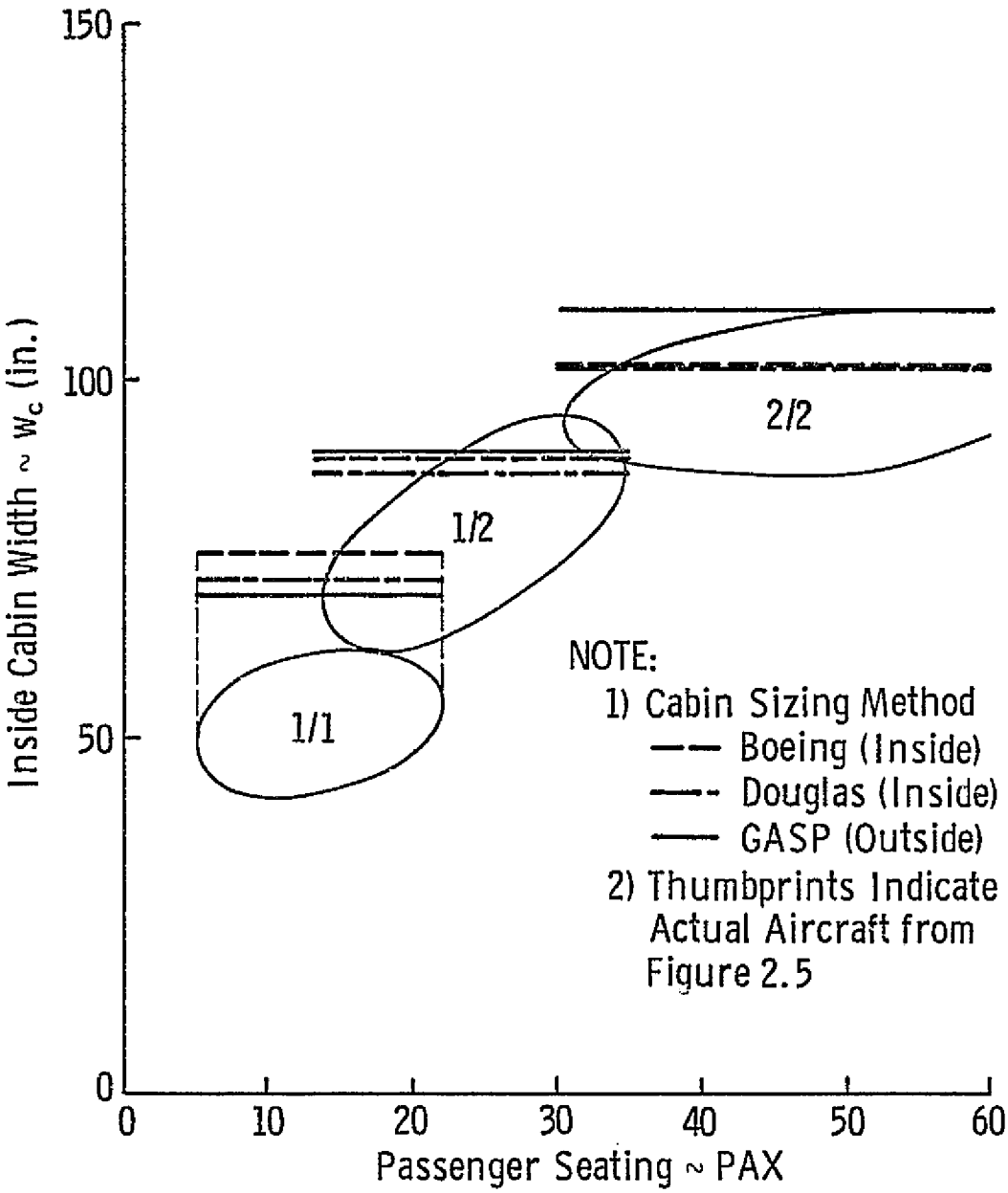

Figure 2.16 Comparison of Computed Adequate Comfort Level Cabin Widths with Existing Aircraft Data

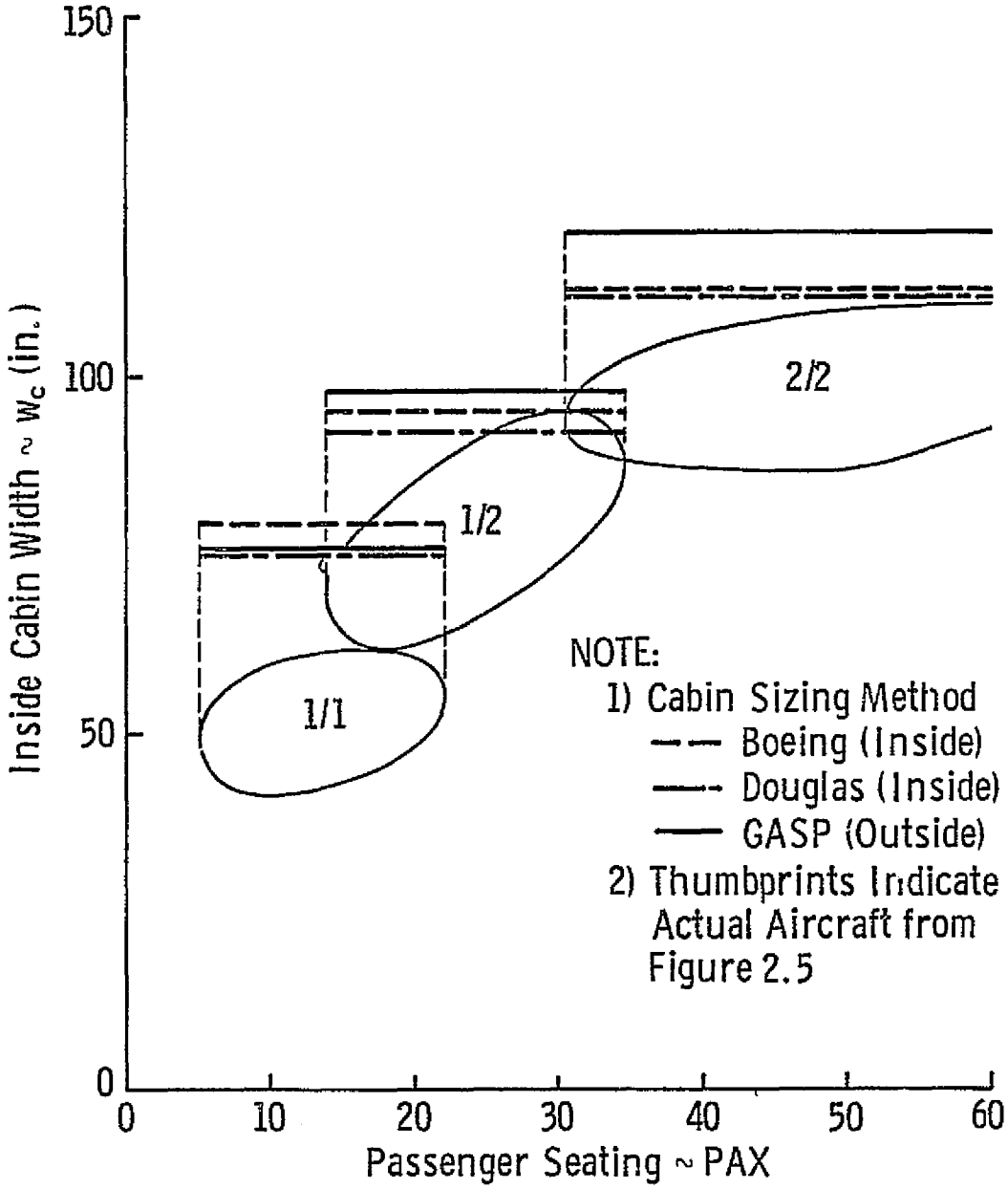

Figure 2.17 Comparison of Computed Maximum Comfort Level Cabin Widths with Existing Aircraft Data

Douglas and Boeing Vertol methods represent very similar results in all cases.

To determine why the Boeing Vertol and McDonnell Douglas methods over-sized cabin width for the smaller seating configurations (i.e. 2 and 3 seats abreast), the extreme case was considered - the 1/1, minimum comfort configuration. The cabin was sized using both methods in Table 2.6. Figure 2.18 presents a drawing showing the resulting cross-sections and seating arrangement. Note that for the Boeing Vertol cross-section control points B, C, and D are not needed and that points A and E become the critical constraints. This results in a large amount of wasted space between the outer armrest and the cabin wall. The same occurs for the McDonnell Douglas cross-section. To provide the seated headroom constraints for these smaller seating configurations the width must be oversized.

Figure 2.19 shows the result of the GASP method which produced a cabin width which was comparable with existing aircraft. The seat used in both Figures 2.18 and 2.19 was a conceptual economy-class seat sized to the minimum comfort level dimensions of Table 2.3. The seated headroom constraint shown in Figure 2.19 is the same as that for the McDonnell Douglas method. The seven inch clearance radius is drawn about the location of the center of a 95 percentile seated man (48 inches above the floor at the seat center line). As the GASP method only sizes for the outside cabin dimension, the Boeing Vertol method for estimating structure was used to determine the inside cabin radius (See Figure 2.13). Figure 2.19 indicates that with these constraints it would be extremely difficult to fit a 95 percentile man in the cabin. Although seat dimensions for smaller seats were not readily available, it is assumed that with such a seat (i.e. lower seat height, greater nominal recline angle, etc.), such a cabin would become cramped but practical. Indeed, several aircraft such as the Gates-Learjets already do this. For a pressurized airplane where a circular cross-section means weight savings, this then would be a viable cabin sizing method.

In the case of unpressurized commuters, a better solution is

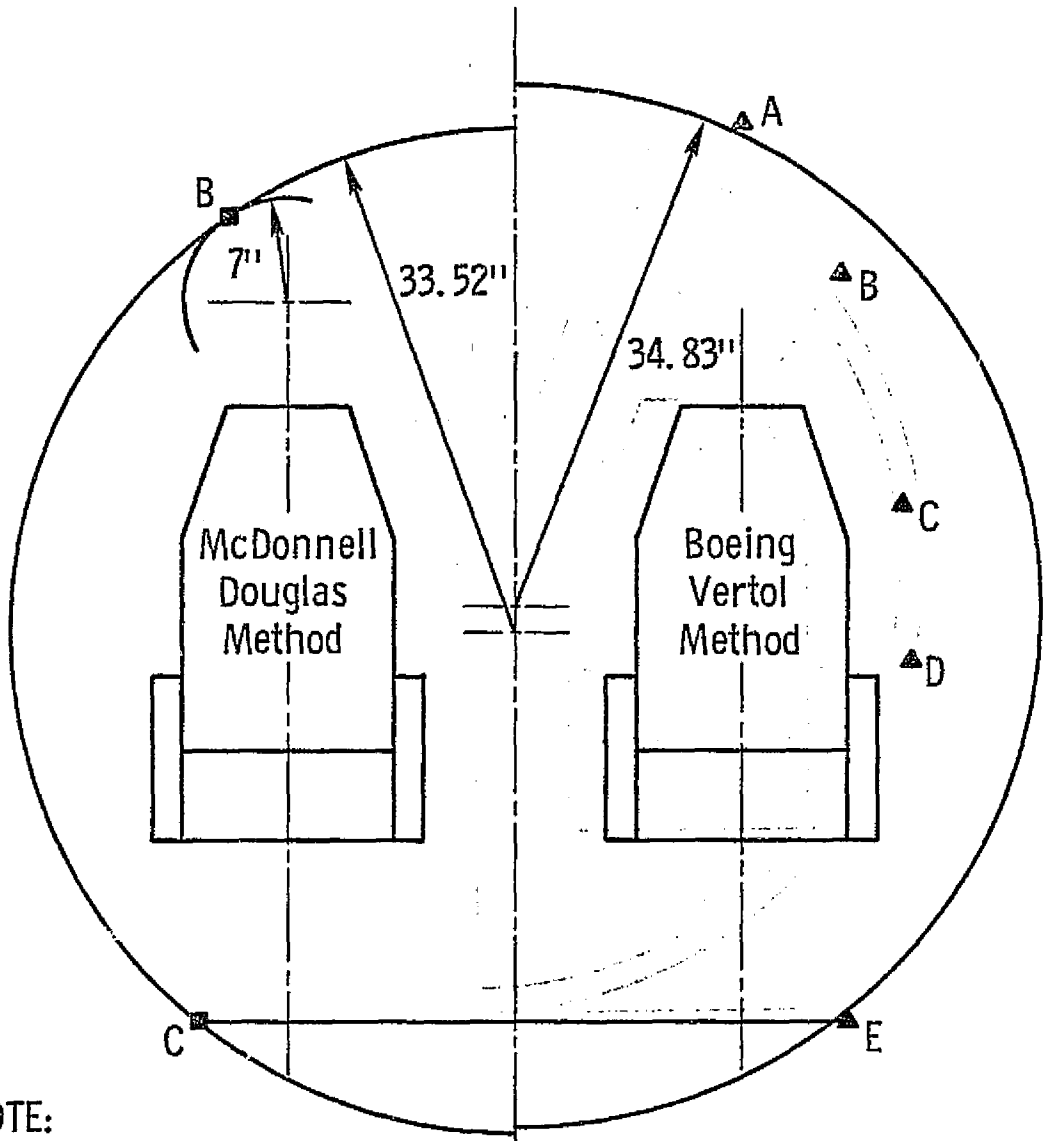

NOTE:

1) Scale in Inches

0 10 20

2) Comfort Level: Minimum
3) Control Points
   - ■ McDonnell Douglas
   - ▲ Boeing Vertol

Figure 2.18 Boeing and Douglas Coin Cross-sections for Minimum Comfort Level

available. The rounded-rectangular cross-section of Figure 2.4 can result in a more comfortable cabin without giving up much in the way of weight or drag. In this case, however it may no longer be assumed that outside body width equals body height. Therefore each must be sized. The values of the round-off radii are for the most part a matter of preference.

Equation 2.8 may be used to determine the inside cabin width. In equation 2.8 it is assumed that the window-side armrest of the seat is placed directly up against the cabin wall.

$$w_c = N_s w_s + N_A w_A \tag{2.8}$$

To determine the fuselage inner height (i.e. total outside body height minus structure), first a control point is established as in control point C for the McDonnell Douglas method. It is assumed that to minimize fuselage inner height, the floor is to be placed as low as this control point will allow (as shown in Figure 2.20). Using the bottom round-off radius fraction, r_{bc}, it should be possible to determine the necessary fuselage height. Let the height below the floor be represented as h_f. The inside fuselage height is then as represented in equation 2.9.

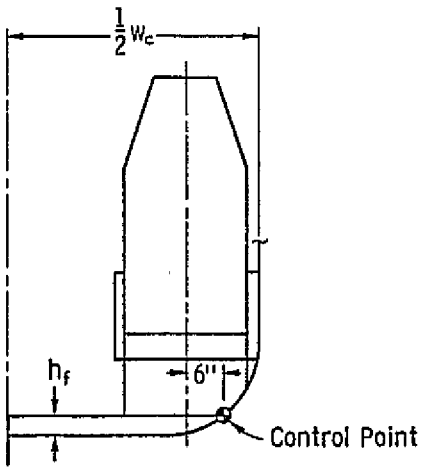

Figure 2.20 Location of Floor Control Point for Rounded-Rectangular Cross-Sections

$$h = h_c + h_f \tag{2.9}$$

The round-off shape is elliptical. Therefore at the control point:

$$\left(\frac{2z}{hr_{bc}}\right)^2 + \left(\frac{2y}{w_c r_{bc}}\right)^2 = 1 \tag{2.10}$$

where,

$$y = \frac{w_c r_{bc}}{2} - \frac{w_s}{2} + 6$$

$$z = \frac{hr_{bc}}{2} - hf$$

Substituting equation 2.9 and solving for h results in:

$$h = \left\{ \left[\frac{\frac{r_{bc}}{2} - \frac{r_{bc}}{2}\sqrt{2\left(\frac{w_s - 12}{w_c r_{bc}}\right) - \left(\frac{w_s - 12}{w_c r_{bc}}\right)^2}}{1 + \frac{r_{bc}}{2} + \frac{r_{bc}}{2}\sqrt{2\left(\frac{w_s - 12}{w_c r_{bc}}\right) - \left(\frac{w_s - 12}{w_c r_{bc}}\right)^2}} \right] + 1 \right\} h_c \tag{2.11}$$

Table 2.9, presents inside cabin widths and inner fuselage height for each comfort level and seating configuration. In Table 2.9 round-off radii of r_{bc} = .2, .5, .8, and 1.0 are used. From Table 2.9 it is apparent that for large round-off radii, r_{bc}, the minimum inside body height, h_b, required to meet comfort level constraints can become overly large. Therefore it would seem that if cabin wetted area is to be minimized, a smaller r_{bc} would be preferable.

To check that adequate room for a passenger is indeed provided, the minimum comfort level 1/1 seating configuration was again used. Figure 2.21 provides the resulting cabin cross-sections for upper round-off radii values of r_{t_c} = .2, .5, .8, and 1.0. In all cases the lower round-off radius is r_{bc} = 0.2. Note that this gives very

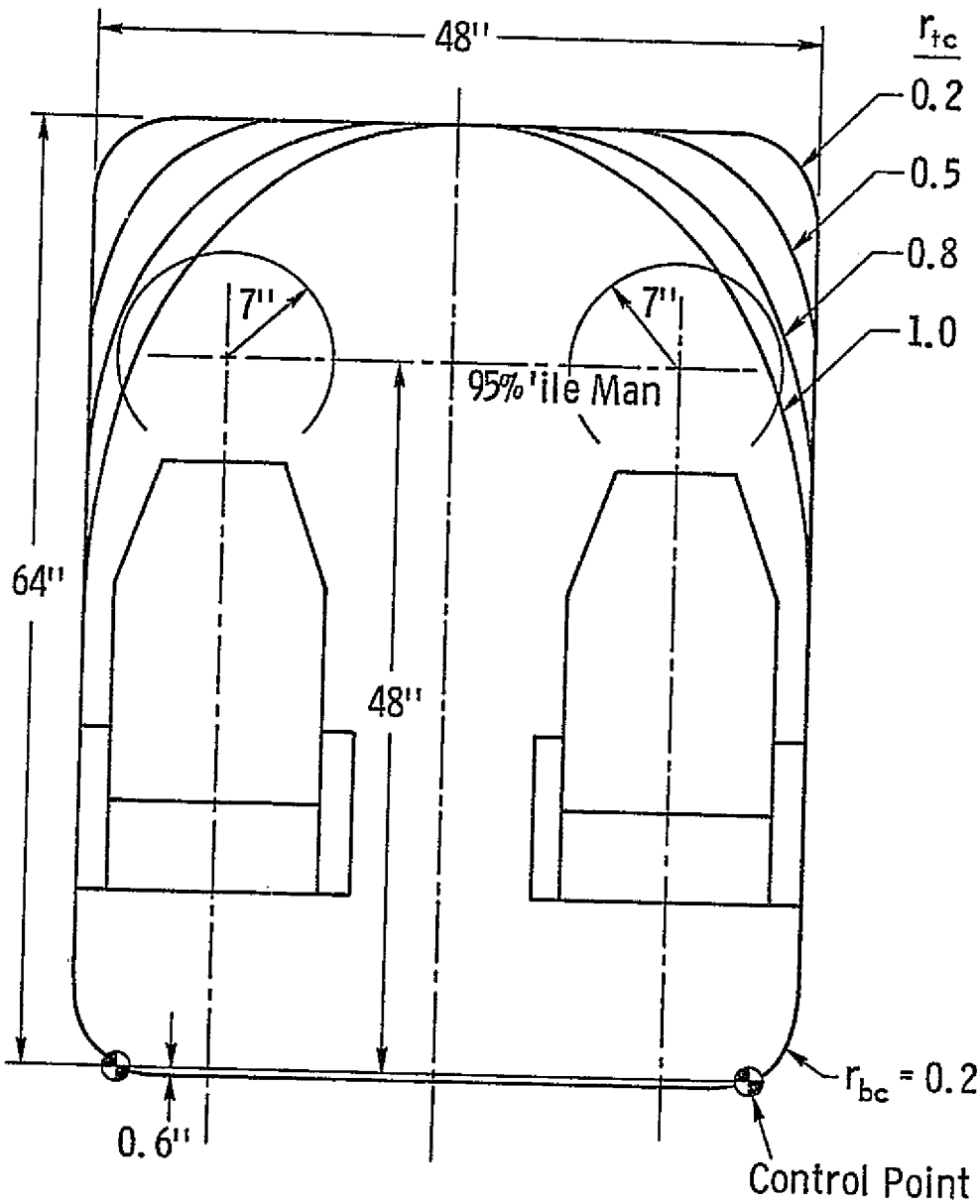

NOTE:
Minimum Comfort Level Dimensions

Figure 2.21 Minimum Cabin Dimensions

Table 2.9 Cabin Dimensions for Rounded-Rectangular Cross-Section

Comfort Level (Table 2.3)	Seat Config.	Cabin Width, w_c (in.)	Inside Body Height, h_b			
			$r_{bc} = .2$	$r_{bc} = .5$	$r_{bc} = .8$	$r_{bc} = 1.0$
Minimum	1/1	48	64.6	73.3	94.8	128.0
Minimum	1/2	66	65.3	75.2	97.1	128.0
Minimum	2/2	84	65.8	76.5	98.6	128.0
Adequate	1/1	58	70.4	79.4	102.7	140.0
Adequate	1/2	78	71.1	81.5	105.4	140.0
Adequate	2/2	98	71.7	82.9	107.0	140.0
Maximum	1/1	64	76.2	85.2	110.1	152.0
Maximum	1/2	86	76.9	87.6	113.3	152.0
Maximum	2/2	108	77.5	89.2	115.2	152.0

reasonable results for $r_{tc} \leq 0.8$. Although other examples are not presented here for the sake of brevity, in general it was found that for $r_{tc} \leq 0.8$ all seated headroom constraints could be met.

It should be noted again that this method sizes the inside cross-section only for the minimum dimensions, given the comfort level constraints. It might be desirable, for instance, to increase the under-the floor height to allow for baggage, wing carry-through structure or landing gear retraction. These considerations are not inherently taken into account by this method.

Methods have been discussed to size both circular and rounded-rectangular cross-sections. It was found that all of the circular cross-section methods provided results which were reasonable for configurations with three and four seats abreast, but that appeared to be either too small (GASP) or too large (Boeing and Douglas) for configurations with only two seats abreast. Of these methods only the GASP method did not directly account for adequate clearances for a seated passenger. Of the other two methods the McDonnell Douglas method seemed to provide the best results for the two-seats-abreast case. Also the McDonnell Douglas method is slightly easier to check and to alter should different seat sizes be chosen. For these reasons it was decided to adopt the McDonnell Douglas method to incorporate into GASP for circular sections. The rounded-rectangular method also appears to provide reasonable results, and in this case, particularly for the smaller seating configurations. This method has the distinct advantage of providing a way of sizing short haul aircraft for cargo payloads, also. The round-off radii may be input as desired, although it was found that for round-off radii greater than 0.8 a circular sizing method would be preferable. Therefore this method will also be used to provide added versatility to the cabin sizing process.

Up until this point only the inner cabin dimensions have been dealt with. Only one method was found to account for structure,

upholstery, etc., in general. The Boeing method determined the inside cabin diameter to be 94% of the outside diameter. Although this is somewhat conservative for smaller unpressurized airplanes, this method will be used to determine the outside dimensions.

2.1.2 Determination of Cabin Length

At this point the cabin length will be determined only as that length required for passenger seating. It will be assumed that for short haul/commuter airplanes of size and range being considered that cabin attendants and lavatory facilities will not be necessary. Baggage compartment requirements will be considered in Section 2.4.

To determine the cabin length for passenger seating equation 2.12 will be used:

$$\ell_{u_{PAX}} = N_{ROWS} \times \ell_s . \qquad (2.12)$$

where,

N_{ROWS} = number of rows of seats

ℓ_s = seat pitch in inches.

2.2 Nose Cone Configuration

The primary consideration in designing the nose cone and windshield geometry is the cockpit arrangement and visibility. The cockpit constraints must be met if the crew are to be able to fly the airplane. Other considerations however include the drag increment resulting from the windshield, nose gear retraction, and some stability characteristics. The main emphasis in this section will be placed upon the design of the nose for adequate cockpit volume and visibility.

The GASP default* size for the cockpit has a flight deck 4.44 ft. long. Based on the data available in References 9 and 10 this might prove inadequate. Figure 2.22 presents the recommended

---

*Note: A "default" quantity is a value stored in the computer routine which is used as the value of a particular variable when no value is input by the user.

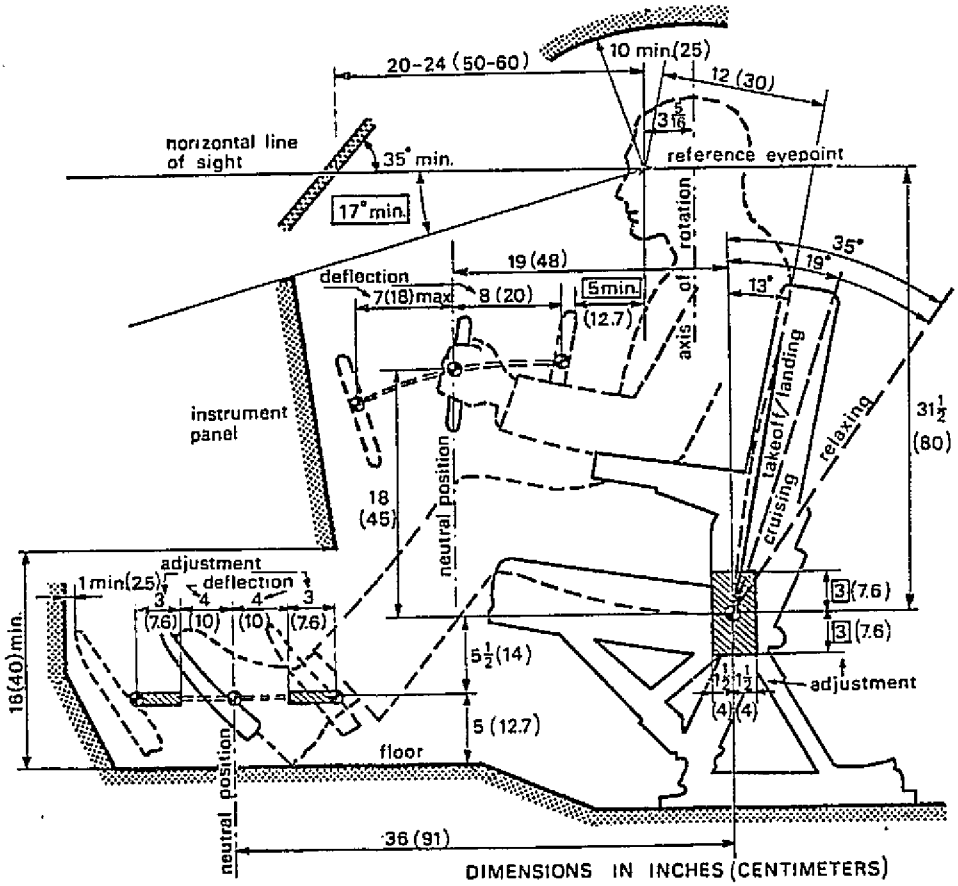

Figure 2.22 Recommended Flight Deck Dimensions For Transport Aircraft (Reproduced from Reference 9)

dimensions for the flight deck. Based on these dimensions it was decided to design a standardized "crewbox" about which the nose might be shaped. The nose is to be modelled by superimposing two elliptical cones as shown in Figure 2.23. The crewbox will be located on the front of the cabin as shown in Figure 2.24. The shorter of the two cones, or cockpit shell will then be sized for the flight deck.

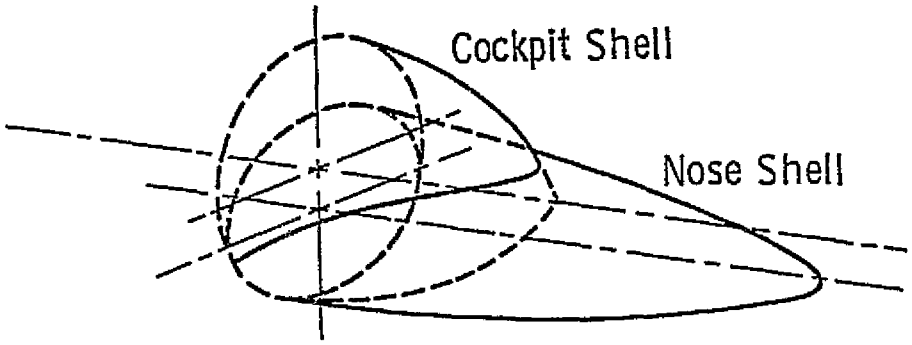

Figure 2.23 Superimposing of Two Elliptical Cones to Define Nose Cone/Windshield Geometry

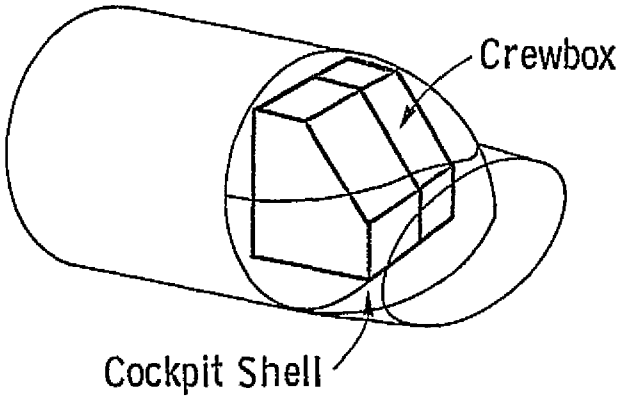

Figure 2.24 Location of the Crewbox

Using the dimensions of Figure 2.22 it was possible to define a more or less standard shape for the crewbox. The dimensions for this crewbox are presented in Figure 2.25. Note from Figure 2.25 that the width of the crewbox is defined as in equation 2.13. The minimum distance between crew seat center lines for the class of aircraft in question should be about thirty inches, according to Reference 9. Also it is assumed that, as a minimum, the crew seats are of the same width as the passenger seats.

$$w_{cb} = w_s + 30 \quad \text{(inches)} \tag{2.13}$$

The length of the nose shell, i.e. the long thin cone of Figure 2.23 is difficult to specify in any generalized form. It was found that the best method is to specify the ratio of the lengths of the two cones. In choosing a length ratio certain factors should be kept in mind. Some of these are:

- Forward and downward visibility on approach
- Nose gear location and retraction method
- Possible installation of radar
- Desirability of a nose baggage compartment
- Longitudinal and directional static stability.

Although attempts were made to develop a method to size the nose shell based on these factors no successful method was derived. Instead, the length ratio approach seems to provide adequate results. It was found that for commuter aircraft the length ratio was normally between 1.5 and 2.5.

2.3 Tail Cone/Empennage Configuration

In line with the objective of minimizing the fuselage/empennage drag and weight while maintaining stability constraints, the Roskam/Fillman method was chosen to be used to size the tail cone and empennage. The Roskam/Fillman method as originally published in Reference 11 represented an approach to optimizing fuselage and

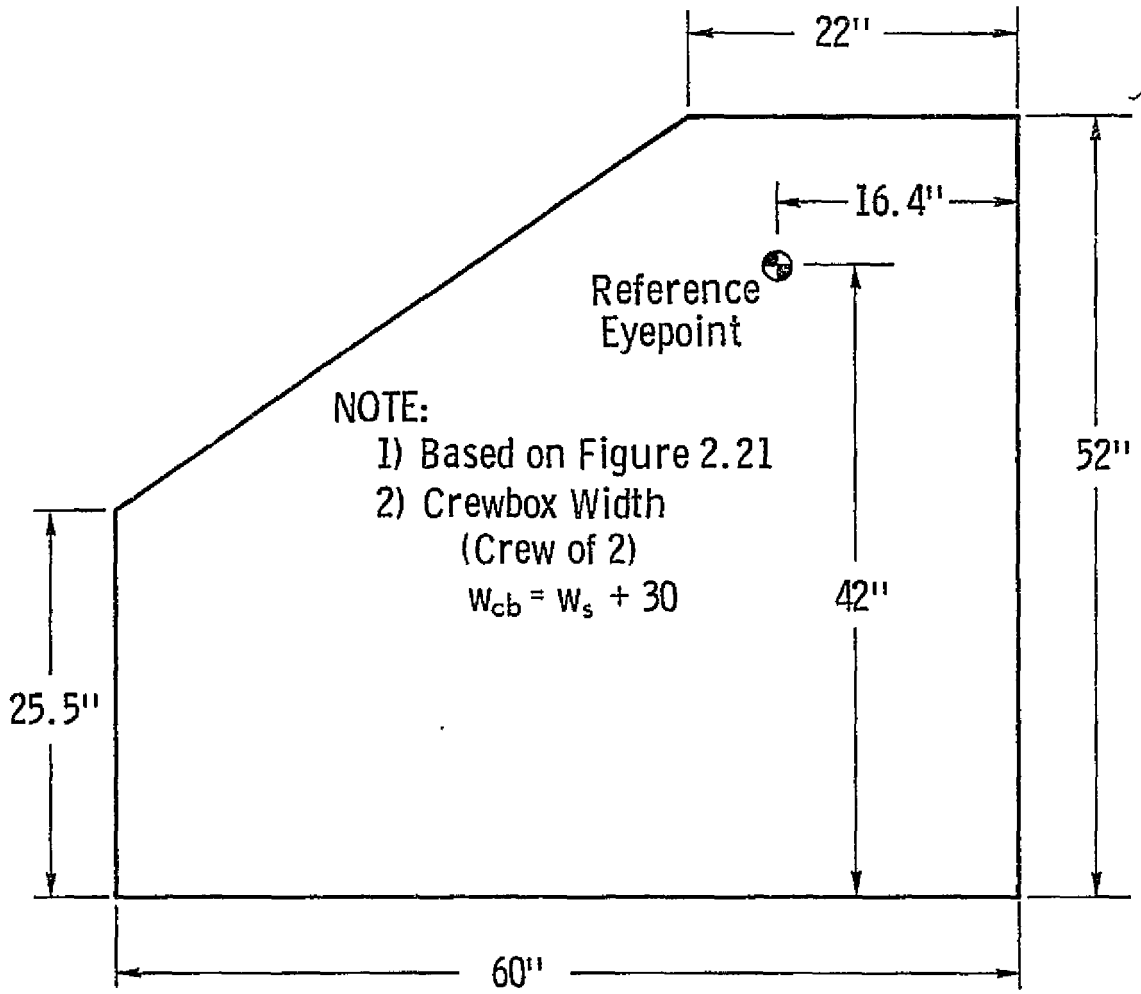

Figure 2.25 Crewbox Dimensions

empennage size with respect to zero-lift drag while maintaining certain stability and control characteristics. The zero-lift drag of the fuselage is a direct function of the fuselage fineness ratio, ℓ_B/D. If it is assumed that the size and shape of the aircraft nose and cabin are dictated by the utility constraints then the fineness ratio may be varied by altering the 'tail cone' length, ℓ_c.

If certain stability and control characteristics are specified as constants, then the optimization process becomes a trade-off between fuselage and empennage drag. Fuselage zero-lift drag may be approximated by equation 2.14 (from Reference 12).

$$C_{D_{0_B}} = C_{f_B}\left[1 + \frac{60}{(\ell_B/D)^3} + .0025\,\frac{\ell_B}{D}\right]\frac{(S_{Wet})\ body}{S_{Wing}} \qquad (2.14)$$

The zero-lift drag of either the vertical or horizontal tail may be estimated by equation 2.15 (from Reference 12).

$$C_{D_{0\ Vor\ H}} = C_f[1 + L(t/c) + 100(t/c)^4]R_{L.S.}\,\frac{S_{Wet\ V\ or\ H}}{S_{Wing}} \qquad (2.15)$$

As the fineness ratio, ℓ_B/D, is increased by lengthening the tail cone the following occur:

- Increasing ℓ_B/D will increase the fuselage Reynolds number decreasing C_{f_B}
- Increasing ℓ_B/D will decrease the value in the brackets of equation (2.14)
- Increasing ℓ_B/D will increase $S_{Wet\ Body}$
- Increasing ℓ_B/D will reduce the empennage wetted area requirements, for constant stability levels.

One simplifying assumption made in the method as originally published in Reference 11 was that the aircraft aerodynamic center location could be considered as a constant as the tail cone was lengthened. The overall intent was to trade off a reduction in empennage drag for an increase in fuselage drag in hopes of finding

the minimum drag configuration.

To use the Roskam/Fillman method to size the fuselage and empennage for minimum weight and drag a number of changes became necessary. Weight estimation of the fuselage and empennage was added as well as a c.g. location method. With these additions static stability constraints could be specified as a constant C_{m_α} for the longitudinal case and a constant C_{n_β} for the directional case. As with the original method, it was assumed that the airplane geometry forward of the tail cone would remain unchanged.

To test the method a computer program was written in FORTRAN IV to facilitate the methods application to both existing and conceptual aircraft. This section will describe the program methods and discuss the results it produced.

2.3.1 Roskam/Fillman Program Description

A flowchart of the program is presented in Figure 2.26. A program listing and an explanation of how the input data are prepared are presented in Appendix B of this report. Explanations of the methods used in each of the main subroutines are provided in the following paragraphs. Note that on Figure 2.26 Section numbers refer to the section in which a discussion of each method is presented.

2.3.1.1 Computation of Wetted Areas

The wetted areas for the fuselage and empennage are computed in the following manner in the subroutine SWET.

The fuselage wetted area is computed in three components: the cabin wetted area, the nose wetted area, and the tail cone wetted area. The cabin is assumed to be a right circular cylinder. The cabin wetted area is expressed as in equation 2.16.

$$S_{\text{Wet}_{\text{Cabin}}} = \pi D \ell_u \qquad (2.16)$$

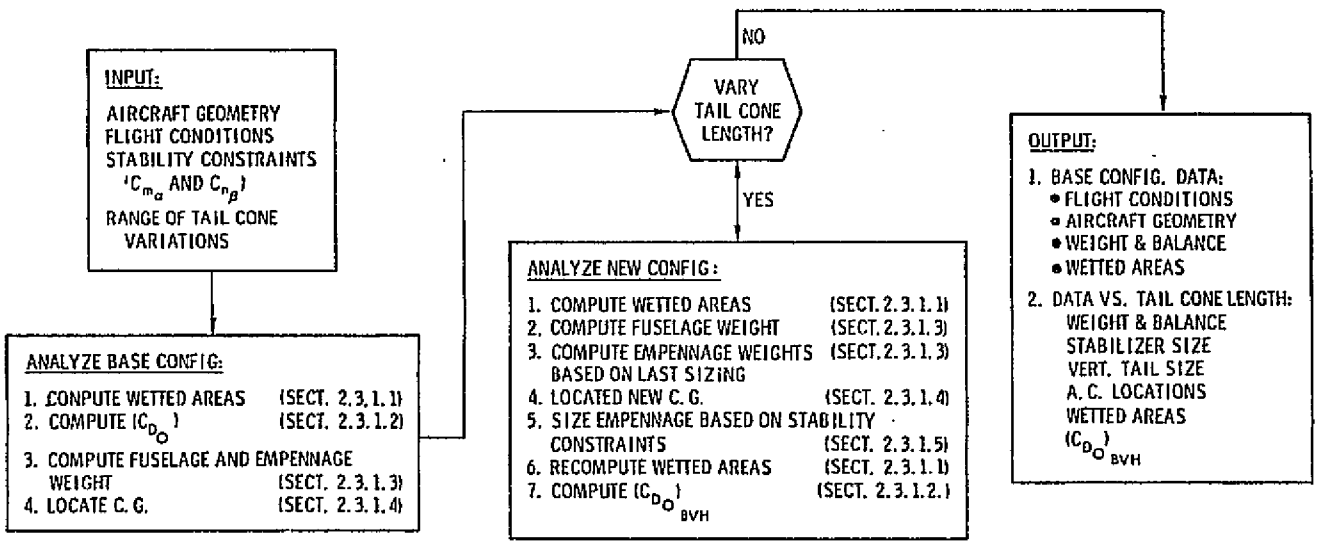

Figure 2.26 Flowchart of Roskam/Fillman Method Program

The wetted areas of the nose cone and tail cone are computed using Torenbeek's elliptical cone methods of Reference 9. This approach is documented in Appendix A of this report. By using Figures A-1 and A-3 of Appendix A to determine the shape parameters, ϕ, for the nose and tail cones, it is possible to determine a wetted area correction factor, k_w, from Figure A-2 of Appendix A. The wetted areas for the nose and tail may then be expressed as in equations 2.17 and 2.18:

NOSE

$$(S_{WET})_{NOSE} = (k_w)_{NOSE} \ell_N \tag{2.17}$$

TAIL

$$(S_{WET})_{TAIL} = (k_w)_{TAIL} \ell_c \tag{2.18}$$

The wetted area of the fuselage is then expressed as:

$$(S_{WET})_B = (S_{WET})_{CABIN} + (S_{WET})_{NOSE} + (S_{WET})_{TAIL} \tag{2.19}$$

The horizontal and vertical tail wetted areas were computed with the aid of a surface area correction factor, K_p, from Corning (Reference 13). This surface area correction factor is a function of the airfoil thickness ratio, t/c, as shown in Figure 2.27.

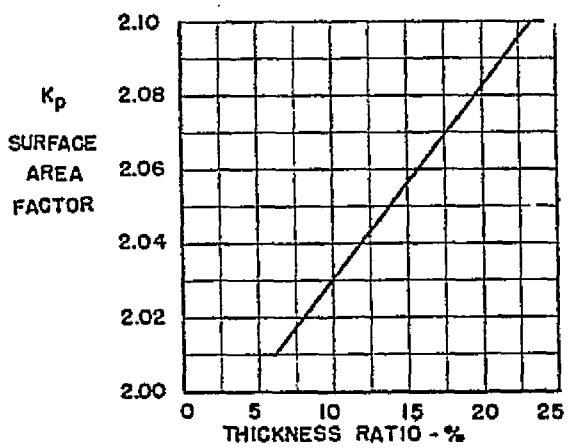

Figure 2.27 Determination of the Surface Area Correction Factor, K_p (Reproduced from Reference 13)

Using Figure 2.27 the wetted areas of the horizontal and vertical tails may be determined as:

$$S_{WET}{}_{H \text{ or } V} = K_p (S)_{H \text{ or } V} \tag{2.20}$$

Where,

$$K_p = 0.52\left(\frac{t}{c}\right) + 1.987$$

2.3.1.2 Calculation of Zero-Lift Fuselage/Empennage Drag

The zero-lift drag of the fuselage and empennage are computed in the subroutine CDO using equations 2.14 and 2.15 as stated earlier.

$$\left(C_{D_o}\right)_B = C_{f_B}\left[1 + \frac{60}{(\ell_B/D)^3} + .0025\,\frac{\ell_B}{D}\right]\frac{(S_{WET})_{BODY}}{S_{WING}} \tag{2.14}$$

$$\left(C_{D_o}\right)_{V \text{ or } H} = C_f\left[1 + L\,\frac{t}{c} + 100\left(\frac{t}{c}\right)^4\right]\; R_{L.S.}\left(\frac{(S_{WET})_{V \text{ or } H}}{S_{WING}}\right) \tag{2.15}$$

The mean skin-friction coefficients, C_f, are a function of Reynolds number, R_N, and Mach as shown in Figure 2.28. The factors L and $R_{L.S.}$ are as defined in Reference 11.

2.3.1.3 Calculation of Fuselage and Empennage Weight

The structural weights of the fuselage and empennage are mainly dependent on their areas and the maximum speed of the aircraft. The following equations were taken from Reference 9. The equation for fuselage shell weight estimation is:

$$W_F = k_{WF}\sqrt{V_D\,\frac{\ell_h}{b_f + h_f}}\cdot\left(S_G\right)^{1.2} \cdot K_1 \cdot K_2 \cdot K_3 \cdot K_4 \tag{2.21}$$

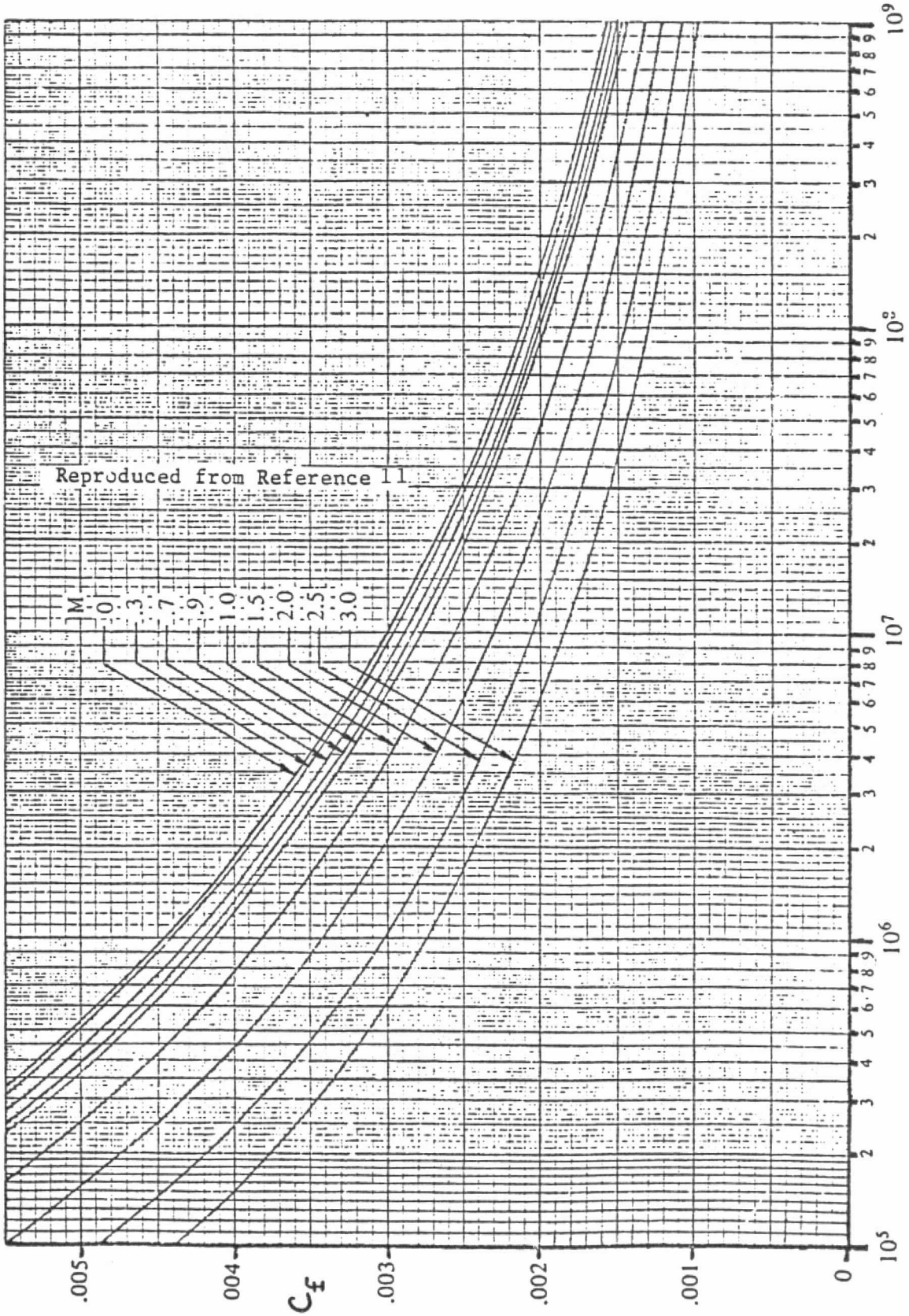

Figure 2.28 Turbulent Mean Skin-Friction Coefficient on an Isolated Flat Plate

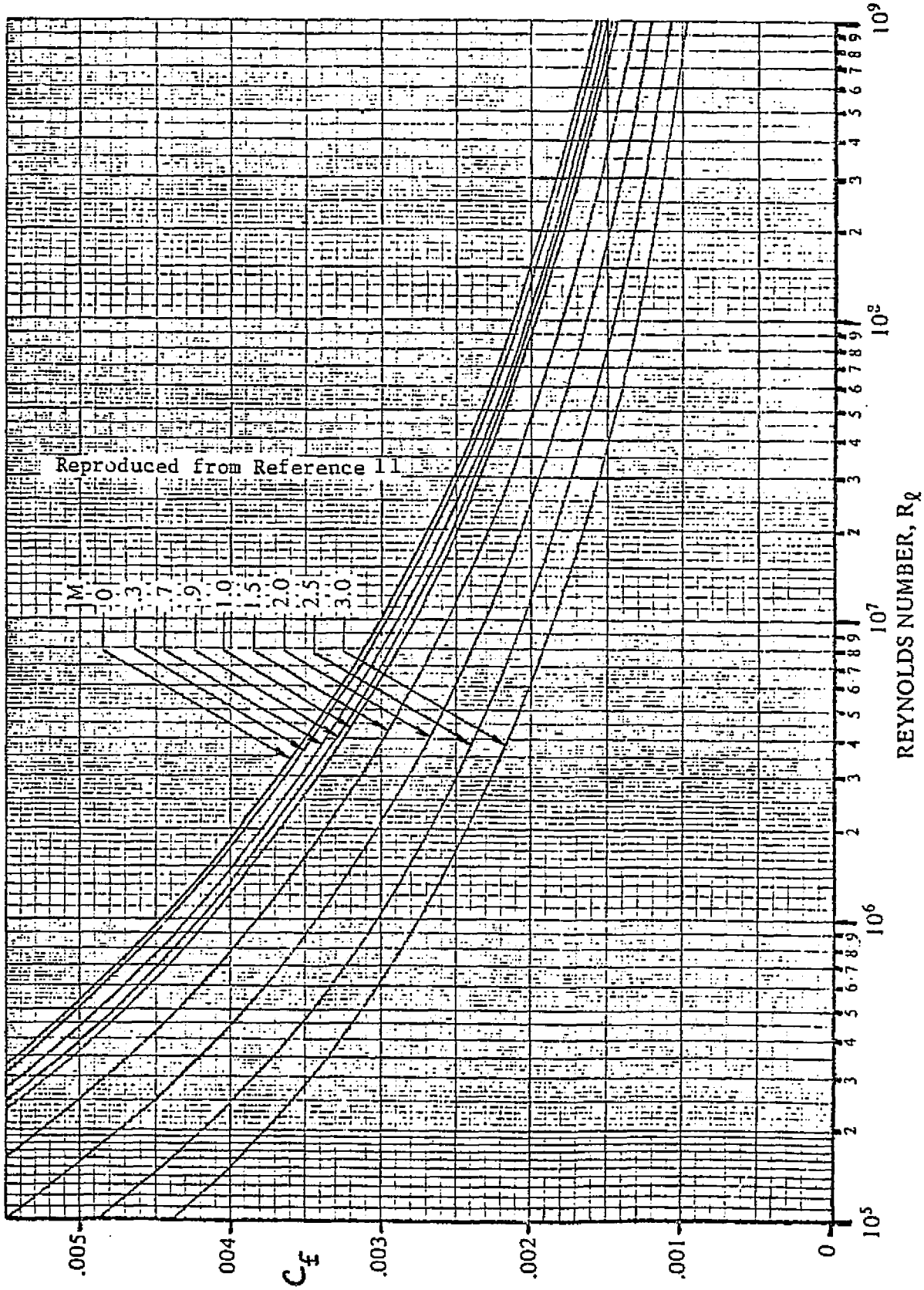

Figure 2.28 Turbulent Mean Skin-Friction Coefficient on an Isolated Flat Plate

Where k_{WF} = .021 for W_F in LBS

W_F = Fuselage Weight (lbs)

V_D = Design dive speed (kts)

S_G = Gross shell area (ft^2)

b_f = Maximum fuselage width (ft.)

h_f = Maximum fuselage height (ft.)

ℓ_h = Distance from wing quarter chord to horizontal tail quarter chord (ft.)

K_1 = 1.00 for unpressurized fuselage

= 1.08 for pressurized fuselage

K_2 = 1.00 for wing mounted engines

= 1.04 for fuselage mounted engines

K_3 = 1.00 for main gear attached to wing

= 1.07 for main gear attached to fuselage

K_4 = 1.00 for main gear bay in the fuselage

= 0.96 for no main gear bay in the fuselage

As can be seen from equation 2.21, the weight is dependent on the square root of the dive speed and the wetted area to the 1.2 power!

The empennage weight is dependent on the load factor and the square of the wetted area for dive speeds less than or equal to 250 kts.

$$W_{EMP} = K_{WT} \left[\eta_{ULT} \, S^2_{EMP} \right]^{0.75} \qquad (2.22)$$

where K_{WT} = 0.04 for V_D in KTS

W_{EMP} in LBS

S_{EMP} in FT^2

η_{ULT} = Ultimate airplane load factor

S_{EMP} = Empennage Planform area

For dive speeds greater than 250 kts. the empennage weight is a direct function of the planform area and the terms F_H and F_V which are defined below.

$$W_{HT} = K_H \cdot S_H \cdot f(F_H) \tag{2.23}$$

$$W_{VT} = K_V \cdot S_V \cdot f(F_V) \tag{2.24}$$

where V_D = Dive speed in kts.

S_H = Horizontal Tail Planform area

S_V = Vertical Tail Planform area

K_H = 1.0 for fixed stabilizer

= 1.1 for variable incidence stabilizer

K_V = 1.0 for fuselage mounted horizontal tails

$$= 1.0 + .15 \frac{S_H b_H}{S_V b_V} \text{ for T-Tails}$$

where b_H = Height of Horizontal Tail above Fin Root

b_V = Vertical Tail span

$$F_H = \frac{V_D \left(S_H \right)^{.2}}{1000 \sqrt{\cos \Lambda_H}} \tag{2.25}$$

$$F_V = \frac{V_D \left(S_V \right)^{.2}}{1000 \sqrt{\cos \Lambda_V}} \tag{2.26}$$

where Λ = sweep in degrees at the maximum airfoil thickness

The values of the parameters dependent on F_H and F_V can be determined from Figure 2.29. These equations were programmed and are used to calculate the shell weights used in the Roskam/Fillman program in the subroutines FUSWGT and EMPWGT.

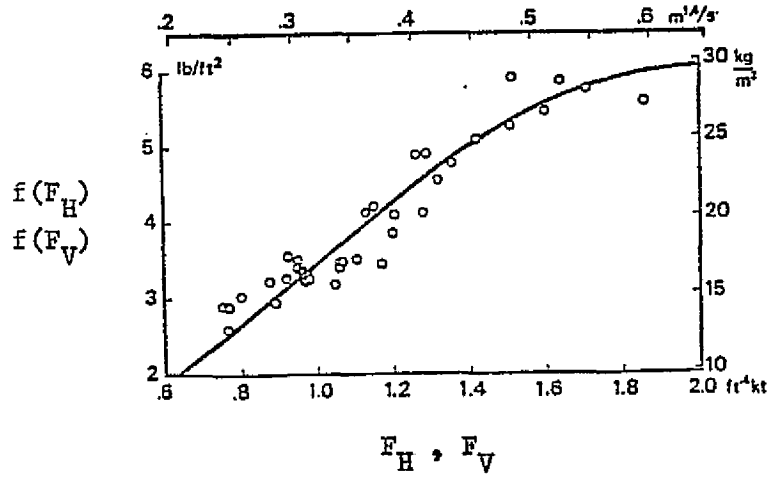

Figure 2.29 Empennage Weight Function
(Reproduced from Reference 9)

One of the input parameters for the Roskam/Fillman program is the baseline airplane's gross weight. Using this gross weight and the baseline shell weights of the fuselage and empennage, it is possible to correct for change in gross weight due to the change in tail cone and empennage configuration. This is done in the following manner. Equation 2.21 shows that the fuselage weight is proportional to fuselage gross wetted area to the power 1.2. It is assumed that to approximate the shell weight of the tail cone equation 2.27 may be applied.

$$W_{TAIL} = \frac{(S_{WET})_{TAIL}}{(S_{WET})_{BODY}} W_F \qquad (2.27)$$

This weight and the weight of the empennage are then subtracted from the baseline gross weight to provide an adjusted gross weight, $(W_{GR})'$. It is then assumed that $(W_{GR})'$ remains constant and that only the tail cone and empennage weights vary.

2.3.1.4 Location of the Center of Gravity

The longitudinal c.g. location is required to size the empennage for stability constraints. The c.g. location subroutine, SBARCG, performs this function. The routine is not intended to locate the c.g. accurately, but rather to estimate the shift in c.g. location due to incrementally lengthening the tail cone. The equation used to locate the c.g. was as expressed in equation 2.28.

$$X_{cg_i} = \frac{\left(W_{GR}\right)^3 \left(X_{cg}\right)_o + \left(W_{TAIL}\right)\left(X_{cg}\right)_{TAIL} + W_H\left(X_{cg}\right)_H + W_V\left(X_{cg}\right)_V}{\left(W_{GROSS}\right)_i} + \varepsilon_{cg} \qquad (2.28)$$

Where,

W_{GR} = adjusted gross weight (lbs) (See Section 2.3.1.3)

$\left(X_{cg}\right)_o$ = baseline c.g. location relative to the nose (ft.)

W_{TAIL} = tail cone shell weight (lbs)

$\left(X_{cg}\right)_{TAIL}$ = tail cone c.g. location relative to the nose (ft.)

W_H = horizontal tail weight (lbs)

$\left(X_{cg}\right)_H$ = horizontal tail c.g. location relative to the nose (ft.)

W_V = vertical tail weight (lbs)

$\left(X_{cg}\right)_V$ = vertical tail c.g. location relative to the nose (ft.)

$\left(W_{GROSS}\right)_i$ = total gross weight for i'th tail cone/empennage configuration (lbs)

ε_{cg} = c.g. correction found as the difference between estimated c.g. location for baseline and actual c.g. location for the baseline.

The tail cone c.g. location $X_{cg_{TAIL}}$ was located at the centroid of a body of revolution having a planform shape modelled by the equation:

$$\left(\frac{x}{a}\right)^n + \left(\frac{y}{b}\right)^m = 1 \qquad (2.29)$$

With a cone shape of this type, it may be shown that the centroid of the tail is located by equation 2.30.

$$\bar{X}_{TAIL} = \frac{\left[\frac{1}{2} - \left(\frac{1}{m(n+2)}\right) + \left(\frac{1-m}{4m^2(2n+2)}\right) - \left(\frac{1-3m+2m^2}{6m^3(3n+2)}\right)\right]_{\ell_c}}{\left[1 - \left(\frac{1}{m(n+1)}\right) + \left(\frac{1-m}{4m^2(2n+1)}\right) - \left(\frac{1-3m+2m^2}{6m^3(3n+1)}\right)\right]} \tag{2.30}$$

Therefore, the c.g. of the tail, relative to the nose is located as:

$$X_{cg_{TAIL}} = \ell_N + \ell_u + \bar{X}_{TAIL} \tag{2.31}$$

The baseline c.g. locations for the horizontal and vertical tails were input parameters, although for preparation of the data, where more accurate data were lacking, it was assumed that the c.g. was at 60% of the mean geometric chord,. To correct for tail cone length changes equation 2.32 was used.

$$\left(X_{cg}\right)_{H \text{ or } V} = X_{cg_{o\ H \text{ or } V}} + \Delta\ell_c \tag{2.32}$$

where,

X_{cg_o} = baseline c.g. location relative to the nose (ft.)

$\Delta\ell_c$ = change in tail cone length relative to the baseline (ft.)

As stated before, this routine was intended to provide only quick and dirty estimations for c.g. location based on the limited input parameters that the program used. It was anticipated that if the method had been integrated into the GASP, that the GASP c.g. location method would provide better results.

2.3.1.5 Empennage Sizing

The horizontal and vertical tails were to be sized to meet specified static stability constraints. The horizontal tail was to be sized to provide a specific C_{m_α} value, and the vertical tail a

specific C_{n_β} value. In addition to this, it was decided to optimize the effectiveness of the horizontal and vertical tails for each tail cone length. These functions were performed for the horizontal and vertical tails in the subroutines STABAREA and VERTAREA respectively.

The effectiveness of each surface was to be optimized by maximizing the product of the lift curve and moment arm for each surface. The variable was to be the sweep of the surface. For instance, by varying the sweep of the horizontal tail, both the horizontal tail moment arm, ℓ_h, and the horizontal tail lift curve slope, $C_{L_{\alpha_H}}$, are affected. The tail may be said to be most effective where the product $C_{L_{\alpha_H}} \times \ell_h$ is a maximum. The value of ℓ_h is easily defined geometrically, and the value of $C_{L_{\alpha_H}}$, from Reference 14, may be expressed as

$$C_{L_\alpha} = \frac{2\pi A}{2+\sqrt{\left(\frac{A\beta}{\kappa}\right)^2 \left(1 + \frac{\tan^2 \Lambda c/2}{\beta^2}\right) + 4}} \qquad (2.33)$$

where,

A = aspect ratio

β = Prandtl-Glauert transformation, $\sqrt{1 - M^2}$

κ = ratio of the actual section lift curve slope to 2π

$\Lambda_{c/2}$ = half-chord sweep

The program assumes that the aspect ratios of the horizontal and vertical tails remain constant, allowing this procedure to be more or less independent of the sizing.

The horizontal tail is to be sized for a constant C_{m_α} value. From Reference 14:

$$C_{m_\alpha} = \left(\bar{X}_{cg} - \bar{X}_{ac}\right) C_{L_\alpha} \qquad (2.34)$$

where all of the above values are total aircraft values.

From Reference 14:

$$\bar{X}_{ac} = \frac{\left(\bar{X}_{ac}\right)_{WB} + \frac{C_{L_{\alpha_H}}}{C_{L_{\alpha_{WB}}}} \eta_H \frac{S_H}{S} \bar{X}_{ac_H} \left(1 - \frac{d\varepsilon}{d\alpha}\right)}{1 + \frac{C_{L_{\alpha_H}}}{C_{L_{\alpha_{WB}}}} \eta_H \frac{S_H}{S} \left(1 - \frac{d\varepsilon}{d\alpha}\right)} \tag{2.35}$$

Solving for S_H renders:

$$S_H = \frac{\left(\bar{X}_{ac_{WB}} - \bar{X}_{ac}\right) S}{\left(\bar{X}_{ac} - \bar{X}_{ac_H}\right) \frac{C_{L_{\alpha_H}}}{C_{L_{\alpha_{WB}}}} \eta_H \left(1 - \frac{d\varepsilon}{d\alpha}\right)} \tag{2.36}$$

All of the variables on the right-hand side of equation 2.36 are determined using the methods of Reference 14. In particular, however, the $\bar{X}_{ac_{WB}}$ is determined as:

$$\bar{X}_{ac_{WB}} = \bar{X}_{ac_W} + \Delta\bar{X}_{ac_B} \tag{2.37}$$

Whereas the $\bar{X}_{ac}$ of the wing, $\bar{X}_{ac_W}$, is an input parameter, the aerodynamic center shift due to the body, $\Delta\bar{X}_{ac_B}$, is computed by performing a Multhopp strip-integration as described in Reference 14. This is accomplished in the subroutine MULTOP.

The total aircraft lift slope in equation 2.34 may be expressed as:

$$C_{L_\alpha} = C_{L_{\alpha_{WB}}} + C_{L_{\alpha_H}} \eta_H \frac{S_H}{S} \left(1 - \frac{d\varepsilon}{d\alpha}\right) \tag{2.38}$$

The program uses equations 2.36 and 2.38 to iterate to find a value for S_H which will meet the C_{m_α} constraint.

The vertical tail size is determined in a similar manner. From Reference 14, the value for the C_{n_β} of the aircraft may be expressed as:

$$C_{n_\beta} = C_{n_{\beta_B}} + C_{n_{\beta_W}} + C_{n_{\beta_V}} \qquad (2.39)$$

where,

$C_{n_{\beta_B}}$ = the body contribution to C_{n_β} (rad^{-1})

$C_{n_{\beta_W}}$ = the wing contribution to C_{n_β} (rad^{-1})

$C_{n_{\beta_V}}$ = the vertical tail contribution to C_{n_β} (rad^{-1})

It is conservative to assume that the wing contribution is negligible. Therefore, equation 2.39 becomes:

$$C_{n_\beta} = C_{n_{\beta_B}} + C_{n_{\beta_V}}$$

or,

$$C_{n_{\beta_V}} = C_{n_\beta} - C_{n_{\beta_B}} \qquad (2.40)$$

From Reference 14 the body contribution may be determined as:

$$C_{n_{\beta_B}} = -57.3 \; K_N \; K_{R_\ell} \; \frac{S_{B_s}}{S} \; \frac{\ell_B}{b} \quad (rad^{-1}) \qquad (2.41)$$

where,

K_N = an empirical factor for body and body + wing effects determined from Figure 7.19 of Reference 14.

K_{R_ℓ} = a Reynold's number factor for the fuselage determined from Figure 7.20 of Reference 14.

S_{B_s} = body side area (ft^2)

ℓ_B = body length (ft)

The side body area is computed using the methods of Appendix A of this report.

The vertical tail contribution, $C_{n_{\beta_V}}$, may be expressed as shown in equation 2.42 (Reference 14).

$$C_{n_{\beta_V}} = -C_{y_{\beta_V}} \left(\frac{\ell_V \cos\alpha + Z_V \sin\alpha}{b} \right) \quad (\text{rad}^{-1}) \tag{2.42}$$

For an airplane in the cruise configuration it is reasonable to assume that the angle of attack is small. Therefore:

$$C_{n_{\beta_V}} = -C_{y_{\beta_V}} \frac{\ell_V}{b} \tag{2.43}$$

From Reference 14:

$$C_{y_{\beta_V}} = -kC_{L_{\alpha_V}} \left(1 + \frac{d\sigma}{d\beta}\right)\eta \frac{S_V}{S} \quad (\text{rad}^{-1}) \tag{2.44}$$

where,

k = an empirical factor from Figure 7.3 of Reference 14.

$C_{L_{\alpha_V}}$ = the vertical tail lift curve slope determined from equation 2.33 using $A = A_{eff.}$ The value of the effective aspect ratio, A_{eff}, is determined by the methods of Reference 14.

The value of the factor $1 + \frac{d\sigma}{d\beta}\eta$ is assumed to be approximately 1.0.

Substitution and solving equation 2.40 for S_V renders:

$$S_V = \frac{Sb\, C_{n_\beta} + 57.3\, K_N\, K_{R_\ell}\, S_{B_s}\, \ell_B}{kC_{L_{\alpha_V}}\, \ell_V} \quad (\text{ft}^2) \tag{2.45}$$

By iterating between the equation for $C_{L_{\alpha_V}}$ and equation 2.45, the value for S_V which meets the C_{n_β} constraint may be determined.

2.3.2 Results of the Roskam/Fillman Program

The Roskam/Fillman method was tested using data for both actual and conceptual baseline aircraft. Although preliminary results for the Gates-Learjet Model 24 seemed to verify the method, later results for both other existing aircraft, and for the conceptual aircraft in particular, were rather disappointing. For the sake of brevity only a generalized discussion of the results and the conclusions based thereon will be presented here. A more detailed discussion of the airplane configurations tested and the results is presented in Reference 15.

When the tests were made, as was expected the vertical tail size required to maintain C_{n_β} decreased with increasing tail cone length. On the other hand, with many of the aircraft tested, as the tail cone length was increased so did the horizontal tail size required to maintain C_{m_α}. This was not as expected. As a result the increasing drag and weight of the horizontal tail and tail cone together over-rode the decreasing drag and weight of the vertical tail.

After carefully evaluating the Roskam/Fillman algorithm the following conclusions as to the cause of the difficulties were arrived at. The method assumes that the wing may be kept at a constant location relative to the nose of the aircraft. Because of this and the fact that the aft portion of the fuselage has very little effect on the shift in aerodynamic center due to the body, the location of the wing + body aerodynamic center remains relatively constant. As the tail cone is lengthened the aircraft c.g. moves aft. It is probable that inherent inaccuracies in the "quick-and-dirty" method used to locate the c.g. pushed it even farther aft than should have been the case. It is also reasonable to assume that the lift slope of the total aircraft is not going to change drastically with changes in tail cone and horizontal tail size. Therefore by referring to equation 2.34 note that

as the c.g. is pulled aft by the tail cone, the aircraft aerodynamic center is also pushed aft to maintain the static margin. Realizing this and the fact that the wing + body aerodynamic center is more or less fixed, note that the numerator of equation 2.36 is going to become considerably larger. At the same time, the $(\bar{X}_{ac} - \bar{X}_{ac_H})$ factor in the denominator may also be decreasing, compounding the effect.

The program was written so that some of the computations made for each tail cone increment relied on some of the data from the previous tail cone increment. This was done to reduce the number of iterative cycles required. In particular, to locate the c.g. at a new tail cone length, the empennage sizes from the previous tail cone length were used. This was originally felt to be reasonable as long as the increments in tail cone length were small. Unfortunately, this also resulted in pushing the c.g. even farther aft in light of the oversized horizontal tail. Thus the problem was doubly compounded.

From this evaluation of the algorithm employed the following conclusions and recommendation as to the usefulness of the method may be made:

Before the method may be applied reliably to determine if an optimum tail cone length (from a weight and drag viewpoint) may be found:

A) An accurate c.g. location routine is needed. Also if this is to be done, it would be wise to include a more accurate estimation of the component weights and how they might be altered by changing tail cone length.

B) The re-balancing of the wing on the fuselage for each new tail cone cone configuration might be investigated to prevent the distance between the wing + body aerodynamic center and the total aircraft aerodynamic center from becoming overly large. One disadvantage to the

re-balancing of the wing would be to reduce the effect of an increased horizontal tail moment arm, with the possible result that the overall objective of the method is cancelled.

C) The algorithm needs to be revised such that the calculations for each new configuration are independent of all previous configuration data. This would reduce the probability of compounding errors.

The most obvious means of accomplishing these revisions was to include the empennage sizing subroutines into the GASP and then to change the tail cone lengths by external manipulations. This would also allow checking the method both with and without re-balancing the wing. Work was being accomplished to this end before the writing of this report but, due to the difficulties encountered in trying to put the GASP into an operational status, could not be completed.

The technical monitor of this project at NASA-Ames, Tom Galloway, performed some preliminary calculations using the GASP to test the method's application. The empennage sizing method in this case was the $\bar{V}$ method currently used by the GASP. The results from Tom Galloway's study (Reference 16) indicate that the increasing weight of the tail cone structure with increasing length will more than overcome the decreasing weight of the empennage. Drag, on the other hand, did decrease as expected. The intent of this procedure, it must be remembered, was to minimize DOC. However, DOC is much more dependent upon weight than drag. Consequently, Tom Galloway's results indicate that a shorter tail cone is better from a DOC point of view. Nevertheless, we believe that by revising the GASP in the manner suggested above to implement the Roskam/Fillman method, studies in this area might prove beneficial.

2.4 Baggage Compartment Study

It is necessary to allow enough room for passenger baggage. Since the shorthaul/commuter airplane is frequently used to

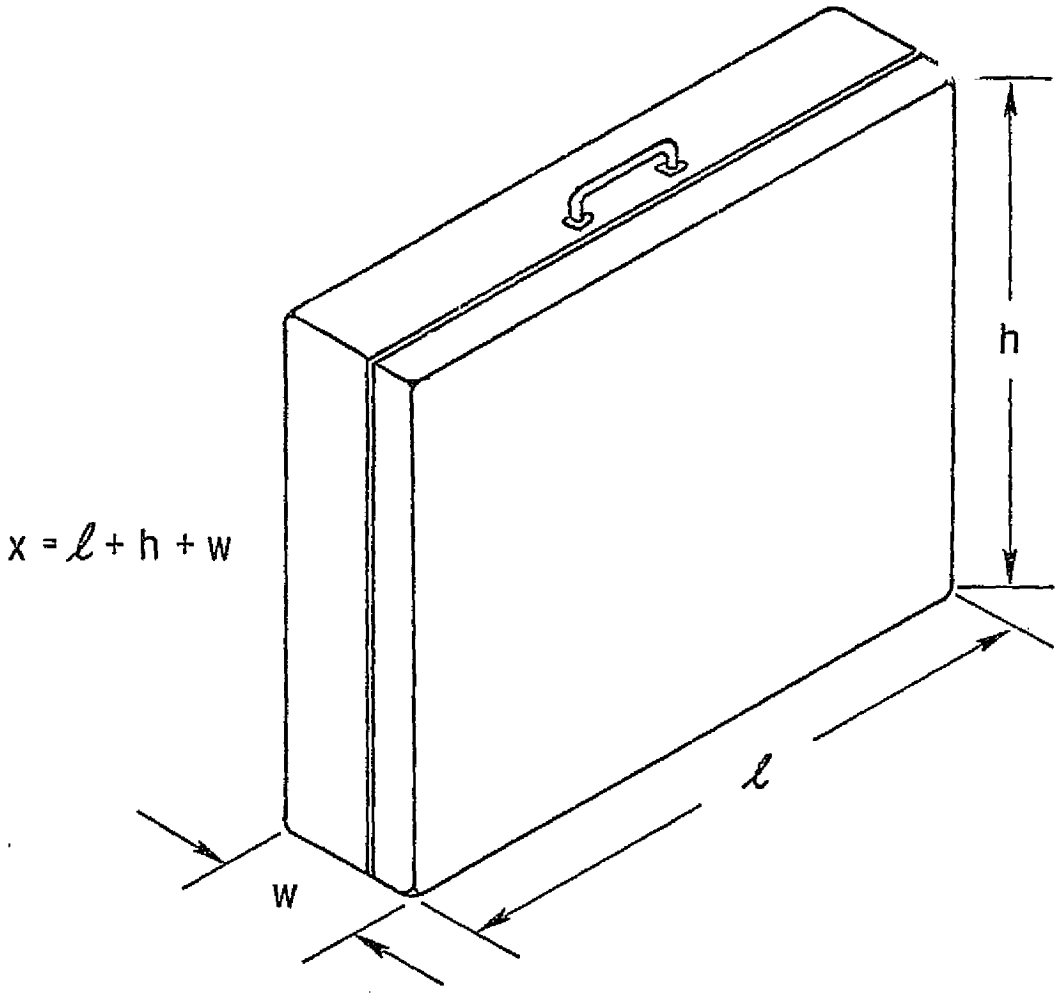

Figure 2.30 Baggage Dimensions

Table 2.10 Baggage Allowance

Large Suitcase	x = 62 inches
Small Suitcase	x = 55 inches
Total Weight - - - - -	70 pounds

where $x = \ell + h + w$

transport passengers to the major airlines, it is desirable to allow for the same amount of baggage as the major airlines specify.

The problem of storage location was investigated in Reference 15, and three storage methods were studied, two of which were cabin oriented and the other, tail cone oriented. For the cabin-oriented storage methods the limitation was availability of required volume. For the tail-cone storage method the critical consideration was c.g. location.

To establish the baggage allowances for shorthaul/commuter airplanes, several major carriers were questioned about their baggage allowances. It was discovered that most major carriers specify baggage allowance by the sum of the baggage dimensions and total weight rather than by volume. The major carriers allow two pieces of checked luggage plus one carry-on piece. These baggage allowances are summarized in Table 2.10. Figure 2.30 defines the baggage dimensions. One major airline allows 5.0 cu. ft. per passenger for its Trijet service.

To attempt to determine a volume corresponding to the allowances of Table 2.10 a survey of baggage dimensions was performed using the catalog of a major retail chain. From the survey the dimensions listed in Table 2.11 were selected as representative. The original baggage compartment study documented in Reference 15 used the baggage volume indicated by Table 2.11. In that study the required baggage compartment volumes for 12, 21, and 30 passenger configurations were computed. It was assumed that no additional allowances were needed for carry-on baggage, as this baggage may be stored under the passengers' seats.

Table 2.11 Representative Baggage

	ℓ	h	w	vol.
Large Suitcase	30 in	22 in	10 in	3.82 ft^3
Small Suitcase	28 in	18 in	9 in	2.62 ft^3
Total Volume				6.44 ft^3

$(\Delta \ell_u)_{BAGGAGE} = 4.566$ ft

The result, although slightly small, looks reasonable. This method will be used to size for the baggage compartment.

2.5 Fuselage Shape Simulation Program, FUSE

A computer program was written to simulate and design commuter aircraft fuselages. The purpose of this program was two-fold. First, the program was intended to provide a method for modelling actual aircraft fuselages to provide node coordinates for use with finite element analysis procedures. This modelling method was to be simple to apply and versatile enough to be used with most commuter aircraft slopes. The second purpose of the program was to provide a means for applying and evaluation the design methods previously discussed in this chapter. In addition to these objectives for the program, an option was included to allow for interactive graphic display of the resulting design or simulation to ensure reasonable configurations. The final version of the program at the time of this report is intended to be used with a Tektronix 4014 or 4015 graphic display terminal using the PLOT 10 graphics software package (Reference 18). The computer program, which will be referred to as FUSE, was written in FORTRAN IV for a Honeywell 66/60 timesharing system. Appendix C of this report contains a complete listing and user's guide for the program.

The program was originally documented in Reference 19. At that time the program was only used in batch operations for actual aircraft simulations and plotting of the simulated fuselages was performed on a Benson Lehner plotter. Although the design mode and the interactive graphics have been added the modelling routines are essentially the same. Section 2.5.1 will discuss the approach taken to model the fuselage. Section 2.5.2 will provide the program description. Section 2.5.3 will discuss the program results.

The three methods of baggage storage considered in Reference 15 are shown in Figures 2.30 through 2.33. Reference 17 provides a more detailed analysis of each method. The results of the analysis indicated that only the fuselage lobe baggage compartment could be considered feasible from a volume requirement standpoint. The carry-on baggage compartment would have required that the cabin be lengthened by approximately 50% and the tail cone compartment resulted in center of gravity difficulties. One very important factor was neglected in considering the fuselage lobe compartment, however. No allowance was made in the study for either the wing-carry through structure or the possibility of main landing gear storage. This would be especially critical for the smaller commuter airplanes where the wing root chord is significant in comparison with cabin length.

For these reasons another form of carry-on compartment was considered. Figure 2.31 shows the baggage compartment to be only on one side of the cabin. McDonnell Douglas found in Reference 6 that baggage compartments on either side of the aisle were more efficient from a design-to-cost point of view than the fuselage lobe method. It was decided to try and develop a method to define the length required for this type of baggage compartment. Also, at the suggestion of Tom Galloway, the project technical monitor at NASA-Ames, it was decided to limit the baggage to 5 cu. ft. per passenger.

It was assumed that the baggage compartment could be represented by a trapezoidal cross-section for either the circular or rounded-rectangular cabin sections. It was also assumed that an aisle of 1.5 the normal aisle width would be maintained. The resulting effective baggage compartment cross-sections were to appear as shown in Figure 2.34.

It will be assumed that the aisle-side of the compartment is essentially equal to the inside cabin height, h_c. The base of each side may be represented as in equation 2.46, if McDonnell Douglas control points are used:

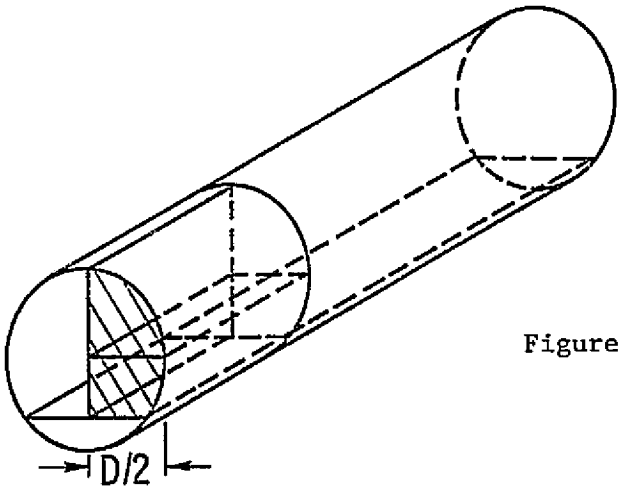

Figure 2.31 Carry-on Baggage Compartment

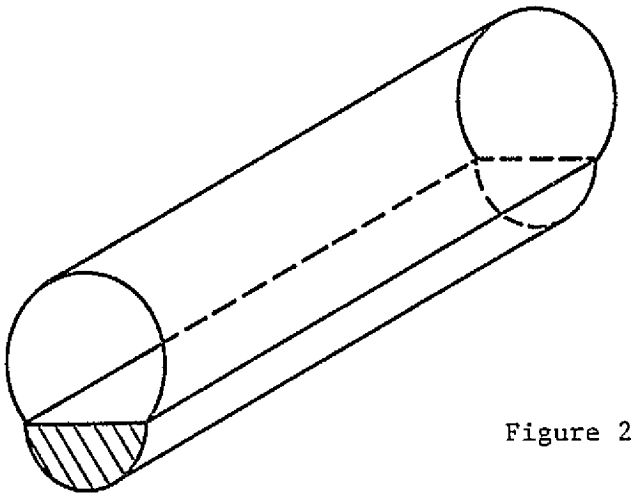

Figure 2.32 Fuselage Lobe Baggage Compartment

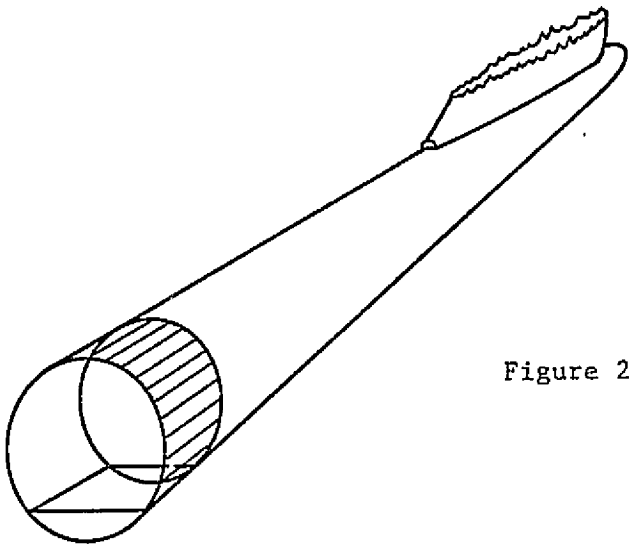

Figure 2.33 Tail Cone Baggage Compartment

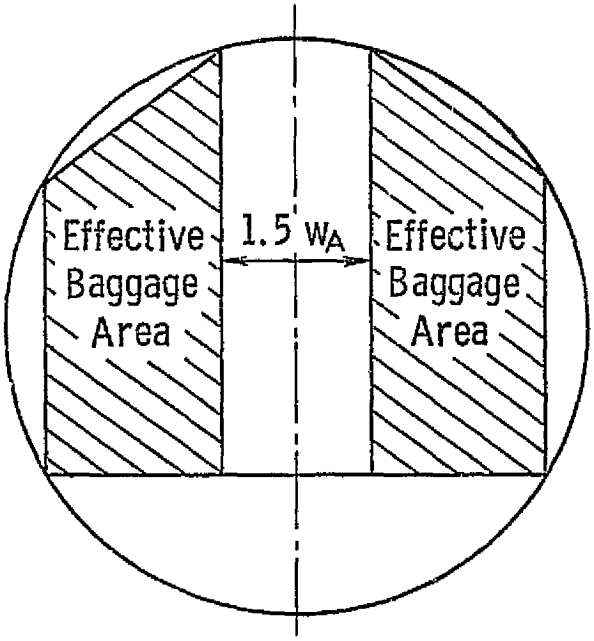

a) Circular Cabin Section

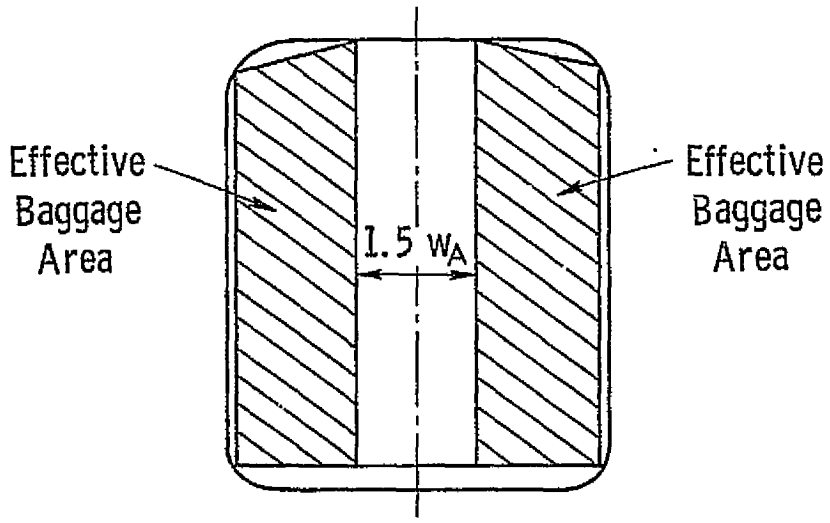

b) Rounded-Rectangular Cabin Section

Figure 2.34 Definition of Effective Baggage Compartment Area

$$w_{bc} = \frac{1}{2}\left[(N_S - 1)\, w_S - .5N_A\, w_A + 12\right] \qquad (2.46)$$

By solving the cross-section equations for a rounded-rectangular section it is possible to find the wall-side compartment height for both circular and rounded rectangular sections as:

$$h_{bc} = h_c - \frac{h}{2}\left[1 - r_{t_c}\sqrt{1 - \frac{1}{4}\left(\frac{w_f - w_c + r_{tc}\, w_c}{r_{tc}\, w_c}\right)^2}\right] \qquad (2.47)$$

where,

h = inside body height (in.)

w_f = floor width (in.) = $(N_S - 1)\, W_S + N_A W_A + 12$

Finally, the additional cabin length required to allow for 5 cu. ft. of baggage per passenger may be expressed as:

$$(\Delta \ell_u)_{\text{BAGGAGE}} = \frac{720 \text{ PAX}}{w_{bc}\left[2h_c - \frac{h}{2}(1 - r_{tc})\sqrt{1 - \frac{1}{4}\left(\frac{w_f - w_c + r_{tc} w_c}{r_{tc} w_c}\right)^2}\right]}$$

where,

PAX = number of passengers

As a check of the method the baggage compartment length for a 30-passenger cabin of the type presented by McDonnell Douglas in Reference 6 was computed. The actual length was chosen as the average of the lengths of the compartments on either side of the aisle. In this case, that implied an actual baggage compartment length of 5.375 ft.

Given:

w_c = 103 in. $\quad w_f$ = 90.5 in.

w_S = 20 in. $\quad N_S$ = 4

w_A = 18.5 in. $\quad N_A$ = 1

h = 103 in. $\quad h_c$ = 78 in.

r_{bc} = 1.0

2.5.1 Approach to Fuselage Shape Simulation

For the majority of short haul/commuter aircraft, the fuselage can be considered to be made up of three distinct sections: the nose, the cabin, and the tail cone, as shown in Figure 2.35. This was the basis for the development of FUSE. The intent was to model each of these sections individually and then assemble them. The methods used to model these three fuselage sections will be explained in Sections 2.4.1.3 through 2.5.1.5. As all of the cross-sections will be modelled in the same manner the cross-sections will be discussed in Section 2.5.1.2.

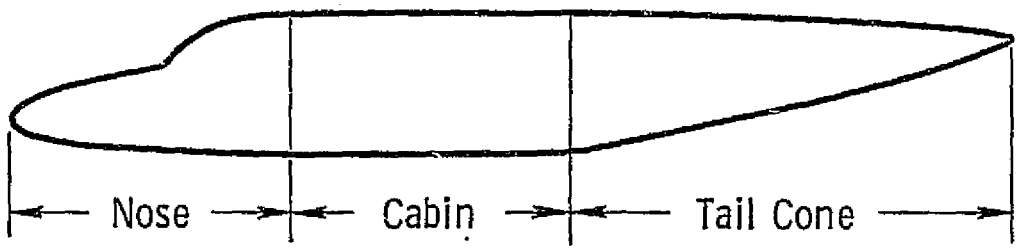

Figure 2.35 Definition of Generalized Fuselage Sections

2.5.1.1 Coordinate Systems

As FUSE was to be used to provide the nodes for finite-element analysis methods, it was necessary to define a book-keeping system by which the nodes might be located and used. As it was hoped to use FUSE in conjunction with the NCSU BODY program of Reference 20, the node numbering and coordinate system were chosen to be compatible with the BODY program. The coordinate system is such that x is positive aft, y is positive left, and z is positive up. The aircraft is assumed to be symmetric about the

XZ-plane. Therefore, nodes are only simulated for half of the fuselage on the positive-y side.

The fuselage will be subdivided both in the lengthwise direction, and radially about some specified central axis. The nodes will be numbered (i,j) in a coordinate system, where the value of i represents the number of the corresponding lengthwise subdivision and the value of j represents the number of the radial segment. For each node, (i,j) values for x, y, and z will be computed and stored.

The NCSU BODY program is written so that the number of lengthwise and radial subdivisions are assigned to each fuselage section (nose, cabin, or tail) individually as input parameters. FUSE was written such that the number of lengthwise divisions are input for each section, but that the number of radial divisions is constant for all sections. This facilitates the definition of each panel.

2.5.1.2 Cross-Section Determination, CRSSEC

The original program as documented in Reference 19 assumed that the airplane cross-sections could be modelled by elliptical or circular sections. Also the cross-sections for the nose, cabin and tail cone were determined independently. This sometimes resulted in a discontinuity at the juncture of two fuselage sections. To avoid this problem and to allow for round-rectangular cross-sections, the subroutine CRSSEC was substituted for all cross-section calculations.

The approach taken to locating the cross-section nodes is similar to that used in Reference 19. The main difference is that the method has been generalized to account for the use of rounded rectangular cross-sections.

Figure 2.36 will be used to help describe the node location procedure. It will be assumed that the cross-section center is vertically offset from the y-z origin by some value, z_o. The

nodes will be located by rotating a radial line through 180° (from -90° to +90° relative to the y-axis) from a center point at y = 0, z = z_{CL}. The nodes will be located at the intersection of the radial and the cross-section shape every $\frac{\pi}{m}$ degrees, where "m" is the number of radial segments desired.

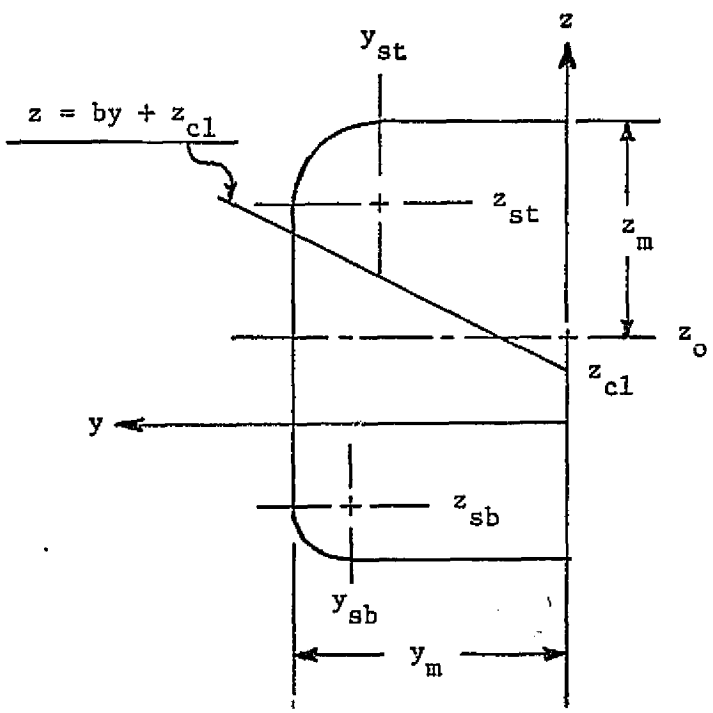

Figure 2.36 Node Location Method

The equation for the radial is as expressed in equation 2.49:

$$z = by + z_{CL} \tag{2.49}$$

where,

$$b = \tan\left[\frac{j-1}{m}\pi - \frac{\pi}{2}\right] \text{ for } j = 1, 2, 3 \ldots, (m+1)$$

m = number of radial segments

Note from Figure 2.34 that for $z_{sb} < z < z_{st}$, $y = y_m$. Similarly,

for $b < 0$ and $y < y_{sb}$, $z = z_o - z_m$, and for $b > 0$ and $y < y_{st}$, $z = z_o + z_m$. The values for y_{st}, z_{st}, y_{sb}, and z_{sb} are easily determined by equations 2.50:

$$y_{st} = y_m (1 - r_t) \tag{2.50a}$$

$$z_{st} = z_m (1 - r_t) + z_o \tag{2.50b}$$

$$y_{sb} = y_m (1 - r_b) \tag{2.50c}$$

$$z_{sb} = z_m (r_b - 1) + z_o \tag{2.50d}$$

where r_t and r_b are the upper and lower round-off radii expressed as a constant fraction of y_m and z_m.

This reduces the node location problem significantly. Only the rounded corners of the section must be dealt with. By solving the cross-section corner equations at either the top or bottom corner it can be shown that:

$$y = \frac{-B + \sqrt{B^2 - 4AC}}{2A} \tag{2.51}$$

where,

$$A = 1 + \left(\frac{by_m}{z_m}\right)^2$$

$$B = -2y' + 2b\,(z_{CL} - z')\left(\frac{y_m}{z_m}\right)^2$$

$$C = 2y_m y' + \left[\left(\frac{z_{CL} - z'}{z_m}\right)^2 - 1\right](y_m)^2$$

and where,

$$y' = \begin{cases} y_{st} & \text{for } b > 0 \\ y_{sb} & \text{for } b < 0 \end{cases}$$

$$z' = \begin{cases} z_{st} & \text{for } b > 0 \\ z_{sb} & \text{for } b < 0 \end{cases}$$

With a value for y at any radial position from equation 2.51, the value for z is easily determined from equation 2.49.

An added advantage of the subroutine CRSSEC is that the discontinuities that could occur at the juncture of two fuselage sections may be "faired-out." This has been done at the nose-to-cabin juncture in the following manner. At any nose section radial the node coordinates of both the nose and cabin are determined as if the cabin shell had been extended forward over the nose. The coordinates which are the least distant from the center line of the fuselage are used. This is not implemented for the tail cone to allow for upswept tails.

2.5.1.3 Nose Shape

The aircraft nose will be modeled as the locus of two superimposed elliptical cones as shown in Figure 2.23. Each of the elliptical cones is constructed such that the top and side view planforms may be modeled by the generalized expression of equation 2.51.

$$\left(\frac{x}{a}\right)^n + \left(\frac{y}{b}\right)^m = 1 \qquad (2.51)$$

Figure 2.37 defines the geometric parameters used to describe the shape of the nose. Using the parameters shown in Figure 2.37 the coordinates at any point on the nose will be determined by the following procedure.

Each of the elliptical cones used for the nose will be such that the top and side view planforms may be described by the general equation 2.51. Appendix A of this report explains the use of elliptical cones as described in Reference 9. Briefly, the shape of the elliptical cone is determined as follows.

Given a specific cone shape, a rectangle may be superimposed about half the planform as shown in Figure 2.38. By constructing the diagonals, $\overline{OS}$ and $\overline{OT}$, it is possible to define the shape parameters ϕ_1 and ϕ_2. In general, the shape parameter ϕ_1 may be considered to be a taper shape parameter, while ϕ_2 may be

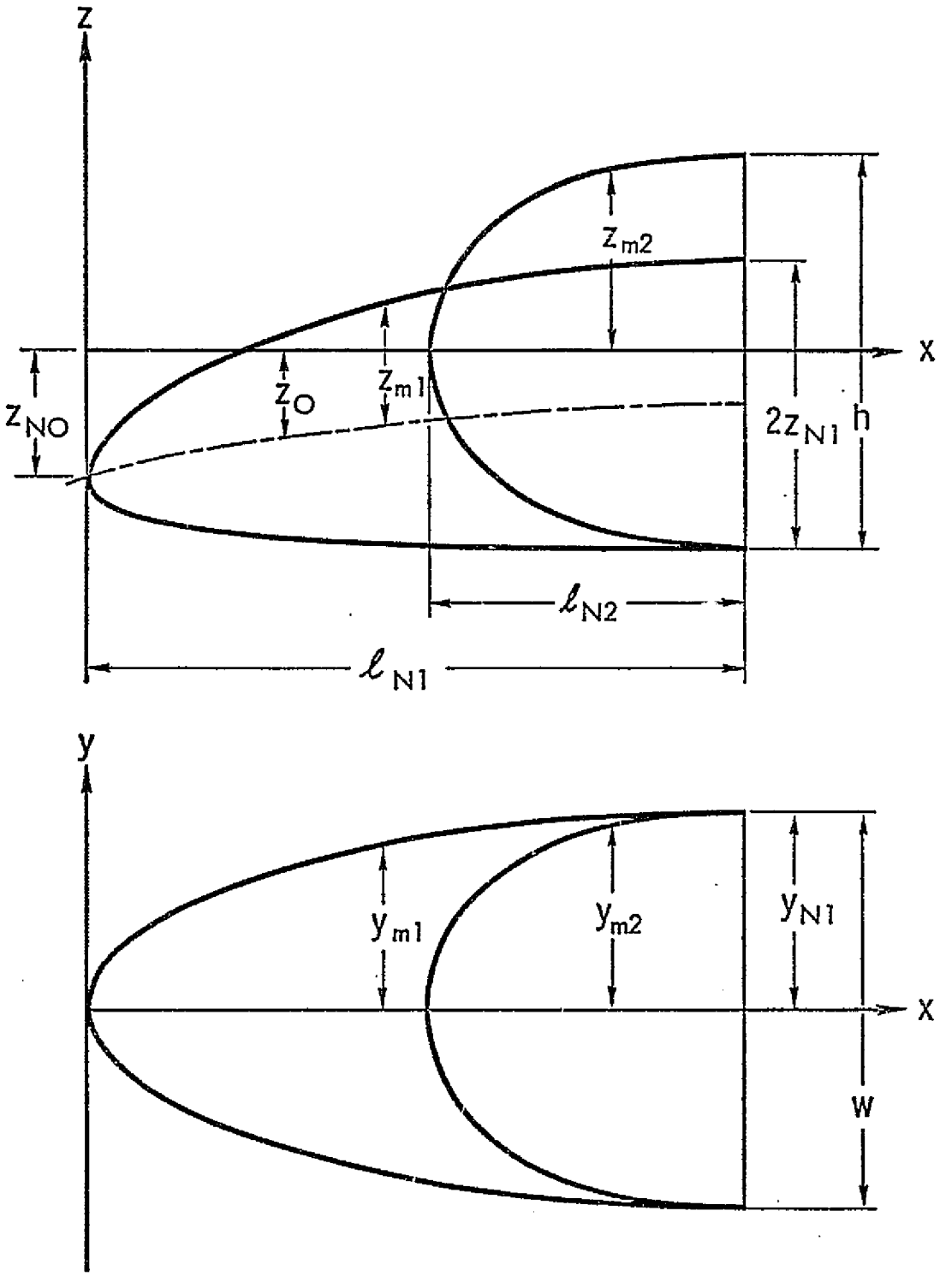

Figure 2.37 Definition of Nose Cone Geometry

defined as the bluntness parameter for the cone. These shape parameters may be used to determine the exponents of equation 2.51 as described in Appendix A.

It will be assumed that Cone N1 may be described by its top and side view shape parameters and that Cone N2 may be described by only its side view shape parameters. The method for determining these shape parameters for FUSE is discussed in detail in Appendix C.

After determining the proper shape parameters and the corresponding exponents for equation 2.51, equation 2.51 may be applied to determine the planform shapes for each cone. The planform equations for Cones N1 and N2 are expressed in equations 2.52 through 2.55, as derived from equation 2.51.

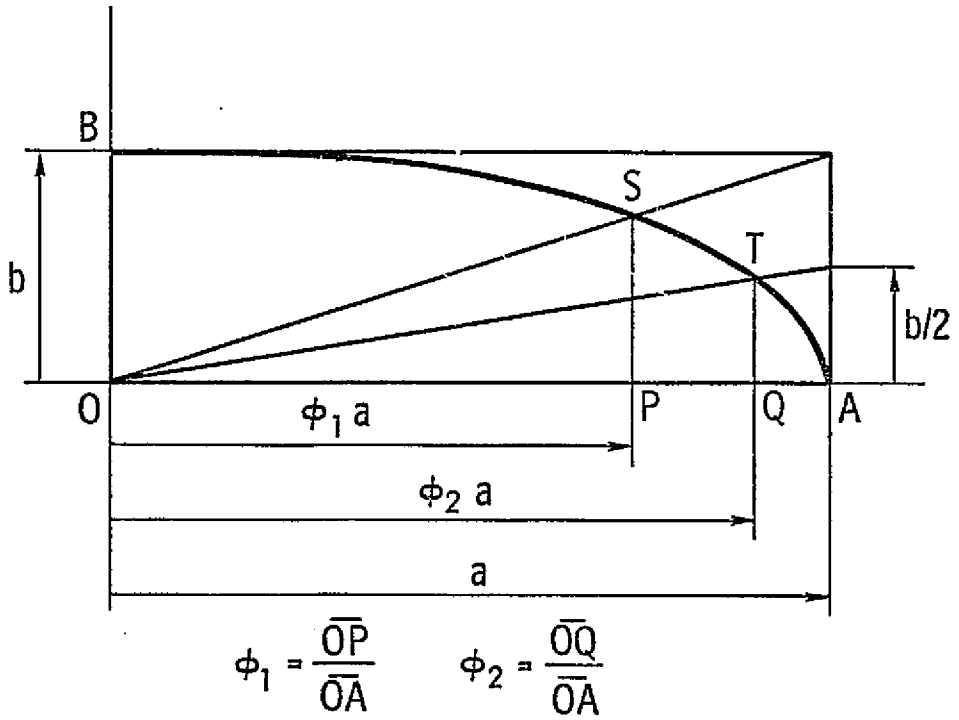

Figure 2.38 Definition of Elliptical Cone Shape Parameters

For Cone N1

Side View:

$$z_{m1}|_x = z_{N1}\left[1 - \left(\frac{\ell_{N1} - x}{\ell_{N1}}\right)^{n_{N1}}\right]^{1/m_{N1}} \qquad (2.52)$$

Top View:

$$y_{m1}|_x = y_{N1}\left[1 - \left(\frac{\ell_{N1} - x}{\ell_{N1}}\right)^{n_{y1}}\right]^{1/m_{y1}} \qquad (2.53)$$

where: m_{N1} and n_{N1} are derived from Cone N1 side view shape parameters ϕ_{11} and ϕ_{21};

and: m_{y1} and n_{y1} are derived from Cone N1 top view shape parameters, ϕ_{y1} and ϕ_{y2}.

For Cone N2

Side View:

$$z_{m2}|_x = \begin{cases} \frac{H}{2}\left[1 - \left(\frac{\ell_{N1} - x}{\ell_{N2}}\right)^{n_{N2}}\right]^{1/m_{N2}} & \text{for } x > (\ell_{N1}-\ell_{N2}) \\ 0 & \text{for } x \leq (\ell_{N1}-\ell_{N2}) \end{cases} \qquad (2.54)$$

Top View:

$$y_{m2}|_x = \begin{cases} \frac{W}{2}\left[1 - \left(\frac{\ell_{N1} - x}{\ell_{N2}}\right)^{n_{N2}}\right]^{1/m_{N2}} & \text{for } x > (\ell_{N1}-\ell_{N2}) \\ 0 & \text{for } x \leq (\ell_{N1}-\ell_{N2}) \end{cases} \qquad (2.55)$$

where: m_{N2} and n_{N2} are derived from Cone N2 side view shape parameters.

With the planform values, y_m and z_m at any x, for both cones, the cross-section shapes may be superimposed according to the methods of Section -.5.1.2. As stated in Section 2.5.1.1, the cross-section at each lengthwise segment will be divided into a specified number of radial segments. To attempt to place the

nodes as effectively as possible, for use in the NCSU BODY program, the following method will be used.

Figure 2.39 pictures the orientation of cones N1 and N2. A line, $\overline{CL}$, has been constructed from the tip of Cone N1 to the centroid at the base of Cone N2.

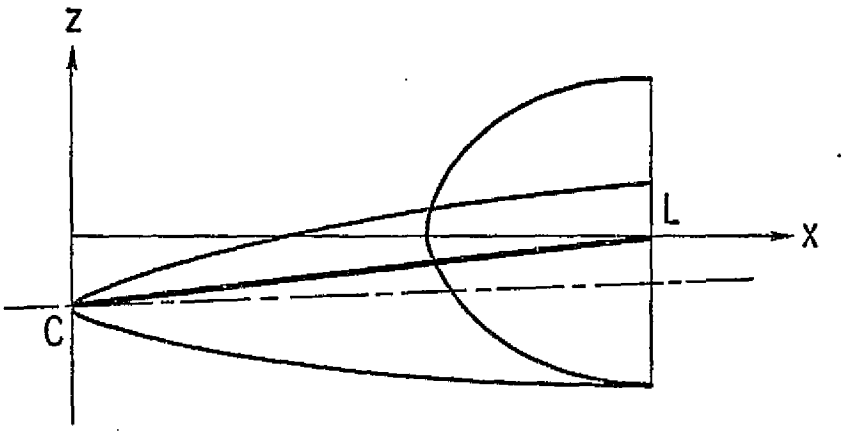

Figure 2.39 Geometric Definition of the Centerline for Radial Divisions

The equation for $\overline{CL}$ may be expressed as in equation 2.56.

$$z_{CL} = \left(\frac{-z_{NO}}{\ell_{N1}}\right) x + z_{NO} \qquad (2.56)$$

This line will be used as a centerline from which the radial divisions will be constructed.

For $x \leq (\ell_{N1} - \ell_{N2})$ nodes will only be determined for Cone N1. For $x > (\ell_{N1} - \ell_{N2})$, the distance of the j'th node for each cone from $\overline{CL}$ will be used to decide which node will be retained. The distance will be determined as:

$$r = \sqrt{y^2 + (z - z_{CL})^2} \qquad (2.57)$$

The node resulting in the greater value of r will be used.

2.5.1.4 Cabin (Utility Section) Shape

The cabin will be modelled by a cylinder of a constant cross-section. No offsets will be used for the cabin. The length of the cabin will be represented as ℓ_u. The cross-section at any point may be represented by the method of Section 2.5.1.2.

2.5.1.5 Tail Cone Shape

The tail cone shape will be modelled as an elliptical cone in much the same manner as Cone N1 of the nose. At present, the shape parameters used by FUSE for the tail cone are the same for both the top and side planform shapes. For this reason, an average of the top and the side view shape parameters is advised for input data to the program. This is discussed in Appendix C in more detail.

With the shape parameters and subsequently the exponents for the equation, the planform shapes may be expressed as in equations 2.58 and 2.59. Figure 2.40 describes the geometric parameters used to describe the tail cone.

Side View:
$$z_{mc}|_x = \frac{H}{2}\left[1 - \left(\frac{x'}{\ell_c}\right)^{n_c}\right]^{1/m_c} \qquad (2.58)$$

$$y_{mc}|_x = \frac{W}{2}\left[1 - \left(\frac{x'}{\ell_c}\right)^{n_c}\right]^{1/m_c} \qquad (2.59)$$

Where: $x' = x - (\ell_{N1} + \ell_u)$

As with Cone N1 of the nose, to allow for upswept tail cone, provision has been made in FUSE for a vertical offset for the tail cone of the form:

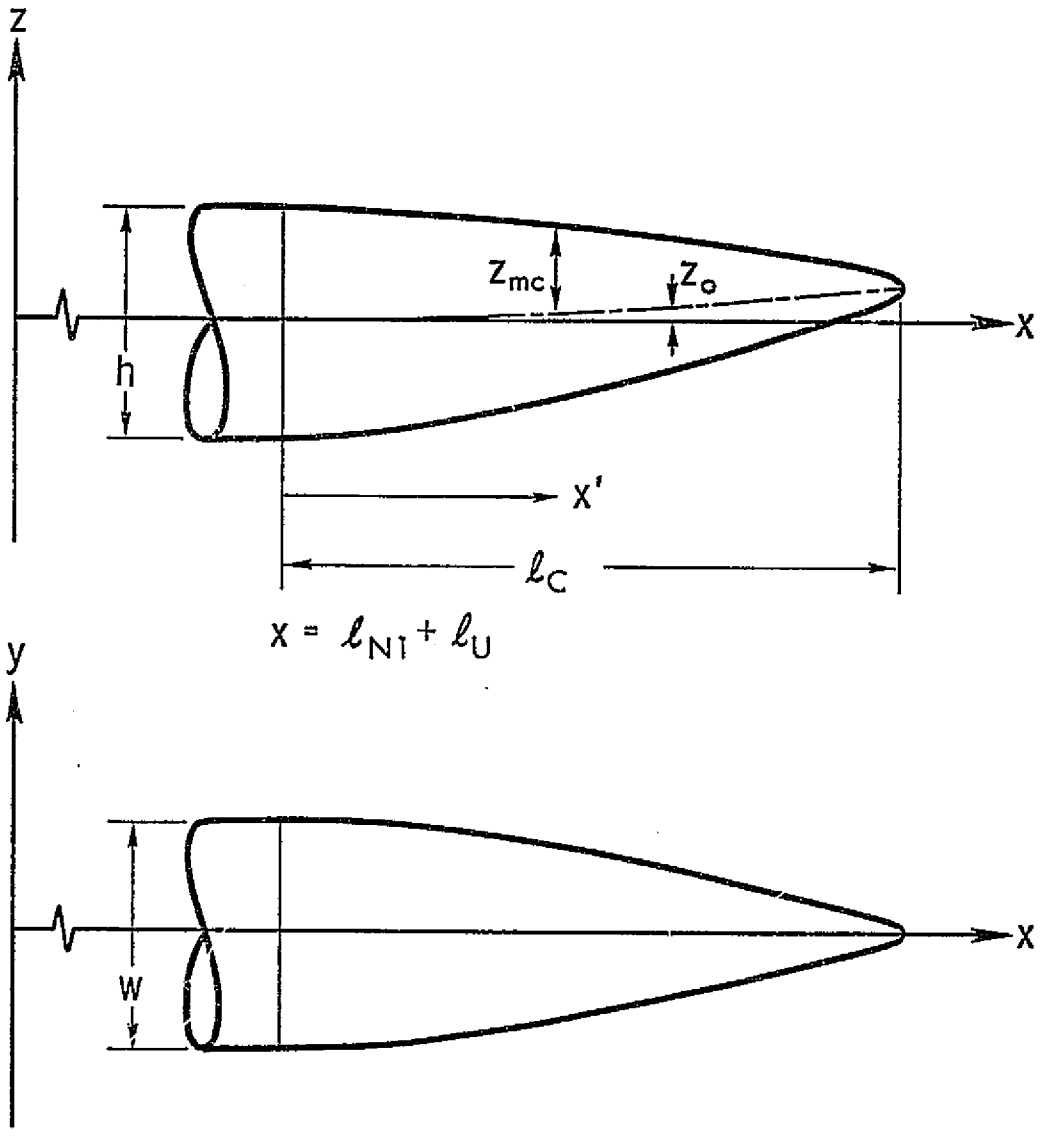

Figure 2.40 Definition of Tail Cone Geometry

$$z_0 = q_{c1}(x') + q_{c2}(x')^2 \qquad (2.60)$$

The cross-section will, again, be determined according to the method of Section 2.5.1.2.

2.5.2 Program Description

Using the model developed in Section 2.51 a program was written in the Fortran IV computer language to compute the coordinates of nodes for finite-element analysis applications for commuter aircraft fuselages. Figure 2.41 presents a simplified flowchart of the program. A complete listing for the program is presented in Appendix C of this report.

The program calls one subroutine to aid in the computation of the node coordinates, CONSHP. CONSHP is a short iteration subroutine used to determine the planform equation exponents from the elliptical cone shape parameters, as stated in Section 2.5.1. A description of the method used in CONSHP is presented as part of the explanation of the elliptical cone method in Appendix A.

It should be noted that fuselage node coordinates are stored in a three-dimensional matrix, SFUS (I, J, K). SFUS has been dimensioned as a 60 x 30 x 3 matrix. This allows a maximum of 1,711 panels for each fuselage. Although this may appear to be an excessive number of panels, the dimensioning was chosen to allow maximum flexibility in choosing lengthwise and radial segment distributions for structural or aerodynamic applications. The I value is the number of the lengthwise segment. The J value is the number of the radial segment, numbered from bottom to top. The K value is the x, y, or z coordinate, with the K values of 1, 2, and 3 corresponding to x, y, and z, respectively.

Although at present, they are not output, the coordinates for the nose cones N1 and N2 are also stored in three-dimensional

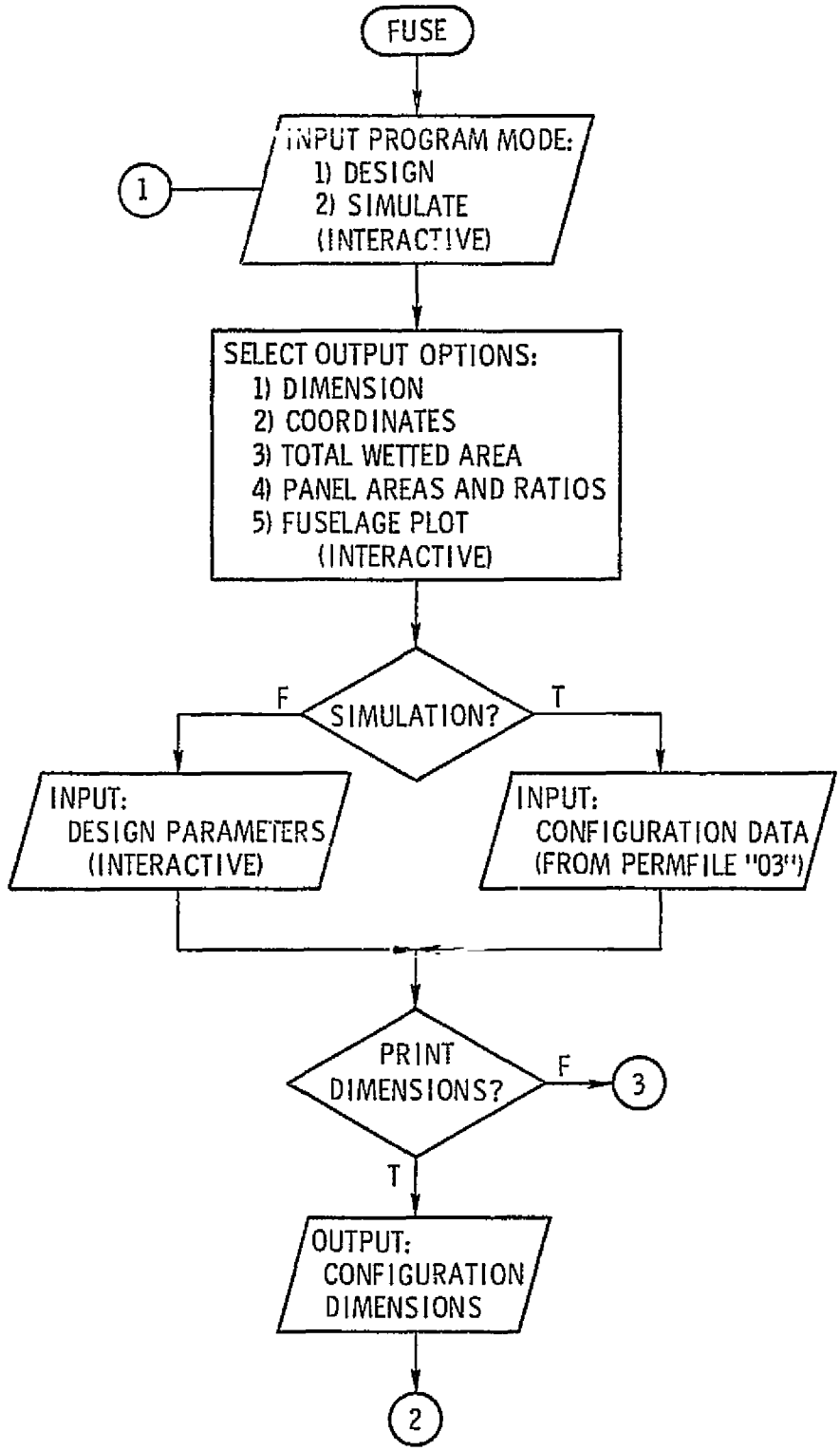

Figure 2.41 Simplified Flowchart for FUSE

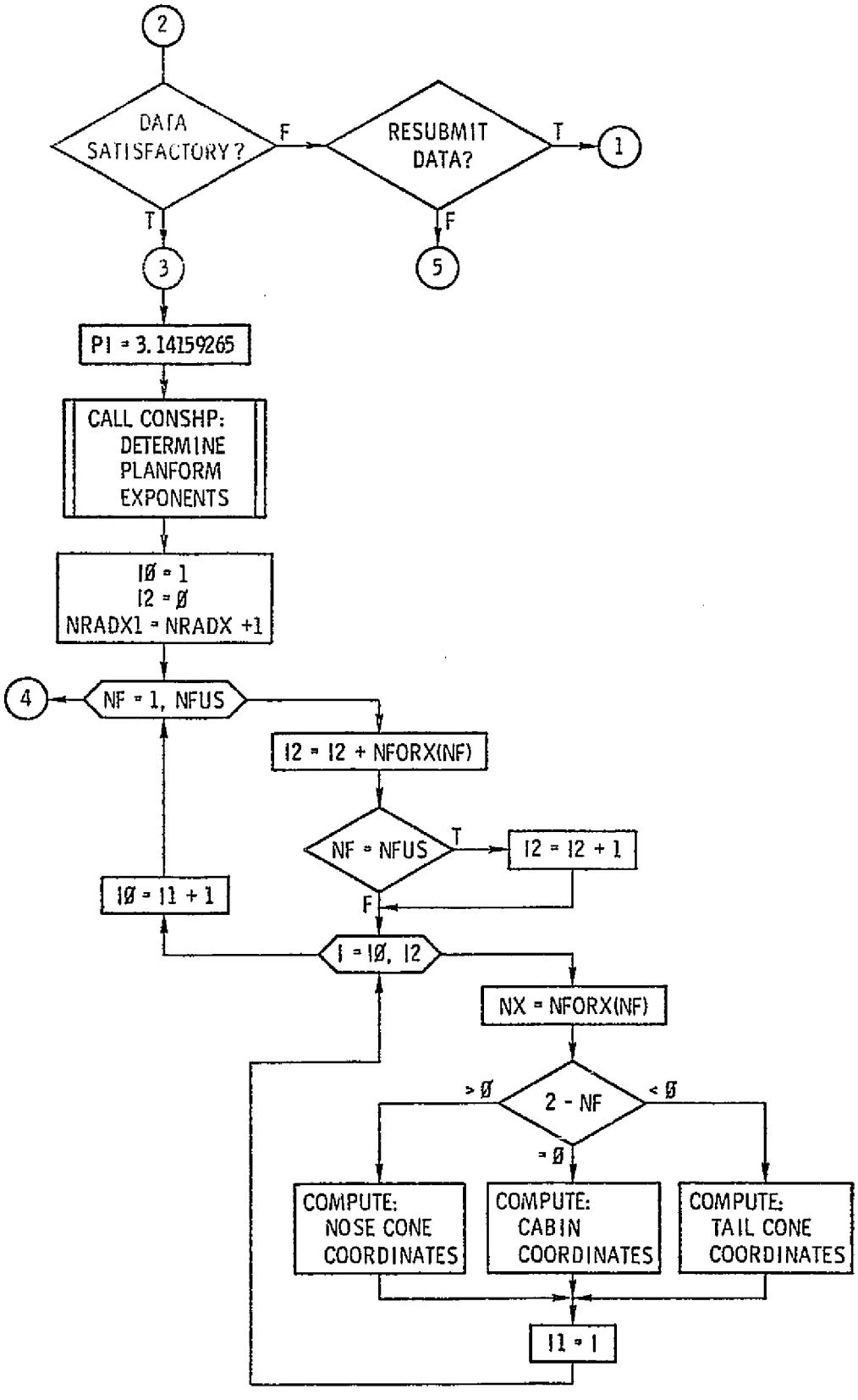

Figure 2.41 (continued)

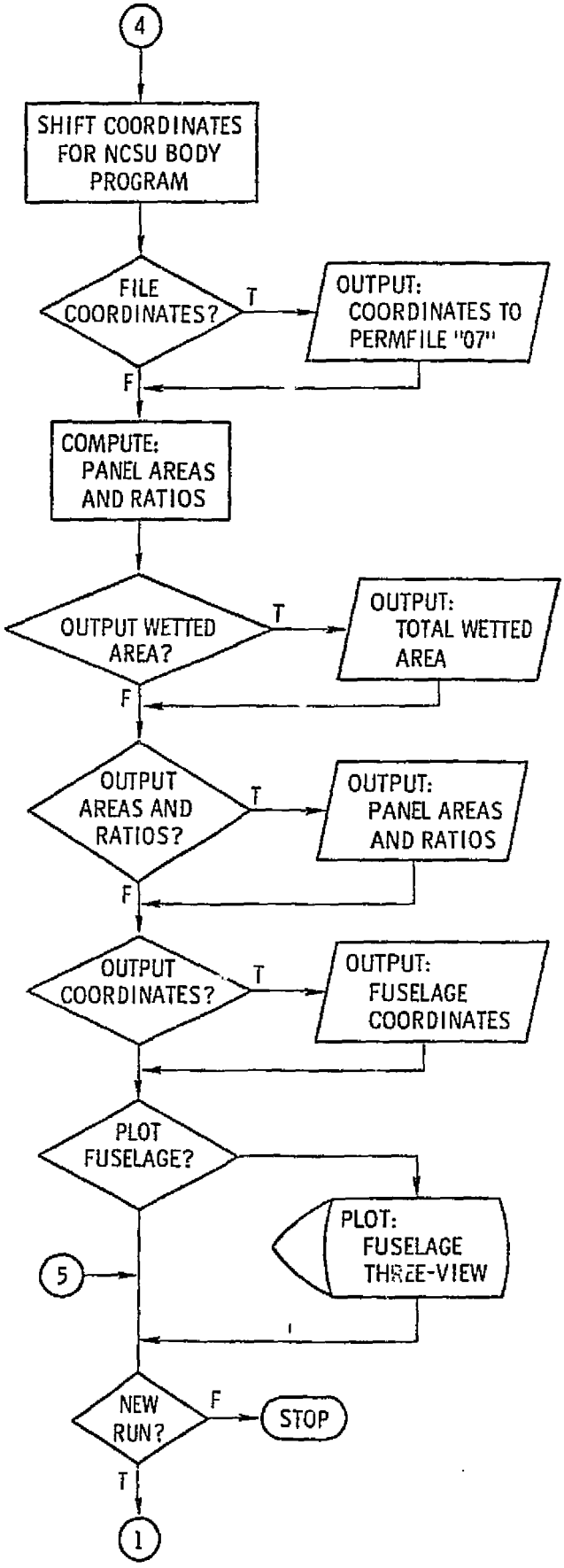

Figure 2.41 (continued)

arrays. These arrays, SNOS1(I, J, K) and SNOS2(I, J, K), are set up in a similar manner to SFUS. The intent is to eventually evaluate the individual nose shells for crew compartment volume, visibility, landing gear stowage, etc.

The program may be operated in either a design mode or a simulation mode. In the simulation mode, the program will read shape parameters for a particular aircraft configuration from a data file already stored on disc. The logical unit number for the READ statements in this case is "03." In the design mode the program will ask the user to input the necessary variables in a question-and-answer process.

One of the original intents for FUSE was to prepare data for use with the NCSU BODY program (or Reference 20) to enable parametric studies for fuselage drag optimization. For this reason the program will re-orient the fuselage coordinates and output them to a disc permfile in a format useful to the BODY program, if desired. The logical unit number for the WRITE statements in this case is "07." Several other output options are available as well. These are discussed in Appendix C.

2.5.3 Program Results

To test FUSE, several simulations of actual aircraft were made. Two of these simulations are presented here as Figures 2.42 and 2.43. Figure 2.42 represents a simulation of the Gates-Learjet Model 35/36. Figure 2.43 represents a simulation of the Fokker-VFW F28 Mk. 4000.

In both cases, the simulation seems to represent the fuselage shape with reasonable accuracy. Discrepancies, however, are apparent. Because of the straight-line-segment method used, for instance, the nose and tail become pointed. The accuracy by which the windshield/body intersection is modelled depends upon the number of panels specified for the nose section of the fuselage. Note, also, that the "flat" portion of the F28 tail cone has been averaged into the overall rounded shape. The mismatch of tail cone lengths is a result of a miscalculation for input data.

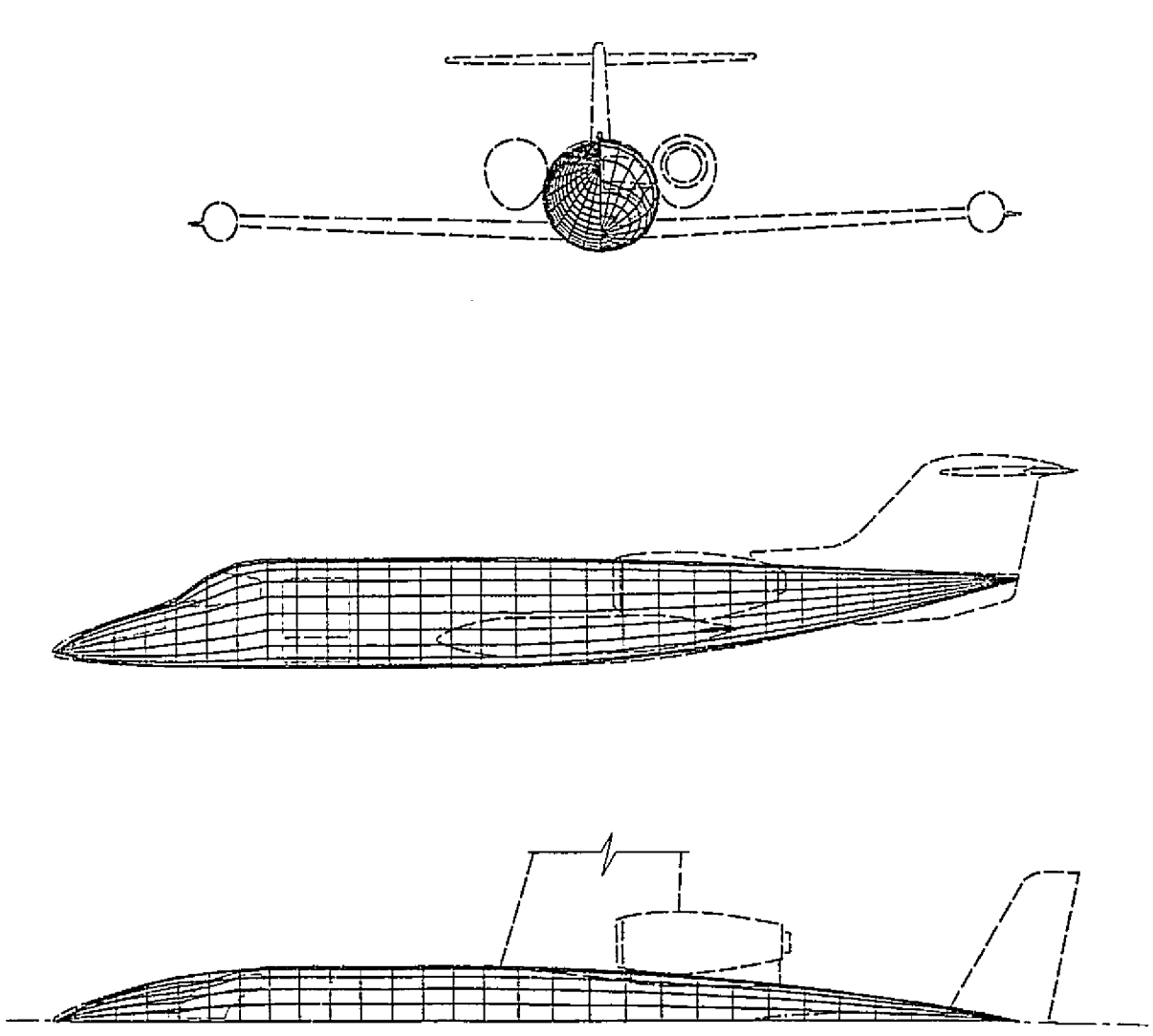

Figure 2.42 Gates Learjet 35/36 Simulation - 580 Panels

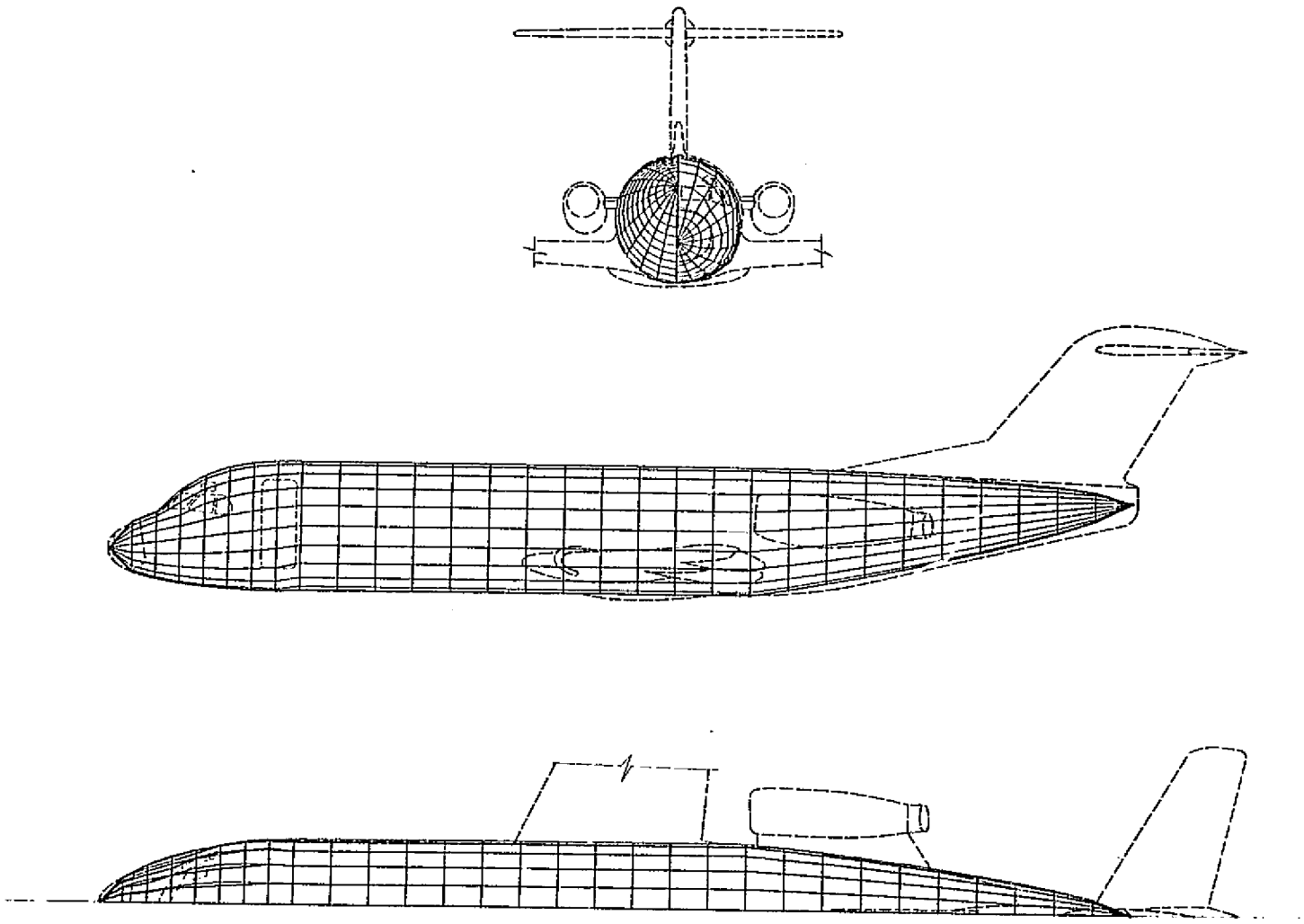

Figure 2.43 Fokker F28 MK. 4000 Simulation - 600 Panels

It is believed that when the analysis of the fuselages is completed using BODY, the results will be close. Also, at that time, to check the sensitivity of the method slight modifications in the shape and geometry will be made to document the effects of simulation discrepancies on aerodynamic predictions of BODY. The most considerable problem to be encountered was the choosing of the fuselage divisions to insure accuracy according to the constraints of Reference 20.

Although several conceptual designs have also been made, hard-copy plots were not available. Preliminary indications are that FUSE-generated designs are reasonable.

CHAPTER 3 WING CONFIGURATION STUDIES

The project objectives as outlined in Chapter 1 called for performing a short study of wing sizing methods and considering a rational approach to wing placement. Although it has not been possible to completely meet the objectives in this area, this chapter will discuss briefly one alternative method to the GASP method for wing sizing, and a method that was considered for wing placement. Section 3.1 will discuss the wing sizing method, and Section 3.2 will describe the wing placement method.

3.1 Wing Sizing

It was proposed to consider the methods of Laurence Loftin of NASA-Langley (References 3, 21, 22, and 23) as an alternative method to sizing the aircraft wing for optimization studies. Time permitted only a quick look at the methods involved, and no formal evaluation was possible.

The methods described by References 3, 21, 22, and 23 may be applied to either jet-propelled or propeller-driven aircraft. The methods used are based on data collected from several aircraft in each category.

The propeller-driven aircraft sizing methods were based on the characteristics of over one hundred forty different aircraft in a gross weight range from approximately 1000 lbs. to over 100,000 lbs. The maximum speed range of these aircraft covered a range from about 100 MPH to over 500 MPH. The methods are intended to size the aircraft to one or more of the following performance objectives (Reference 21):

A. Airport Performance
   1. Stalling Speed
   2. Landing Field Length

3. Take-off Field Length
4. Climb Performance

B. Cruise Performance

1. Maximum or cruising speed usually at a specified altitude and power setting
2. Range, again at a specified altitude and power setting
3. Payload

By specifying these performance objectives, and by using the aircraft data and the analysis methods proposed, it is possible to rapidly estimate the following aircraft characteristics:

- Gross Weight
- Empty Weight
- Fuel Weight
- Wing Area and Wing Loading
- Power and Power Loading
- Performance Characteristics at Values of Altitude and Power other than those Specified

Figure 3.1 provides a simplified flowchart of the method as applied to propeller-driven aircraft.

The performance and size estimation method for jet-propelled aircraft was accomplished in a similar manner. The methods were based on the characteristics of approximately 35 aircraft with gross weight ranging from about 10,500 to 800,000 lbs. For the jet-propelled aircraft the following performance objectives were considered (Reference 22):

A. Airport Performance

1. FAR (Federal Air Regulations) landing field length including missed approach requirement
2. FAR take-off field length including second segment climb requirement

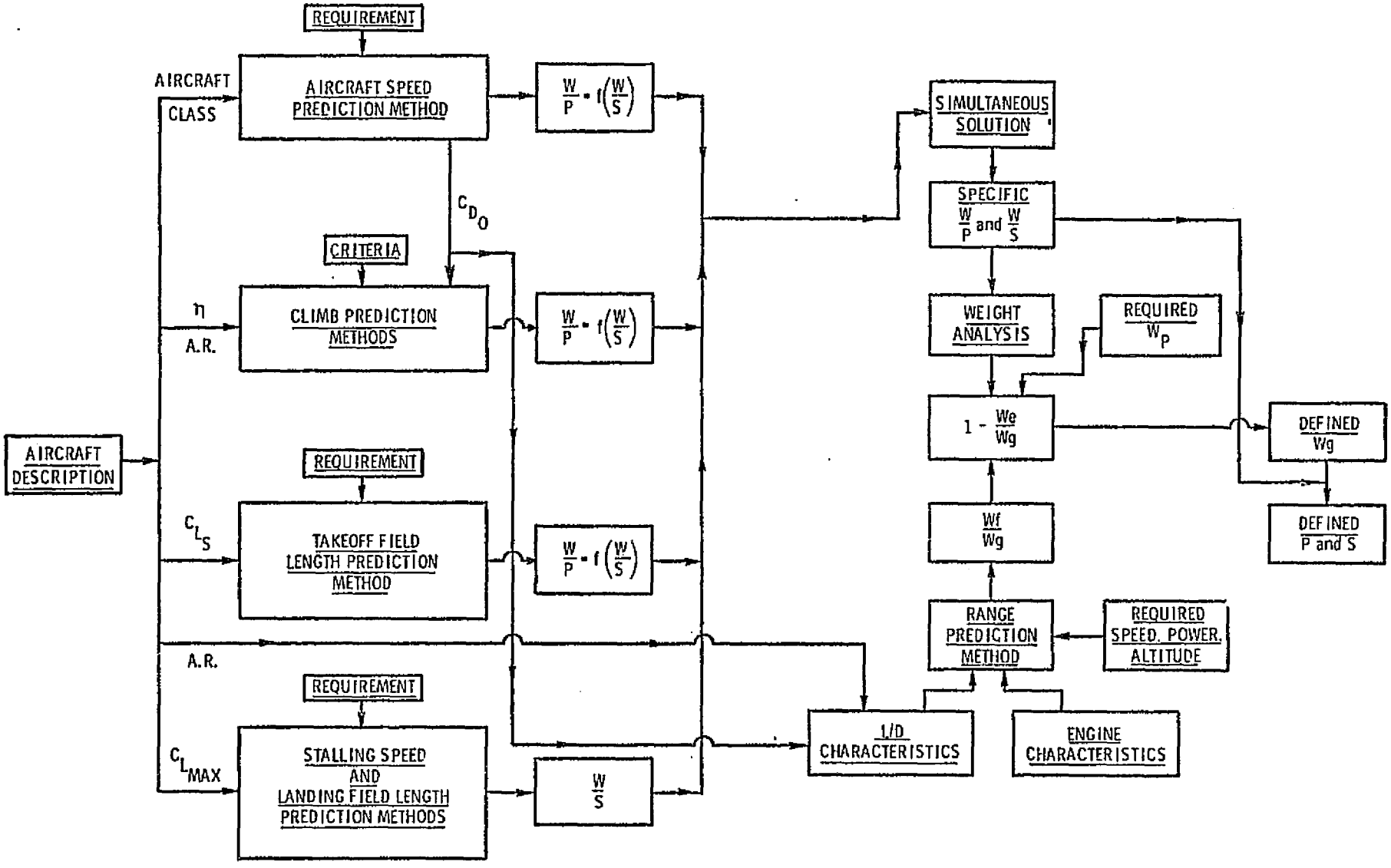

Figure 3.1 Aircraft Sizing Flow Diagram for Propeller-Driven Aircraft (Reproduced from Reference 21)

B. Cruise Performance

1. Cruise speed and altitude
2. Range
3. Payload

In this case by using the performance objectives, the aircraft data, and the proposed analysis methods, the following aircraft characteristics may be rapidly estimated:

- Gross Weight
- Fuel Weight
- Wing Area and Wing Loading
- Thrust and Thrust Loading
- Altitude for Cruise, if not specified

Figure 3.2 provides a simplified flowchart of the methods as applied to jet-propelled aircraft.

Although a formal evaluation of the methods was not made, a preliminary study of the method indicated that very good results could be expected. The intent of Loftin's method was to allow one person to rapidly estimate the performance and size of an aircraft without having to rely on expensive computer aids. As a result the method is very much oriented towards graphical approximations. The GASP, on the other hand, accomplishes the same basic objectives through computer applications. At this time, it is not felt necessary to pursue the evaluations of Loftin's approach for use in the design optimization of commuter airplanes.

3.2 Wing Placement

When the proposal for the first continuation of this research project was submitted to NASA-Ames in December 1976 (Reference 2), a misunderstanding of the wing location method used by the GASP inclined KU-FRL personnel to believe that an improved method was available. This method, provided in

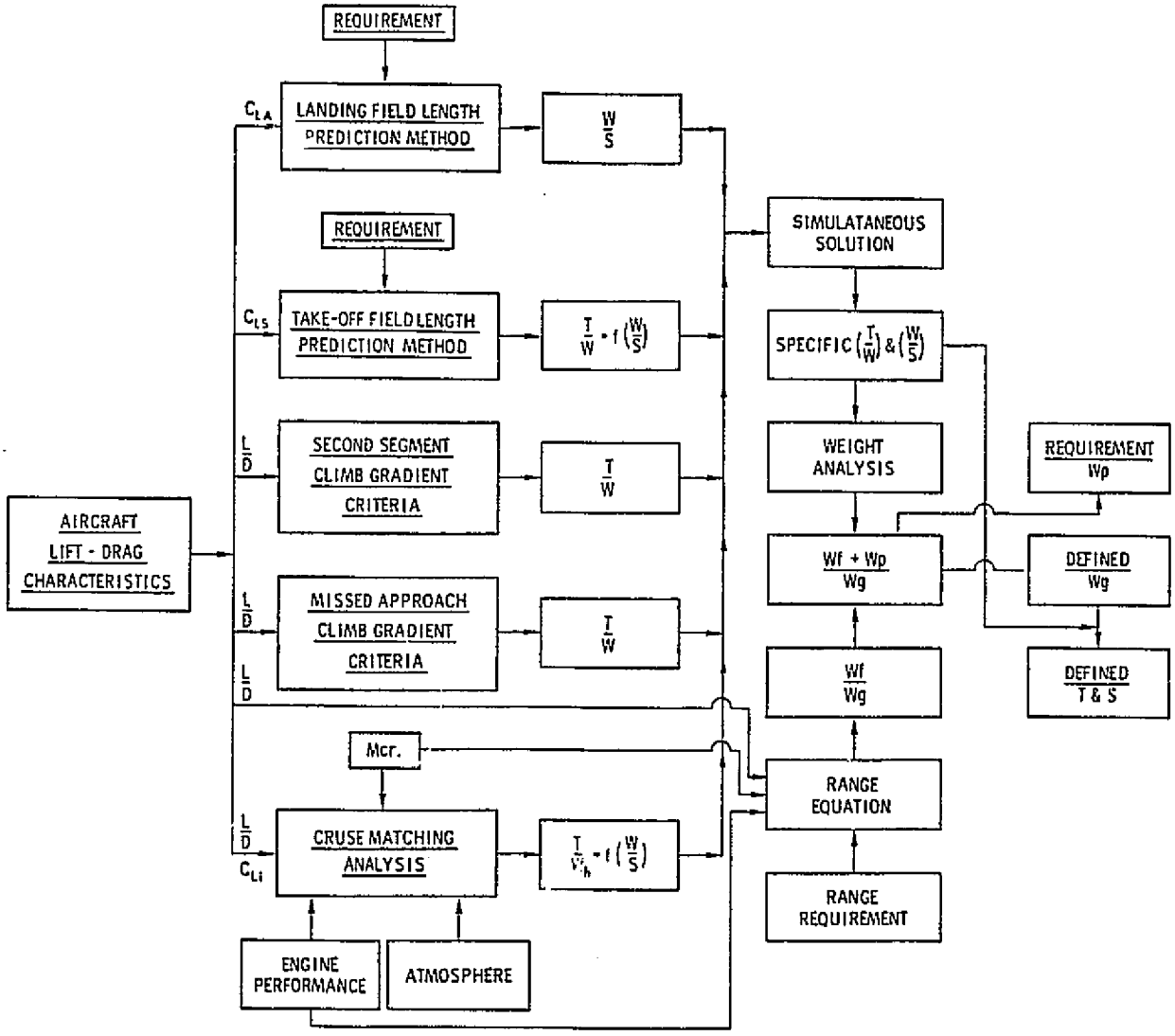

Figure 3.2 Aircraft Sizing Flow Diagram for Jet-Propelled Aircraft
(Reproduced from Reference 22)

Chapter 8 of Reference 9, however, was in fact essentially what the GASP already used. For this reason work to incorporate a wing location routine based on Reference 9 was discontinued.

One other aspect of the GASP wing location routine did raise some questions. In locating the wing to provide a specified static margin value, the GASP assumes that the aerodynamic center of the wing (alone) is at 25% of the MAC. This is satisfactory for essentially unswept wings ($\Lambda_{LE} < 10°$) at low Mach numbers ($M < 0.3$). For business jet configurations this is not necessarily the case. The methods of Reference 14 were to be used to locate the aerodynamic center, given a specific wing geometry at cruise Mach number, but time did not permit the completion of the associated routines. Also, it appeared that, in the GASP, it was assumed that the effect of the body is to shift the aerodynamic center aft. Subsequently it was assumed in the GASP that any static margin allowed would be conservative. On the other hand, the effect of the body is, in fact, to shift the aerodynamic center forward, tending to destabilize the aircraft. For this reason it was intended to use the Multhopp strip integration routine mentioned in Section 2.3 to compute the body effect and then to iterate to find the wing location that would result in the proper static margin. Figure 3.3 presents a flow diagram to illustrate this approach.

As the GASP is still inoperational, these methods have not yet been implemented.

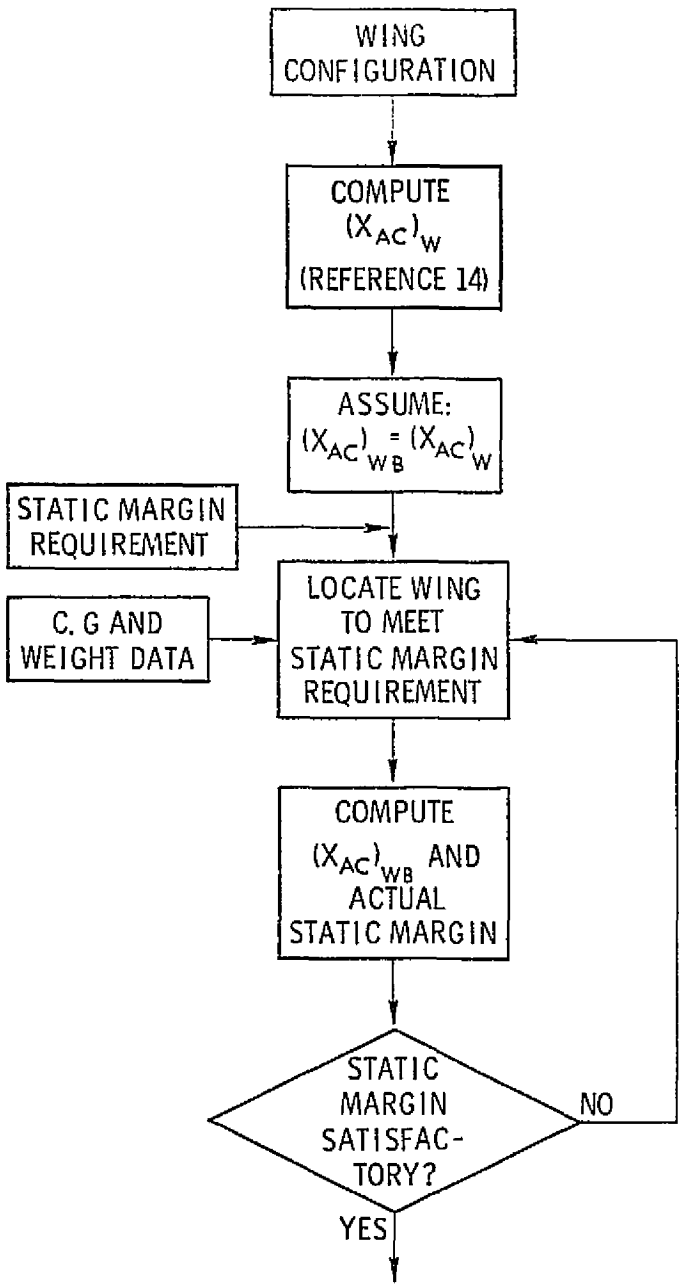

Figure 3.3 Flow Diagram of the Proposed Wing Location Approach

CHAPTER 4 WETTED AREA, DRAG, AND WEIGHT STUDIES

Towards the objective of determining a minimum weight and drag configuration to aid in minimizing DOC, studies were made to determine whether a minimum drag configuration could be defined for the fuselage. Weight and drag studies were both to have been conducted using the GASP, but due to the inoperational status of the program this has not been possible. It was also hoped that additional drag data could have been compiled to compare with the GASP results by using the NCSU BODY program of Reference 20. Higher priorities had to be placed on the GASP program, and therefore the BODY program transliteration process was put aside.

Wetted area studies were conducted using FUSE for both actual and conceptual aircraft. As wetted area may be related to both drag and weight, some implication of the wetted area study may be used to predict what might be expected with drag and weight. The wetted area study will be discussed in Section 4.1. Section 4.2 redocuments the slipstream drag study presented in Reference 15.

4.1 Wetted Area Studies

The zero-lift drag of an airplane is proportional to its wetted area as shown in equation 2.4. The weight of the fuselage structure may be said to be proportional to its wetted area to the power 1.2, as shown in equation 2.21. Therefore by studying the wetted areas of various airplane configurations, it should become possible to derive some conclusions as to the trends in weight and drag to be expected.

Early in the research program, an attempt was made to correlate both total fuselage wetted area and fuselage section (nose, cabin, and tail) wetted area with their characteristic length. Data were compiled using wetted areas either acquired directly from the airframe manufacturer, or acquired by estimations from available

drawings. In an attempt to derive mathematical relationships, linear, exponential, and logarithmic least-squares curve-fits were applied to these data. These relationships are presented as Figures 4.1 through 4.12.* The results of these correlations were not very promising.

With the completion of FUSE (Section 2.5) another approach to determining wetted areas became available. Several aircraft were modelled using FUSE and the resultant wetted areas were compared with their actual wetted areas. These results are presented as Figure 4.13. With the exception of the Fokker F28, FUSE seems to provide good results.

Having determined that the wetted areas computed by FUSE were reasonable, a quick study was performed to determine the effect of cabin seating arrangement and total passenger capacity on fuselage wetted area. Conceptual aircraft were designed by FUSE to consider 10, 20, and 30 passengers in 2, 3, and 4 seats abreast configurations. Also these designs were made for circular cross-sections and for round-rectangular sections with a round-off radii value of 0.5. In all cases the default** values for a piston aircraft were used for the shape parameters and ratios. Adequate comfort level values were assumed, and baggage compartments allowing for 5 cu. ft. of baggage per passenger were also included. The significant parameters for each configuration are presented in Table 4.1. Figure 4.14 presents a plot of fuselage wetted area as a function of passengers for the circular fuselage configurations. Similarly, Figure 4.15 presents the results for the rounded-rectangular fuselage configurations.

From Figure 4.14 note that for all of the passenger capacities considered the number of seats abreast seems to be the controlling factor. For the twenty to thirty passenger range, however, the

---

*In figures 4.1 through 4.12, gross wetted area is the wetted area of the entire fuselage; net wetted area is gross wetted area minus the area of wing-body and tail-body intersections.

**See footnote page

Table 4.1 Conceptual Aircraft Design Parameters for the Wetted Area Study

Note: 1) Adequate Comfort Level is Assumed

2) Baggage Compartment ∿ 5 cu. ft./passenger

Conceptual Config.	Total Passengers	Seats Abreast	Round-off Radii	Outside Width (ft)	Outside Height (ft)	Nose Length (ft)	Cabin Length (ft)	Tail Length (ft)	Wetted Area (ft^2)
A	10	2	1.0	6.40	6.40	9.19	17.57	22.38	878.17
B	20	2	1.0	6.40	6.40	9.19	35.13	22.38	1237.46
C	30	2	1.0	6.40	6.40	9.19	52.70	22.38	1494.43
D	10	3	1.0	7.71	7.71	10.87	12.43	27.00	1017.94
E	20	3	1.0	7.71	7.71	10.87	22.36	27.00	1264.58
F	30	3	1.0	7.71	7.71	10.87	32.29	27.00	1526.47
G	10	4	1.0	9.20	9.20	12.09	8.98	34.11	1331.11
H	20	4	1.0	9.20	9.20	12.09	15.47	32.19	1403.99
I	30	4	1.0	9.20	9.20	12.09	24.45	32.19	1683.11
J	10	2	0.5	5.25	6.74	10.55	17.68	20.98	929.07
K	20	2	0.5	5.25	6.74	10.55	35.35	20.98	1328.55
L	30	2	0.5	5.25	6.74	10.55	53.03	20.98	1686.99
M	10	3	0.5	6.92	6.88	11.54	12.78	24.15	955.47
N	20	3	0.5	6.92	6.88	11.54	23.06	24.15	1201.46
O	30	3	0.5	6.92	6.88	11.54	33.33	24.15	1470.86
P	10	4	0.5	8.58	6.99	11.78	9.40	27.26	1017.50
Q	20	4	0.5	8.58	6.99	11.78	16.30	27.26	1198.44
R	30	4	0.5	8.58	6.99	11.78	25.70	27.26	1460.11

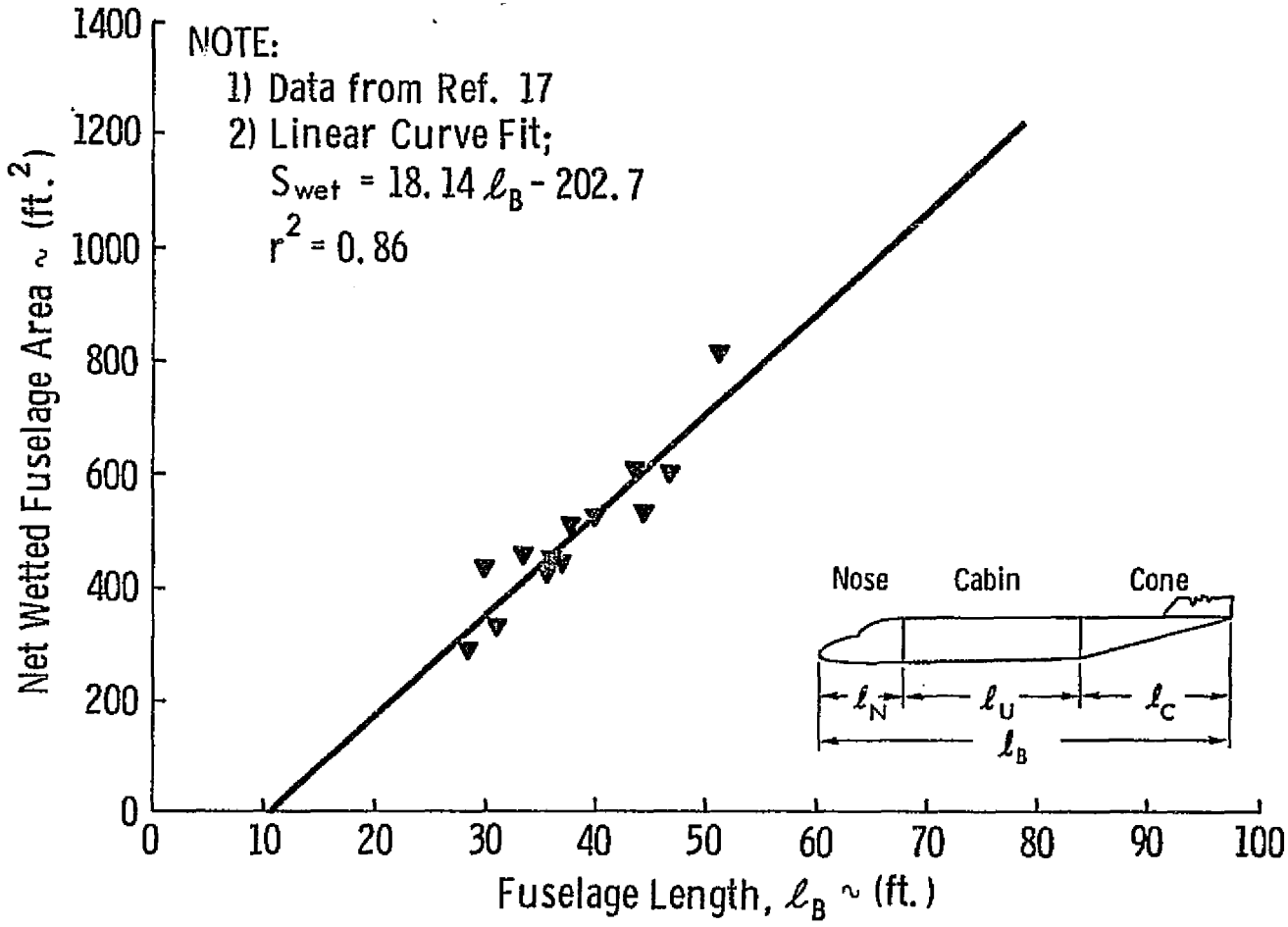

Figure 4.1 Linear Correlation Between Fuselage Length and Fuselage Wetted Area

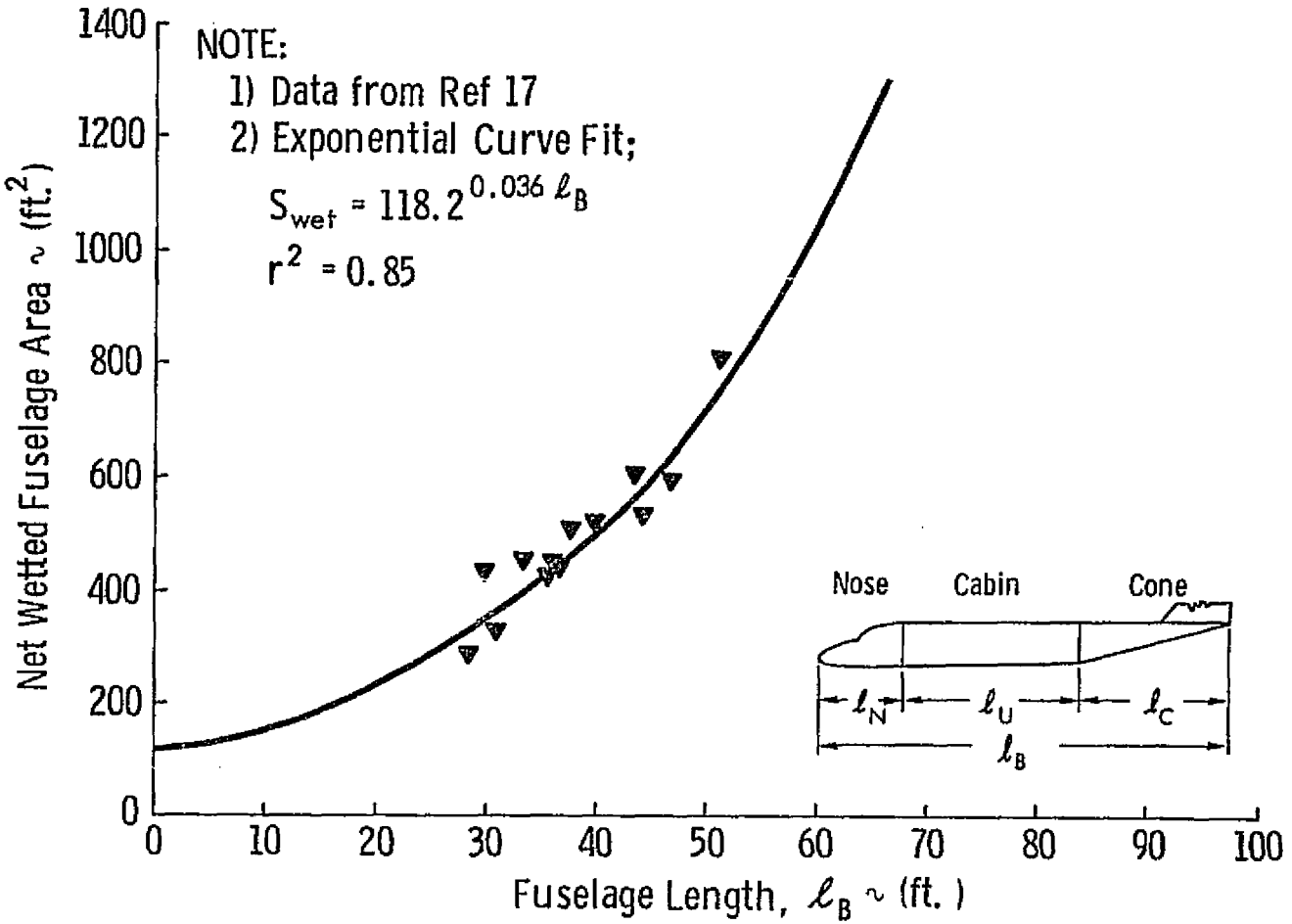

Figure 4.2 Exponential Correlation Between Fuselage Length and Fuselage Wetted Area

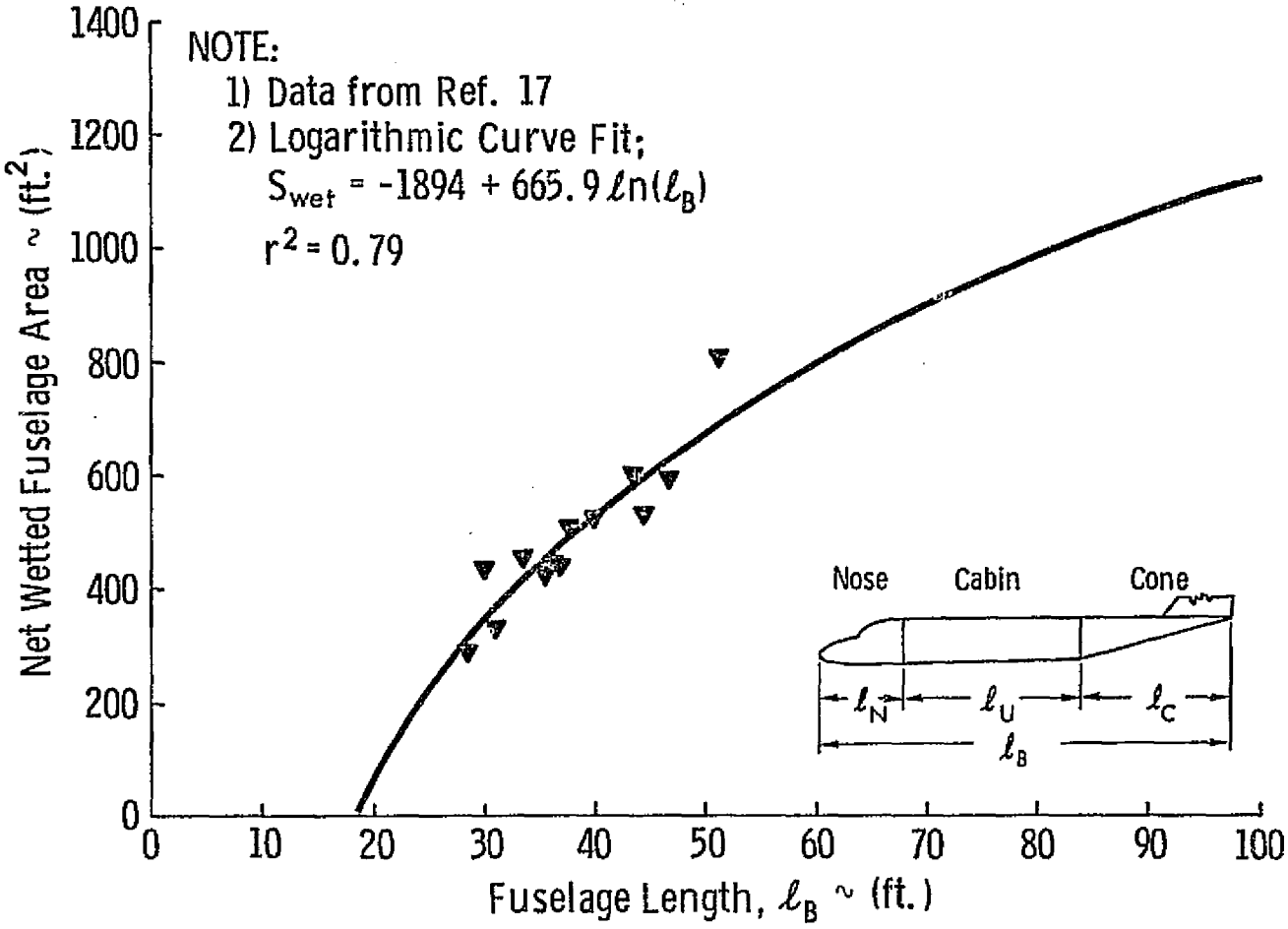

Figure 4.3 Logarithmic Correlation between Fuselage Length and Fuselage Net Wetted Area

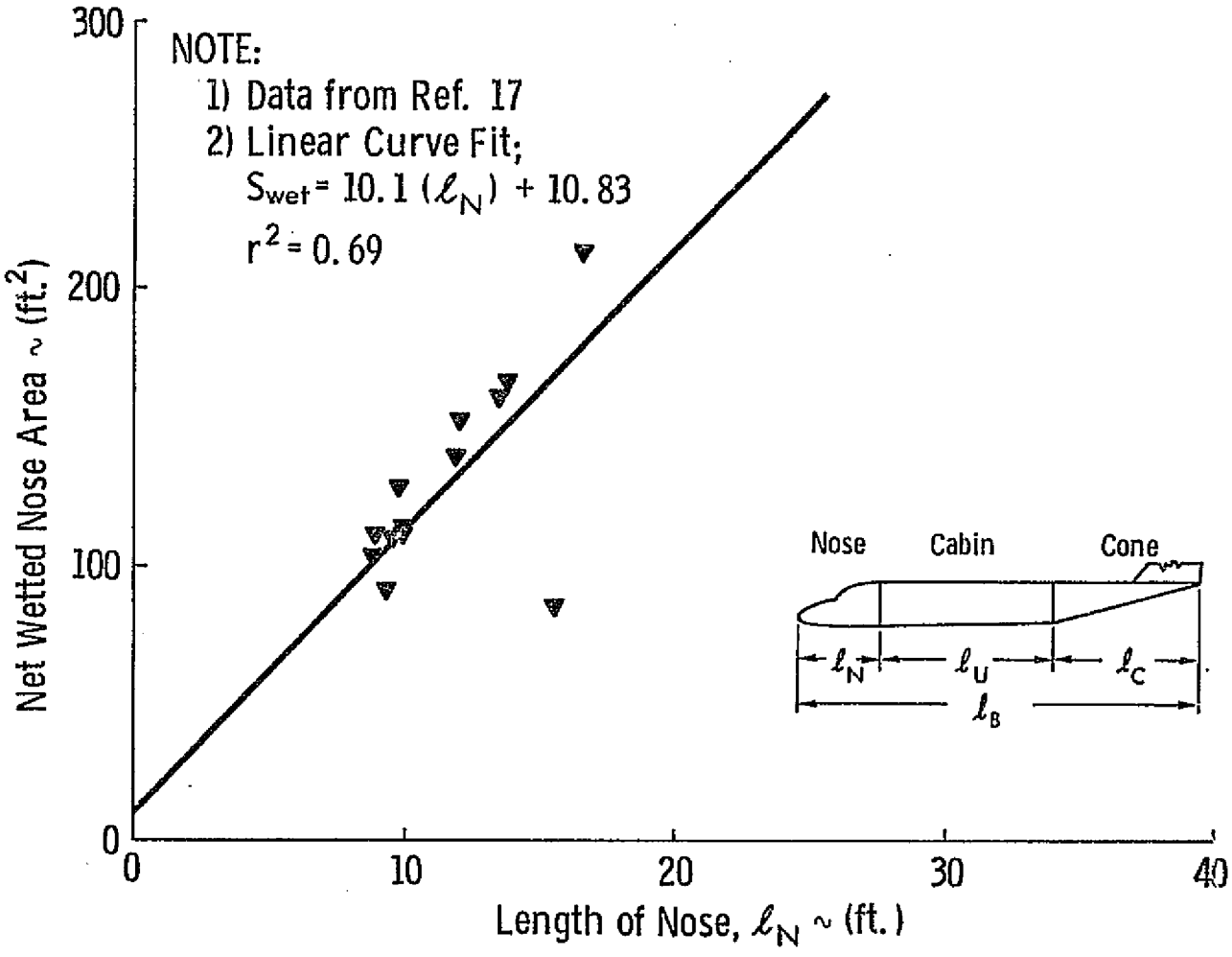

Figure 4.4 Linear Correlation Between Nose Length and Nose Wetted Area

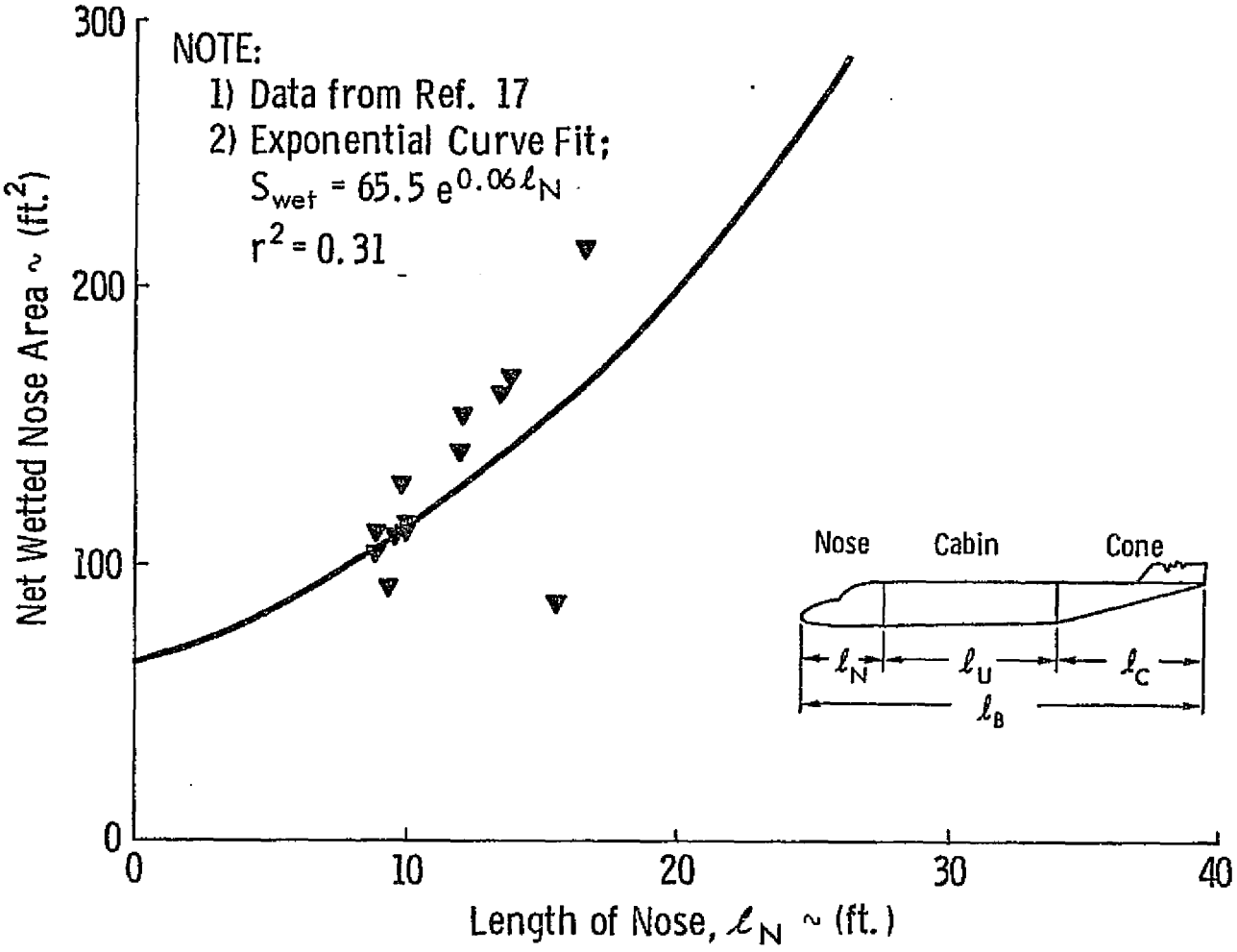

Figure 4.5 Exponential Correlation Between Nose Length and Nose Wetted Area

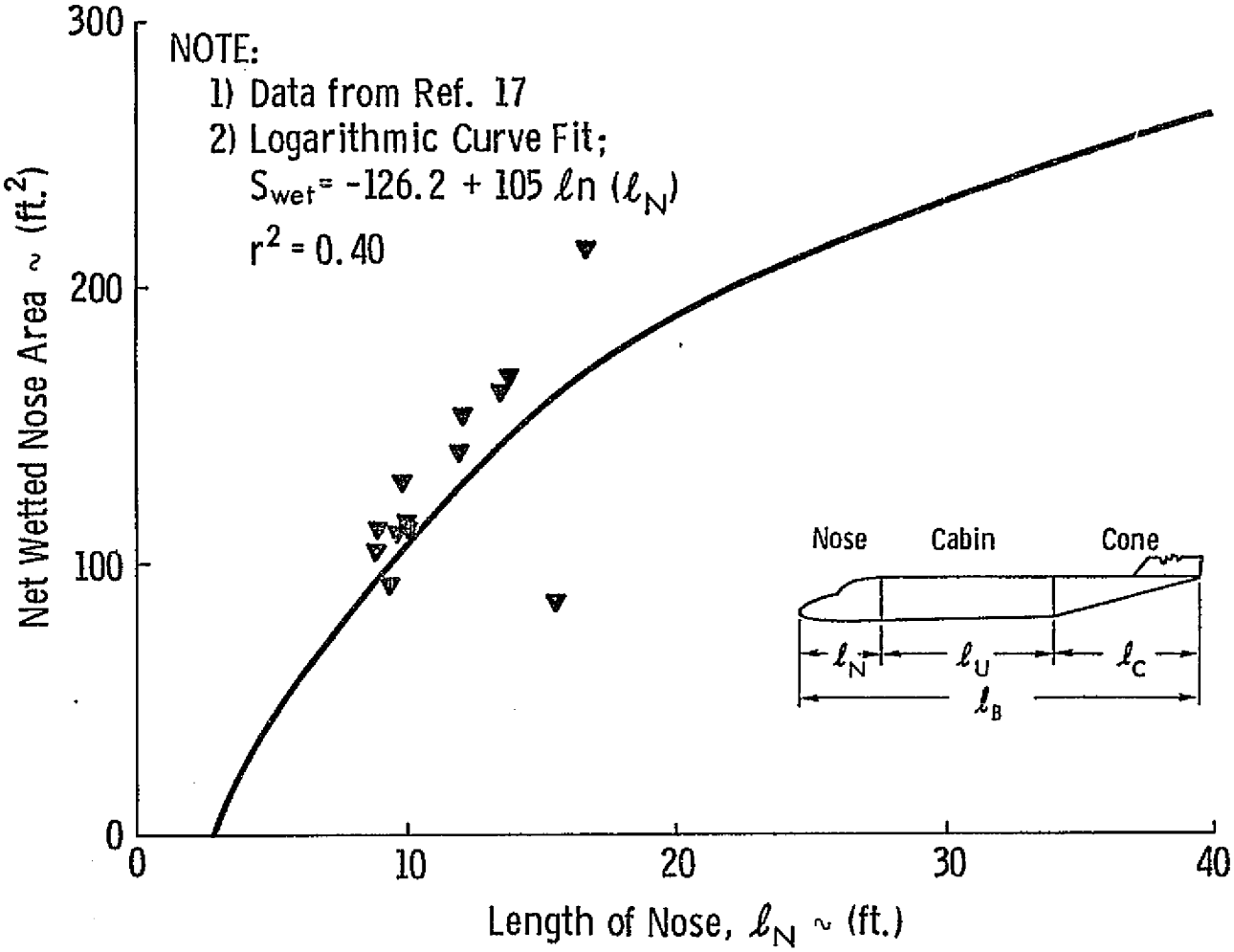

Figure 4.6 Logarithmic Correlation Between Nose Length and Nose Wetted Area

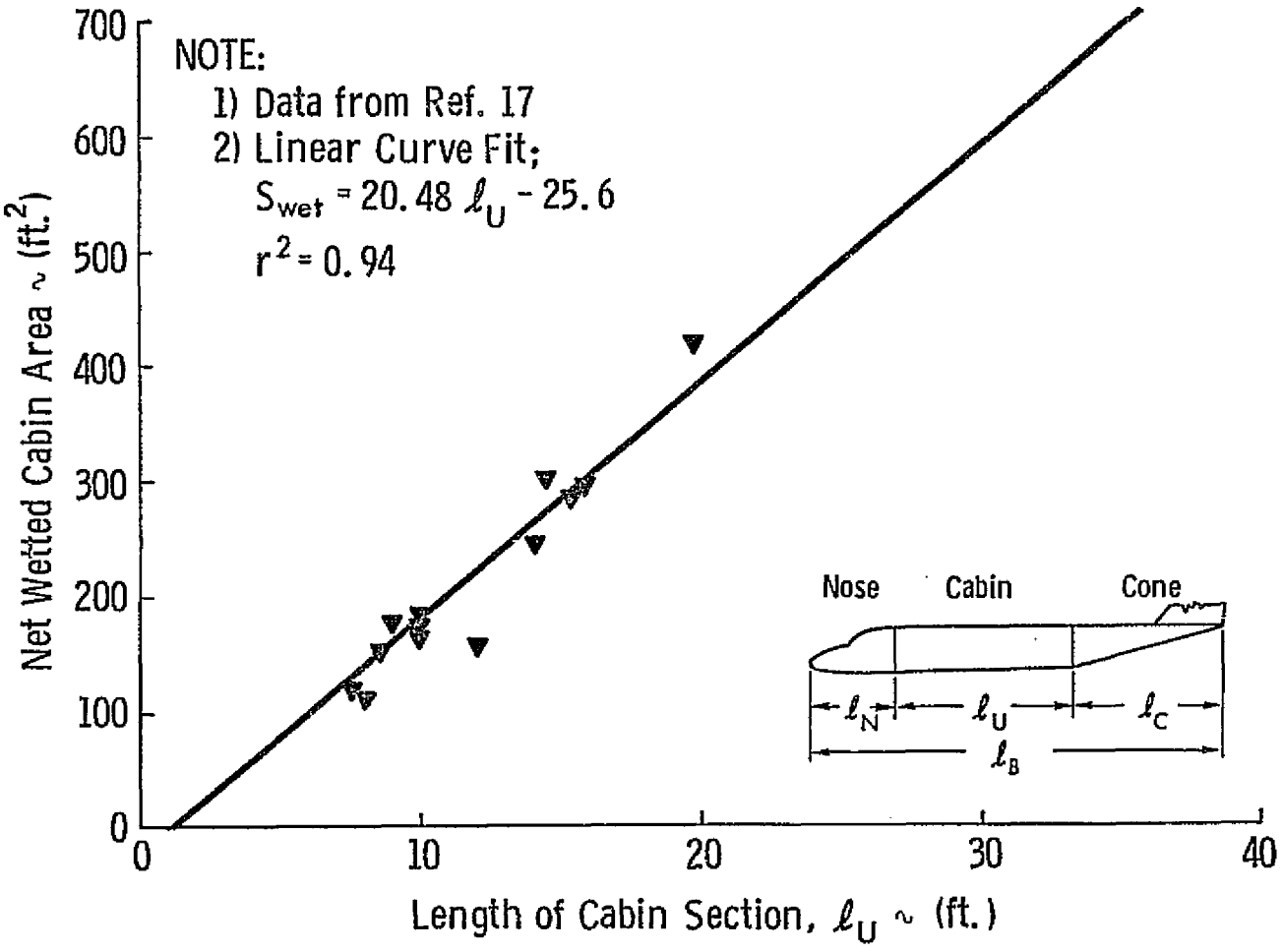

Figure 4.7 Linear Correlation Between Cabin Length and Cabin Wetted Area

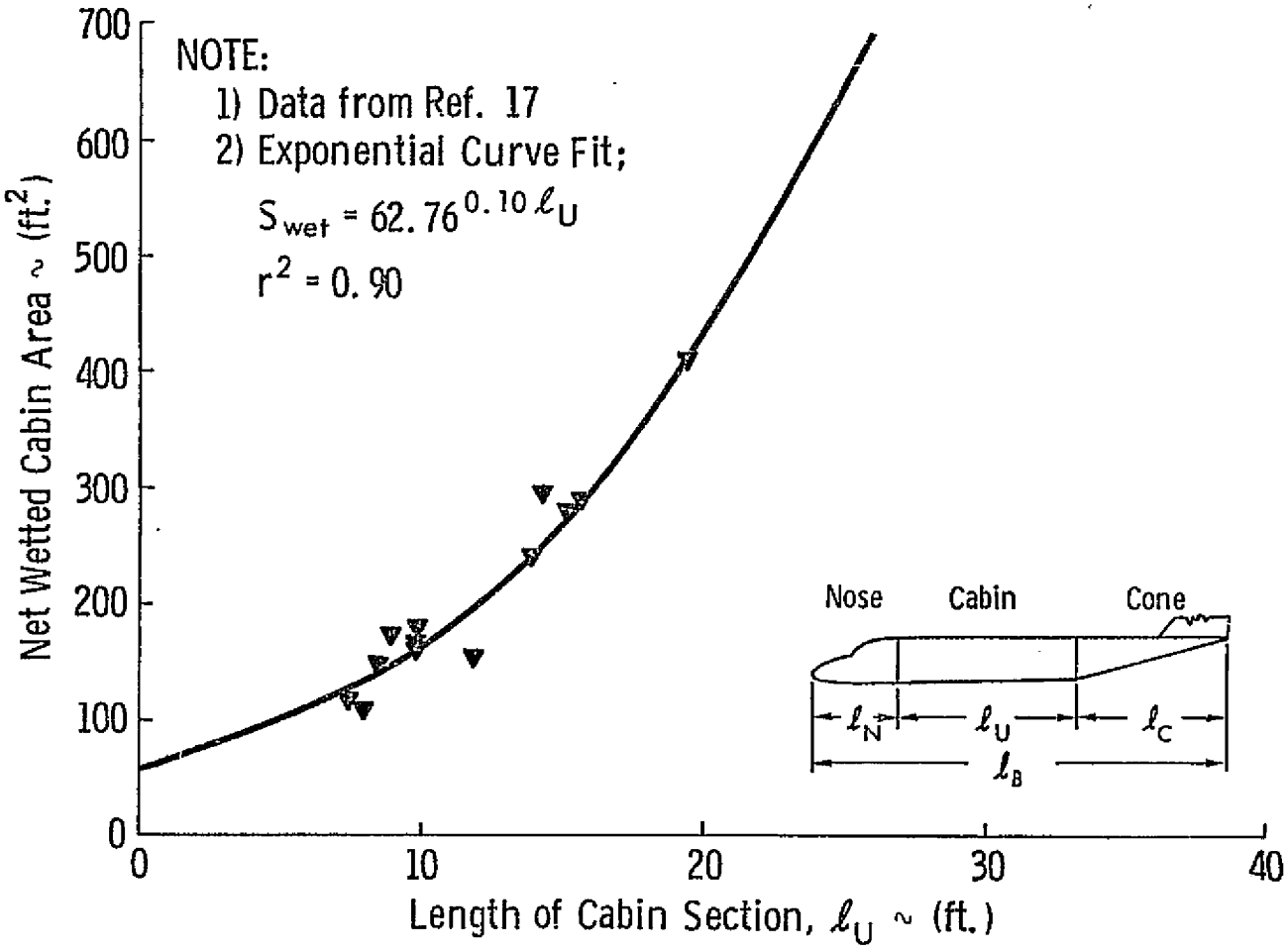

Figure 4.8 Exponential Correlation Between Cabin Length and Cabin Wetted Area

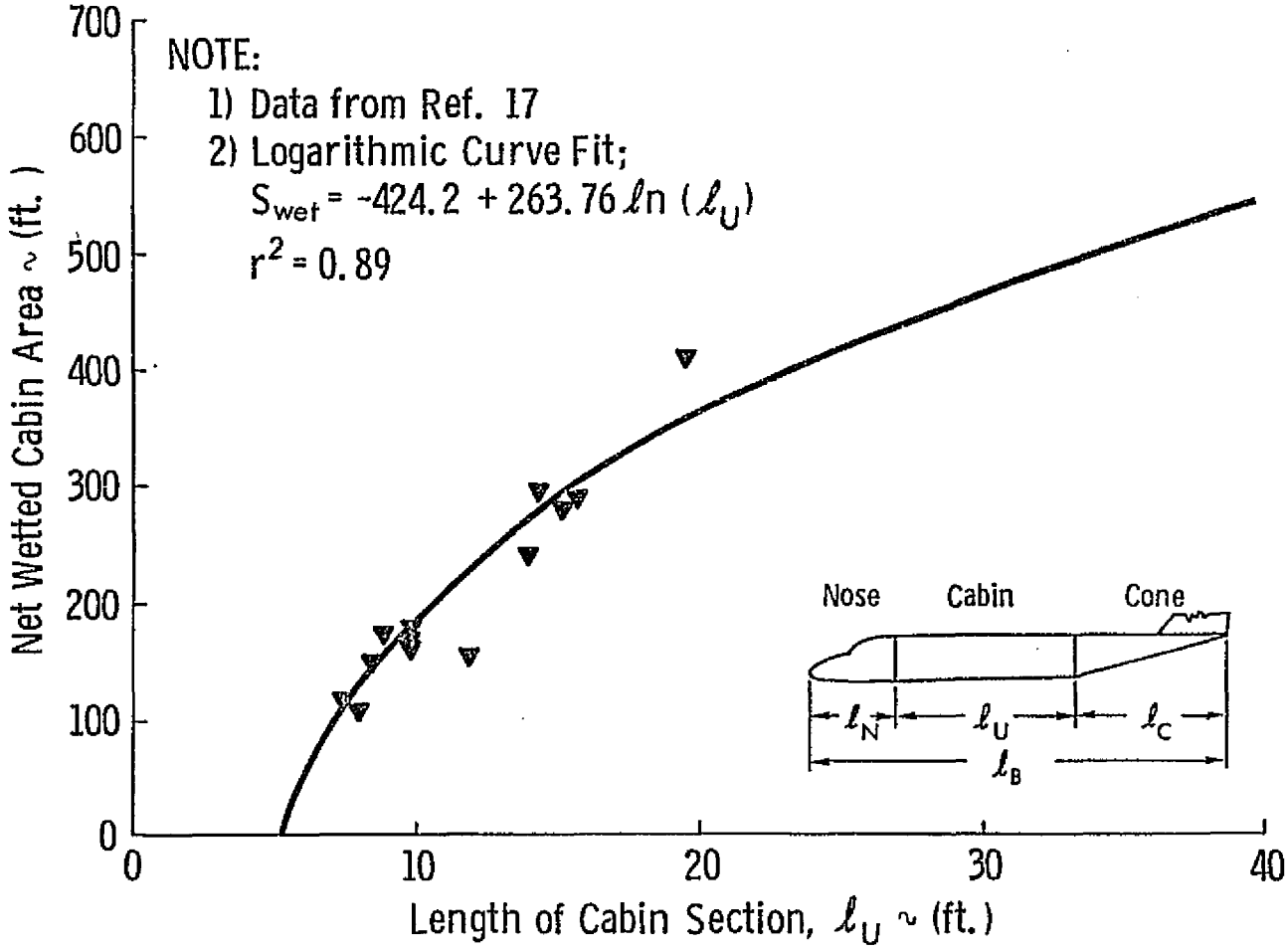

Figure 4.9 Logarithmic Correlation Between Cabin Length and Cabin Wetted Area

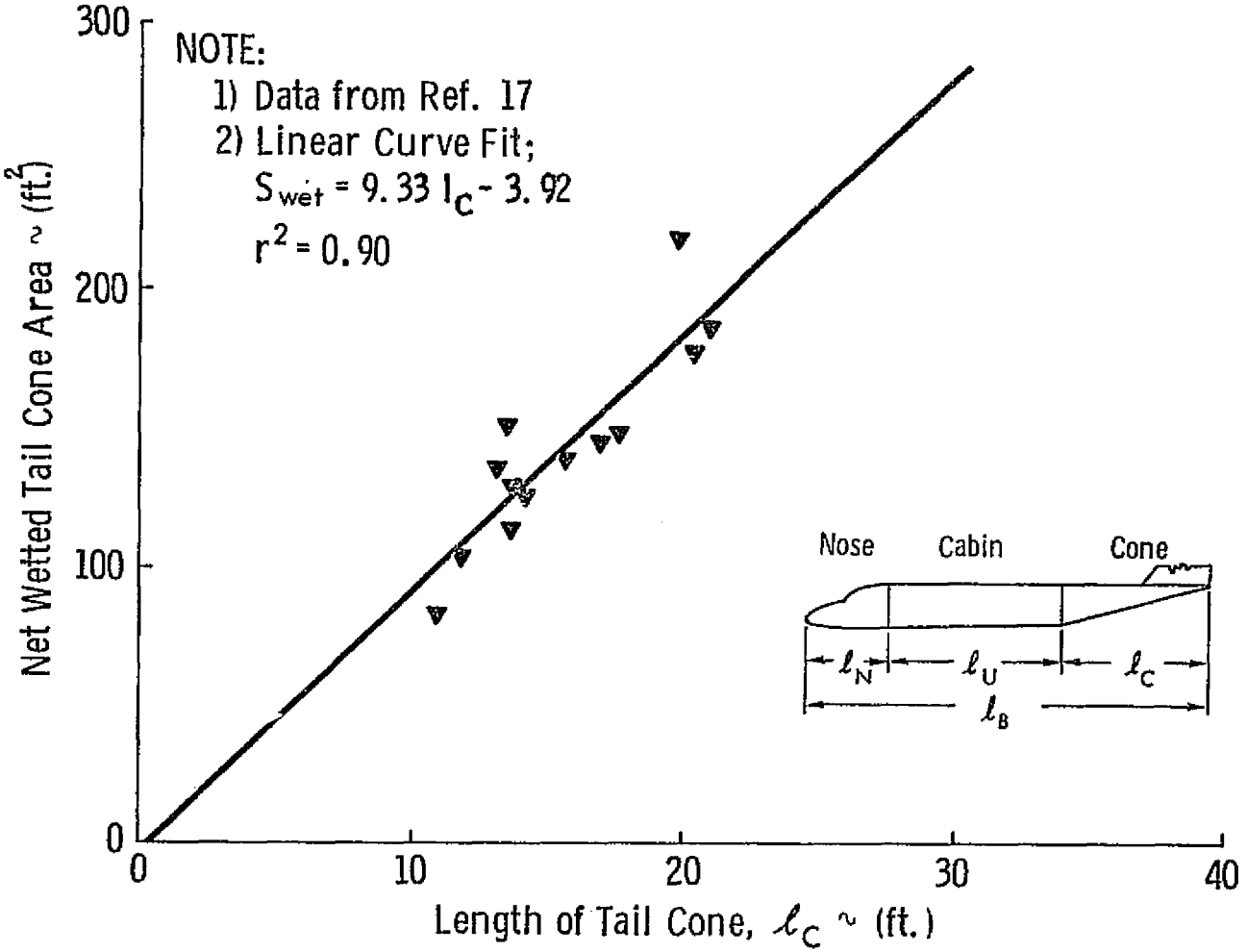

Figure 4.10 Linear Correlation Between Tail Cone Length and Tail Cone Wetted Area

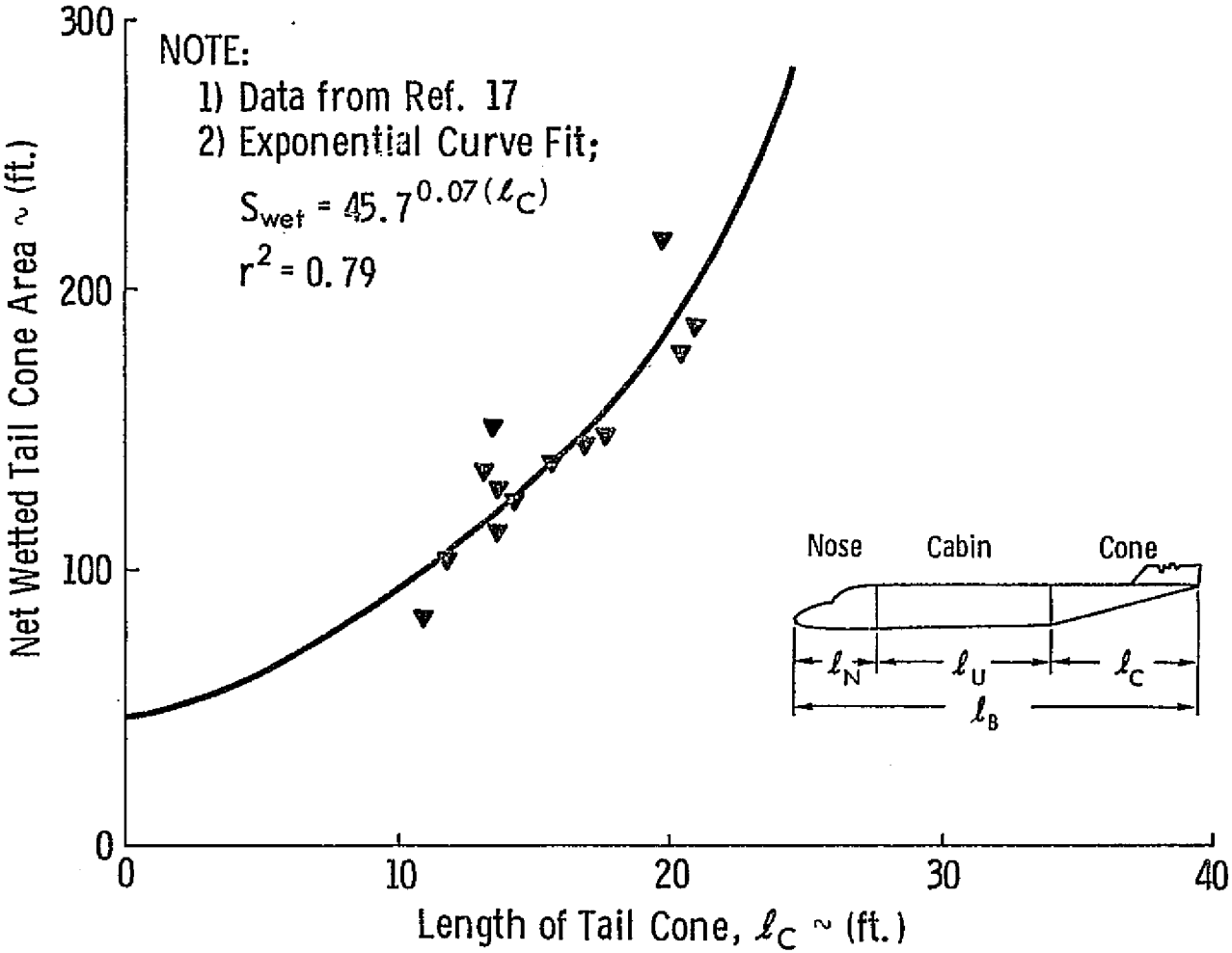

Figure 4.11 Exponential Correlation Between Tail Cone Length and Tail Cone Wetted Area

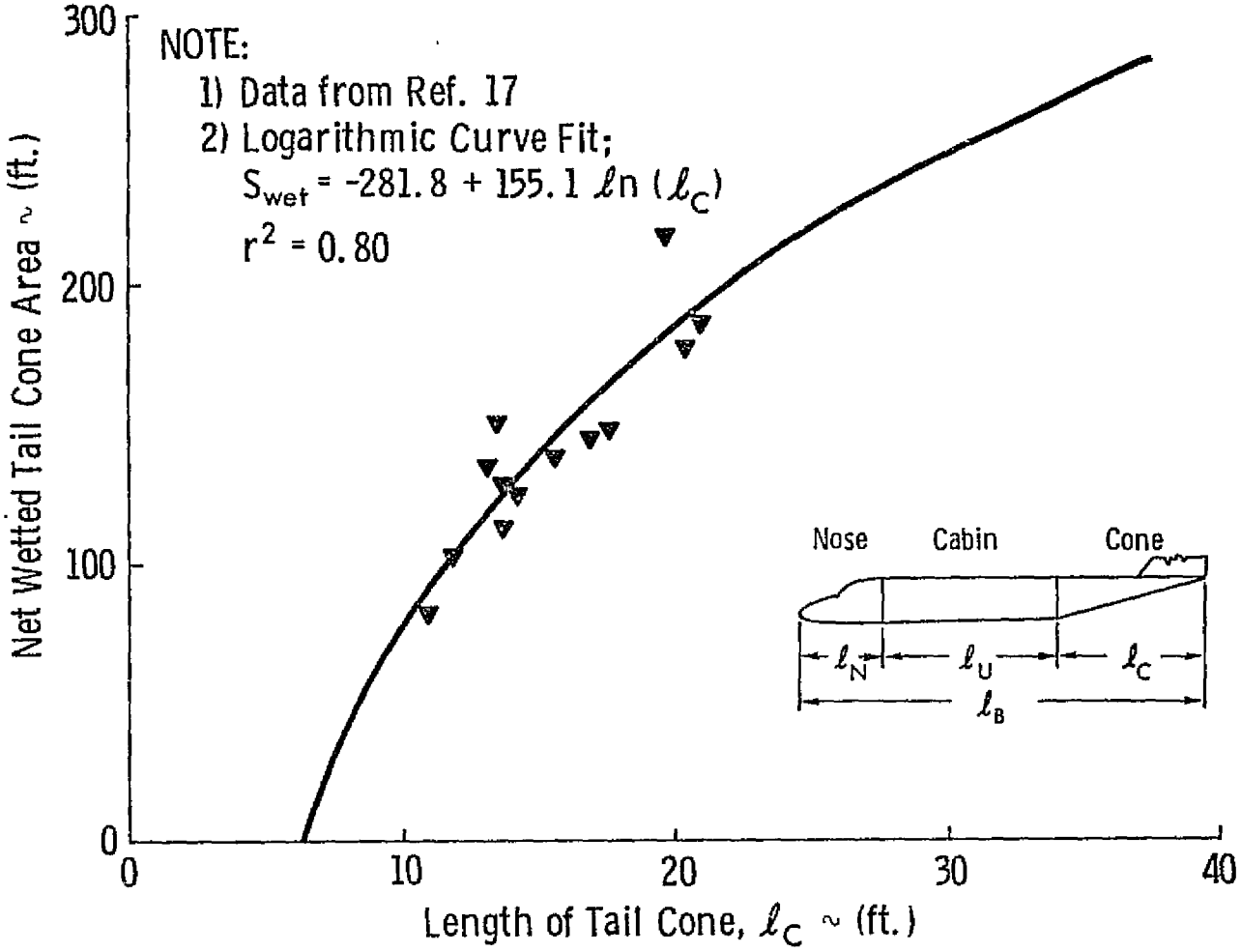

Figure 4.12 Logarithmic Correlation Between Tail Cone Length and Tail Cone Wetted Area

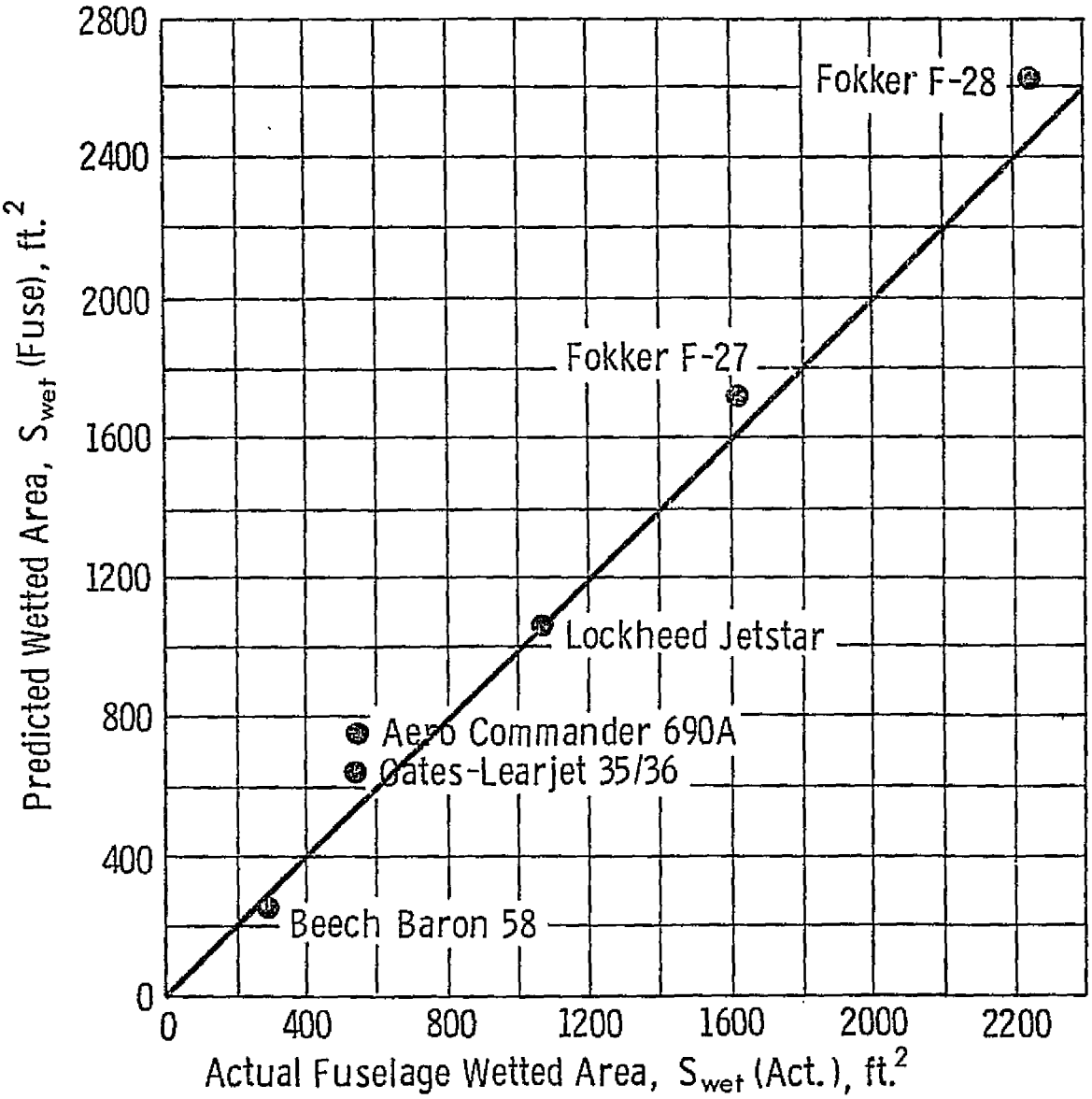

Figure 4.13 Comparison of Actual Fuselage Wetted Areas with Wetted Areas Predicted by FUSE

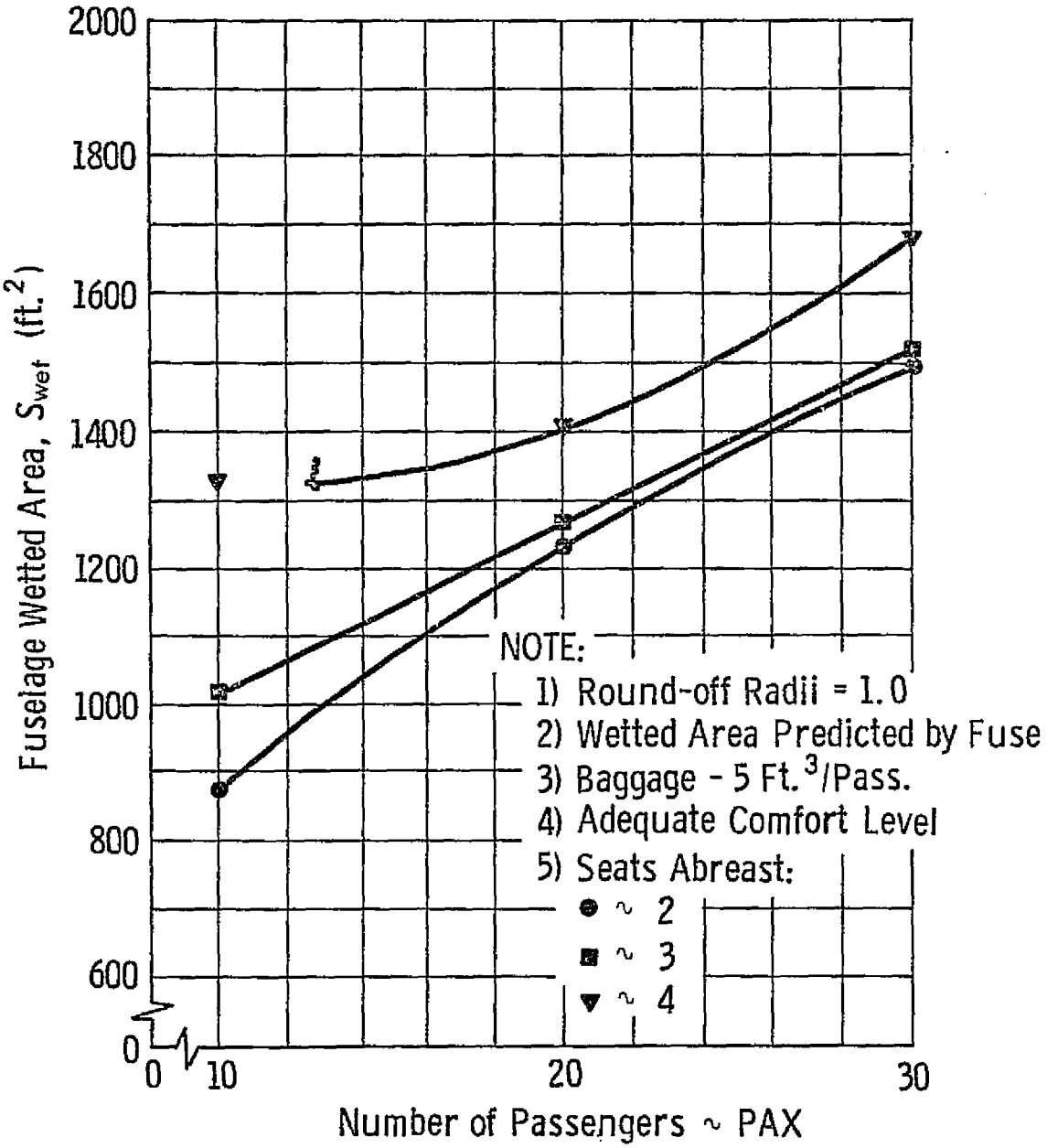

Figure 4.14 Gross Wetted Area as a Function of Passengers for Circular Fuselages

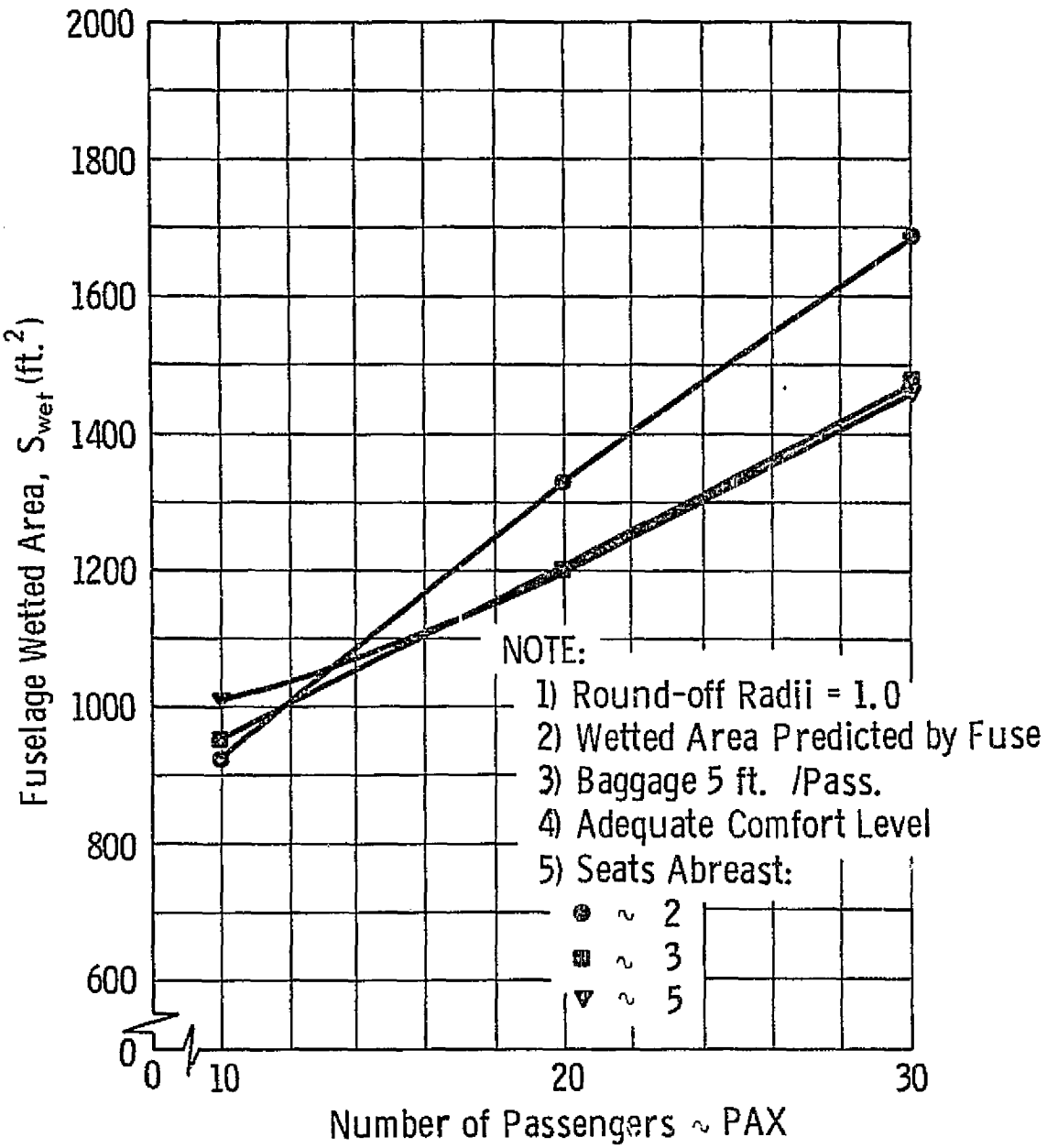

Figure 4.15 Gross Wetted Area as a Function of Passengers for Rounded-Rectangular Fuselages

wetted areas for the 2 and 3 seats abreast configurations are very close. Considering drag, in this case, the 2 seats abreast configuration is still best. A longer fuselage length results in higher Reynolds numbers and therefore lower skin friction coefficients. From a weight standpoint, as weight may be considered as proportional to wetted area to the power of 1.2, the 2 seats abreast configuration also prevails.

Figure 4.15 produced some rather unexpected results. Note here, that the wetted areas for the 2 seats abreast configurations rapidly become very much greater than the other seating arrangements. Checking Table 4.1, it is apparent that the nose cone lengths for this configuration appear overly large. This might indicate that the standard crewbox is too large for this configuration. Looking at the 3 and 4 seats abreast configurations, note that 4 seats abreast become more efficient, from a wetted area standpoint above 16 passengers. This could mean a drag trade-off as the 3 seats abreast configurations will have longer fuselages and therefore lower skin friction coefficients. From a weight standpoint the 4 seats abreast configuration is still preferable.

These assumptions and conclusions are of course based solely on the wetted areas. Such factors as comfort, pressurization, ease of construction, etc., should also be considered before selecting a configuration.

4.2 Approach to the Prediction of Zero-Lift Drag in a Propeller Slipstream

When a rotating propeller is working in the presence of a body (wing, nacelle, fuselage), the flow through the propeller disc and about the body will change. The flow through the propeller disc will change because it will work in a perturbed flow field. These perturbations alter the local angle of attack and effective airspeed at each blade section, and thus the overall propeller characteristics.

The flow over the body will change due to the existence of a slipstream. The body can be either immersed in the slipstream or be close to it; in either case the airflow about the body will change. As a result, lift and drag of the aircraft parts in the slipstream and propeller thrust and power-required will change.

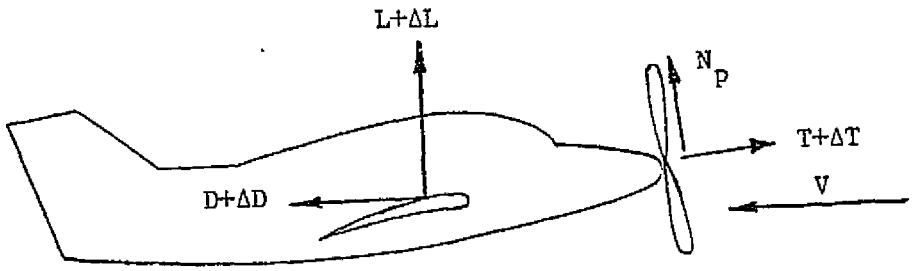

Figure 4.16 Change in Aerodynamic Forces due to the Slipstream

The lift dependent drag is affected by propeller power in the following ways:

1. The components of propeller thrust and normal force that are parallel to and have the same direction as the wing lift reduce the wing lift required, thereby reducing the wing drag due to lift. A method to compute the magnitude of this effect can be found in Reference 24.

2. The propeller slipstream modifies the downwash and dynamic pressure over portions of the wing thus changing the wing drag due to lift. Two different methods are available to compute the magnitude of this change in drag: a) Reference 25, Section 4.6.4 (essentially empirical) and b) theoretical methods, for example: Reference 26.

Sophisticated methods exist that predict lift dependent drag changes. Therefore, the topic of this investigation will be: changes in zero-lift drag and propeller performance.

4.2.1 Zero-Lift Drag

Methods to predict the increase in zero lift drag of bodies immersed in a propeller slipstream are presented in several publications. According to all these publications, the drag increase is proportional to the average increase in dynamic pressure in the slipstream and an appropriate drag area.

Reference 24:

$$\Delta C_{D_0} = \frac{1}{S q_\infty} \int_{S_I} C_{D_f} \Delta q_S \, dS \qquad (4.1)$$

where: $\Delta q_S = T/\pi R^2$

S_I = area, immersed in slipstream

Reference 28:

$$V_R = \sqrt{(V_0 + V_1 \cos\alpha_T)^2 + V_1^2 \sin^2\alpha_T} \qquad (4.2)$$

where: V_R = resultant velocity about body

$V_1 = \sqrt{V^2 + \frac{2T}{A\rho}} - V$

= average velocity increase in slipstream far behind propeller according to momentum theory.

Reference 27:

$$\eta_{eff} = F \times \eta_{is} \qquad (4.3)$$

where: $F = 1 - 1.558 \frac{\Sigma C_D S}{D^2}$

Except for an additional correction factor, this method is the same as the methods of References 24 and 28 because these can also be written as follows:

with: $\Delta q = T/\pi R^2$

$$F = 1 - \frac{4}{\pi} \frac{\Sigma C_D S_I}{D^2} \qquad (4.4)$$

$$\Delta D = \Delta q C_D S_I$$

Instead of $\frac{4}{\pi}$ a factor of 1.558 is used in the Reference 27 method (22% higher). In all these methods the slipstream is represented as shown in Figure 4.17.

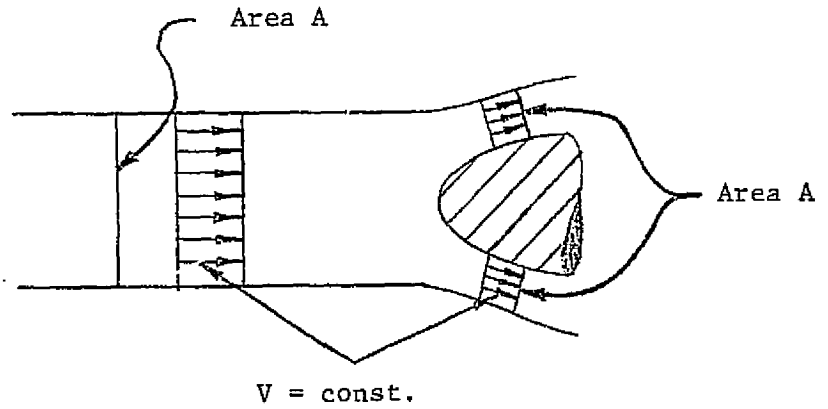

Figure 4.17 Representation of Slipstream

4.2.1.1 Theoretical Considerations

Theoretically it can be proven that the spanwise axial velocity distribution behind a propeller is as shown in Figure 4.18. These results have been verified experimentally.

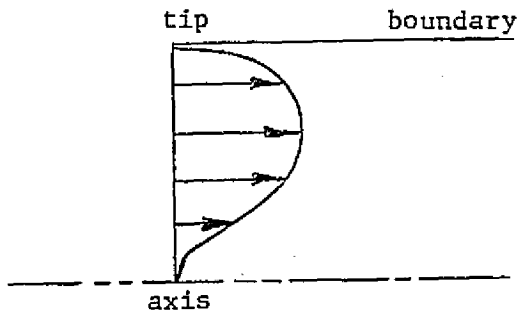

Figure 4.18 Spanwise Axial Velocity Distribution Behind a Propeller

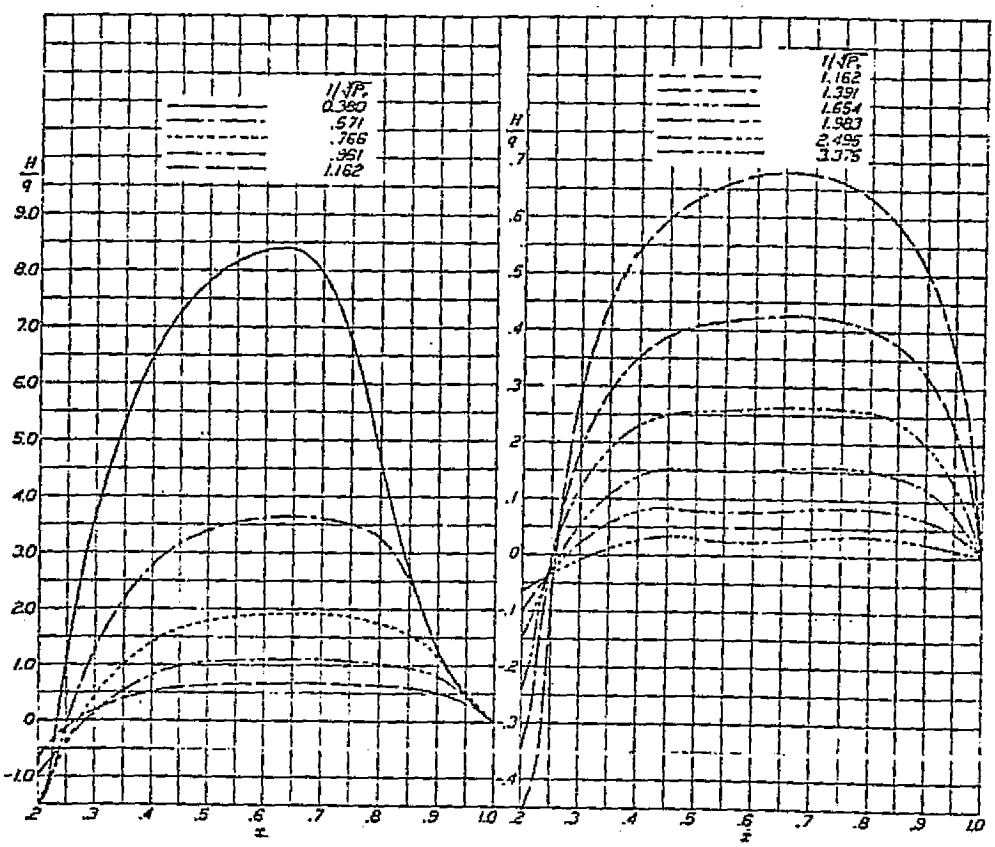

Figure 4.19 Curves of H/q against x for NACA cowling

Figure 4.19 (from Reference 29) shows distributions of total pressure increase (H) divided by q (ambient dynamic pressure).

Considering these curves it seems unlikely that both slender and wide bodies are equally affected (as far as drag increases are concerned) by a slipstream. This suspicion is reinforced by experimental results presented in Figure 4.20 from Reference 30.

Apparently, the drag increase of bodies with a small propeller (high d/D) is higher than the increase in zero lift drag of bodies with a larger propeller at the same conditions (i.e. same Δq_s and q_0)

N.B.: $T_{c_a} = \frac{\Delta q}{q_0} \frac{\pi}{8}$

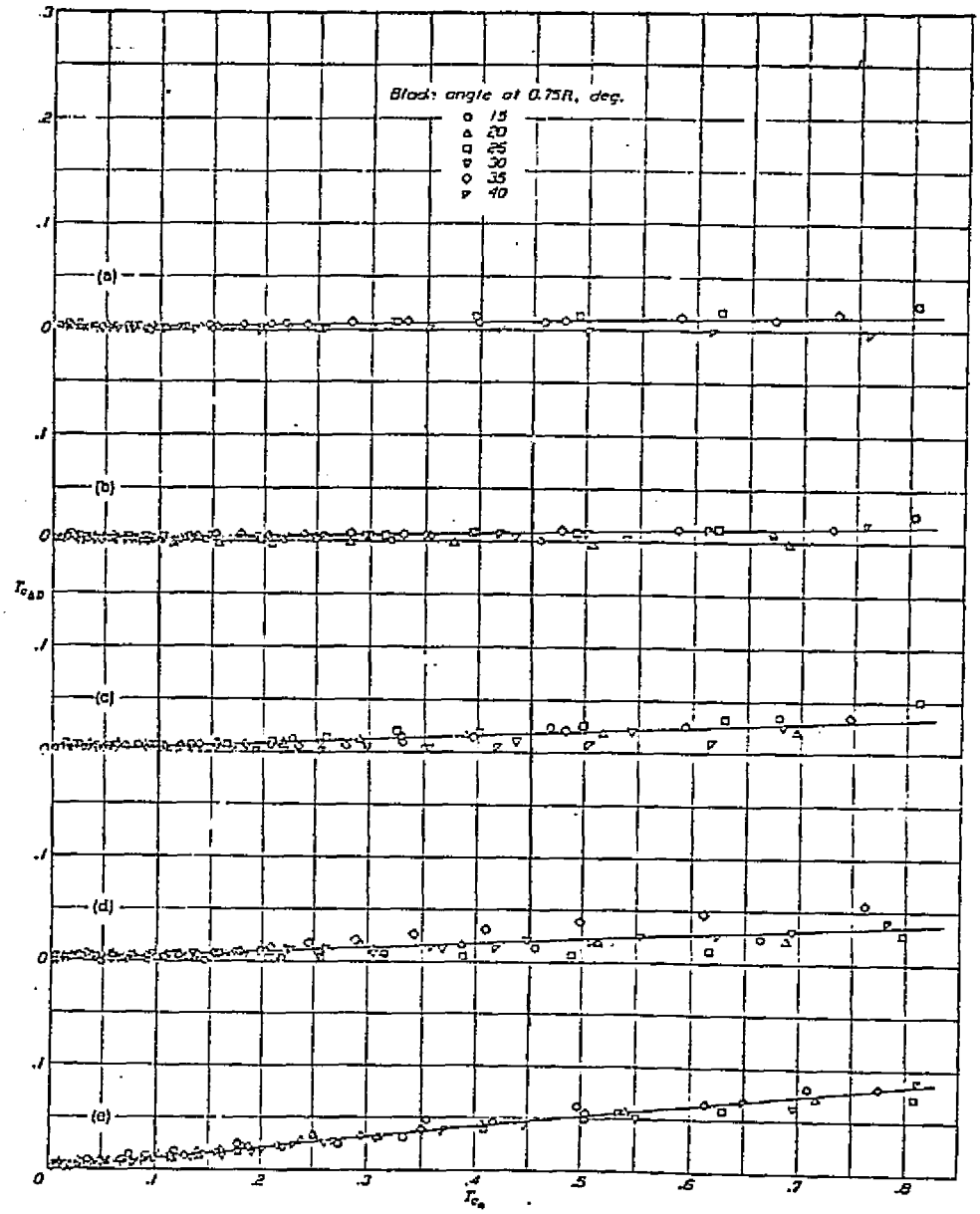

(a) 48-in. propeller; 12-in. nacelle (with spinner); d/D = 0.25
(b) 48-in. propeller; 12-in. nacelle; d/D = .25
(c) 48-in. propeller; 16-in. nacelle; d/D = .33
(d) 36-in. propeller; 12-in. nacelle; d/D = .33
(e) 36-in. propeller; 16-in. nacelle; d/D = .44

Figure 4.20 The variation of slipstream-drag coefficients with apparent propeller thrust-loading coefficients.

N.B. $T_{C_{\Delta D}} = \Delta D_{fus}/\rho V_0^2 D_p^2$ $\qquad T_{c_a} = T/\rho V_0^2 D_p^2$

An obvious explanation for this phenomenon has not been found.

It appears necessary to know the development of the slipstream in streamwise direction accurately, in order to provide better predictions of zero-lift drag increases than those presented in Reference 24.

Reference 29 presents dynamic pressure contours in the plane of the elevator hingeline of some propeller driven airplanes. Some of the results are shown in Figure 4.21.

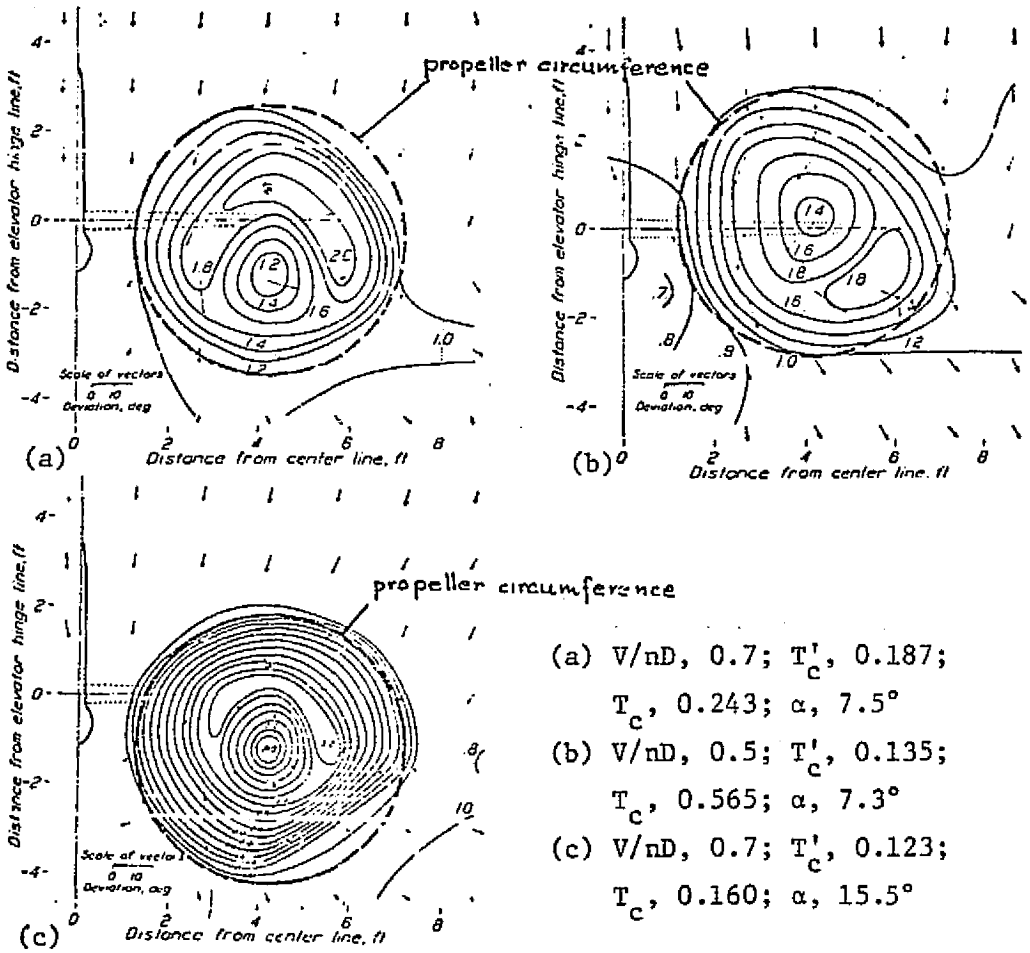

(a) V/nD, 0.7; T_c', 0.187; T_c, 0.243; α, 7.5°

(b) V/nD, 0.5; T_c', 0.135; T_c, 0.565; α, 7.3°

(c) V/nD, 0.7; T_c', 0.123; T_c, 0.160; α, 15.5°

Figure 4.21 Dynamic pressure (q/q_0) contours and inclination of the air stream in the plane of the elevator hinge line. Vectors show deviation of air flow from the free-stream direction. View looking forward. Circle shows projection of propeller center.

These figures show the velocity distribution in a cross-section of the slipstream some distance behind the propeller.

It can be seen that in this case (where the slipstream is not influenced by a body) the slipstream diameter some distance behind the propeller is still the same as the propeller diameter. The dynamic pressure distribution however is quite different from the one right behind the propeller, suggesting that mixing processes can be quite important. The results shown in Figure 4.22 are similar.

Such a slipstream development rules out quick, but accurate, predictions of its influence on drag.

Detailed theoretical or experimental investigations appear necessary to yield an accurate prediction method. A simplified approach is given in Section 4.2.1.2. At the moment, however, it seems best to use the average Δq (cross sectional) in ΔC_{D_0} calculations.

The use of this "easy" method seems even more attractive, after looking at Figures 4.23a and b, showing dynamic pressure contours of slipstreams that have been influenced by bodies.

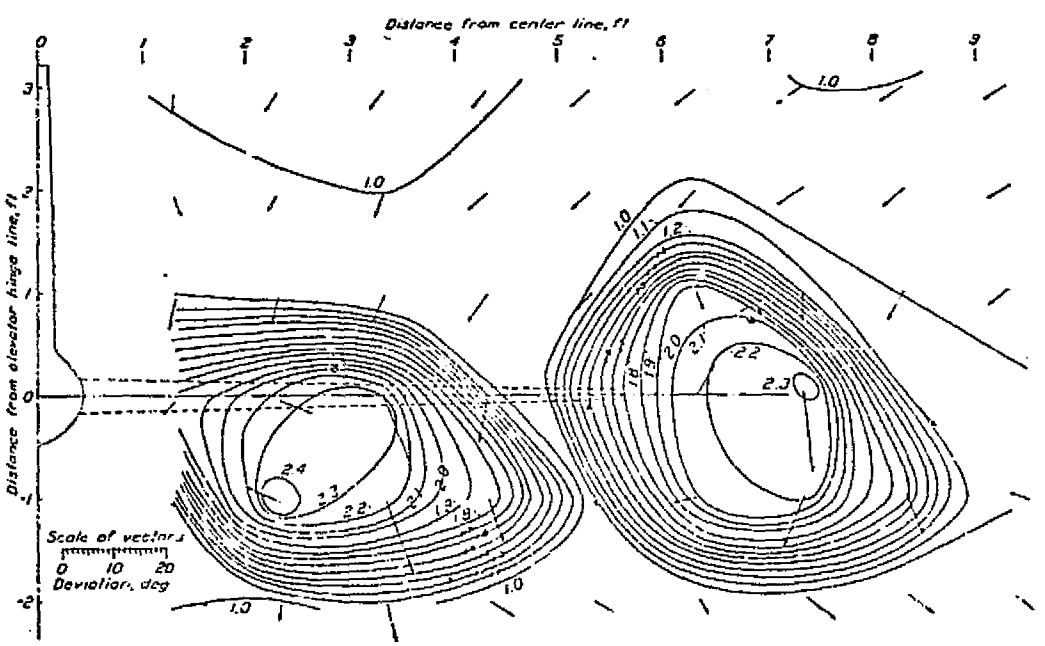

(a) V/nD, 0.489; T_c', 0.183; T_c,0.373; α, 4.1°

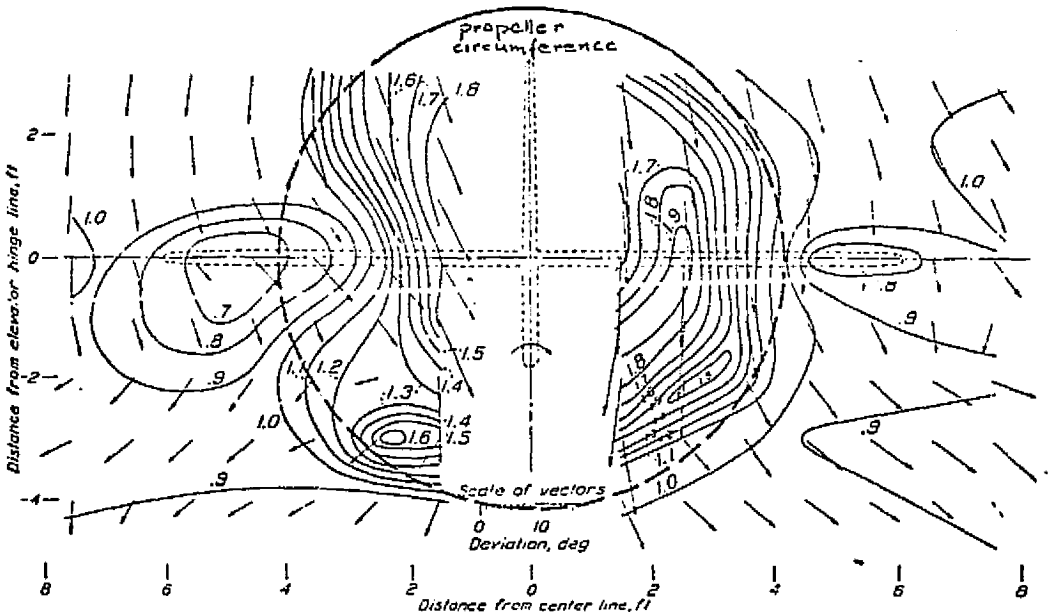

(a) With fillet and cowling; T_c', 0.165; T_c, 0.248; α, 13.7°

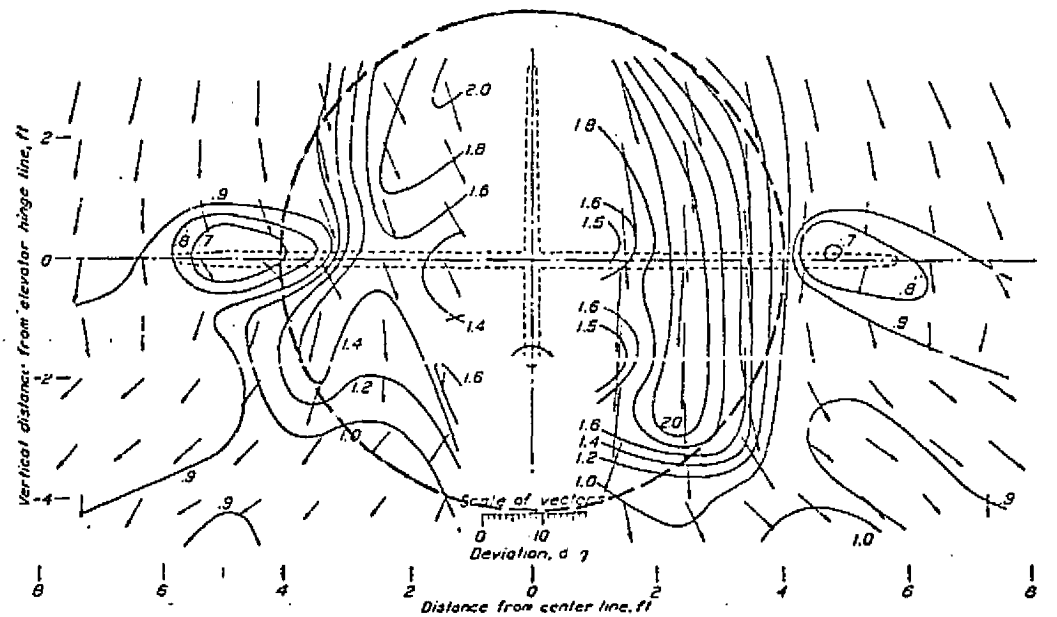

(b) Original condition; T_c', 0.194; T_c, 0.292; α, 13.7°

Figure 4.23 Dynamic pressure (q/q_0) contours and inclination of the airstream in the plane of the elevator hinge line. Vectors show deviation of air flow from the freestream direction. View looking forward. The McDonnell airplane.

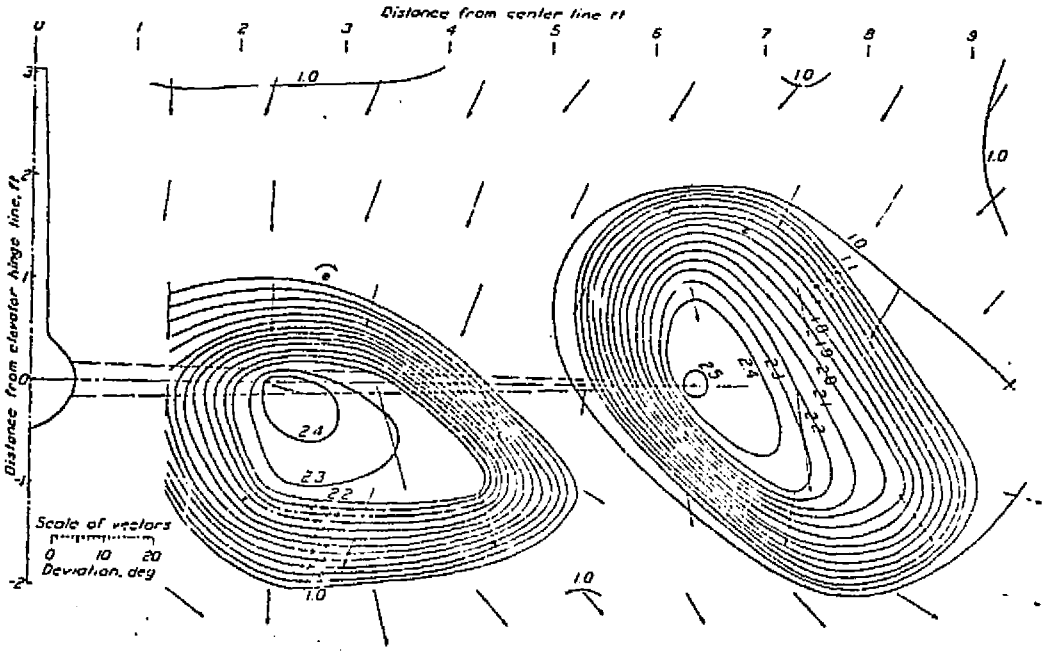

(b) V/nD, 0.170; T_c', 0.205; T_c, 0.418; α, 10.2°

Figure 4.22 Dynamic pressure (q/q_0) contours and inclination of the air stream in the plane of the elevator hinge line. Vectors show deviation of air flow from free-stream direction. View looking forward. Circles show projections of propeller centers. The four-engine pusher model.

It is hard to tell what the influence on fuselage drag is, of a slipstream, the dynamic pressure distribution of which has changed from the one shown at the beginning of this section, to the ones shown in Figure 4.23.

It is therefore suggested to use an average $\Delta q_S = T/\pi R^2$ in ΔC_{D_0} calculations, possibly together with one of the following correction factors:

$$\Delta D = \Delta q_S \, C_D S_I \times k \qquad (4.5)$$

where $\Delta q_S = T/\pi R^2$

$k = 1$ (Reference 24)

or: $k = 1.224$ (Reference 27)

or: k 5.8 d/D (Reference 30)

An attempt has been made to show that dynamic pressure changes in streamwise direction due to mixing, etc. do exist and make accurate drag predictions virtually impossible (i.e. in a fast and simple way). But, even when a very simple theory is used (Momentum Theory), neglecting all effects like mixing and viscosity, it can be shown that the dynamic pressure (and static pressure) change in streamwise direction (Figure 4.24).

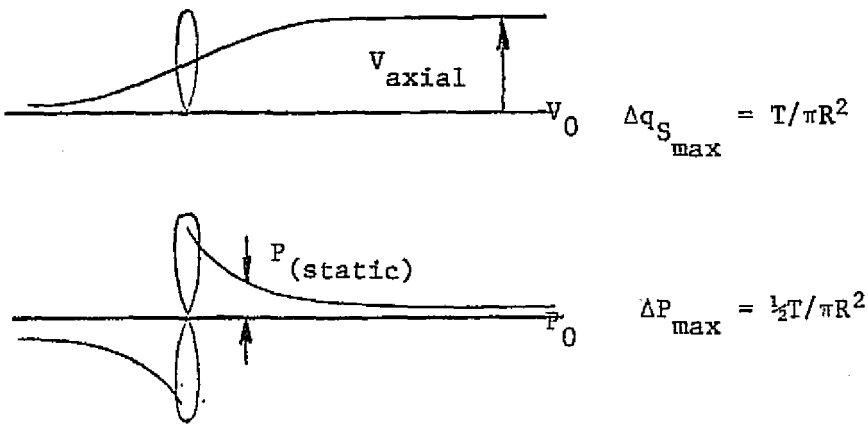

Figure 4.24 Change in Pressure Behind a Propeller

In the region of the fuselage nose, Δq_S is apparently lower than far behind the propeller, while ΔP_S is higher. The influence of both effects on fuselage drag however can be approximated by assuming that $\Delta P = 0$ and Δq_S = constant = Δ_q far behind propeller. This assumption might lead to erroneous results when short fuselages with a blunt nose are considered.

4.2.1.2 A Simplified Approach to Zero-Lift Drag Prediction

An approach to the zero-lift drag prediction problem might be:

1. Calculate velocity distribution in slipstream (using continuity expression).
2. Determine dV/ds at nacelle boundary (s = distance to nacelle boundary) (Inviscid).
3. Determine influence of dV/ds on boundary layer development and wall skin friction.

This approach has not been developed completely. The following explanations might help in such a development.

If local speed at a particular blade section is $V_0+V_{a_i}$, then there must be a speed $V_0+2V_{a_i}$; in the fully developed slipstream. These speeds are along one slipstream line.

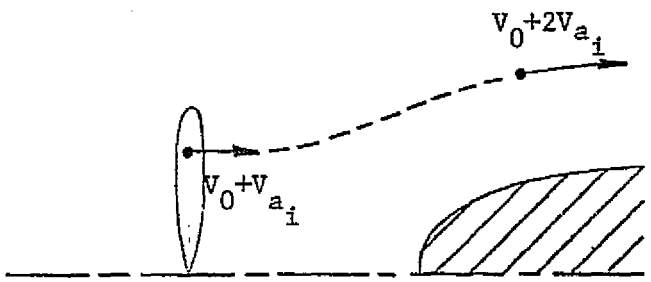

Figure 4.25 Velocity Profile in a Slipstream

With the continuity expression it follows: (4.6)

$$\rho\pi(r_{pi}^2 - r_{pi-1}^2) \times V^2_{Pav.\,r_{pi}-r_{pi-1}} = \rho\pi(r_{s_i}^2 - r_{s_{i-1}}^2) \times V^2_{sav.\,r_{s_i}\to r_{s_{i-1}}}$$

where: r_{pi-1} and r_{pi} are ends (inboard and outboard) of a blade section.

$V_{Pav.\,r_{pi}-r_{pi-1}}$ = average speed at this blade section = $V_0+V_{a_i}$

$r_{s_{i-1}}$ and r_{s_i} are boundaries of streamline tube (boundaries of which at propeller disc are: r_{pi-1} and r_{pi}) in slipstream.

$V_{sav.\,r_{s_i}\to r_{s_{i-1}}}$ = average speed through this streamline tube = $V_0+2V_{a_i}$

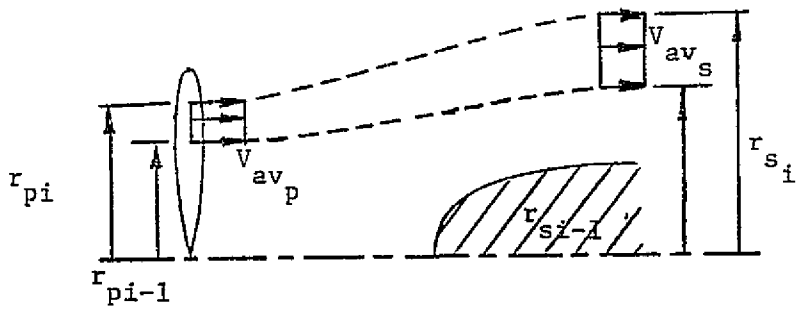

Figure 4.26 Velocity Profile in a Streamline Tube

Therefore: $(r_{pi}^2 - r_{pi-1}^2) \times (2V_0 + V_{a_i} + V_{a_{i-1}})^2 =$ (4.7)

$$(r_{s_i}^2 - r_{s_{i-1}}^2) \times (2V_0 + 2V_{a_i} + 2V_{a_{i-1}})^2$$

With the known axial velocity distribution at the propeller disc (theory or experiments), the velocity distribution in the slipstream about a nacelle can be obtained by numerical integration.

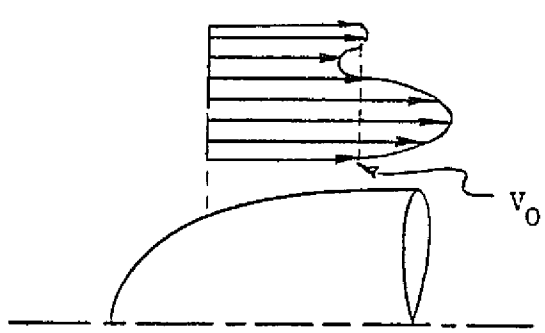

Figure 4.27 Velocity Distribution in the Slipstream Around a Nacelle.

At nacelle boundary: $V = V_0$ (inviscid!).

According to boundary layer theory:

$$\int_0^{\delta} \left(\frac{\partial u}{\partial x} + \frac{\partial v}{\partial y}\right) dy = 0 \rightarrow V(\delta) - V(0) = -\int_0^{\delta} \frac{\partial u}{\partial x}\, dy \qquad (4.8)$$

N.B. δ is distance to wall, where viscous speed u is equal to inviscid local speed U = speed according to 1 of Section 4.2.1.2.

$$\int_0^{\delta} \left\{\frac{\partial}{\partial x}(u^2) + \frac{\partial}{\partial y}(uv) - u\frac{\partial u}{\partial x} - \nu\frac{\partial^2 u}{\partial y^2}\right\} dy = 0 \qquad (4.9)$$

where: $-\nu\int_0^{\delta} \frac{\partial^2 u}{\partial y^2}\, dy = \nu\left\{\left(\frac{\partial u}{\partial y}\right)_0 - \left(\frac{\partial u}{\partial y}\right)_{\delta}\right\} = \frac{\tau_0}{\rho} - \nu\left(\frac{\partial u}{\partial y}\right)_{\delta}$

Rewritten:

$$-\frac{\partial}{\partial x}\left\{\int_0^{\delta} u(U-u)dy\right\} - \frac{\partial u}{\partial y}\int_0^{\delta}(U-u)dy - \nu\left(\frac{\partial u}{\partial y}\right)_{\delta} = -\frac{\tau_0}{\rho} \qquad (4.10)$$

Assuming that U hardly changes over the boundary layer, and that $\frac{du}{dy} \neq 0$ and can be determined by the method explained in Section 3.1.2.1, the increment in skin friction drag can be determined using boundary layer theory.

A first order approximation (assuming velocity profile in boundary layer doesn't change) is:

$$\Delta\tau = \rho\nu\left(\frac{\partial u}{\partial y}\right)_{\delta} = \zeta\nu\left(\frac{\partial u}{\partial y}\right)_{\substack{\text{at wall}\\ \text{according}\\ \text{to } \underline{1}}} \qquad (4.11)$$

Reference 30 presents a method to compute changes in lift due to a propeller slipstream. In the first part of the method velocities at the propeller disc and in the slipstream (including swirl) are calculated. This method is more complicated than the one explained above, but could also be used instead of the method in Section 3.1.2.1 to yield similar results.

4.2.2 Propeller Blockage.

Only Reference 27 gives a method to account for propeller blockage effects:

$$J_{eff} = (1-h)\, J_{is} \qquad (4.12)$$

where $J_{is} = \frac{V_0}{nD}$

$$1-h = 1-.32g\,\frac{S}{D^2}$$

By using J_{eff} instead of J_{is} in propeller performance charts (for isolated propellers), thrust and power required of a propeller (operating in a flowfield that is perturbed by a body) can be found.

4.2.2.1 Theoretical Considerations.

In the presence of a body, the axial velocity relative to a blade section is not the velocity of advance V_0 but a velocity u caused by the blocking effect of the body. As a result, the geometric pitch will be modified:

instead of: $P/D = V/nD$ (4.13)

$P/D\ V/u = V/nD$

It means that the blade sections will work at a different angle of attack.

According to Reference 29, the true propeller efficiency may be computed according to the following relation:

$$\eta = \eta_{is} \frac{\int_0^1 \frac{u}{V}\frac{dC_T}{dx}\,dx}{\int_0^1 \frac{dC_T}{dx}\,dx} \qquad \text{(Approximate!)} \qquad (4.14)$$

In order to calculate η, both the velocity distribution through the propeller disc and the spanwise propeller load distribution have to be known. Both can be found either experimentally or theoretically. A Blade-Element theory could be used to predict theoretical load distribution. Source-sink distributions can be convenient when calculating velocity distributions in the propeller disc. Figure 4.28 shows the body shapes that can be simulated by a combination of 1 sink and 1 source.

Figure 4.29 shows some u/v distributions in the propeller disc according to this potential flow theory.

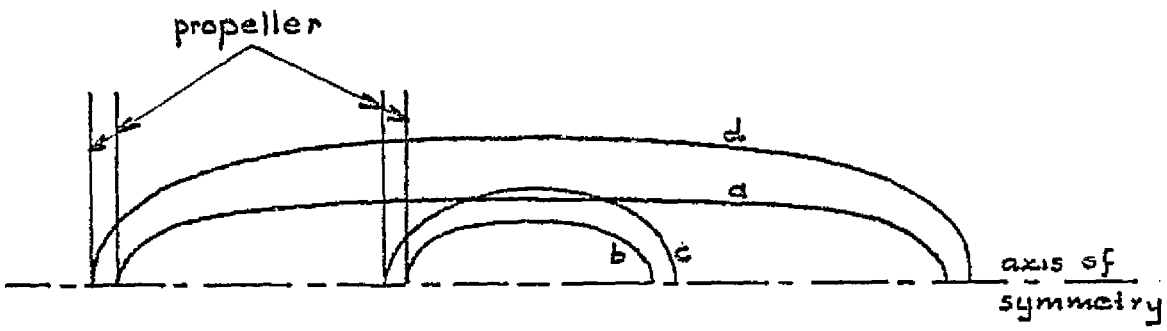

Figure 4.28 Body Shapes Simulated by a Source/Sink Combination

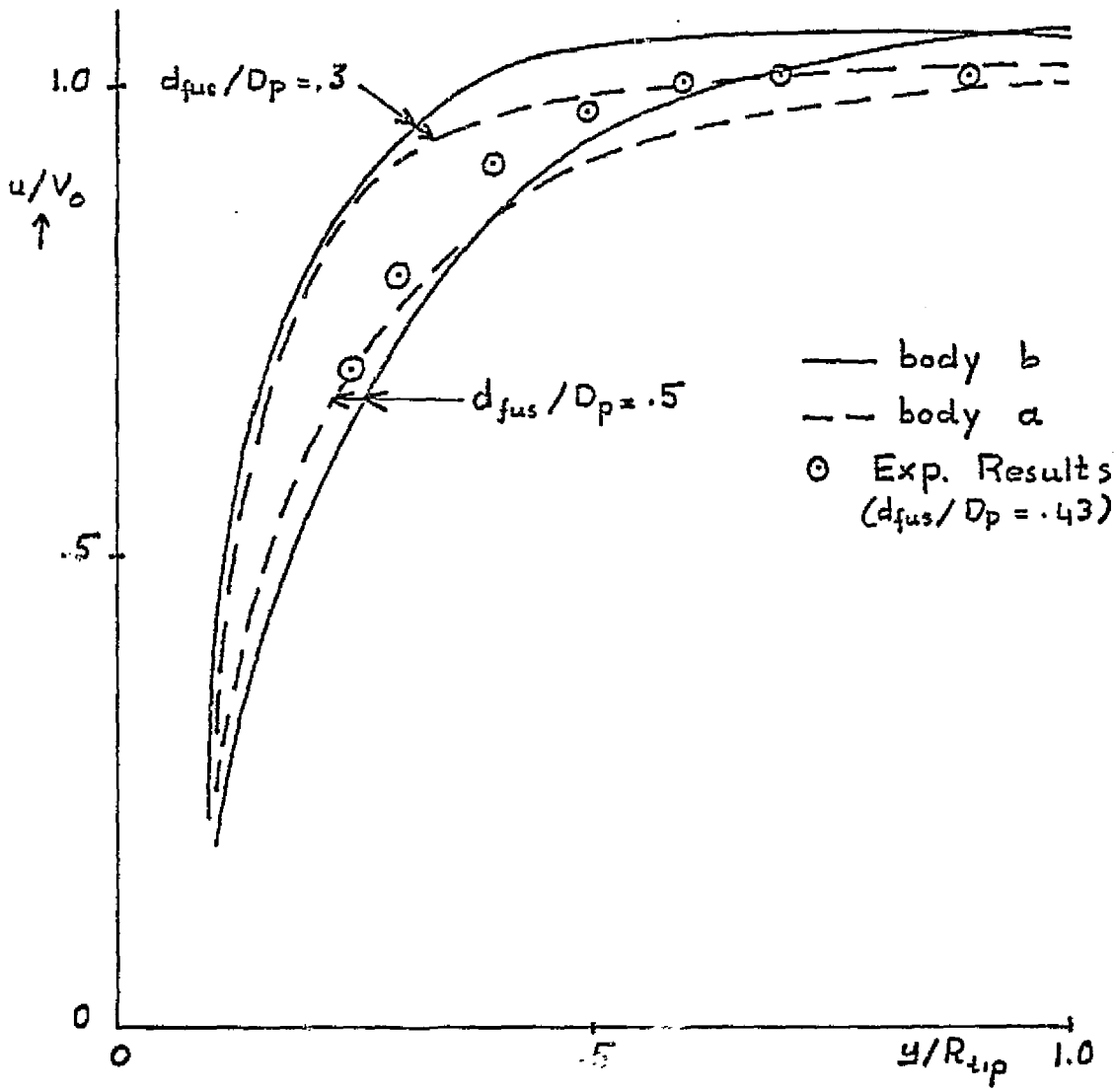

Figure 4.29 Velocity Distributions in the Propeller Disc by Potential Flow Theory

4.2.2.2 Experimental Results.

Some of the results presented in Reference 29 are shown in Figure 4.30.

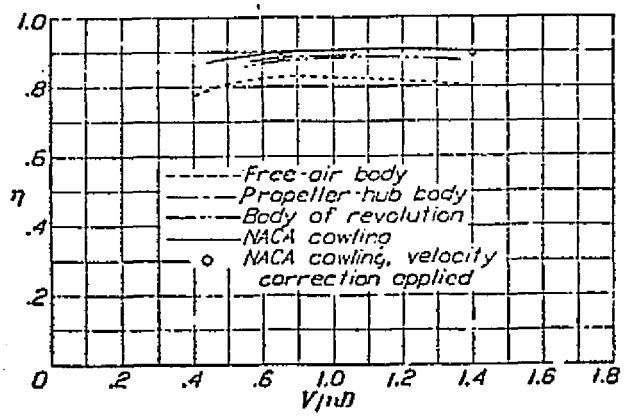

Figure 4.30 Comparison of apparent propeller efficiency envelopes for four body shapes.

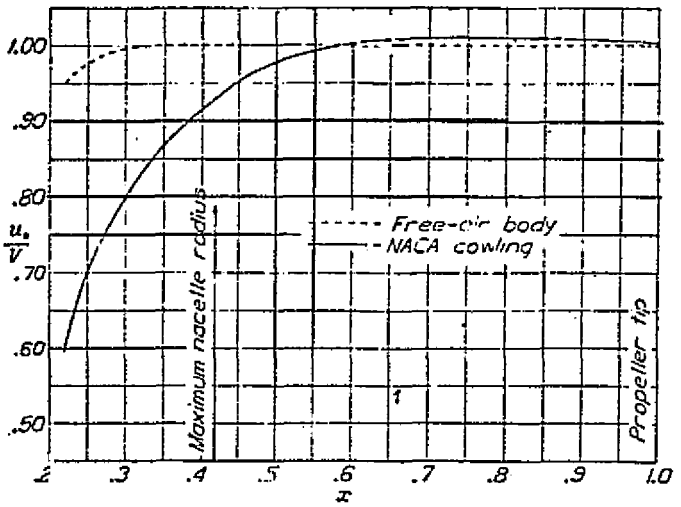

Figure 4.31 Velocity distribution of propeller (propeller removed). V, 93 miles per hour.

Depending on the accuracy required, either the method of Reference 26 can be used, or a blade element theory combined with a method that predicts velocity distributions in the propeller disc.

Further studies should be conducted to develop this approach to the estimation of slipstream drag (along with the approach of Reference 26) into a programmable method. Eventually the intent is to include this method into the drag estimation portion of the GASP.

CHAPTER 5 THE GENERAL AVIATION SYNTHESIS PROGRAM, GASP

As has been stated at several points throughout this report, the means by which all of the design optimization methods were to be implemented was the General Aviation Synthesis Program (GASP) developed for the NASA-Ames research center by the University of Minnesota. The KU-FRL research staff has been working continuously now for approximately one year to put an up-to-date version of the GASP into an operational status on the University of Kansas Honeywell 66/60 computer. At this time the program is still not implemented on the University of Kansas facilities, although it is believed that for reasons that will be explained in the next section, this will be accomplished in the near future.

The difficulties encountered in putting the GASP into operational status have also prevented the KU-FRL research staff from making revisions to the GASP to reflect the research that has been completed. This chapter will therefore discuss, first, the steps taken in attempting to transliterate the GASP, in Section 5.1, and second, how the design constraints were to be implemented in the GASP, in Section 5.2.

5.1 Transliteration Process

A copy of the GASP was first received at the KU-FRL in June 1976. The program was forwarded to the KU-FRL by Tom Galloway at NASA-Ames on magnetic tape. Also provided with the magnetic tape were a complete listing, a copy of Reference 31 describing the general flow of the program, a description of input parameters, and a sample output. Unfortunately, the magnetic tape parity was incompatible with the University of Kansas computer system. The Tape was returned to NASA-Ames for a copy with the proper parity. The new magnetic tape was in the following format:

- IBM compatible
- 9-track

- 1600 BPI
- EBCDIC -80 BYTE records
- No Label
- Even Parity

Transliteration procedures were started for this tape; and although all compilation errors were finally eliminated, the program could not be coerced to execute. At that time no explanation was available.

A card deck version of the GASP was acquired from the Cessna Aircraft Company with the assistance of Don Halverstadt. This version was designed to be run on an IBM 360 computer system. After completing preliminary transliterations it was determined that the free-field input routines of this version and the previous NASA version were incompatible with the Honeywell 66/60 system. The Cessna input routines proved easier to revise. In early March two runs were made of the Cessna version with only minor difficulties.

The Cessna version of the GASP was an older version and consequently it became necessary to update the program to reflect NASA revisions. Revisions were made to the program using the Honeywell 66/60 timesharing system editor and by storing the GASP on disc subroutine by subroutine. This process was proving to be extremely time consuming with no guarantee of success. It was decided to acquire a new magnetic tape from NASA-Ames with the intent of splicing the revised Cessna input routines onto a transliterated NASA version. This was the status at the end of June 1977. Fiscal year end administration difficulties prevented the completion of this process.

Negotiations have been carried out with the University of Kansas Computation Center to gain what is referred to as "internal project status" for the GASP. This status has now been assigned by the computation center, and they will implement the program using its more experienced staff at no charge.

Previously it was understood that such status would not be possible for the GASP. To have the GASP implemented on an "external project status" would have resulted in prohibitive costs. It is expected that the GASP will be finally operational by the end of September.

5.2 Implementation of Design Constraints

In Chapter 1 it was assumed that the aircraft configuration could be designed to meet four specific constraints:

a) Utility Constraints
b) Stability and Control Constraints
c) Mission Constraints
d) Performance Constraints

The GASP already will account for the last two constraints adequately and therefore those constraints will not be discussed here. The utility and stability and control constraints were in need of some revision, however. The methods that were to be used to revise the GASP accordingly will be discussed in the following paragraphs.

5.2.1 Cabin-Utility Constraints

In Chapter 2 a number of methods for sizing for the utility constraints were discussed. These methods were brought together in the form of the design mode of the program FUSE. It was intended to replace the fuselage sizing portion of the subroutine SIZE in the GASP with a call to a subroutine FUSIZE. FUSIZE would have consisted of the design mode and wetted area calculation portion of FUSE. This could have been readily implemented with one minor exception. The Honeywell 66/60 allows only 59 arguments for SIZE. This would mean that to add the needed data for FUSIZE, a namelist input method would be necessary. This, however, should present no great difficulties.

5.2.2 Stability and Control Constraints

Two forms of stability and control constraints were considered for implementation in the GASP--static constraints and dynamic constraints. The methods that were considered for each will be discussed in turn.

The static stability and control constraints that were considered were: longitudinal static stability in the stick-fixed case, implemented through C_{m_α}; and directional static stability, implemented through C_{n_β}. Both constraints were to have been accomplished in the empennage sizing process in the following manner. The first time the SIZE is called, the weight and c.g. data are usually lacking. As the c.g. location is required for both constraints, it was intended to use $\bar{V}$ methods to size the empennage. The next time SIZE is called, when a c.g. location is known, the subroutines STABAREA and VERTAREA (Section 2.3) would be used to size the horizontal and vertical tails for the stability constraints. In this manner the preliminary use of a $\bar{V}$ method would provide the required "seeds" for the iterative processes of STABAREA and VERTAREA.

The dynamic stability and control characteristics presented more of a problem. To determine the dynamic characteristics of the aircraft all of the non-dimensional stability and control derivatives, and the airplane inertias must be known. It was intended that rather than to attempt to constrain the design for dynamic characteristics, the configuration would simply be analyzed for dynamic stability and control characteristics. To accomplish this the non-dimensional derivatives would be determined using the methods of Reference 14, and the analysis would be implemented by appending the appropriate portion of the program described in Reference 32 to the GASP. An inertia determining routine would also be required, but this was not felt to present any great difficulty.

These characteristics, plus a number of others, will be the subject of the next chapter.

CHAPTER 6 PROPOSED FUTURE RESEARCH

With the exception of integrating the design methods into the GASP, most of the design constraints mentioned in Chapter 1 were accounted for. Only the stability and control constraints have not been adequately enforced. Considering this, a proposal for the continuation of the project was submitted to NASA-Ames (Reference 33), placing sole emphasis on stability and control methods. This chapter will present what is essentially a reprint of the statement of work of that proposal.

Care will be exercised not to duplicate any work already done in this area by other GASP investigators.

6.1 Objectives

It is proposed that work on the design optimization of short haul and commuter airplanes be continued with the following objectives:

a) To determine those stability and control characteristics which are critical to the preliminary design process.

b) To evaluate stability and control analysis methods currently available to determine those methods most appropriate for the preliminary design function which GASP performs.

c) To determine how the methods of b) may be used to provide the proper constraints and/or analysis functions for GASP.

d) To develop the appropriate subroutines for the methods of c) and how they may be appended into GASP.

In line with these objectives, emphasis will be placed on the stability and control characteristics of both jet and propeller driven airplanes. Also specific attention will be given to the determination of the following stability and control characteristics in the preliminary design process:

a) Static longitudinal stability;

b) Static directional stability;

c) Engine-out control;

d) Calculation of rotation velocity, V_R;

e) Longitudinal dynamic stability;

f) Lateral-directional dynamic stability;

g) Trim at low speed and forward C.G.

The following section will outline briefly the approach that will be taken to meet the objectives with respect to the above stability and control characteristics.

6.2 Stability and Control Analysis Methods

The primary references that will be used to determine and evaluate the stability and control analysis methods will be References 9, 14, 24, and 34. In the following paragraphs each of the stability and control characteristics listed in the previous section and its proposed analysis method will be discussed briefly.

6.2.1 Static Longitudinal Stability

Using the methods of References 14 and 34, the configuration will be analyzed for static margin (dC_m/dC_L), static longitudinal stability (C_{m_α}), and the neutral point for both and stick-fixed and stick-free cases. To facilitate the calculation of these values a simple Multhopp integration procedure for the body (and engine nacelles in the case of wing-mounted engines; see Section 2.3) will be used. Correlations with on-hand tunnel data actual configurations will be made.

Using Equation 4.35 on page 4.23 of Reference 34, the stick-fixed neutral point will be defined as in Equation 6.1. The stick-free neutral point will be defined by Equation 5.99 on page 5.47 of Reference 34 as shown in Equation 6.2. In both cases the variables are as defined in Reference 34.

Stick-Fixed Case:

$$\bar{X}_{c.g.(C_{m_\alpha}=0)} = \text{N.P.} = \frac{\bar{X}_{AC_{WB}} + \frac{C_{L_{\alpha_H}}}{C_{L_{\alpha_{WB}}}} \eta_H \frac{S_H}{S} \bar{X}_{AC_H}\left(1 - \frac{d\varepsilon}{d\alpha}\right)}{1 + \frac{C_{L_{\alpha_H}}}{C_{L_{\alpha_{WB}}}} \eta_H \frac{S_H}{S}\left(1 - \frac{d\varepsilon}{d\alpha}\right)} \quad (6.1)$$

Stick-Free Case:

$$\bar{X}_{c.g.(C_{m_\alpha}=0)} = \text{N.P.} = \frac{\bar{X}_{AC_{WB}} + \frac{C_{L_{\alpha_H}}}{C_{L_{\alpha_{WB}}}} \eta_H \frac{S_H}{S} \bar{X}_{AC_H}\left(1 - \frac{d\varepsilon}{d\alpha}\right)\left(1 - \frac{C_{h_\alpha} T_E}{C_{h_{\delta_e}}}\right)}{1 + \frac{C_{L_{\alpha_H}}}{C_{L_{\alpha_{WB}}}} \eta_H \frac{S_H}{S_H}\left(1 - \frac{d\varepsilon}{d\alpha}\right)\left(1 - \frac{C_{h_\alpha} T_E}{C_{h_{\delta_e}}}\right)} \quad (6.2)$$

Propeller effects will be accounted for using the method of Reference 34, Chapter 4.

6.2.2 Static Directional Stability

Values for static directional stability, C_{n_β}, will be computed using the methods of References 9 and 14. Also propeller effects on directional stability will be considered using the methods of References 9, 24, 34, and 35.

6.2.3 Engine-Out Control

The methods of References 9 and 34 will be used to analyze the configuration for the minimum engine-out control speed, V_{mc}. Engine-out control will be considered from both the single-degree-of-freedom

and three-degree-of-freedom points of view. Drag due to stopped engines and/or propeller will be accounted for.

6.2.4 Calculation of Rotation Velocity, V_R

The speed required to rotate on take-off, V_R, will be calculated using the method of Reference 9.

6.2.5 Dynamic Longitudinal Stability

Dynamic longitudinal stability characteristics will be considered using the methods of both References 9 and 34 for the stick-fixed case. The dynamic longitudinal stability characteristics upon which primary emphasis will be placed will be the short period damping and undamped natural frequency. Phugoid damping and frequency will also be considered. The methods considered will include both the two-degree-of-freedom short period and phugoid approximations and the complete three-degree-of-freedom solutions of Reference 34. Also the relatively simple dynamic stability relationships of Torenbeek in Chapter 9 of Reference 9 will be investigated as to their validity.

One possible method for analyzing a configuration for dynamic stability in the GASP that will be considered will be a revised version of the dynamic stability and control analysis program document in Reference 32.

6.2.6 Lateral-Directional Dynamic Stability

In analyzing the dynamic lateral-directional stability the characteristics of the spiral, roll, and dutch roll modes will be considered. Using the methods of Reference 34, these methods will be analyzed from the approximate and complete three-degree-of-freedom points of view.

REFERENCES

1. Roskam, J., et. al.; "A Study of Commuter Airplane Design Optimization", Modified Proposal to NASA-Ames Research Center; February 1976.

2. Roskam, J., et. al.; "A Study of Commuter Airplane Design Optimization", Continuation Proposal to NASA-Ames Research Center; December 1976.

3. Loftin, Laurence; "A Rapid Method for Estimating the Performance and Size of Propeller Driven Aircraft"; NASA-Langley; April 1973.

4. Galloway, Tom; Correspondence of August 10, 1976.

5. Schoen, A. H., "User's Manual for VASCOMP II - The V/STOL Aircraft Sizing and Performance Computer Program, Vol. VI"; The Boeing Co., Vertol Div.; Boeing Document D8-0375; March 1968, revised October 1971.

6. Anonymous; "Analysis of Operational Requirements for Medium Density Air Transportation - Final Report"; Douglas Aircraft Company; Douglas MDC-J4484, NASA CR-137604; March 1975.

7. Anonymous; "Study of Short-Haul Aircraft Operating Economics - Final Report"; Douglas Aircraft Company; Douglas MDC-J6970, NASA CR-137685; September 1975.

8. Anonymous; "Operational Factors of Air Service to Small Communities - Final Report"; Douglas Aircraft Company; Douglas MDC J7131, NASA CR-137820; December 1975.

9. Torenbeek, E.; Synthesis of Subsonic Airplane Design, Delft University Press, 1976.

10. Roskam, J.; "Handbook of Aircraft Design Data - Part III Fuselage and Cockpit Arrangements and Interior Dimensions"; The University of Kansas Department of Aerospace Engineering, Lawrence, Kansas; August 1975.

11. Roskam, J. and Fillman, G.; "Design for Minimum Fuselage Drag"; Journal of Aircraft, Vol. 13, No. 8, pg. 639; August 1976.

12. Roskam, J.; Methods for Estimating Drag Polars of Subsonic Airplanes; Roskam Aviation and Engineering Corporation, Lawrence, Kansas ; 1971.

13. Corning, G.; Supersonic and Subsonic, CTOL and VTOL, Airplane Design; Published by the author; 1960.

14. Roskam, J.; Methods for Estimating Stability and Control Derivatives of Conventional Subsonic Airplanes; Roskam Aviation and Engineering Corporation, Lawrence, Kansas; 1971.

15. Roskam, J., Wyatt, R. D., et. al.; "A Study of Commuter Airplane Design Optimization", Second Status Report on NASA Grant NSG-2145, Kansas University Flight Research Laboratory Report No. KU-FRL 902; December 1976.

16. Galloway, Tom; Correspondence of October 19, 1976.

17. Roskam, J., Wyatt, R. D., et. al.; "A Study of Commuter Airplane Design Optimization", First Status Report on NASA Grant NSG-2145, Kansas University Flight Research Laboratory Report No. KU-FRL 901; June 1976.

18. Anonymous; "PLOT-10 Terminal Control System User's Manual"; Tektronix, Inc.; Document No. 062-1474-00; Beaverton, Oregon; July 1976.

19. Wyatt, R. D.; "A Computer Program for Commuter Aircraft Fuselage Shape Simulation"; Kansas University Flight Research Laboratory Report No. KU-FRL 313-3; May 1977.

20. Smetana, Frederick O., et. al.; "Light Aircraft Lift, Drag, and Moment Prediction - A Review and Analysis"; North Carolina State University; NASA CR-2523, May 1975.

21. Loftin, Laurence; "The Sizing of Propeller-Driven Aircraft"; NASA-Langley, Unpublished.

22. Loftin, Laurence; "A Rapid Method for Estimating the Size and Performance of Jet-Powered Aircraft"; NASA-Langley; Unpublished.

23. Loftin, Laurence; "Application of Sizing Method for Jet-Powered Cruising Aircraft"; NASA-Langley; Unpublished.

24. Hoak, D. E., Ellison, D. E., et. al.; "USAF Stability and Control DATCOM"; Flight Control Division, Wright-Patterson AFB, Ohio, 1974.

25. Roskam, J.; "Overview of Fuselage Drag"; Proceedings of the NASA/Industry/University General Aviation Drag Reduction Workshop; July 14-16, 1975; pp. 89-96; The University of Kansas Center for Research, Inc., Lawrence, Kansas 66045.

26. Lan, C.; "Wing-Slipstream Interaction with Mach Number Nonuniformity"; Journal of Aircraft, Vol. 12, No. 10, October 1975, pp. 759-760.

27. Anonymous; "Standard Method of Propeller Performance Estimation"; The Society of British Aircraft Construction; 1940.

28. Dommasch, D. O., Sherby, S. S., Connolly, T. F.; "Airplane Aerodynamics"; Pitman Publishing Corporation, New York, 1964.

29. Stickle, G. W., Crigler, J. L.; "Propeller Analysis from Experimental Data"; NACA Report Number 712, 1941.

30. McHugh, J. G., Derring, E. H.; "Effect of Nacelle-Propeller Diameter Ratio on Body Interference and on Propeller and Cooling Characteristics"; NACA Report Number 680, 1939.

31. Galloway, T. L., and Waters, M. H.; "Computer Aided Parametric Analysis for General Aviation Aircraft"; SAE Paper 730 332, presented at SAE National Business Aircraft Meeting, Wichita, Kansas; April 1973.

32. Postai, Mark; "A Computer Program for Determining Open and Closed Loop Dynamic Stability Characteristics of Airplanes and Control Systems"; University of Kansas Flight Research Laboratory, May 1973.

33. Roskam, J., et al.; "A Study of Commuter Airplane Design Optimization"; Continuation Proposal to NASA-Ames Research Center; Submitted July 1977.

34. Roskam, J.; Flight Dynamics of Rigid and Elastic Airplanes, Part I; published by the author, Lawrence, Kansas 1972.

35. Perkins, C. D., and Hage, R. E.; Airplane Performance Stability and Control; John Wiley and Sons, Inc.; New York, 1949.

APPENDIX A USE OF POLYNOMIALS WITH FRACTIONAL EXPONENTS TO APPROXIMATE EXTERNAL AIRCRAFT LINES

Appendix B of Reference 9 describes a method for approximating the external lines of aircraft for the estimation of wetted areas, volumes, cross-sections, etc. This appendix will discuss that method and how it has been applied to fuselage shape simulation.

A1 General Background

In Reference 9, Torenbeek uses polynomials with fractional exponents to approximate the external lines of aircraft fuselages. These polynomials are of the form expressed in equation A-1.

$$\left(\frac{x}{a}\right)^n + \left(\frac{y}{b}\right)^m = 1;\ m,\ n \geq 1 \qquad \text{(A-1)}$$

Figure A-1 presents a generalized curve of this type. In Reference 9, Torenbeek assumes that the plan view curves of aircraft may be generalized by equation A-1. As shown in Figure A-1, a shape parameter ϕ may be determined from the plan view of an aircraft's external lines. This shape parameter may then be used to determine certain factors, k_A, k_C, k_V and k_W, according to Figure A-2. These k-factors may

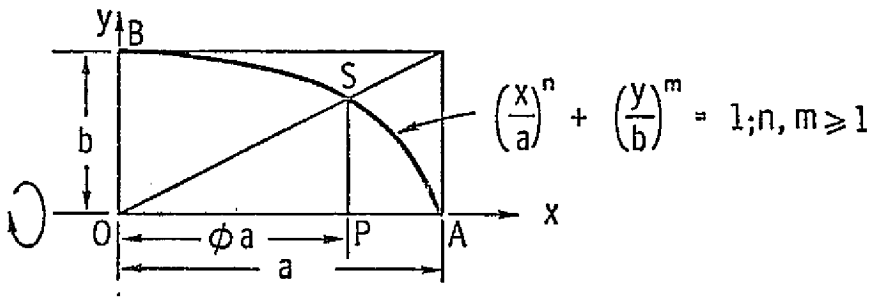

Figure A-1 Definition of Shape Parameter, ϕ, for the Generalized Curve

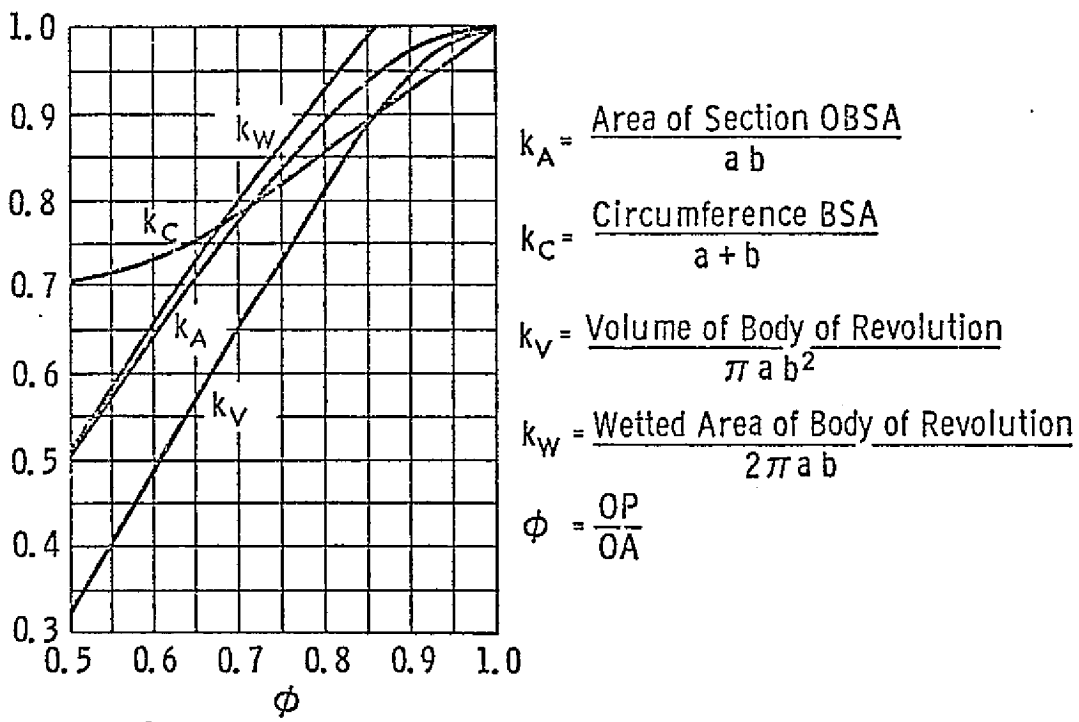

Figure A-2 Nondimensional Geometric Constants Defined by ϕ

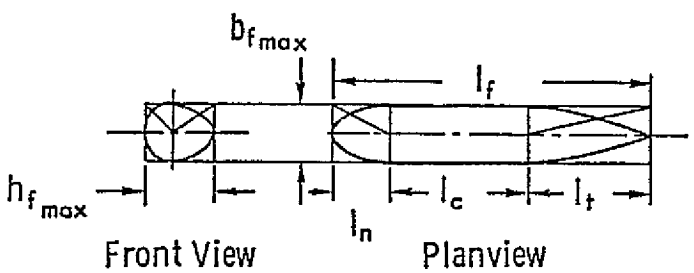

Figure A-3 Fuselage Geometry Used to Define Characteristic Areas and Volume

be used to calculate the characteristic areas and volume. Using the geometry of Figure A-3:

Cross-sectional area*:

$$A_C = k_A \, b_{f_{max}} \, h_{f_{max}} \qquad \text{(A-2)}$$

Circumferential length of the cross-section:

$$C_f = 2k_C \, (b_{f_{max}} + h_{f_{max}}) \qquad \text{(A-3)}$$

Fuselage volume:

$$V_f = A_C(\ell_c + k_{V_n} \ell_n + k_{V_t} \ell_t) \qquad \text{(A-4)}$$

Fuselage wetted area:

$$S_{f_{wet}} = C_f(\ell_c + k_{W_n} \ell_n + k_{W_t} \ell_t) \qquad \text{(A-5)}$$

It may be noted that Torenbeek's method precludes the necessity of knowing the values of m and n in equation A-1. To use these curves to simulate fuselage shapes, however the values for m and n become a pre-requisite.

---

*At the fuselage station where the width and height are maximum

As the intent was to develop a program to aid in the preliminary design of fuselage shapes, it was desired to find a method to specify cone shapes for the nose and tail that was relatively easy to use. The use of m and n in this regard proved to be rather cumbersome, as it was difficult to develop a 'feel' for their values. As an alternative, the shape parameter, ϕ, was chosen to specify the shapes. In addition a second shape parameter was defined to enable the determination of the values of m and n within the program. Figure A-4 defines the geometry of the two shape parameters, ϕ_1 and ϕ_2.

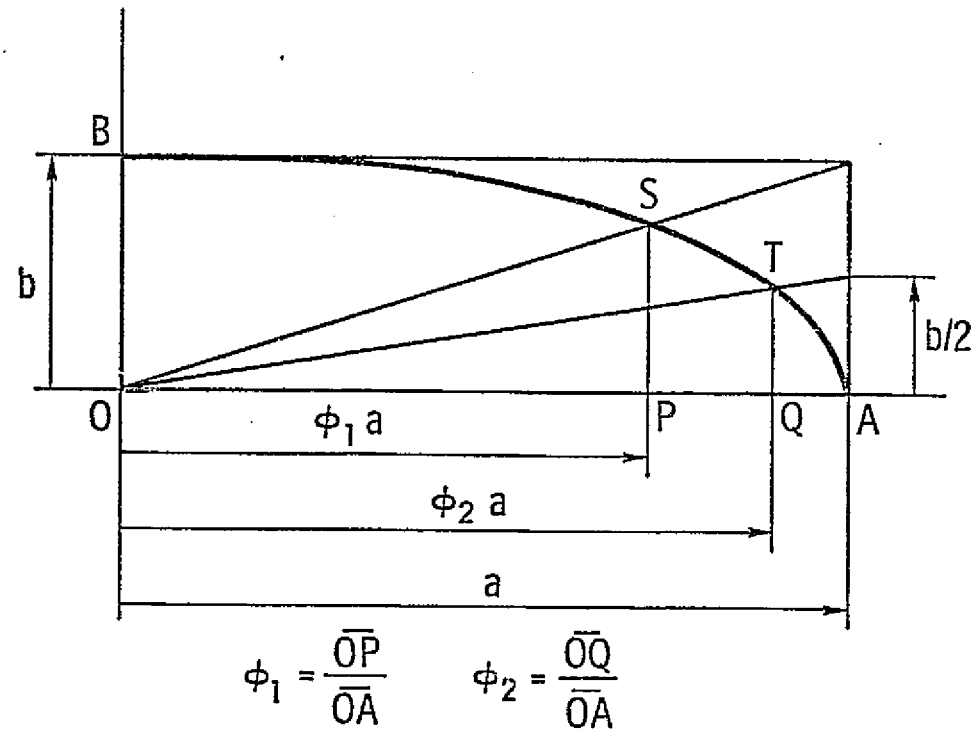

Figure A-4 Definition of Elliptical Cone Shape Parameters

From Figure A-4 it may be seen that ϕ_1 may be considered to indicate the taper characteristics of the cone, while ϕ_2 indicates the bluntness characteristics of the cone.

These shape parameters may be used to determine the values of m and n in the following manner. From Figure A-4 it may be seen that the line $\overline{OS}$ may be represented by the equation A-6.

$$y = \frac{b}{a} x \qquad \text{(A-6)}$$

Similarly the line $\overline{OT}$ may be represented by equation (A-7).

$$y = \frac{b}{2a} x \qquad \text{(A-7)}$$

Substituting for y in equation A-1 gives the following:

$$\left(\frac{x}{a}\right)^n + \left(\frac{x}{a}\right)^m = 1 \qquad \text{(A-8a)}$$

$$\left(\frac{x}{a}\right)^n + \left(\frac{x}{2a}\right) = 1 \qquad \text{(A-8b)}$$

At the points S and T, x equals $\phi_1 a$ and $\phi_2 a$ respectively. Substituting these values for x into equations A-8 a and b respectively renders:

$$(\phi_1)^n + (\phi_2)^m = 1 \qquad \text{(A-9a)}$$

$$(\phi_2)^n + \left(\frac{\phi_2}{2}\right)^m = 1 \qquad \text{(A-9b)}$$

By solving these two equations for m:

$$m = \frac{\ln[1 - (\phi_1)^n]}{\ln \phi_1} \qquad \text{(A-10a)}$$

$$m = \frac{\ln[1 - (\phi_2)^n]}{\ln \left(\frac{\phi_2}{2}\right)} \qquad \text{(A-10b)}$$

Equations A-10 may be used to solve for m and n by iteration. Such a method was used in the subroutine CONSHP, for which the listing is presented in Section A3. It should be noted here that the exponents m and n are purely a function of the shape parameters and a completely independent of the cone fineness ratio, a/2b.

A2 Example Cone Shapes

To provide a 'feel' for the cone shapes resulting from various shape parameters a program was written for a Hewlett-Packard 9100B desktop calculator that would compute the exponents for and plot various cone shapes. Figures A-5 and A-6 provide cone shapes for

cones of fineness ratios (a/2b) of 1.5 and 2.0 respectively where ϕ_1 is held constant and ϕ_2 is varied. Table A-1 provides the values of m and n for these figures. Figures A-7 and A-8 provide cone shapes for cone fineness of 1.5 and 2, where ϕ_2 has been held constant and ϕ_1 is varied. Table A-2 presents the values of m and n for these figures.

It is interesting to note that for each value of ϕ_1, there is a practical range for ϕ_2. If ϕ_2 is too small, the value of m drops below 1.0 and an inflection occurs near the nose of the cone. If ϕ_2 is too large, the value of n drops below 1.0 and an inflection occurs near the base of the cone. It has been found that the windshield shape can sometimes best be simulated by the former of these two cases. The inflection that occurs in cone N2 will normally be buried in cone N1.

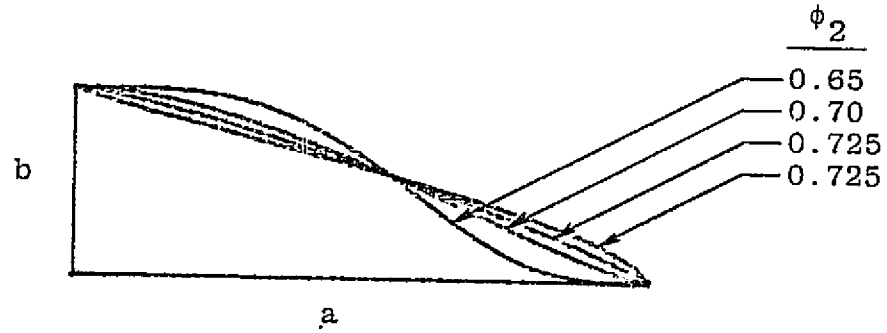

a) $\phi_1 = 0.55$

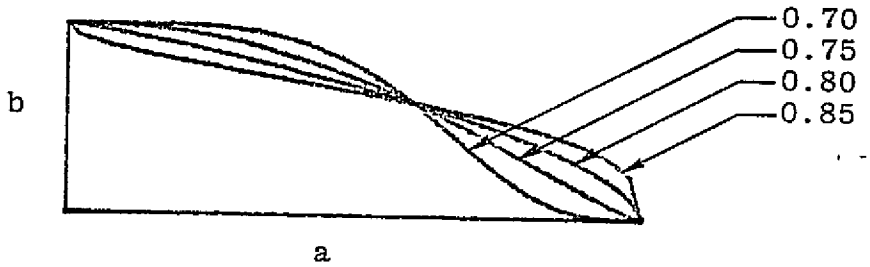

b) $\phi_1 = 0.6$

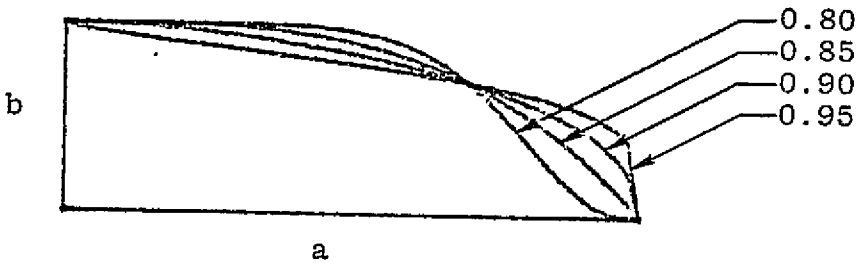

c) $\phi_1 = 0.70$

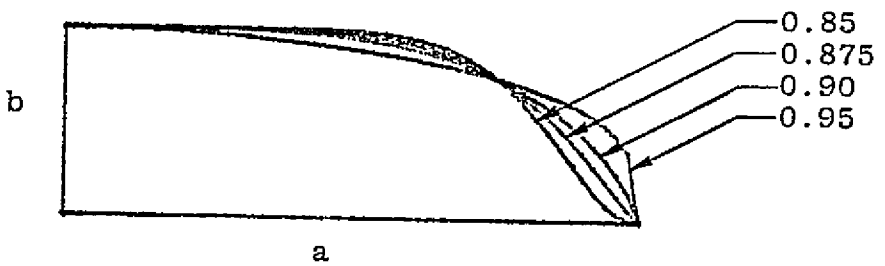

d) $\phi_1 = 0.75$

Figure A-5 Various Cone Shapes for a/2b = 1.5

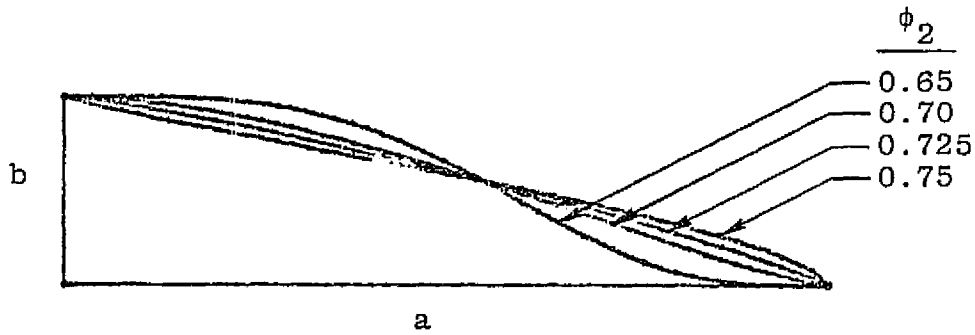

a) $\phi_1 = 0.55$

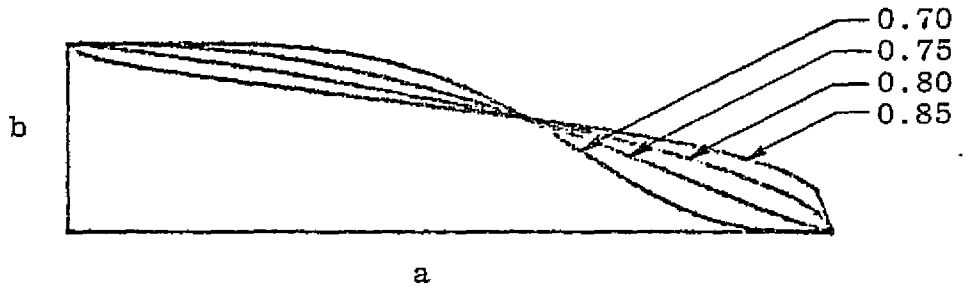

b) $\phi_1 = 0.60$

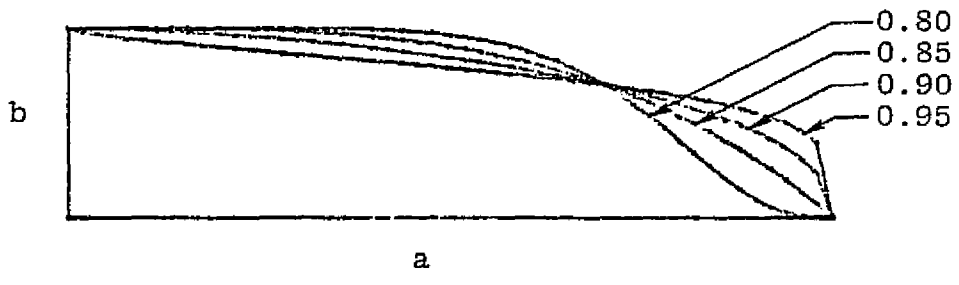

c) $\phi_1 = 0.70$

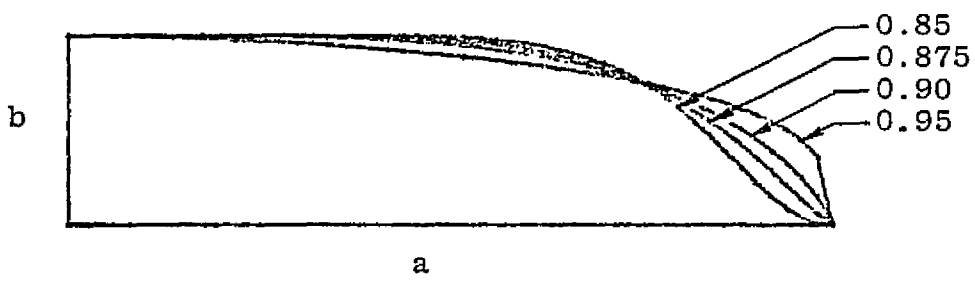

d) $\phi_1 = 0.75$

Figure A-6 Various Cone Shapes for a/2b = 2.0

Table A-1 Values of m and n for Various Shape Parameters

ϕ_1	ϕ_2	m	n
.55	.65	.2350	3.3990
	.70	.7523	1.6987
	.725	1.1320	1.1874
	.75	1.5982	.8118
.60	.70	.2375	4.2468
	.75	.7808	2.1769
	.80	1.6865	1.0749
	.85	3.0995	.4498
.70	.80	.2970	6.4413
	.85	1.0216	3.3258
	.90	2.3345	1.6001
	.95	4.7857	.5613
.75	.85	.3810	7.8740
	.875	.7802	5.5762
	.90	1.3559	3.9285
	.95	3.3668	1.6596

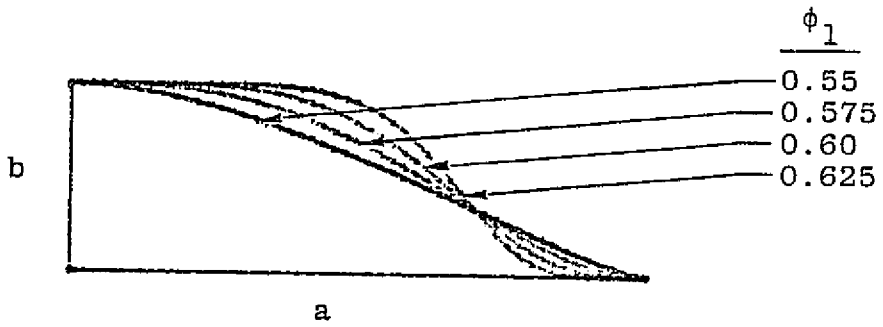

a) ϕ_2 = 0.70

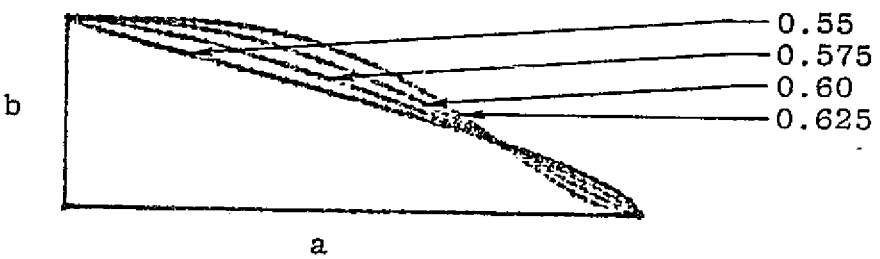

b) ϕ_2 = 0.75

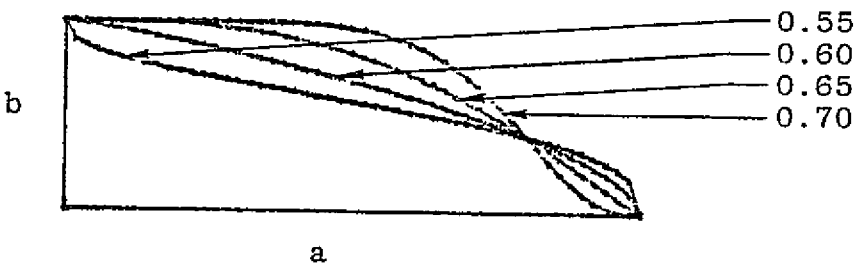

c) ϕ_2 = 0.80

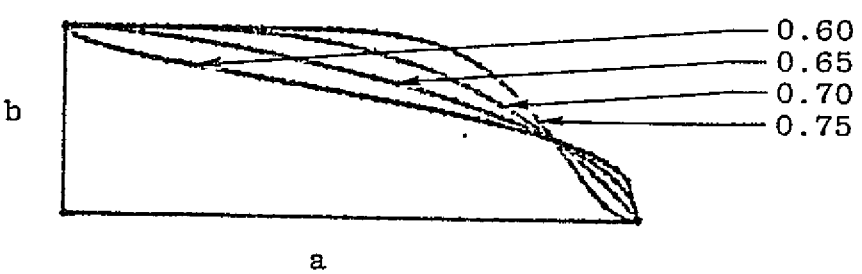

d) ϕ_2 = 0.85

Figure A-7 Various Cone Shapes for a/2b = 1.5

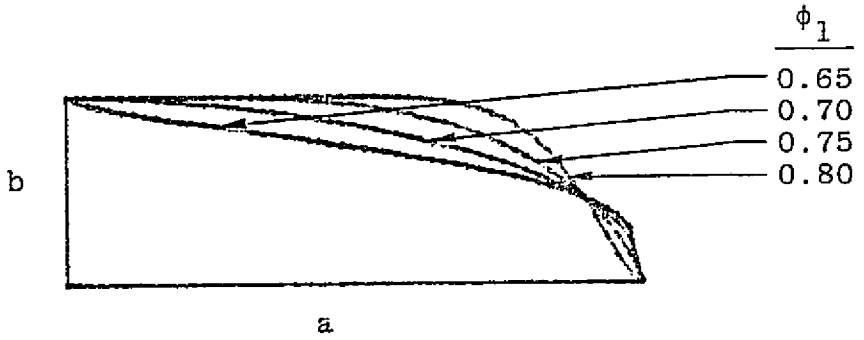

e) ϕ_2 = 0.90

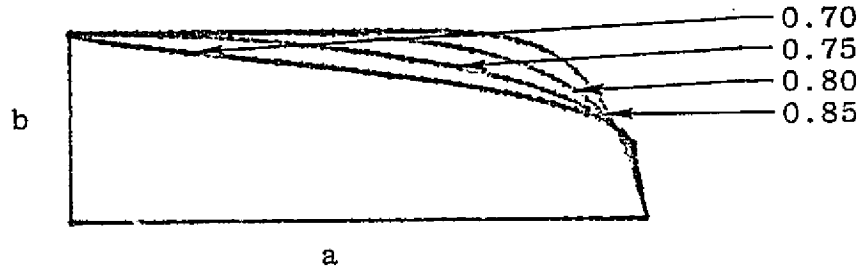

f) ϕ_2 = 0.95

Figure A-7 (continued)

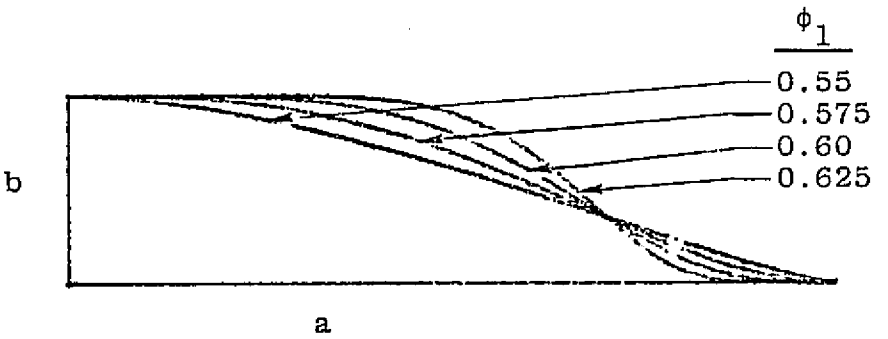

a) ϕ_2 = 0.70

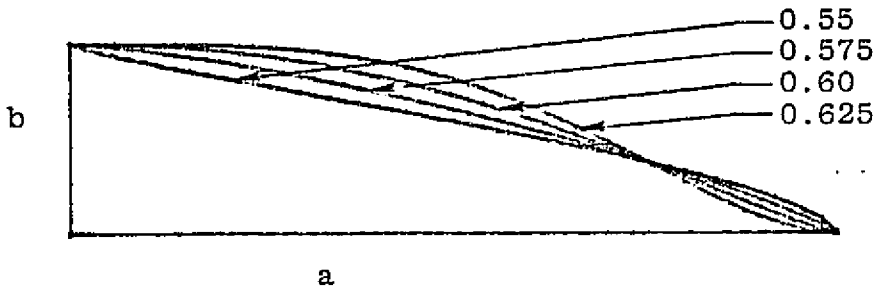

b) ϕ_2 = 0.75

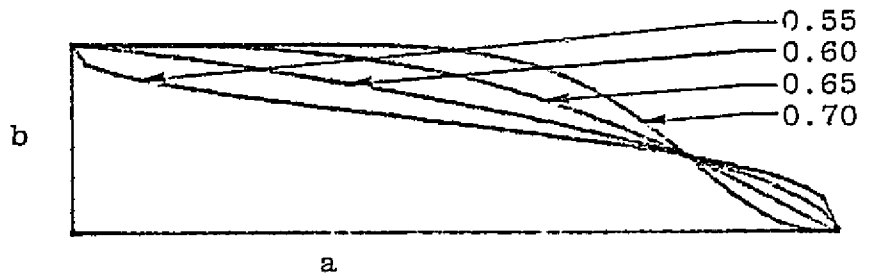

c) ϕ_2 = 0.80

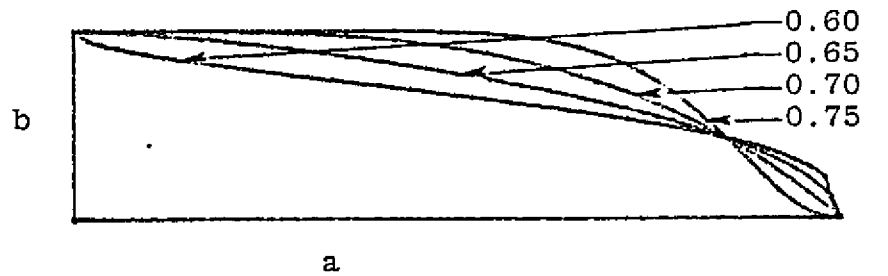

d) ϕ_2 = 0.85

Figure A-8 Various Cone Shapes for a/2b - 2.0

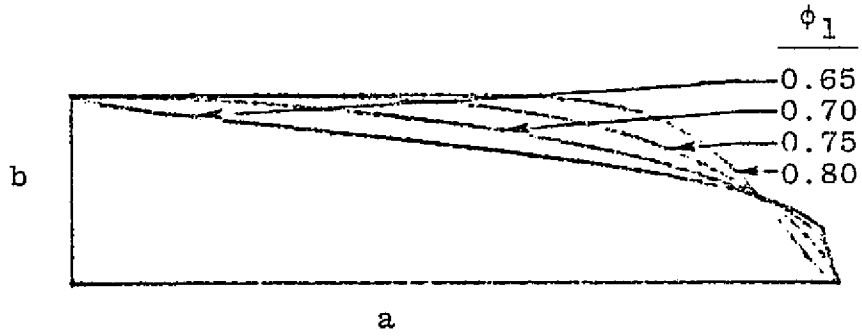

e) ϕ_2 = 0.90

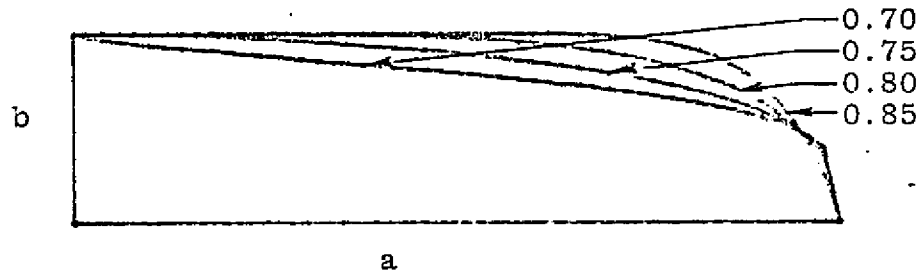

f) ϕ_2 = 0.95

Figure A-8 (continued)

Table A-2 Values of m and n for Various Shape Parameters

ϕ_2	ϕ_1	m	n
.70	.55	.7523	1.6987
	.575	.4482	2.7038
	.60	.2375	4.2468
	.625	.0902	6.7696
.75	.55	1.5988	.8118
	.575	1.1494	1.3620
	.60	.7808	2.1769
	.625	.4841	3.3876
.80	.55	2.9056	.3239
	.60	1.6885	1.0734
	.65	.8597	2.7225
	.70	.2970	6.4413
.85	.60	3.0982	.4502
	.65	1.8974	1.3526
	.70	1.0216	3.3258
	.75	.3834	7.8530
.90	.65	3.5879	.5566
	.70	2.3345	1.6001
	.75	1.3559	3.9285
	.80	.5768	9.4732
.95	.70	4.7857	.5613
	.75	3.3668	1.6596
	.80	2.1867	4.2647
	.85	1.1343	10.9631

A3 Listing for the Subroutine CONSHP

This section contains a listing of the iterative subroutine used to determine the values of m and n.

```
      SUBROUTINE CONSHP(PHI1,PHI2,TOL,M,N)
      REAL M,N,M1,M2
      I=1
      J=1
      N=1.0
      DM2 = 10.0
   10 M1 = ALOG(1.0 -(PHI1**N))/ALOG(PHI1)
      M2 = ALOG(1.0 -(PHI2**N))/ALOG(PHI2/2.0)
      J = J+1
      IF(J.EQ.100)    GO TO 80
      DM1 = M1-M2
      IF(DM1.LE.0.) GO TO 30
      IF(DM1.GT.DM2) GO TO 50
   20 N = N+(0.05/I)
      DM2 = DM1
      GO TO 10
   30 IF(ABS(DM1).LT.TOL)GO TO 60
      I = I*5
   40 N = N - (0.05/I)
      M1 = ALOG(1.0 -(PHI1**N))/ALOG(PHI1)
      M2 = ALOG(1.0 -(PHI2**N))/ALOG(PHI2/2.0)
      J = J+1
      IF(J.EQ.100)    GO TO 80
      DM1 = M2-M1
      IF(DM1.LT.0.) GO TO 20
      IF(ABS(DM1).LT.TOL) GO TO 60
      GO TO 40
   50 WRITE(6,1)
      M = 1.0
      N = 1.0
      GO TO 70
   60 M = (M1 + M2)*0.5
   70 RETURN
   80 WRITE(6,4)
      GO TO 60
    1 FORMAT(10X,'***ITERATION FOR M AND N DIVERGES***'/15X,'SET-  M=1.0
     X'/22X,'N=1.0'//)
    4 FORMAT(10X,'***100 STEPS COMPLETE--DID NOT CONVERGE***'//)
      RETURN

      END
```

APPENDIX B THE ROSKAM/FILLMAN PROGRAM

This appendix documents the Roskam/Fillman program's use and provides a copy of the listing. Appendix B1 will define all input and output acronyms and explain how to prepare the input data. Appendix B2 will provide a complete program listing. Appendix B3 provides an example output.

B1 Preparation of Input Data

Table B-1 defines all of the input and output computer acronyms.

Table B-2 presents the input card formats. All input cards must be in the order specified by Table B-2. Data for more than one baseline aircraft may be input by stacking data decks. For multiple data decks the last card of each set of data corresponds with the first card of the next set of data. The last card of the total data deck must be blank. This tells the program that the next set of data is a null set and terminates execution.

Of particular interest are K1, K2, K3, K4, KEMP1 and KEMP2. These correspond with the weight correction factors of Section 2.3.1.3. In this case an input value of zero will result in a correction factor of unity. An input value of one will result in the corresponding non-unity correction factor.

Table B-1 Roskam/Fillman Program

Input/Output Acronyms

Acronyms	Variable	Description	Units
AEFF	A_{EFF}	Effective aspect ratio of the vertical tail (Reference 14)	
AIRCRAFT	-	Aircraft or configuration name	
AH	A_H	Horizontal tail aspect ratio	
ALT	h	Altitude	ft
AV	A_V	Vertical tail aspect ratio	
AW	A	Wing aspect ratio	
BHO	b_h	Baseline horizontal tail span	ft
BVO	b_v	Baseline vertical tail span	ft
BW	b	Wing span	ft
CBAR	$\bar{c}$	Wing mean aerodynamic chord	ft
CHO	$\bar{c}_H$	Baseline horizontal tail MAC	ft
CMA	C_{m_α}	Static longitudinal stability	rad^{-1}
CNB	C_{n_β}	Static directional stability	rad^{-1}
CVO	$\bar{c}_v$	Baseline vertical tail MAC	ft
DENSIT	P	Atmospheric density	$slugs/ft^3$
DFUS	D	Fuselage equivalent outside diameter	ft

Table B-1 Roskam/Lillman Program

Input/Output Acronyms (Cont'd)

Acronym	Variable	Description	Units
DIVE	V_D	Dive speed	Knots
EP	-	Tail sizing span tolerance for iteration process	ft
ETA	η	Dynamic pressure ratio at the empennage $\bar{q}_E/\bar{q}_W$	
FUSHGT	H	Fuselage outside height	ft
FUSWID	W	Fuselage outside width	ft
H1	h_1	Fuselage height at $.25\ell_B$	ft
H2	h_2	Fuselage height at $.75\ell_B$	ft
HH	h_H	Vertical distance from aircraft center line to horizontal tail root chord (positive down)	ft
IF	-	Number of different tail cones to be considered	
K	k	Empirical vertical tail factor from Figure 7.3 of Reference 14	
K1,K2,K3,K4	-	Weight estimation constant controls for fuselage (See text)	
KAPAH	κ_H	Ratio of horizontal tail section lift slope to 2π	
KAPAV	κ_V	Ratio of vertical tail section lift slope to 2π	
KAPAW	κ_W	Ratio of wing section lift slope to 2π	

Table B-1 Roskam/Fillman Program

Input/Output Acronyms (Cont'd)

Acronym	Variable	Description	Units
KEMP1	K_H	Empennage weight estimation constant control (See text)	
KEMP2	K_V	Empennage weight estimation constant control (See text)	
LBOLD	ℓ_B	Baseline Fuselage Length	ft
LC1	-	Minimum tail cone length to be considered	
LCF	-	Maximum tail cone length to be considered	
LCOLD	ℓ_c	Baseline tail cone length	ft
LHOLD	ℓ_H	Baseline horizontal tail moment arm	ft
LN	ℓ_{N1}	Nose length	ft
LU	ℓ_u	Cabin length	ft
LVOLD	ℓ_V	Baseline vertical tail moment arm	ft
MACH	M	Mach number	
PHIC1	ϕ_{C1}	Tail cone shape parameters	
PHIC2	ϕ_{C2}		
PHIN1	ϕ_{N1}	Nose cone shape parameters	
PHIN2	ϕ_{N2}		
SBSC1	-	Side view projected area of the baseline tail cone	ft^2

Table B-1 Roskam/Fillman Program

Input/Output Acronyms (Cont'd)

Acronym	Variable	Description	Units
SBSN	-	Side view projected area of the nose	ft^2
SBSU	-	Side view projected area of the cabin	ft^2
SHO	S_H	Baseline horizontal tail area	ft^2
SVO	S_V	Baseline vertical tail area	ft^2
SW	S	Reference wing area	ft^2
SWPHO	Λ_{LE_H}	Baseline horizontal tail leading edge sweep	deg
SWPVO	-	Baseline vertical tail leading edge sweep	deg
TAPRH	λ_H	Horizontal tail taper ratio	
TAPRV	λ_V	Vertical tail taper ratio	
TAPRW	λ	Wing taper ratio	
TAS	V_T	True airspeed	ft/sec
TEST	-	Test run number	
THICKH	$(t/c)_H$	Horizontal tail thickness ratio	
THICKV	$(t/c)_V$	Vertical tail thickness ratio	
TOL	-	Tolerance for the iteration in CONSHP (See Appendix A3)	
ULTLOAD	n_{ULT}	Ultimate load factor	g's

Table B-1 Roskam/Fillman Program

Input/Output Acronyms (Cont'd)

Acronym	Variable	Description	Units
VISCOS	μ	Kinematic viscosity	ft^2/sec
WGROSS	W_G	Gross weight	lbs
WSWPLE	Λ_{LE}	Wing Leading Edge Sweep	deg
XBARHO	-	Baseline horizontal tail aerodynamic center location as a fraction of $\bar{c}$	
XBARW	$(\bar{X}_{ac})_W$	Wing aerodynamic center location as a fraction of $\bar{c}$	
XCBAR	-	Location of the leading edge of $\bar{c}$, relative to the nose	ft
XCG	X_{cg}	Baseline c.g. location relative to the nose	ft
XCGH	$(X_{cg})_H$	Baseline horizontal tail c.g. relative to the nose	ft
XCGV	$(X_{cg})_V$	Baseline vertical tail c.g. location relative to the nose	ft

Table B-2 Roskam/Fillman Program Input Card Formats

INPUT CARD NO. 1 - (13A6, A2)

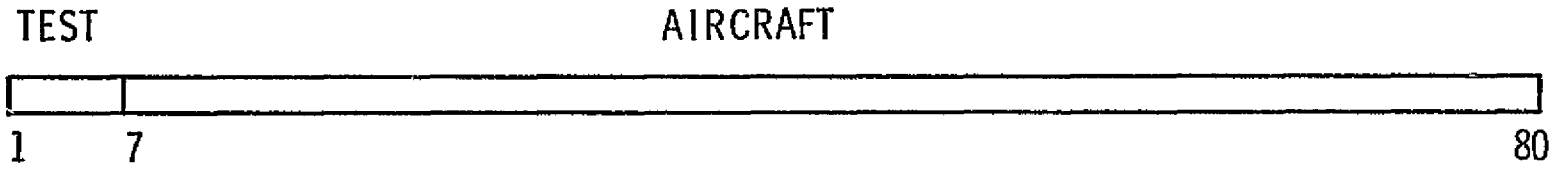

INPUT CARD NO. 2 - (7F10.0)

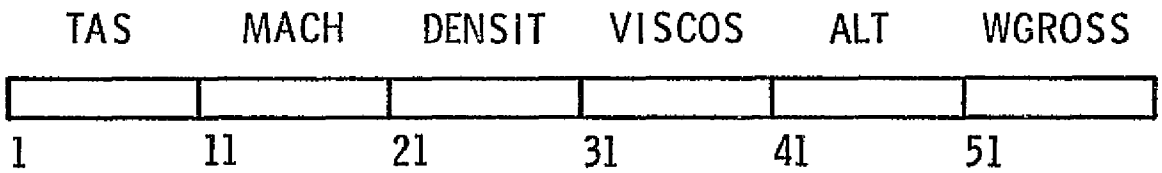

INPUT CARD NO. 3 - (7F10.

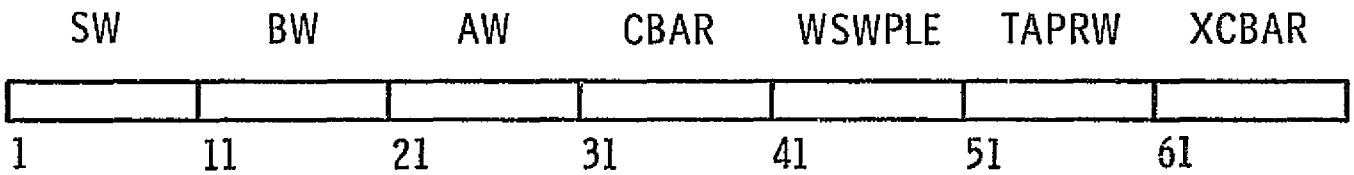

INPUT CARD NO. 4 - (7F10.0)

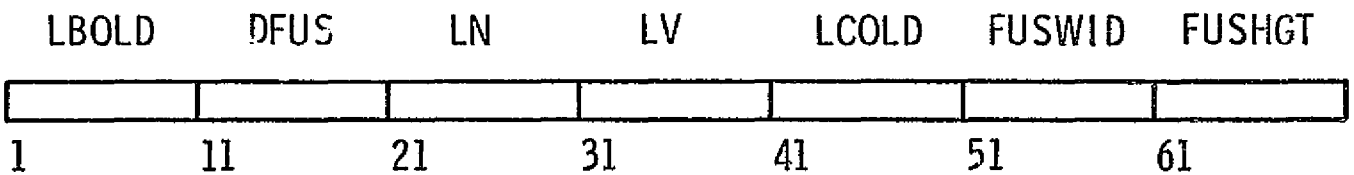

Table B-2 (Continued)

INPUT CARD NO. 5 - (7F10.0)

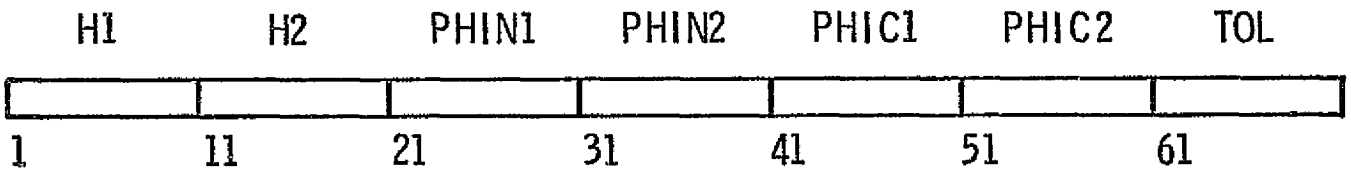

INPUT CARD NO. 6 - (4I2)

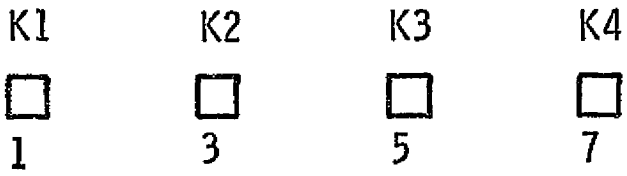

INPUT CARD NO. 7 - (7F10.0)

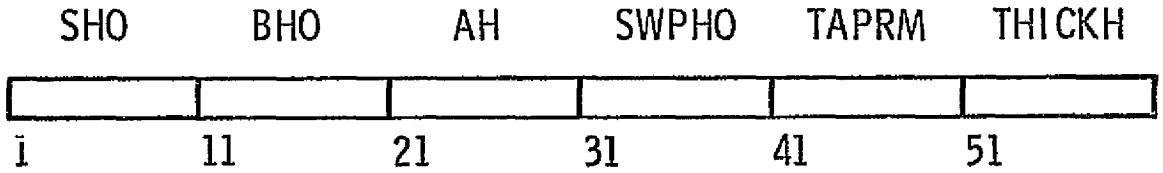

INPUT CARD NO. 8 - (7F10.0)

Table B-2 (Continued)

INPUT CARD NO. 9 - (7F10.0)

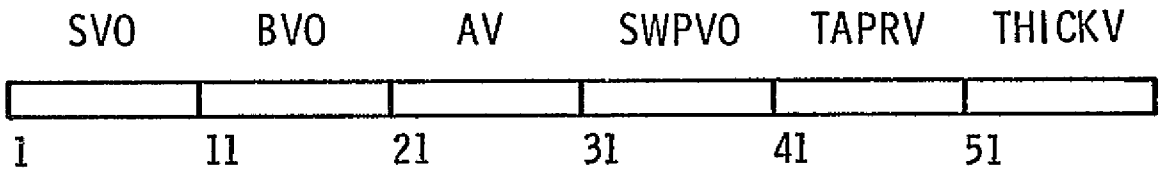

INPUT CARD NO. 10 - (7F10.0)

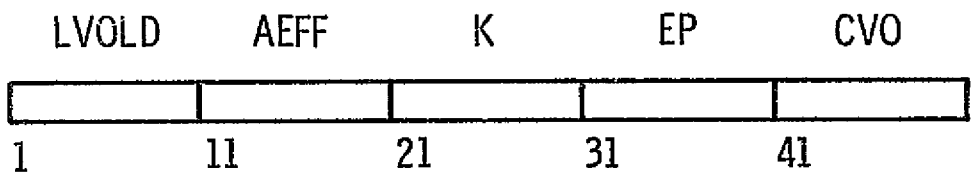

INPUT CARD NO. 11 - (412)

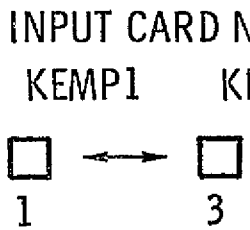

INPUT CARD NO. 12 - (7F10.0)

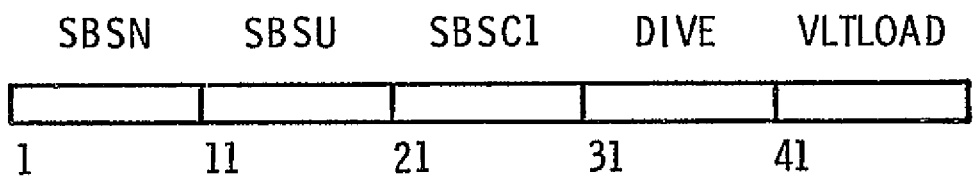

Table B-2 (Continued)

INPUT CARD NO. 13 - (7F10.0)

XC6 XC6H XC6V

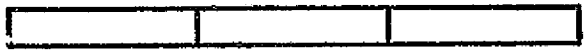

INPUT CARD NO. 14 - (7F10.0)

XBARW XBARHO CMA CNB

INPUT CARD NO. 15 - (7F10.0)

KAPAW KAPAH KAPAV ETA

INPUT CARD NO. 16 - (3F10.0, 1X, I3)

LC1 LCP IF1 IF

Table B-2 (Continued)

INPUT CARD NO. 17 - SHOULD BE BLANK AS THE LAST CARD OF THE TOTAL DATA DECK. OTHERWISE, THIS CARD CORRESPONDS WITH THE INPUT CARD NO. 1 OF THE NEXT DATA SET.

B2 Program Listing

This section provides a complete listing of the Roskam/Fillman Program.

```
      DIMENSION LCOD(500),L(500),SVL(500),SHL(500),LCODO(1),LO(1),CDO(1
     *),CDOL(500),SVO(1),BVO(1),SHO(1),BHO(1),SWPHO(1),SWPVO(1),SWETFO(1
     *),SWETEO(1),SWETNO(1),SWETCO(1),SWETUO(1),WAITFO(1),WAITEO(1),BVL
     *(500),BHL(500),SWPHL(500),SWPVL(500),SWF(500),SWE(500),SWC(500),SW
     *N(500),SWU(500),WAITF(500),WAITE(500),LBL(500),XCGL(500),CBH(500)
     *,CBV(500),SWH(500),SWV(500),SWT(500),LABEL1(14),LABEL2(14),
     *LABEL3(14),ARCRFT(13)
      DIMENSION XBW(500),XBB(500),XBWB(500),XBH(500),XBA(500)
      COMMON TAS,AMACH,VISCOS,SW,BW,AW,CBAR,WSWPLE,TAPRW,XCBAR,LBOLD,
     1DFUS,LN,LU,LCOLD,FUSWID,FUSHGT,H1,H2,PHIN1,PHIN2,PHIC1,PHIC2,TOL,
     2K1,K2,K3,K4,SHO,BHO,AH,SWPHO,TAPRH,THICKH,LHOLD,HH,SVO,BVO,AV,
     3SWPVO,TAPRV,THICKV,LVOLD,AEFF,K,KEMP1,KEMP2,SBSN,SBSU,SBSC1,DIVE,
     4ULTLOAD,XCG,XCGH,XCGV,XBARWB,XBARHO,CMA,CNB,KAPAW,KAPAH,KAPAV,
     5ETA,DELTLC,EP
      COMMON/STAB/XBARW,XBARAC,DXACB,XBARH
      COMMON/RHO/DENSIT
      COMMON/WEIGHT/WN,WU,WC,WF,WH,WV,WEMP,CGERR,WGROSS,WGR
      REAL LCOD,L,LCODO,LO,LBL,LN,LU,LCOLD,LHOLD,KAPAW,KAPAH,
     *LVOLD,LBOLD,KAPAV,LC,L,LC2,LBNEW,LCNEW
      REAL LC1,LCF,IF1
      DATA (LABEL1(I),I=1,5)/6HLCOD V,6HS. CDO,6H - SCA,6HLED VA,
     14HLUES/
      DATA  (LABEL2(I),I=1,5)/6HLC VS.,6H SH - ,6HSCALED,6H VALUE,1HS/
      DATA  (LABEL3(I),I=1,5)/6HLC VS.,6H SV - ,6HSCALED,6H VALUE,1HS/
      DATA TERM/6H      /
   10 READ(5,1)TEST,(ARCRFT(I),I=1,13)
      IF(TEST.EQ.TERM) STOP
      READ(5,2)TAS,AMACH,DENSIT,VISCOS,ALT,WGROSS
      READ(5,2)SW,BW,AW,CBAR,WSWPLE,TAPRW,XCBAR
      READ(5,2)LBOLD,DFUS,LN,LU,LCOLD,FUSWID,FUSHGT
      READ(5,2)H1,H2,PHIN1,PHIN2,PHIC1,PHIC2,TOL
      READ(5,3)K1,K2,K3,K4
      READ(5,2)SHO,BHO,AH,SWPHO,TAPRH,THICKH
      READ(5,2)LHOLD,HH,CHO
      READ(5,2)SVO,BVO,AV,SWPVO,TAPRV,THICKV
      READ(5,2)LVOLD,AEFF,K,EP,CVO
      READ(5,3)KEMP1,KEMP2
      READ(5,2)SBSN,SBSU,SBSC1,DIVE,ULTLOAD
      READ(5,2)XCG,XCGH,XCGV
      READ(5,2)XBARW ,XBARHO,CMA,CNB
      READ(5,2)KAPAW,KAPAH,KAPAV,ETA
      READ(5,4)LC1,LCF,IF1,IF
      DLC=(LCF-LC1)/IF1
      DELTC = 0.
      CALL SWET(PHIN1,PHIC1,SHO,SVO,LCOLD,SWETNO,SWETUO,SWETCO,
     *SWETHO,SWETVO)
      SWETFO=SWETNO+SWETUO+SWETCO
      SWETEO=SWETHO+SWETVO
      CALL CDO(LBOLD,SWPV,SWPH,SWETHO,SWETVO,SWETFO,CHO,CVO,CDOBHV)
      CALL FUSWGT(SWETFO,SWETNO,SWETUO,SWETCO,WF,WN,WU,WC)
      CALL EMPWGT(SWETHO,SWETVO,SWETEO,SHO,BHO,SVO,BVO,SWPH,SWPV,WV,WH,
     *WEMP)
```

```
                CALL XBARCG(0,XBCG)
                SWPW = WSWPLE * 57.3
                WRITE(6,5)TEST,ARCRFT
                WRITE(6,6)ALT,TAS,AMACH,DENSIT,VISCOS
                WRITE(6,7)SW,BW,AW,CBAR,XCBAR,SWPW,TAPRW
                WRITE(6,8)LBOLD,LN,LU,LCOLD,FUSWID,FUSHGT,DFUS
                WRITE(6,9)SHO,BHO,AH,CHO,TAPRH,THICKH
                WRITE(6,11)SVO,BVO,AV,CVO,TAPRV,THICKV
                WRITE(6,12)TEST,ARCRFT,WGROSS
                WRITE(6,13)WN,WU,WC,WF,WH,WV,WEMP,XBCG
                WRITE(6,14)TEST,ARCRFT
                WRITE(6,15)SWETNO,SWETUO,SWETCO,SWETFO,SWETHO,SWETVO,SWETEO
                SWPH=SWPHO
                SWPV=SWPVO
                SWETF=SWETFO
                SWETN=SWETNO
                SWETE=SWETEO
                SWETC=SWETCO
                SWETU=SWETUO
                SH = SHO
                BH = BHO
                SV = SVO
                BV = BVO
                CH=CHO
                CV=CVO
                LCODO(1) = LCOLD/DFUS
                CDO(1) = CDOBHV
                SVO(1) = SVO
                SHO(1) = SHO
                BVO(1) = BVO
                BHO(1) = BHO
                SWPHO(1) = SWPH * 57.3
                SWPVO(1) = SWPV * 57.3
                SWETFO(1) = SWETFO
                SWETEO(1) = SWETEO
                SWETNO(1) = SWETNO
                SWETCO(1) = SWETCO
                WAITFO(1) = WF
                WAITEO(1) = WEMP
                LO(1) = LCOLD
                DO 100 I=1,IF
                LC2=LC1+((I-1)*DLC)
                LBNEW = LN+LU+LC2
                DELTLC=LC2-LCOLD
                CALL SWET(PHIN1,PHIC1,SH,SV,LC2,SWETN,SWETU,SWETC,SWETH,SWETV)
                CALL FUSWGT(SWETF,SWETN,SWETU,SWETC,WF,WN,WU,WC)
                CALL EMPWGT(SWETH,SWETV,SWETE,SH,BH,SV,BV,SWPH,SWPV,WV,WH,WEMP)
               100 CALL XBARCG(I,XBCG)
*****W  1457 DO LOOP INDEX I MAY NOT BE REDEFINED IN CALL OR ABNORMAL FUNCTION
               101 CALL STABAREA(XBCG,HSWPLE,SH,BH,CH)
               102 CALL VERTAREA(VSWPLE,SV,BV,CV)
               103 CALL SWET(PHIN1,PHIC1,SH,SV,LC2,SWETN,SWETU,SWETC,SWETH,SWETV)
```

```
104           SWETF = SWETN + SWETU + SWETC
105           SWETE = SWETH + SWETV
106           CALL CDO(LBNEW,VSWPLE,HSWPLE,SWETH,SWETV,SWETF,CH,CV,CDOBHV)
107           SWV(I) = SWETV
108           SWH(I) = SWETH
109           SWT(I) = SWETF + SWETE
110           LCDO(I) = LC2/DFUS
111           L(I) = LC2
112           XBW(I) = XBARW
113           XBB(I) = DXACB
114           XBWB(I) = XBARWB
115           XBH(I) = XBARH
116           XBA(I) = XBARAC
117           SVL(I) = SV
118           SHL(I) = SH
119           CDOL(I) = CDOBHV
120           BVL(I) = BV
121           BHL(I) = BH
122           SWPHL(I) = HSWPLE * 57.3
123           SWPVL(I) = VSWPLE * 57.3
124           SWF(I) = SWETF
125           SWE(I) = SWETE
126           SWC(I) = SWETC
127           SWN(I) = SWETN
128           SWU(I) = SWETU
129           WAITF(I) = WGR + WC
130           WAITE(I) = WEMP
131           LBL(I) = LBNEW
132           XCGL(I) = XBCG
133           CBH(I) = CH
134           CBV(I) = CV
135       100 CONTINUE
136           WRITE(6,16)TEST,ARCRFT,WGR,((I,L(I),LBL(I),WAITF(I),WAITE(I),
137          *XCGL(I)),I=1,IF)
138           WRITE(6,17)TEST,ARCRFT,CMA,AH,TAPRH
139           WRITE(6,18)((I,L(I),SHL(I),BHL(I),CBH(I),SWPHL(I)),I=1,IF)
140           CALL M15A(2,L,SHL,IF,LO,SHO,1,LABEL2)
141           WRITE(6,19)TEST,ARCRFT,CNB,AV,TAPRV
142           WRITE(6,18)((I,L(I),SVL(I),BVL(I),CBV(I),SWPVL(I)),I=1,IF)
143           CALL M15A(2,L,SVL,IF,LO,SVO,1,LABEL3)
144           WRITE(6,25) TEST,ARCRFT,CMA
145           WRITE(6,26)((I,L(I),XBW(I),XBB(I),XBWB(I),XBH(I),XBA(I),XCGL(I)),
146          *I=1,IF)
147           WRITE(6,21)TEST,ARCRFT
148           WRITE(6,22)((I,L(I),SWF(I),SWH(I),SWV(I),SWT(I)),I=1,IF)
149           WRITE(6,23)TEST,ARCRFT,CDO(1)
150           WRITE(6,24)((I,L(I),LCDO(I),CDOL(I)),I=1,IF)
151           CALL M15A(2,LCDO,CDOL,IF,LCDO0,CDO,1,LABEL1)
152           GOTO 10
153         1 FORMAT(13A6,A2)
154         2 FORMAT(7F10.0)
155         3 FORMAT(4I2)
```

```
      4 FORMAT(3F10.0,1X,I3)
      5 FORMAT(1H1,10X,'TABLE ',A6,'.1A ROSKAM-FILLMAN METHOD'/27X,12A6,
     *A2/27X,'ORIGINAL FLIGHT CONDITIONS AND'/27X,'GEOMETRIC DEFINITIONS
     *'//10X,65('*')//)
      6 FORMAT(10X,'FLIGHT CONDITIONS'//15X,'ALTITUDE',T50,F10.3,' FT'/
     *15X,'AIRSPEED',T50,F10.3,' FPS '/15X,'MACH',T50,F10.3/15X,'DENSITY
     *',T50,F10.5,' SLUGS/CU.FT.'/15X,'KINEMATIC VISCOSITY',T50,F10.5,
     *' SQ.FT./SEC'//)
      7 FORMAT(10X,'GEOMETRIC'//15X,'WING'/20X,'REFERENCE AREA',T50,F10.3,
     *' SQ.FT.'/20X,'SPAN',T50,F10.3,' FT'/20X,'ASPECT RATIO',T50,F10.3/
     *20X,'M.A.C.',T50,F10.3,' FT'/22X,'F.S.',T50,F10.3,' FT'/20X,'L.E.
     *SWEEP',T50,F10.3,' DEG'/20X,'TAPER',T50,F10.3//)
      8 FORMAT(15X,'FUSELAGE'/20X,'OVERALL LENGTH',T50,F10.3,' FT'/20X,
     *'NOSE LENGTH',T50,F10.3,' FT'/20X,'CABIN LENGTH',T50,F10.3,' FT'/
     *20X,'TAIL CONE LENGTH',T50,F10.3,' FT'/20X,'MAX WIDTH',T50,F10.3,
     *' FT'/20X,'MAX HEIGHT',T50,F10.3,' FT'/20X,'EQUIV. DIAMETER',T50,
     *F10.3,' FT'//)
      9 FORMAT(15X,'HORIZONTAL TAIL'/20X,'REFERENCE AREA',T50,F10.3,
     *'SQ.FT.'/20X,'SPAN',T50,F10.3,' FT'/20X,'ASPECT RATIO',T50,F10.3/
     *20X,'M.A.C.',T50,F10.3,' FT'/
     *20X,'TAPER',T50,F10.3/20X,'THICKNESS',T50,F10.3//)
     11 FORMAT(15X,'VERTICAL TAIL'/20X,'REFERENCE AREA',T50,F10.3,
     *'SQ.FT.'/20X,'SPAN',T50,F10.3,' FT'/20X,'ASPECT RATIO',T50,F10.3/
     *20X,'M.A.C.',T50,F10.3,' FT'/
     *20X,'TAPER',T50,F10.3/20X,'THICKNESS',T50,F10.3//)
     12 FORMAT(1H1,10X,'TABLE ',A6,'.1B ROSKAM-FILLMAN METHOD'/27X,12A6,
     *A2/27X,'ORIGINAL WEIGHT AND BALANCE STATEMENT'//10X,65('*')//
     *T52,'(LBS.)'//10X,'GROSS WEIGHT',T55,F10.3//)
     13 FORMAT(10X,'APPROXIMATED SHELL WEIGHTS',          //15X,
     *'FUSELAGE'//20X,'NOSE SECTION',T50,F10.3/20X,'CABIN SECTION',T50,
     *F10.3/20X,'TAIL CONE SECTION',T50,F10.3//20X,'TOTAL FUSELAGE',T50,
     *F10.3//15X,'EMPENNAGE'//20X,'HORIZONTAL TAIL',T50,F10.3/20X,
     *'VERTICAL TAIL',T50,F10.3//20X,'TOTAL EMPENNAGE',T50,F10.3//10X,
     *'CENTER OF GRAVITY -- FRACTION OF M.A.C.',T50,F10.3//)
     14 FORMAT(1H1,10X,'TABLE ',A6,'.1C ROSKAM-FILLMAN METHOD'/27X,12A6,
     *A2/27X,'ORIGINAL WETTED AREA BREAKDOWN'//10X,65('*')//)
     15 FORMAT(10X,'FUSELAGE',T51,'(SQ.FT.)'//15X,'NOSE SECTION',T50,F10.3
     */15X,'CABIN SECTION',T50,F10.3/15X,'TAIL SECTION',T50,F10.3//
     *15X,'TOTAL FUSELAGE',T50,F10.3//10X,'EMPENNAGE'//15X,'HORIZONTAL T
     *AIL',T50,F10.3,/15X,'VERTICAL TAIL',T50,F10.3//15X,'TOTAL EMPENNAG
     *E',T50,F10.3//)
     16 FORMAT(1H1,10X,'TABLE ',A6,'.2A ROSKAM-FILLMAN METHOD'/27X,12A6,
     *A2/27X,'OPTIMIZATION WEIGHT AND BALANCE'/27X,'STATEMENT'//10X,65('
     **')//10X,'GROSS WEIGHT( W/O TAIL OR EMP.)',T55,F10.3,' (LBS.)'
     *   //T12,'I',T18,'LC',T31,'LB',T41,'FUSELAGE',T54,'EMPENNAGE',T69,
     *'C.G.'/T44,'WI',T58,'WT'/T17,'(FT)',T30,'(FT)',T43,'(LB)',T57,
     *'(LB)',T67,'(FR CBAR)'//(10X,I3, 5(F10.3,3X)/))
     17 FORMAT(1H1,10X,'TABLE ',A6,'.2B ROSKAM-FILLMAN METHOD'/27X,12A6,
     *A2/27X,'OPTIMIZATION STABILIZER'/27X,'SIZING'//27X,'CHA = ',T55,
     *F10.3/27X,'ASPECT RATIO = ',T55,F10.3/27X,'TAPER RATIO = ',T55,
     *F10.3//10X,65('*')//T12,'I',T18,'LC',T31,'SH',T44,'BH',T57,'CBARH'
     *,T68,'SWEEPH'/T17,'(FT)',T28,'(SQ.FT.)',T43,'(FT)',T58,'(FT)',T69,
```

```
      208          *'(DEG)'//)
      209        18 FORMAT((10X,I3,5(F10.3,3X)/))
      210        19 FORMAT(1H1,10X,'TABLE ',A6,'.2C ROSKAM-FILLMAN METHOD'/27X,12A6,
      211          *A2/27X,'OPTIMIZATION VERTICAL TAIL'/27X,'SIZING'//27X,'CNB = ',T55
      212          *,F10.3/27X,'ASPECT RATIO =',T55,F10.3/27X,'TAPER RATIO =',T55,
      213          *F10.3//10X,65('*')//T12,'I',T18,'LC',T31,'SV',T44,'BV',T57,'CBARV'
      214          *,T68,'SWEEPV'/T17,'(FT)',T28,'(SQ.FT.)',T43,'(FT)',T58,'(FT)',T69,
      215          *'(DEG)'//)
      216        21 FORMAT(1H1,10X,'TABLE ',A6,'.3A ROSKAM-FILLMAN METHOD'/27X,12A6,
      217          *A2/27X,'SENSITIVITY OF WETTED AREA'/27X,'TO TAIL CONE LENGTH'//1 X
      218          *,65('*')//T12,'I',T20,'LC',T29,'FUSELAGE',T42,'HORIZ',T55,'VERT'
      219          *,T67,'TOTAL'/T19,'(FT)',T29,'(SQ.FT.)',T41,'(SQ.FT.)',T53,'(SQ.FT.
      220          *)',T65,'(SQ.FT.)'//)
      221        22 FORMAT((10X,I3,2X,5(F10.3,2X)/))
      222        23 FORMAT(1H1,10X,'TABLE ',A6,'.3B ROSKAM-FILLMAN METHOD'/27X,12A6,
      223          *A2/27X,'SENSITIVITY OF ZERO-LIFT',/27X,'DRAG TO TAIL CONE LENGTH'
      224          *//27X,'ORIGINAL CD0BHV',T50,F10.5
      225          *//10X,65('*')//T12,'I',T23,'LC',T35,'LC/D',T47,'CD0BHV'/T22,'(FT)'
      226          *//)
      227        24 FORMAT ((11X,I3,2X,2(F10.3,3X),F10.5/))
      228        25 FORMAT(1H1,10X,'TABLE ',A6,'.2D ROSKAM-FILLMAN METHOD'/27X,12A6,
      229          *A2,/27X,'STATIC MARGIN COMPONENTS'//27X,'CMA =',T50,F10.3//
      230          *10X,65('*')//)
      231        26 FORMAT(12X,'I',5X,'LC',6X,'XDW',4X,'XBB',4X,'XBWB',2X,' XBH',4X,
      232          *'XBA',4X,'XBCG'//(10X,I3,F10.3,6F7.3/))
      233          END
*****W  1470 EQUALITY OR NON-EQUALITY COMPARISON MAY NOT BE MEANINGFUL IN LOGICAL IF EXPRESSIONS
```

```
      SUBROUTINE SWET(PHIN,PHIC,SH,SV,TALLGT,SWETN,SWETU,SWETC,
     *SWETH,SWETV)
      COMMON TAS,AMACH,VISCOS,SW,BW,AW,CBAR,WSWPLE,TAPRW,XCBAR,LBOLD,
     1DFUS,NOSLGT,CABLGT,LCOLD,FUSWID,FUSHGT,H1,H2,PHIN1,PHIN2,PHIC1,
     *   PHIC2,  TOL,
     2K1,K2,K3,K4,SHO,BHO,AH,SWPHO,TAPRH,THICKH,LHOLD,HH,SVO,BVO,AV,
     3SWPVO,TAPRV,THICKV,LVOLD,AEFF,K,KEMP1,KEMP2,SBSN,SBSU,SBSC1,DIVE,
     4ULTLOAD,XCG,XCGH,XCGV,XBARWB,XBARHO,CNA,CNB,KAPAW,KAPAH,KAPAV,
     5ETA,DELTLC,EP
      REAL KW,KV,KC,KA,NOSLGT
      DATA PI/3.14159/
      CIRCUM = DFUS * PI
      SWETU = CIRCUM * CABLGT
      CALL CONPAR(PHIN,KA,KV,KC,KW)
      SWETN = CIRCUM * NOSLGT * KW
      CALL CONPAR(PHIC,KA,KV,KC,KW)
      SWETC = CIRCUM * TALLGT * KW
      CKP = .52 * THICKH + 1.987
      SWETH = CKP * SH
      CKP = .52 * THICKV + 1.987
      SWETV = CKP * SV
      RETURN
      END
```

```
      SUBROUTINE CDO (ALB,SWPVT,SWPHT,SWETHT,SWETVT,SWETF,CBARH,CBARV,
     1CDOBHV)
      COMMON TAS,AMACH,VISCOS,SW,BW,AW,CBAR,WSWPLE,TAPRW,XCBAR,LBOLD,
     1DFUS,LN,LJ,LCOLD,FUSWID,FUSHGT,H1,H2,PHIN1,PHIN2,PHIC1,PHIC2,TOL,
     2K1,K2,K3,K4,SHO,BHO,AH,SWPHO,TAPRH,THICKH,LHOLD,HH,SVO,BVO,AV,
     3SWPVO,TAPRV,THICKV,LVOLD,AEFF,K,KEMP1,KEMP2,SBSN,SBSU,SBSC1,DIVE,
     4ULTLOAD,XCG,XCGH,XCGV,XBARWB,XBARHO,CMA,CNB,KAPAW,KAPAH,KAPAV,
     5ETA,DELTLC,EP
      RENUMF = RENUM(DENSIT,VISCOS,TAS,ALB)
      CFMO=0.455/(ALOG10(RENUMF)**2.58)
      CFCM=6.899*AMACH-16.226*AMACH**2+15.741*AMACH**3-5.4894*AMACH**4
      SKIN = CFMO *CFCM
      FINE = ALB / DFUS
      CDOFUS = SKIN*SWETF/SW*(1+60/FINE**3+.0025*FINE)
      RENUMH = RENUM(DENSIT,VISCOS,TAS,CBARH)
      CFMO = .455/(ALOG10(RENUMH)**2.58)
      SKIN = CFMO *CFCM
      HSWPC3=ATAN((SIN(SWPHT)/COS(SWPHT))-(4./AH*(.333*(1-TAPRH)/
     *(1.+TAPRH))))
      VSWPC3=ATAN((SIN(SWPVT)/COS(SWPVT))-(4./AV*(.333*(1.-TAPRV)/
     *(1.+TAPRV))))
      SWPH = COS(HSWPC3)
      SWPV = COS(VSWPC3)
      IF(AMACH.LT.0.25) GOTO 650
      Y=13.36-79.39*AMACH+212.8*AMACH**2-232.9*AMACH**3+94.3*AMACH**4
      RLIFT=Y-16.12*SWPH+33.15*SWPH**2-27.82*SWPH**3+8.32*SWPH**4
      GOTO 660
  650 RLIFT=3.541-16.12*SWPH+33.15*SWPH**2-27.82*SWPH**3+8.32*SWPH**4
  660 CDOHT=SKIN*SWETHT/SW*RLIFT*(1+1.2*THICKH+100*THICKH**4)
      RENUMV = RENUM(DENSIT,VISCOS,TAS,CBARV)
      CFMO = 0.455/(ALOG10(RENUMV)**2.58)
      SKIN = CFMO *CFCM
      IF(AMACH.LT.0.25) GOTO 670
      RLIFT=Y-16.12*SWPV+33.15*SWPV**2-27.82*SWPV**3+8.32*SWPV**4
      GOTO 680
  670 RLIFT=3.541-16.12*SWPV+33.15*SWPV**2-27.82*SWPV**3+8.32*SWPV**4
  680 CDOVT=SKIN*RLIFT*SWETVT/SW*(1+1.2*THICKV+100*THICKV**4)
      CDOBHV = CDOFUS + CDOHT + CDOVT
      RETURN
      END
```

```
      SUBROUTINE FUSWGT(SWETF,SWETN,SWETU,SWETC,WF,WN,WU,WC)
      COMMON TAS,AMACH,VISCOS,SW,BW,AW,CBAR,WSWPLE,TAPRW,XCBAR,LBOLD,
     1BFUS,LN,LU,LCOLD,FUSWID,FUSHGT,H1,H2,PHIN1,PHIN2,PHIC1,PHIC2,TOL,
     2K1,K2,K3,K4,SHO,BHO,AH,SWPHO,TAPRH,THICKH,LHOLD,HH,SVO,BVO,AV,
     3SWPVO,TAPRV,THICKV,LVOLD,AEFF,K,KEMP1,KEMP2,SBSN,SBSU,SBSC1,DIVE,
     4ULTLOAD,XCG,XCGH,XCGV,XBARWB,XBARHO,CMA,CNB,KAPAW,KAPAH,KAPAV,
     5SETA,DELTLC,EP
      REAL LHOLD
C
C     THIS SUBROUTINE, FUSWGT, ESTIMATES THE FUSELAGE WEIGHT WHEN HTE
C     DIVE SPEED, WETTED AREA, FUSELAGE GEOMETRY, AND FOUR CORRECTION
C     FACTORS TO ACCOUNT FOR PRESSURIZATION, ENGINE LOCATION, AND
C     LANDING GEAR LOCATION ARE KNOWN
C
C
C     DETERMINATION OF FUSELAGE CORRECTION FACTORS FROM OPTIONCODES
C
      IF(K1-1)130,120,130
  120 FUSK1=1.08
      GOTO140
  130 FUSK1=1.00
  140 IF(K2-1)160,150,160
  150 FUSK2=1.04
      GOTO170
  160 FUSK2=1.
  170 IF(K3-1)190,180,190
  180 FUSK3=1.07
      GOTO200
  190 FUSK3=1.
  200 IF(K4-1)220,210,220
  210 FUSK4=0.96
      GOTO230
  220 FUSK4=1.
C
C     FROM THE INPUT DATA AND THE FUSELAGE CORRECTION FACTORS, THE
C     ESTIMATED FUSELAGE WEIGHT CAN BE COMPUTED
C
  230 FUSK = FUSK1*FUSK2*FUSK3*FUSK4
      QCWHT = LHOLD + DELTLC
      A = DIVE * QCWHT
      B = FUSWID + FUSHGT
      C = A/B
      D = SWETF**1.2
      E = SQRT(C)
      WF = 0.021*FUSK*D*E
      AFUSK = WF / SWETF
      WN = AFUSK * SWETN
      WU = AFUSK * SWETU
      WC = AFUSK * SWETC
      RETURN
      END
```

```
      SUBROUTINE EMPWGT(SWETH,SWETV,SWETE,HTAREA,HTSPAN,VTAREA,VTSPAN,
     *HSWPLE,VSWPLE,VTWGT,HTWGT,EMPWGH)
      COMMON TAS,AMACH,VISCOS,SW,BW,AW,CBAR,WSWPLE,TAPRW,XCBAR,LBOLD,
     1DFUS,LN,LU,LCOLD,FUSWID,FUSHGT,H1,H2,PHIN1,PHIN2,PHIC1,PHIC2,TOL,
     2K1,K2,K3,K4,SHO,BHO,AH,SWPHO,TAPRH,THICKH,LHOLD,HH,SVO,BVO,AV,
     3SWPVO,TAPRV,THICKV,LVOLD,AEFF,K,KEMP1,KEMP2,SBSN,SBSU,SBSC1,DIVE,
     4ULTLOAD,XCG,XCGH,XCGV,XBARWB,XBARHO,CMA,CNB,KAPAW,KAPAH,KAPAV,
     5ETA,DELTLC,EP
C
C      THIS SUBROUTINE, EMPWGT, CALCULATES THE ESTIMATED WEIGHT OF AN
C     EMPENNAGE WHEN THE DIVE SPEED, WETTED AREA, AND EMPENNAGE
C     GEOMETRY ARE KNOWN
C
C          EMPENNAGE WEIGHT FOR DIVE SPEED LESS THAN 250 KTS
C
      IF(DIVE.GT.250)GOTO500
      EMPWGH=.74*(ULTLOAD*SWETE**2)**.75
      HTWGT = EMPWGH*SWETH/SWETE
      VTWGT = EMPWGH*SWETV/SWETE
      GOTO 630
C
C              EMPENNAGE WEIGHT WHEN DIVE SPEED GREATER THAN 250 KTS
C
C       DETERMINATION OF EMPENNAGE CORRECTION FACTORS
C
500   IF(KEMP1-1)530,520,530
520   EMPKH=1.1
      GOTO540
530   EMPKH=1.
540   IF(KEMP2-1)560,550,560
550   EMPKV=1.+.15*(HTAREA*HTSPAN/VTAREA/VTSPAN)
      GOTO570
560   EMPKV=1.
C
C     DETERMINATION OF HORIZONTAL AND VERTICAT TAIL CORRECTION FACTORS
C
570   HTCF=HTAREA**.2*DIVE/1000./(SQRT(COS(HSWPLE)))
      VTCF=VTAREA**.2*DIVE/1000./(SQRT(COS(VSWPLE)))
      IF(HTCF.GT.1.40)GOTO580
      HTWGT=(3.9*HTCF-.419)*HTAREA*EMPKH
      GOTO590
580   HTWGT=(5.74-2.29*ALOG(HTCF))*HTAREA*EMPKH
590   IF(VTCF.GT.1.40)GOTO600
      VTWGT=(3.9*VTCF-.419)*VTAREA*EMPKV
600   VTWGT=(5.74-2.29*ALOG(VTCF))*VTAREA*EMPKV
      GOTO610
610   EMPWGH = HTWGT + VTWGT
630   CONTINUE
      RETURN
      END
```

```
      SUBROUTINE XBARCG(I,XBCG)
      COMMON TAS,AMACH,VISCOS,SW,BW,AW,CBAR,WSWPLE,TAPRW,XCBAR,LBOLD,
     1DFUS,LN,LU,LCOLD,FUSWID,FUSHGT,H1,H2,PHIN1,PHIN2,PHIC1,PHIC2,TOL,
     2K1,K2,K3,K4,SHO,BHO,AH,SWPHO,TAPRH,THICKH,LHOLD,HH,SVO,BVO,AV,
     3SWPVO,TAPRV,THICKV,LVOLD,AEFF,K,KEMP1,KEMP2,SBSN,SBSU,SBSC1,DIVE,
     4ULTLOAD,XCG,XCGH,XCGV,XBARWB,XBARHO,CMA,CNB,KAPAW,KAPAH,KAPAV,
     5ETA,DELTLC,EP
      COMMON/WEIGHT/WN,WU,WC,WF,WH,WV,WEMP,CGERR,WGROSS,WGR
      COMMON/CEEGEE/XCG1
      COMMON/SHAPE/MN,NN,MC,NC
C
C        THIS SUBROUTINE ESTIMATES THE LOCATION OF THE C.G. OF THE
C        AIRCRAFT ALONG THE LONGITUDINAL AXIS.  THE METHOD USED IS NOT
C        INTENDED TO ACCURATELY LOCATE THE C.G., BUT RATHER TO AID
C        IN LOCATING THE C.G. SHIFT DUE TO INCREMENTALLY LENGTHENING THE
C        AIRCRAFT TAIL CONE.  INPUTS REQUIRED FOR THIS SUBROUTINE
C        ARE LISTED BELOW, AND MUST BE ENTERED INTO THE SUBROUTINE
C        THROUGH EITHER READ STATEMENTS OR COMMON.
C        LN          NOSE LENGTH  (FT)
C        LU          CABIN LENGTH   (FT)
C        LC          TAIL CONE LENGTH   (FT)
C        WFUS        FUSELAGE WEIGHT   (LB)
C        WEMP        EMPENNAGE WEIGHT   (LB)
C        PHIN1,      NOSE CONE SHAPE PARAMETERS
C        PHIN2
C        PHIC1,      TAIL CONE SHAPE PARAMETERS
C        PHIC2
C        XCGH        HORIZ. TAIL C.G. LOCATION   (FT)
C        XCGV        VERT. TAIL C.G. LOCATION   (FT)
C        I           TAIL CONE INCREMENT NUMBER
C
      REAL M,N,LN,LU,LC,MN,NN,MC,NC,LCOLD
      X(A,M,N) =(.5-(1.0/(M*(N+2.0)))+(1.0-M)/(4.0*(M**2)*(2.0*
     *N+2.0))-((1.0-3.0*M+2.0*M**2)/(6.0*(M**3)*(3.0*N+2.0))))*A/(1.0-(1
     *.0/(M*(N+1.0)))+((1.0-M)/(4.0*(M**2)*(2.0*N+1.0)))-(1.0-3.0*M+2.0*
     *(M**2))/(6.0*(M**3)*(3.0*N+1.0)))
C
C        COMPUTE FUSELAGE COMPONENT C.G. LOCATIONS
C
      LC = LCOLD + DELTLC
      CALL CONSHP(PHIN1,PHIN2,TOL,MN,NN)
      IF(I.GT.0)GOTO 50
      WGR = WGROSS - (WC+WV+WH)
   50 CALL CONSHP(PHIC1,PHIC2,TOL,MC,NC)
      XC = X(LC,MC,NC) + LN + LU
      ARM1 = WGR * XCG + WC * XC
C
C        COMPUTE EMPENNAGE COMPONENT C.G. LOCATIONS
C
      XV = XCGV + DELTLC
      XH = XCGH + DELTLC
      ARM2 = WH*XH + WV*XV
```

```
      C
      C        ESTIMATE AIRCRAFT C.G. LOCATION
      C
            WEST = WGR + WC + WH + WV
            XCGEST = (ARM1 + ARM2)/WEST
            IF(I.GT.0) GO TO 100
      C
      C        COMPUTE CORRECTION FACTOR -- CGERR
      C
            CGERR = (XCG - XCGEST)
            XCG1 = XCG
            GO TO 200
        100 XCG1 = XCGEST + CGERR
        200 XBCG =(XCG1 -XCBAR)/CBAR
            RETURN
            END
```

```
      SUBROUTINE STABAREA(XBARCG,HSWPLE,SH,BH,CH)
      COMMON/STAB/XBARW,XBARAC,DXACB,XBARH
      COMMON TAS,AMACH,VISCOS,SW,BW,AW,CBAR,WSWPLE,TAPRW,XCBAR,LBOLD,
     1DFUS,LN,LU,LCOLD,FUSWID,FUSHGT,H1,H2,PHIN1,PHIN2,PHIC1,PHIC2,TOL,
     2K1,K2,K3,K4,SHO,BHO,AH,SWPHO,TAPRH,THICKH,LHOLD,HH,SVO,BVO,AV,
     3SWPVO,TAPRV,THICKV,LVOLD,AEFF,K,KEMP1,KEMP2,SBSN,SBSU,SBSC1,DIVE,
     4ULTLOAD,XCG,XCGH,XCGV,XBARWB,XBARHO,CMA,CNB,KAPAW,KAPAH,KAPAV,
     5ETA,DELTLC,EP
      COMMON/CLDATA/ASPECT,BATA,SWPC2,KAPPA
      REAL LHOLD,LHNEW,HH,KWB,KAPPA,KAPAH,KAPAW,KA,KTAPR,KH
      SH=SHO
      BH=BHO
      HSWPLE=SWPHO
C
C     THIS PART OF THE PROGRAM OPTOMIZES THE SWEEP ANGLE OF THE
C     HORIZONTAL TAIL, FIRST WE CONVERT THE INPUT VALUE OF THE LE SWEEP
C     TO THE HALF-CHORD SWEEP ANGLE
C
      HSWPC2=ATAN((SIN(HSWPLE)/COS(HSWPLE))-(4./AH*(.5*(1.-TAPRH)/
     *(1.+TAPRH))))
C
C     FIRST WE CONVERT THE INPUT VALUES OF SURFACE SWEEP ANGLES
C     TO USEABLE FORM FOR CALCULATION PURPOSES
C
      WSWPC2=ATAN((SIN(WSWPLE)/COS(WSWPLE))-(4./AW*(.5*(1.-TAPRW)
     */(1.+TAPRW))))
      WSWPC4=ATAN((SIN(WSWPLE)/COS(WSWPLE))-(4./AW*(.25*(1.-TAPRW)
     */(1.+TAPRW))))
      BETA=SQRT(1.-AMACH**2.)
    1 CLLH1=0.
      HSWP1=0.
      DO 10 I=1,181
      HSWP2=HSWP1+.008727
      ASPECT=AH
      BATA=BETA
      SWPC2=HSWP2
      KAPPA=KAPAH
      CALL LSLOPE (SLOPE)
      CLAH=SLOPE
      LHNEW=LHOLD+DELTLC+(((BH/6.)*(1.+2.*TAPRH)/(1.+TAPRH))*
     *((SIN(HSWP2)/COS(HSWP2 ))-(SIN(HSWPC2)/COS(HSWPC2))))
      CLLH2=CLAH*LHNEW
      IF (CLLH1.GE.CLLH2 ) GO TO 20
      CLLH1=CLLH2
   10 HSWP1=HSWP2
   20 CONTINUE
C
C     NOW WE COMPUTE THE PARAMETERS TO THE EQUATION FOR SH
C     FIRST WE COMPUTE CLAH
C
      SWPC2=HSWP1
      CALL LSLOPE (SLOPE )
```

```
      CLAH=SLOPE
C
C     NOW WE COMPUTE XBARACH
C
      XBARH=XBARHO+DELTLC/CBAR+(((BH/6.)*(1.+2.*TAPRH)/(1.+TAPRH))*
     *((SIN(HSWP2 )/COS(HSWP2 ))-(SIN(HSWPC2)/COS(HSWPC2))))/CBAR
C
C     NOW WE CALCULATE D EPSILON / D ALPHA
C
      ASPECT =AW
      SWPC2=WSWPC2
      BATA=BETA
      KAPPA=KAPAW
      CALL LSLOPE (SLOPE)
      CLAWM=SLOPE
      BATA=1.
      CALL LSLOPE (SLOPE)
      CLAWO=SLOPE
      KA=(1./AW)-(1./(1.+AW**1.7))
      KTAPR=(10.-(3.*TAPRW))/7.
      KH=(1.-(HH/BW))/((2.*LHNEW)/BW)**.3333
      DEPDAL=(CLAWM/CLAWO)*(4.44*(KA*KTAPR*KH*SQRT(COS(WSWPC4)))**1.19)
C
C     NEXT COMPUTE CL ALPHA WB
C
      KWB = 1.-(.25*(DFUS/BW)**2)+.025*DFUS/BW
      CLAWB=KWB*CLAWM
C
C     NEXT COMPUTE THE TOTAL AIRPLANE CL ALPHA
C
      CLAA=CLAWB+CLAH*ETA*SH/SW*(1.-DEPDAL)
C
C     COMPUTE XBARAC
C
      XBARAC=XBARCG-CMA/CLAA
      CALL MULTOP(LHNEW,CLAWM,DEPDAL,DXACB)
      XBARWB =XBARW  +DXACB
C
C     NOW THAT ALL PARAMETERS ARE KNOWN WE CAN COMPUTE THE NEW AREA
C
      SHNEW=(XBARWB-XBARAC)/((XBARAC-XBARH)*(CLAH/CLAWB)*
     *(ETA/SW)*(1.-DEPDAL))
      BHNEW=SQRT(SHNEW*AH)
      BHDIF=ABS(BHNEW-BH)
      IF (BHDIF.LE.EP) GO TO 30
      SH=SHNEW
      BH=BHNEW
      GO TO 1
   30 CONTINUE
      SH=SHNEW
      BH=BHNEW
      CH=(4.*SH)/(3.*BH)*((1.+TAPRH+TAPRH**2.)/(1.+TAPRH)**2.)
```

```
105           HSWPLE=ATAN((SIN(HSWP1)/COS(HSWP1))-(4./AH*(-.5*(1.-TAPRH)/
106          *(1.+TAPRH))))
107           SWP = HSWPLE * 57.3
108           RETURN
109           END
```

```
      SUBROUTINE VERTAREA(VSWPLE,SV,BV,CV)
      COMMON TAS,AMACH,VISCOS,SW,BW,AW,CBAR,WSWPLE,TAPRW,XCBAR,LBOLD,
     1DFUS,LN,LU,LCOLD,FUSWID,FUSHGT,H1,H2,PHIN1,PHIN2,PHIC1,PHIC2,TOL,
     2K1,K2,K3,K4,SHO,BHO,AH,SWPHO,TAPRH,THICKH,LHOLD,HH,SVO,BVO,AV,
     3SWPVO,TAPRV,THICKV,LVOLD,AEFF,K,KEMP1,KEMP2,SBSN,SBSU,SBSC1,DIVE,
     4ULTLOAD,XCG,XCGH,XCGV,XBARVB,XBARHO,CMA,CNB,KAPAW,KAPAH,KAPAV,
     5ETA,DELTLC,EP
      COMMON/CEEGEE/XCG1
      REAL K,LVOLD,LVNEW,KN,KRL,KA,LCOLD,LCNEW,LBOLD,LBNEW,LB2SBS
      REAL H1,H2,H1H2,M1,HWRAT,M2,KAPPA,KAPAV,KV,KC,KW,LN
      COMMON/CLDATA/ASPECT,BATA,SWPC2,KAPPA
      BV=BVO
      VSWPLE=SWPVO
C
C     THE FIRST PART OF THIS ROUTINE OPTOMIZES THE SWEEP ANGLE OF
C     THE VERTICAL TAIL  FIRST WE CONVERT THE INPUT VALUE OF LE SWEEP
C     TO HALF CHORD SWEEP
C
      VSWPC2=ATAN((SIN(VSWPLE)/COS(VSWPLE))-(4./AV*(.5*(1.-TAPRV)/
     *(1.+TAPRV))))
      BETA=SQRT(1.-AMACH**2.)
    1 CLLV1=0.
      VSWP1=0.
      DO 10 I=1,181
      VSWP2=VSWP1+.008727
      ASPECT=AEFF
      BATA=BETA
      SWPC2=VSWP2
      KAPPA=KAPAV
      CALL LSLOPE (SLOPE)
      CLAV=SLOPE
      XVOLD = LVOLD - (XCG1-XCG)
      LVNEW=XVOLD+DELTLC+(((BV/3.)*(2.+2.*TAPRV) /(1.+TAPRV ))*
     *((SIN(VSWP2)/COS(VSWP2))-(SIN(VSWPC2)/COS(VSWPC2))))
      CLLV2=CLAV*LVNEW
      IF (CLLV1.GE.CLLV2) GO TO 20
      CLLV1=CLLV2
   10 VSWP1=VSWP2
   20 CONTINUE
C
C     THIS PART OF THE ROUTINE COMPUTES THE NEW VERTICAL TAIL AREA
C     AND VERTICAL TAIL SPAN
C     FIRST WE CALCULATE KRL
C
      LBNEW=LBOLD+DELTLC
      RENUMF=RENUM(DENSIT,VISCOS,TAS,LBNEW)
      KRL= -1.830754+.20494*ALOG(RENUMF)
C
C     NOW WE CALCULATE THE BODY SIDE AREA OF THE NEW AIRPLANE
C
      LCNEW=LCOLD+DELTLC
      CALL CONPAR (PHIC1,KA,KV,KC,KW)
```

```
      SBSEC1=KA*LCOLD*DFUS
      SBSRAT = 1.00
      SBSEC2=KA*LCNEW*DFUS
      CALL CONPAR(PHIN1,KA,KV,KC,KW)
      SBSN = KA*LN*DFUS
      SBS=SBSN+SBSU+SBSRAT*SBSEC2
C
C     NOW WE CALCULATE KN BY A THREE STEP
C     METHOD IT WAS ARRIVED AT BY APPLYING CURVFITTING TECHNIQUES
C     TO THE CHASE AROUND CHART IN DATCOM
C
      LB2SBS=LBNEW**2./SBS
      IF (LB2SBS.GE.8.) GO TO 30
      SHIFT1=6.0942-1.3516*LB2SBS+.13525*LB2SBS**2.-.0062*LB2SBS**3.+
     *.0001*LB2SBS**4.
      GO TO 50
   30 IF (LB2SBS.GE.12.) GO TO 40
      SHIFT1=-.12*LB2SBS+1.91
      GO TO 50
   40 SHIFT1=-.05875*LB2SBS+1.175
   50 CONTINUE
      YVALUE=2.8333*XCG/LBNEW-.41667+SHIFT1
      H1H2=SQRT(H1/H2)
      M1=3.6497-3.5796*H1H2-.39*H1H2**2.+2.0149*H1H2**3.-.6946*H1H2**4.
      ZVALUE=YVALUE/M1
      HWRAT=FUSHGT/FUSWID
      M2=(-1.0147+4.4649*HWRAT-3.3626*HWRAT**2.+1.0794*HWRAT**3.-.1217*
     *HWRAT**4.)*.001
       KN=M2*ZVALUE-.0005
      SWPC2=VSWP1
      CALL LSLOPE (SLOPE)
      CLAV=SLOPE
C
C     COMPUTATION OF THE NEW PLANFORM PARAMETERS
C
      SVNEW=(SW*BW*CNB+57.3*KN*KRL*SBS*LBNEW)/(K*CLAV*LVNEW)
C
C     CALCULATION OF THE NEW SPAN AND COMPARISON WITH THE TOLERANCE
C     OF THE ITERATION
C
      BVNEW=SQRT(AV*SVNEW)
      BVDIF=ABS(BVNEW-BV)
      IF (BVDIF.LE.EP) GO TO 110
      SV=SVNEW
      BV=BVNEW
      GO TO 1
  110 CONTINUE
      SV=SVNEW
      BV=BVNEW
      CV=(4.*SV)/(3.*BV)*((1.+TAPRV+TAPRV**2.)/(1.+TAPRV)**2.)
      VSWPLE=ATAN((SIN(VSWP1)/COS(VSWP1 ))-(4./AV*(-.5*(1.-TAPRV)/
     *(1.+TAPRV))))
```

```
105             SWP = VSWPLE * 57.3
106             RETURN
107             END
```

```
                1            SUBROUTINE MULTOP(LHNEW,CLAWM,DEPDAL,DXACB)
                2            COMMON/RHO/DENSIT
                3            COMMON TAS,AMACH,VISCOS,SW,BW,AW,CBAR,WSWPLE,TAPRW,XCBAR,LBOLD,
                4           1DFUS,LN,LU,LCOLD,FUSWID,FUSHGT,H1,H2,PHIN1,PHIN2,PHIC1,PHIC2,TOL,
                5           2K1,K2,K3,K4,SHO,BHO,AH,SWPHO,TAPRH,THICKH,LHOLD,HH,SVO,BVO,AV,
                6           3SWPVO,TAPRV,THICKV,LVOLD,AEFF,K,KEMP1,KEMP2,SBSN,SBSU,SBSC1,DIVE,
                7           4ULTLOAD,XCG,XCGH,XCGV,XBARWB,XBARHO,CMA,CNB,KAPAW,KAPAH,KAPAV,
                8           5ETA,DEL LC,EP
                9            COMMON/SHAPE/MN,NN,MC,NC
               10            DATA C0,C1,C2,C3,C4 /1.90,-1.6958,1.5759,-0.7292,0.1302/
               11            DATA D0,D1,D2,D3,D4/6.2503,-23.0908,60.3553,-78.4540,38.2895/
               12            REAL LN,NN,MN,LT,LBOLD,LCOLD,LCNEW,NC,MC,LH,LHNEW
               13            POLY(X,C,C1,C2,C3,C4)=C+C1*X+C2*X**2.+C3*X**3.+C4*X**4.
               14            CLAWM = CLAWM/57.2958
               15            QBAR = 0.5*DENSIT*TAS*TAS
               16            XLE=XCBAR-(((BH/6.)*(1.+2.*TAPRH)/(1.+TAPRH))-.5*DFUS)*SIN(WSWPLE)
*****W   412 BH IS NOT DEFINED
               17           */COS(WSWPLE)
               18            CR = 1.5*CBAR*(1.+TAPRW)/(1.+TAPRW+TAPRW**2)
               19            CRF = DFUS*CR*(TAPRW-1.)/BW +CR
               20            DXI = XLE/50.
               21            SUM = 0.
               22            DO 100 I=1,50
               23            XI = XLE - (DXI*0.5)- DXI*(I-1)
               24            IF(XI.LE.(XLE-LN)) GO TO 10
               25            WFI = DFUS*((1.-(((LN+XI-XLE)/LN)**NN))**(1./MN))
               26            GO TO 20
               27         10 WFI = DFUS
               28         20 XCF = XI/CRF
               29            DEDA = POLY(XCF,C0,C1,C2,C3,C4)
               30            IF(I.GE.45) DEDA = POLY(XCF,D0,D1,D2,D3,D4)
               31            DEDAI = DEDA*CLAWM/4.58
               32        100 SUM = SUM + (DXI*WFI*WFI*DEDAI)
               33            LT = LBOLD + DELTLC - XLE - CRF
               34            DXI = LT/50.
               35            LCNEW =LCOLD +DELTLC
               36            DO 200 I=1,50
               37            XI = DXI*(I-1)+(0.5*DXI)
               38            IF(XI.LE.(LT-LCNEW)) GO TO 30
               39            WFI = DFUS*((1.-(((LCNEW+XI-LT)/LCNEW)**NC))**(1./MC))
               40            GO TO 40
               41         30 WFI = DFUS
               42         40 LH = LHNEW-CRF+.25*CBAR+((BW/6.)*(1.+2.*TAPRW)/(1.+TAPRW)-DFUS/2.)
               43           **SIN(WSWPLE)/COS(WSWPLE)
               44            DEDAI = (1.-DEPDAL)*XI/LH
               45        200 SUM = SUM + (DXI*WFI*WFI*DEDAI)
               46            DMDA = (QBAR/36.5)*SUM
               47            DXACB = -1.*DMDA/(QBAR*CBAR*SW*CLAWM)
               48            RETURN
               49            END
```

```
                1            SUBROUTINE CONSHP(PHI1,PHI2,TOL,M,N)
                2            REAL M,N,M1,M2
                3            I=1
                4            J=1
                5            N=1.0
                6            DM2 = 10.0
                7         10 M1 = ALOG(1.0 -(PHI1**N))/ALOG(PHI1)
                8            M2 = ALOG(1.0 -(PHI2**N))/ALOG(PHI2/2.0)
                9            J = J+1
               10            IF(J.EQ.100)   GO TO 80
               11            DM1 = M1-M2
               12            IF(DM1.LE.0.) GO TO 30
               13            IF(DM1.GT.DM2) GO TO 50
               14         20 N = N+(0.05/I)
               15            DM2 = DM1
               16            GO TO 10
               17         30 IF(ABS(DM1).LT.TOL)GO TO 60
               18            I = I*5
               19         40 N = N - (0.05/I)
               20            M1 = ALOG(1.0 -(PHI1**N))/ALOG(PHI1)
               21            M2 = ALOG(1.0 -(PHI2**N))/ALOG(PHI2/2.0)
               22            J = J+1
               23            IF(J.EQ.100)   GO TO 80
               24            DM1 = M2-M1
               25            IF(DM1.LT.0.) GO TO 20
               26            IF(ABS(DM1).LT.TOL) GO TO 60
               27            GO TO 40
               28         50 WRITE(6,1)
               29            M = 1.0
               30            N = 1.0
               31            GO TO 70
               32         60 M = (M1 + M2)*0.5
               33         70 RETURN
               34         80 WRITE(6,4)
               35            GO TO 60
               36          1 FORMAT(10X,'***ITERATION FOR M AND N DIVERGES***'/15X,'SET-  M=1.0
                            X'/22X,'N=1.0'//)
               37          4 FORMAT(10X,'***100 STEPS COMPLETE--DID NOT CONVERGE***'//)
               38            RETURN
*****W   209 STATEMENT CANNOT BE REACHED
               39            END
```

```
      1            SUBROUTINE CONPAR(PHI,KA,KV,KC,KW)
      2            REAL KA,KV,KC,KW
      3        C   THIS SUBROUTINE COMPUTES THE AREA CORRECTION FACTORS
      4        C    KA, KV, KC, AND KW WHEN THE SHAPE PARAMETER PHI IS INPUTTED
      5        C   THIS SUBROUTINE WAS DERIVED FROM TORENBEEK PG. 447
      6        C
      7            DATA AK,AK1,AK2,AK3,AK4/-0.59,3.8109,-5.721,6.4168,-2.9167/
      8            DATA VK,VK1,VK2,VK3,VK4/-.9095,5.803,-13.0927,16.5927,-7.4074/
      9            DATA CK,CK1,CK2,CK3,CK4/2.96,-12.0488,22.8752,-18.3335,5.5556/
     10            DATA WK,WK1,WK2,WK3,WK4/-172.721,1008.8388,-2162.25,2023.9877,-69
     11           *7.9097/
     12            POLY(X,C,C1,C2,C3,C4)=C+C1*X+C2*X**2.+C3*X**3.+C4*X**4.
     13            KA=POLY(PHI,AK,AK1,AK2,AK3,AK4)
     14            KV=POLY(PHI,VK,VK1,VK2,VK3,VK4)
     15            KC=POLY(PHI,CK,CK1,CK2,CK3,CK4)
     16            KW=POLY(PHI,WK,WK1,WK2,WK3,WK4)
     17            CONTINUE
     18            RETURN
     19            END
```

```
1          SUBROUTINE LSLOPE (SLOPE)
2          REAL KAPPA
3          COMMON /CLDATA/ASPECT,BATA,SWPC2,KAPPA
4          SLOPE=(2.*3.14159*ASPECT)/(2.+SQRT((ASPECT**2.*BATA**2./KAPPA**2.)
5         **(1.+(((SIN(SWPC2)/COS(SWPC2))*(SIN(SWPC2)/COS(SWPC2)))/BATA**2))
6         **4.))
7          RETURN
8          END
```

```
1            FUNCTION RENUM(DENSIT,VISCOS,TAS,ALNGTH)
2       C
3       C    THIS FUNCTION COMPUTES THE REYNOLDS NUMBER OF A BODY
4       C
5            RENUM=(TAS*ALNGTH)/VISCOS
6            RETURN
7            END
```

B3 Example Output

This section provides Roskam/Fillman Program output for a conceptual aircraft configuration. This conceptual aircraft is not to be confused with any of those mentioned in Chapter 4.

TABLE 2.15.1A ROSKAM-FILLMAN METHOD
CONFIGURATION J (31 PAX, 2/2)
ORIGINAL FLIGHT CONDITIONS AND
GEOMETRIC DEFINITIONS

****

FLIGHT CONDITIONS

ALTITUDE	25000.000	FT
AIRSPEED	366.750	FPS
MACH	0.361	
DENSITY	0.00107	SLUGS/CU.FT.
KINEMATIC VISCOSITY	0.00030	SQ.FT./SEC

GEOMETRIC

WING		
REFERENCE AREA	440.000	SQ.FT.
SPAN	66.330	FT
ASPECT RATIO	10.000	
M.A.C.	6.880	FT
F.S.	19.840	FT
L.E. SWEEP	0.	DEG
TAPER	0.500	
FUSELAGE		
OVERALL LENGTH	56.350	FT
NOSE LENGTH	14.620	FT
CABIN LENGTH	20.000	FT
TAIL CONE LENGTH	21.760	FT
MAX WIDTH	8.080	FT
MAX HEIGHT	8.080	FT
EQUIV. DIAMETER	8.080	FT
HORIZONTAL TAIL		
REFERENCE AREA	55.600	SQ.FT.
SPAN	14.910	FT
ASPECT RATIO	4.000	
M.A.C.	3.870	FT
TAPER	0.500	
THICKNESS	0.090	
VERTICAL TAIL		
REFERENCE AREA	48.380	SQ.FT.
SPAN	6.960	FT
ASPECT RATIO	1.000	
M.A.C.	7.210	FT
TAPER	0.500	
THICKNESS	0.090	

TABLE 2.15.1B ROSKAM-FILLMAN METHOD
CONFIGURATION J (31 PAX, 2/2)
ORIGINAL WEIGHT AND BALANCE STATEMENT

****

	(LBS.)
GROSS WEIGHT	22000.000
APPROXIMATED SHELL WEIGHTS	
FUSELAGE	
NOSE SECTION	754.560
CABIN SECTION	1246.399
TAIL CONE SECTION	1264.082
TOTAL FUSELAGE	3265.040
EMPENNAGE	
HORIZONTAL TAIL	115.226
VERTICAL TAIL	330.431
TOTAL EMPENNAGE	445.657
CENTER OF GRAVITY -- FRACTION OF M.A.C.	0.250

TABLE 2.15.1C ROSKAM-FILLMAN METHOD
CONFIGURATION J (31 PAX, 2/2)
ORIGINAL WETTED AREA BREAKDOWN

****

	(SQ.FT.)
FUSELAGE	
NOSE SECTION	307.346
CABIN SECTION	507.681
TAIL SECTION	514.883
TOTAL FUSELAGE	1329.910
EMPENNAGE	
HORIZONTAL TAIL	113.079
VERTICAL TAIL	98.395
TOTAL EMPENNAGE	211.475

TABLE 2.15.2A ROSKAM-FILLMAN METHOD
CONFIGURATION J (31 PAX, 2/2)
OPTIMIZATION WEIGHT AND BALANCE
STATEMENT

****

GROSS WEIGHT(W/O TAIL OR EMP.) 20290.261 (LBS.)

I	LC (FT)	LB (FT)	FUSELAGE WT (LB)	EMPENNAGE WT (LB)	C.G. (FR CBAR)
1	15.000	49.620	21066.239	439.115	0.148
2	15.250	49.870	21062.912	793.682	0.205
3	15.500	50.120	21080.119	832.915	0.216
4	15.750	50.370	21097.460	797.579	0.214
5	16.000	50.620	21114.933	791.182	0.217
6	16.250	50.870	21132.538	788.696	0.221
7	16.500	51.120	21150.275	786.583	0.224
8	16.750	51.370	21168.142	784.563	0.228
9	17.000	51.620	21186.141	782.504	0.232
10	17.250	51.870	21204.269	782.219	0.236
11	17.500	52.120	21222.527	780.213	0.240
12	17.750	52.370	21240.915	777.981	0.243
13	18.000	52.620	21259.432	775.626	0.247
14	18.250	52.870	21278.077	773.334	0.251
15	18.500	53.120	21296.850	771.047	0.255
16	18.750	53.370	21315.751	768.685	0.259
17	19.000	53.620	21334.780	766.367	0.263
18	19.250	53.870	21353.936	764.168	0.267
19	19.500	54.120	21373.218	761.934	0.271
20	19.750	54.370	21392.627	759.563	0.275
21	20.000	54.620	21412.161	757.193	0.279
22	20.250	54.870	21431.821	754.873	0.283
23	20.500	55.120	21451.606	752.560	0.287
24	20.750	55.370	21471.516	750.194	0.291

25	21.000	55.620	21491.551	747.872	0.295
26	21.250	55.870	21511.709	745.562	0.299
27	21.500	56.120	21531.991	743.249	0.303
28	21.750	56.370	21552.397	740.889	0.307
29	22.000	56.620	21572.926	738.564	0.312
30	22.250	56.870	21593.578	736.295	0.316
31	22.500	57.120	21614.352	733.949	0.320
32	22.750	57.370	21635.248	731.628	0.325
33	23.000	57.620	21656.266	729.313	0.329
34	23.250	57.870	21677.406	726.967	0.333
35	23.500	58.120	21698.667	724.654	0.338
36	23.750	58.370	21720.049	722.344	0.342
37	24.000	58.620	21741.551	720.008	0.347
38	24.250	58.870	21763.174	717.700	0.351
39	24.500	59.120	21784.916	715.396	0.356
40	24.750	59.370	21806.779	713.066	0.360
41	25.000	59.620	21828.761	710.760	0.365
42	25.250	59.870	21850.862	708.514	0.369
43	25.500	60.120	21873.081	706.203	0.374
44	25.750	60.370	21895.420	703.907	0.379
45	26.000	60.620	21917.876	701.620	0.383
46	26.250	60.870	21940.451	699.313	0.388
47	26.500	61.120	21963.143	697.024	0.393
48	26.750	61.370	21985.953	694.747	0.398
49	27.000	61.620	22008.880	692.450	0.402
50	27.250	61.870	22031.925	690.174	0.407
51	27.500	62.120	22055.085	687.907	0.412
52	27.750	62.370	22078.362	685.621	0.417
53	28.000	62.620	22101.756	683.353	0.422
54	28.250	62.870	22125.265	681.076	0.427

55	28.500	63.120	22148.890	678.815	0.432
56	28.750	63.370	22172.630	676.561	0.437
57	29.000	63.620	22196.486	674.343	0.442
58	29.250	63.870	22220.457	672.099	0.447
59	29.500	64.120	22244.542	669.856	0.452
60	29.750	64.370	22268.741	667.599	0.458
61	30.000	64.620	22293.055	665.359	0.463

TABLE 2.15.28 ROSKAM-FILLMAN METHOD
CONFIGURATION J (31 PAX, 2/2)
OPTIMIZATION STABILIZER
SIZING

CMA = -1.000
ASPECT RATIO = 4.000
TAPER RATIO = 0.500

****

I	LC (FT)	SH (SQ.FT.)	BH (FT)	CBARH (FT)	SWEEPH (DEG)
1	15.000	34.337	11.720	3.038	18.472
2	15.250	49.338	14.048	3.642	19.854
3	15.500	51.615	14.369	3.725	19.854
4	15.750	50.622	14.230	3.689	19.854
5	16.000	50.847	14.261	3.697	19.854
6	16.250	51.238	14.316	3.712	19.854
7	16.500	51.667	14.376	3.727	19.394
8	16.750	52.081	14.433	3.742	19.394
9	17.000	52.492	14.490	3.757	19.394
10	17.250	52.978	14.557	3.774	19.394
11	17.500	53.388	14.613	3.789	19.394
12	17.750	53.786	14.668	3.803	19.394
13	18.000	54.179	14.721	3.817	19.394
14	18.250	54.574	14.775	3.831	19.394
15	18.500	54.935	14.824	3.843	19.394
16	18.750	55.346	14.879	3.858	19.394
17	19.000	55.776	14.937	3.872	18.933
18	19.250	56.192	14.992	3.887	18.933
19	19.500	56.956	15.041	3.899	18.933
20	19.750	56.941	15.092	3.913	18.933
21	20.000	57.326	15.143	3.926	18.933
22	20.250	57.713	15.194	3.939	18.933
23	20.500	58.099	15.245	3.952	18.933

24	20.750	58.483	15.295	3.965	18.933
25	21.000	58.869	15.345	3.978	18.933
26	21.250	59.254	15.395	3.991	18.933
27	21.500	59.639	15.445	4.004	18.933
28	21.750	60.021	15.495	4.017	18.933
29	22.000	60.421	15.546	4.031	18.472
30	22.250	60.805	15.596	4.043	18.472
31	22.500	61.186	15.644	4.056	18.472
32	22.750	61.568	15.693	4.069	18.472
33	23.000	61.950	15.742	4.081	18.472
34	23.250	62.330	15.790	4.094	18.472
35	23.500	62.712	15.838	4.106	18.472
36	23.750	63.093	15.886	4.119	18.472
37	24.000	63.474	15.934	4.131	18.472
38	24.250	63.854	15.982	4.143	18.472
39	24.500	64.234	16.029	4.156	18.472
40	24.750	64.613	16.076	4.168	18.472
41	25.000	65.011	16.126	4.181	18.008
42	25.250	65.394	16.173	4.193	18.008
43	25.500	65.773	16.220	4.205	18.008
44	25.750	66.154	16.267	4.217	18.008
45	26.000	66.534	16.314	4.229	18.008
46	26.250	66.913	16.360	4.242	18.008
47	26.500	67.294	16.407	4.254	18.008
48	26.750	67.675	16.453	4.266	18.008
49	27.000	68.055	16.499	4.278	18.008
50	27.250	68.436	16.545	4.289	18.008
51	27.500	68.817	16.591	4.301	18.008
52	27.750	69.197	16.637	4.313	18.008
53	28.000	69.577	16.683	4.325	18.008

54	28.250	69.958	16.728	4.337	18.008
55	28.500	70.339	16.774	4.349	18.008
56	28.750	70.738	16.821	4.361	17.544
57	29.000	71.121	16.867	4.373	17.544
58	29.250	71.503	16.912	4.385	17.544
59	29.500	71.885	16.957	4.396	17.544
60	29.750	72.266	17.002	4.408	17.544
61	30.000	72.649	17.047	4.420	17.544

TABLE 2.15.2C ROSKAM-FILLMAN METHOD
CONFIGURATION J (31 PAX, 2/2)
OPTIMIZATION VERTICAL TAIL
SIZING

CNB =	0.120
ASPECT RATIO =	1.000
TAPER RATIO =	0.500

****

I	LC (FT)	SV (SQ.FT.)	BV (FT)	CBARV (FT)	SWEEPV (DEG)
1	15.000	117.219	10.827	11.228	69.183
2	15.250	117.577	10.843	11.245	69.183
3	15.500	110.428	10.508	10.898	68.272
4	15.750	109.786	10.478	10.866	68.272
5	16.000	109.238	10.452	10.839	67.971
6	16.250	108.698	10.426	10.812	67.673
7	16.500	108.156	10.400	10.785	67.376
8	16.750	107.614	10.374	10.758	67.080
9	17.000	107.380	10.362	10.746	66.786
10	17.250	106.814	10.335	10.718	66.494
11	17.500	106.244	10.307	10.689	66.203
12	17.750	105.658	10.279	10.660	66.203
13	18.000	105.085	10.251	10.631	65.914
14	18.250	104.511	10.223	10.602	65.626
15	18.500	103.940	10.195	10.573	65.340
16	18.750	103.355	10.166	10.543	65.340
17	19.000	102.780	10.138	10.514	65.054
18	19.250	102.207	10.110	10.484	64.770
19	19.500	101.633	10.081	10.455	64.488
20	19.750	101.050	10.052	10.425	64.488
21	20.000	100.475	10.024	10.395	64.206
22	20.250	99.901	9.995	10.365	63.926
23	20.500	99.318	9.966	10.335	63.926

24	20.750	98.743	9.937	10.305	63.647
25	21.000	98.170	9.908	10.275	63.369
26	21.250	97.596	9.879	10.245	63.092
27	21.500	97.015	9.850	10.214	63.092
28	21.750	96.441	9.820	10.184	62.816
29	22.000	95.868	9.791	10.154	62.541
30	22.250	95.289	9.762	10.123	62.541
31	22.500	94.716	9.732	10.093	62.267
32	22.750	94.144	9.703	10.062	61.994
33	23.000	93.567	9.673	10.031	61.994
34	23.250	92.995	9.643	10.001	61.721
35	23.500	92.424	9.614	9.970	61.450
36	23.750	91.849	9.584	9.939	61.450
37	24.000	91.278	9.554	9.908	61.180
38	24.250	90.709	9.524	9.877	60.910
39	24.500	90.135	9.494	9.846	60.910
40	24.750	89.566	9.464	9.814	60.641
41	25.000	88.998	9.434	9.783	60.373
42	25.250	88.426	9.404	9.752	60.373
43	25.500	87.859	9.373	9.720	60.105
44	25.750	87.292	9.343	9.689	59.838
45	26.000	86.722	9.312	9.657	59.838
46	26.250	86.156	9.282	9.626	59.572
47	26.500	85.592	9.252	9.594	59.307
48	26.750	85.024	9.221	9.562	59.307
49	27.000	84.459	9.190	9.531	59.042
50	27.250	83.896	9.160	9.499	58.777
51	27.500	83.330	9.129	9.467	58.777
52	27.750	82.768	9.098	9.435	58.513
53	28.000	82.203	9.067	9.402	58.513

54	28.250	81.642	9.036	9.370	58.250
55	28.500	81.081	9.005	9.338	57.987
56	28.750	80.519	8.973	9.306	57.987
57	29.000	79.959	8.942	9.273	57.724
58	29.250	79.400	8.911	9.241	57.462
59	29.500	78.839	8.879	9.208	57.462
60	29.750	78.281	8.848	9.175	57.200
61	30.000	77.721	8.816	9.142	57.200

TABLE 2.15.20 ROSKAM-FILLMAN METHOD
CONFIGURATION J (31 PAX, 2/2)
STATIC MARGIN COMPONENTS

CMA = -1.000

I	LC	XBW	XBB	XBWB	XBH	XBA	XBCG
1	15.000	0.230	-0.023	0.207	3.771	0.333	0.148
2	15.250	0.230	-0.023	0.207	3.821	0.388	0.205
3	15.500	0.230	-0.023	0.207	3.858	0.398	0.216
4	15.750	0.230	-0.023	0.207	3.894	0.396	0.214
5	16.000	0.230	-0.023	0.207	3.930	0.399	0.217
6	16.250	0.230	-0.023	0.207	3.966	0.403	0.221
7	16.500	0.230	-0.023	0.207	3.999	0.406	0.224
8	16.750	0.230	-0.023	0.207	4.035	0.410	0.228
9	17.000	0.230	-0.023	0.207	4.071	0.413	0.232
10	17.250	0.230	-0.024	0.206	4.108	0.417	0.236
11	17.500	0.230	-0.024	0.206	4.144	0.421	0.240
12	17.750	0.230	-0.024	0.206	4.181	0.425	0.243
13	18.000	0.230	-0.024	0.206	4.217	0.428	0.247
14	18.250	0.230	-0.024	0.206	4.253	0.432	0.251
15	18.500	0.230	-0.024	0.206	4.290	0.436	0.255
16	18.750	0.230	-0.024	0.206	4.326	0.440	0.259
17	19.000	0.230	-0.025	0.205	4.358	0.443	0.263
18	19.250	0.230	-0.025	0.205	4.395	0.447	0.267
19	19.500	0.230	-0.025	0.205	4.431	0.451	0.271
20	19.750	0.230	-0.025	0.205	4.467	0.455	0.275
21	20.000	0.230	-0.025	0.205	4.504	0.459	0.279
22	20.250	0.230	-0.025	0.205	4.540	0.463	0.283
23	20.500	0.230	-0.025	0.205	4.576	0.467	0.287
24	20.750	0.230	-0.026	0.204	4.613	0.471	0.291
25	21.000	0.230	-0.026	0.204	4.649	0.475	0.295

26	21.250	0.230	-0.026	0.204	4.686	0.479	0.299
27	21.500	0.230	-0.026	0.204	4.722	0.483	0.303
28	21.750	0.230	-0.026	0.204	4.758	0.487	0.307
29	22.000	0.230	-0.026	0.204	4.790	0.491	0.312
30	22.250	0.230	-0.026	0.204	4.827	0.496	0.316
31	22.500	0.230	-0.027	0.203	4.863	0.500	0.320
32	22.750	0.230	-0.027	0.203	4.899	0.504	0.325
33	23.000	0.230	-0.027	0.203	4.936	0.508	0.329
34	23.250	0.230	-0.027	0.203	4.972	0.513	0.333
35	23.500	0.230	-0.027	0.203	5.008	0.517	0.338
36	23.750	0.230	-0.027	0.203	5.045	0.521	0.342
37	24.000	0.230	-0.027	0.203	5.081	0.526	0.347
38	24.250	0.230	-0.028	0.202	5.117	0.530	0.351
39	24.500	0.230	-0.028	0.202	5.154	0.534	0.356
40	24.750	0.230	-0.028	0.202	5.190	0.539	0.360
41	25.000	0.230	-0.028	0.202	5.222	0.543	0.365
42	25.250	0.230	-0.028	0.202	5.258	0.548	0.369
43	25.500	0.230	-0.028	0.202	5.294	0.552	0.374
44	25.750	0.230	-0.028	0.202	5.331	0.557	0.379
45	26.000	0.230	-0.029	0.201	5.367	0.562	0.383
46	26.250	0.230	-0.029	0.201	5.403	0.566	0.388
47	26.500	0.230	-0.029	0.201	5.440	0.571	0.393
48	26.750	0.230	-0.029	0.201	5.476	0.576	0.398
49	27.000	0.230	-0.029	0.201	5.512	0.580	0.402
50	27.250	0.230	-0.029	0.201	5.549	0.585	0.407
51	27.500	0.230	-0.029	0.201	5.585	0.590	0.412
52	27.750	0.230	-0.030	0.200	5.621	0.595	0.417
53	28.000	0.230	-0.030	0.200	5.658	0.600	0.422
54	28.250	0.230	-0.030	0.200	5.694	0.605	0.427
55	28.500	0.230	-0.030	0.200	5.730	0.610	0.432

56	28.750	0.230	-0.030	0.200	5.762	0.614	0.437
57	29.000	0.230	-0.030	0.200	5.798	0.619	0.442
58	29.250	0.230	-0.030	0.200	5.835	0.624	0.447
59	29.500	0.230	-0.031	0.199	5.871	0.630	0.452
60	29.750	0.230	-0.031	0.199	5.907	0.635	0.458
61	30.000	0.230	-0.031	0.199	5.944	0.640	0.463

TABLE 2.15.3A ROSKAM-FILLMAN METHOD
CONFIGURATION J (31 PAX, 2/2)
SENSITIVITY OF WETTED AREA
TO TAIL CONE LENGTH

****

I	LC (FT)	FUSELAGE (SQ.FT.)	HORIZ (SQ.FT.)	VERT (SQ.FT.)	TOTAL (SQ.FT.)
1	15.000	1169.956	69.834	238.400	1478.190
2	15.250	1175.871	100.344	239.129	1515.343
3	15.500	1181.786	104.976	224.589	1511.351
4	15.750	1187.702	102.955	223.282	1513.939
5	16.000	1193.617	103.413	222.168	1519.198
6	16.250	1199.533	104.208	221.069	1524.809
7	16.500	1205.448	105.081	219.967	1530.496
8	16.750	1211.364	105.923	218.865	1536.152
9	17.000	1217.279	106.759	218.389	1542.427
10	17.250	1223.195	107.746	217.239	1548.180
11	17.500	1229.110	108.581	216.078	1553.770
12	17.750	1235.026	109.390	214.887	1559.302
13	18.000	1240.941	110.189	213.721	1564.851
14	18.250	1246.857	110.992	212.555	1570.404
15	18.500	1252.772	111.728	211.394	1575.894
16	18.750	1258.688	112.562	210.203	1581.453
17	19.000	1264.603	113.438	209.035	1587.076
18	19.250	1270.519	114.282	207.868	1592.669
19	19.500	1276.434	115.023	206.701	1598.158
20	19.750	1282.350	115.807	205.515	1603.671
21	20.000	1288.265	116.590	204.346	1609.201
22	20.250	1294.181	117.377	203.178	1614.736
23	20.500	1300.096	118.162	201.993	1620.251
24	20.750	1306.012	118.943	200.824	1625.778
25	21.000	1311.927	119.727	199.658	1631.312

26	21.250	1317.842	120.511	198.492	1636.845
27	21.500	1323.758	121.294	197.309	1642.361
28	21.750	1329.673	122.070	196.142	1647.886
29	22.000	1335.589	122.885	194.976	1653.450
30	22.250	1341.504	123.665	193.800	1658.969
31	22.500	1347.420	124.440	192.634	1664.495
32	22.750	1353.335	125.217	191.471	1670.023
33	23.000	1359.251	125.994	190.296	1675.540
34	23.250	1365.166	126.767	189.134	1681.068
35	23.500	1371.082	127.543	187.972	1686.598
36	23.750	1376.997	128.319	186.802	1692.118
37	24.000	1382.913	129.093	185.642	1697.647
38	24.250	1388.828	129.866	184.483	1703.178
39	24.500	1394.744	130.639	183.316	1708.699
40	24.750	1400.659	131.411	182.159	1714.228
41	25.000	1406.575	132.220	181.004	1719.799
42	25.250	1412.490	132.998	179.841	1725.329
43	25.500	1418.406	133.770	178.687	1730.862
44	25.750	1424.321	134.543	177.535	1736.399
45	26.000	1430.237	135.317	176.376	1741.930
46	26.250	1436.152	136.088	175.225	1747.465
47	26.500	1442.068	136.862	174.076	1753.006
48	26.750	1447.983	137.637	172.921	1758.541
49	27.000	1453.899	138.410	171.774	1764.082
50	27.250	1459.814	139.184	170.629	1769.627
51	27.500	1465.729	139.960	169.477	1775.166
52	27.750	1471.645	140.732	168.333	1780.710
53	28.000	1477.560	141.506	167.185	1786.252
54	28.250	1483.476	142.280	166.043	1791.799
55	28.500	1489.391	143.055	164.903	1797.350

56	28.750	1495.307	143.866	163.759	1802.932
57	29.000	1501.222	144.645	162.621	1808.488
58	29.250	1507.138	145.422	161.484	1814.044
59	29.500	1513.053	146.199	160.343	1819.595
60	29.750	1518.969	146.975	159.208	1825.152
61	30.000	1524.884	147.753	158.070	1830.707

TABLE 2.15.33 ROSKAM-FILLMAN METHOD
CONFIGURATION J (31 PAX, 2/2)
SENSITIVITY OF ZERO-LIFT
DRAG TO TAIL CONE LENGTH

ORIGINAL CDOBHV 0.00937

I	LC (FT)	LC/D	CDOBHV
1	15.000	1.856	0.00894
2	15.250	1.887	0.00911
3	15.500	1.918	0.00909
4	15.750	1.949	0.00909
5	16.000	1.980	0.00910
6	16.250	2.011	0.00911
7	16.500	2.042	0.00912
8	16.750	2.073	0.00913
9	17.000	2.104	0.00915
10	17.250	2.135	0.00917
11	17.500	2.166	0.00918
12	17.750	2.197	0.00919
13	18.000	2.228	0.00921
14	18.250	2.259	0.00923
15	18.500	2.290	0.00924
16	18.750	2.321	0.00926
17	19.000	2.351	0.00928
18	19.250	2.382	0.00930
19	19.500	2.413	0.00932
20	19.750	2.444	0.00933
21	20.000	2.475	0.00935
22	20.250	2.506	0.00937
23	20.500	2.537	0.00939
24	20.750	2.568	0.00941

25	21.000	2.599	0.00943
26	21.250	2.630	0.00945
27	21.500	2.661	0.00947
28	21.750	2.692	0.00949
29	22.000	2.723	0.00951
30	22.250	2.754	0.00953
31	22.500	2.785	0.00955
32	22.750	2.816	0.00958
33	23.000	2.847	0.00959
34	23.250	2.877	0.00962
35	23.500	2.908	0.00964
36	23.750	2.939	0.00966
37	24.000	2.970	0.00968
38	24.250	3.001	0.00971
39	24.500	3.032	0.00972
40	24.750	3.063	0.00975
41	25.000	3.094	0.00977
42	25.250	3.125	0.00979
43	25.500	3.156	0.00981
44	25.750	3.187	0.00984
45	26.000	3.218	0.00986
46	26.250	3.249	0.00988
47	26.500	3.280	0.00991
48	26.750	3.311	0.00992
49	27.000	3.342	0.00995
50	27.250	3.373	0.00997
51	27.500	3.403	0.00999
52	27.750	3.434	0.01002
53	28.000	3.465	0.01004
54	28.250	3.496	0.01006

55	28.500	3.527	0.01009
56	28.750	3.558	0.01011
57	29.000	3.589	0.01013
58	29.250	3.620	0.01015
59	29.500	3.651	0.01017
60	29.750	3.682	0.01020
61	30.000	3.713	0.01022

APPENDIX C FUSELAGE SHAPE SIMULATION PROGRAM, FUSE

This appendix documents the program FUSE and how to use it. Appendix C1 will describe the preparation of input data for both the simulation and design modes of the program. Default values for the design mode are also documented in this section. Appendix C2 will explain how the program was operated on the Honeywell 66/60 timesharing system and about the different operation options that were available. Appendix C3 provides a copy of the program listing.

C1 Preparation of Input Data

FUSE may be operated in either of two modes--the simulation mode or the design mode. In the simulation mode input data are read from a separate disc file set up like a card data deck (Logical unit no. 03). In the design mode data are input by means of an interactive question and answer sequence. Each of these methods will be dealt with in turn. To aid in understanding the input computer acronyms, Table C-1 has been prepared.

Table C-1 FUSE Input Acronyms

Acronym	Variable	Description	Units
H	H	Cabin height	ft
LBD	ℓ_B/D	Fuselage fineness ratio	
LC	ℓ_c	Tail cone length	ft
LCD	ℓ_c/D	Tail cone fineness ratio	
LLN	ℓ_{N1}/ℓ_{N2}	Ratio of nose cone lengths	
LN1	ℓ_{N1}	Cone N1 length	ft
LN2	ℓ_{N2}	Cone N2 length	ft
LU	ℓ_u	Cabin (utility) length	ft
NFORX	-	Array containing number of lengthwise divisions per fuselage section	
NFORX(1)	-	Number of lengthwise divisions for the nose	
NFORX(2)	-	Number of lengthwise divisions for the cabin	
NFORX(3)	-	Number of lengthwise divisions for the tail cone	
NFUS	-	Number of fuselage sections to be simulated; ≤ 3	
NRADX	-	Number of radial divisions	
PH11	ϕ_{11}	Cone N1 taper shape parameter (Side view)	
PH21	ϕ_{21}	Cone N1 bluntness shape parameter (Side view)	

Table C-1 FUSE Input Acronyms (Cont'd)

Acronym	Variable	Description	Units
PH12	ϕ_{12}	Cone N2 taper shape parameter (Side view)	
PH22	ϕ_{22}	Cone N2 bluntness shape parameter (Side view)	
PHY1	ϕ_{Y1}	Cone N1 taper shape parameter (Top view)	
PHY2	ϕ_{Y2}	Cone N1 bluntness shape parameter (Top view)	
PHC1	ϕ_{C1}	Tail cone taper shape parameter	
PHC2	ϕ_{C2}	Tail cone bluntness shape parameter	
QC1	q_{C1}	Coefficient of (x') for the cone offset equation	
QC2	q_{C2}	Coefficient of $(x')^2$ for the tail cone offset equation	
QN1	q_{N1}	Coefficient of x for the cone N1 offset equation	
QN2	q_{N2}	Coefficient of x^2 for the cone N1 offset equation	
RB1	r_{b1}	Cone N1 round-off radius, bottom	
RB2	r_{b2}	Cone N2 round-off radius, bottom	
RBC	r_{bc}	Cabin round-off radius, bottom	
RBT	r_{bt}	Tail round-off radius, bottom	

Table C-1 FUSE Input Acronyms (Cont'd)

Acronym	Variable	Description	Units
RT1	r_{t1}	Cone N1 round-off radius, top	
RT2	r_{t2}	Cone N2 round-off radius, top	
RTC	r_{tc}	Cabin round-off radius, top	
RTT	r_{tt}	Tail round-off radius, top	
W	w	Cabin width	ft
YN1	y_{N1}	Half width of Cone N1 at $x = \ell_{N1}$	
ZN0	z_{N0}	Vertical offset of Cone N1 at x = 0	ft
ZN1	z_{N1}	Half height of Cone N1 at $x = \ell_{N1}$	ft
ZZC	$\frac{2z_o\|_{x=\ell_B}}{H}$	Tail cone offset	
ZZN	$2z_{N1}/H$	Ratio of nose cone heights	

C1.1 Simulation Mode Input Data

As was stated, in the simulation mode data are read from a disc file set up like a data card deck. In other words, each line of the file represents a different data card. The file must be sequential. Also only one simulation data deck may be run at a time. Table C-2 provides a guide for the "card" formats.

Most of the input data required for FUSE are relatively simple to derive from a drawing of the fuselage desired. The nose, however, and the offset cones in general can sometimes present difficulties. In checking out FUSE several methods for determining the shape parameters for the nose were tried. The method that will be described in the following paragraphs consistently produced the best results.

Figures C-1 and C-2 provide the top, side, and front views for the nose of the Gates Learjet 35/36. These views will be used to determine the nose shape input parameters for FUSE.

The length of the nose, ℓ_{N1}, is chosen to extend to the point where the fuselage cabin cross-section can best be said to become constant. Usually this will occur just aft of the crew compartment. The elliptical cones are modelled such that the planform curves are perpendicular to the cross-sectional plane at the base of nose section ($x = \ell_{N1}$). This should also be considered when the nose section length is chosen. The length of Cone N2, ℓ_{N2}, is determined by fairing the windshield curve down to the fuselage centerline as shown in Figure C-1.

Table C-2 Simulation Mode Input Data

Card Format

INPUT CARD NO. 1 - (5I3)

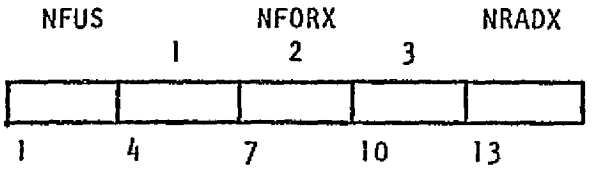

INPUT CARD NO. 2 - (18A4)

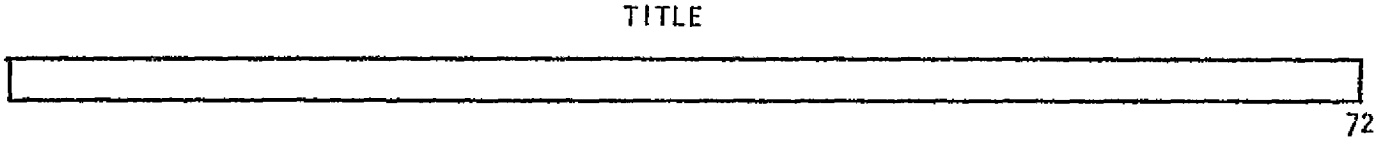

INPUT CARD NO. 3 - (7F10.0)

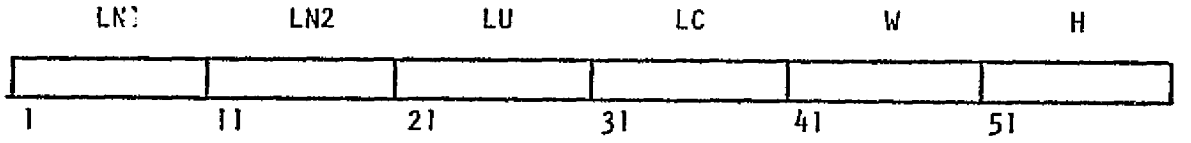

INPUT CARD NO. 4 - (7F10.0)

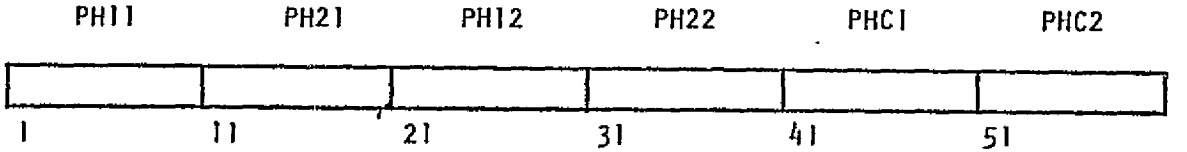

Table C-2 (Continued)

INPUT CARD NO. 5 - (7F10.0)

PHY1 PHY2

INPUT CARD NO. 6 - (7F10/0)

YN1 ZN1 ZNØ QN1 QN2 QC1 QC2

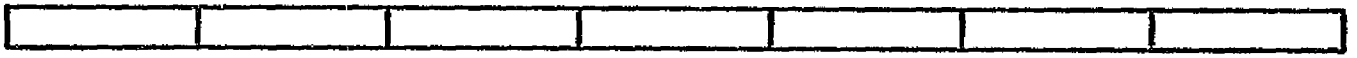

INPUT CARD NO. 7 - (7F10.0)

RT1 RB1 RT2 RB2

INPUT CARD NO. 8 - (7F10.0)

RTC RBC RTT RBT

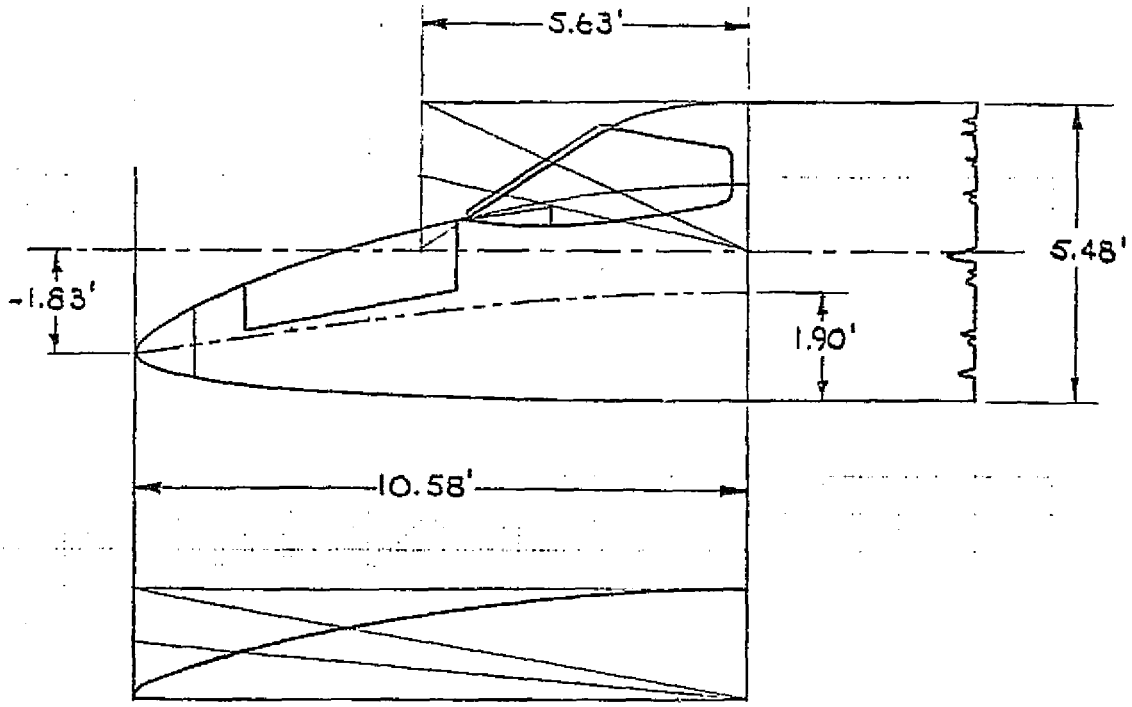

NOTE: SCALE: 1/40

NOSE SHAPE PARAMETERS (SIDE VIEW)

ℓ_{N1} = 10.58 ft. $z_0 = -1.83 + .195x - .00834x^2$

ℓ_{N2} = 5.63 ft. ϕ_{11} = 0.651

H = 5.48 ft. ϕ_{21} = 0.825

z_{NO} = - 1.83 ft. ϕ_{12} = 0.598

z_{N1} = 1.90 ft. ϕ_{22} = 0.749

CALC	R.D.W.	28MAR	REVISED	DATE	Figure C-1 Gates Learjet 35/36 Nose Shape Input Parameters (Side View).	
CHECK						
APPD						
APPD					30 UNIVERSITY OF KANSAS	PAGE

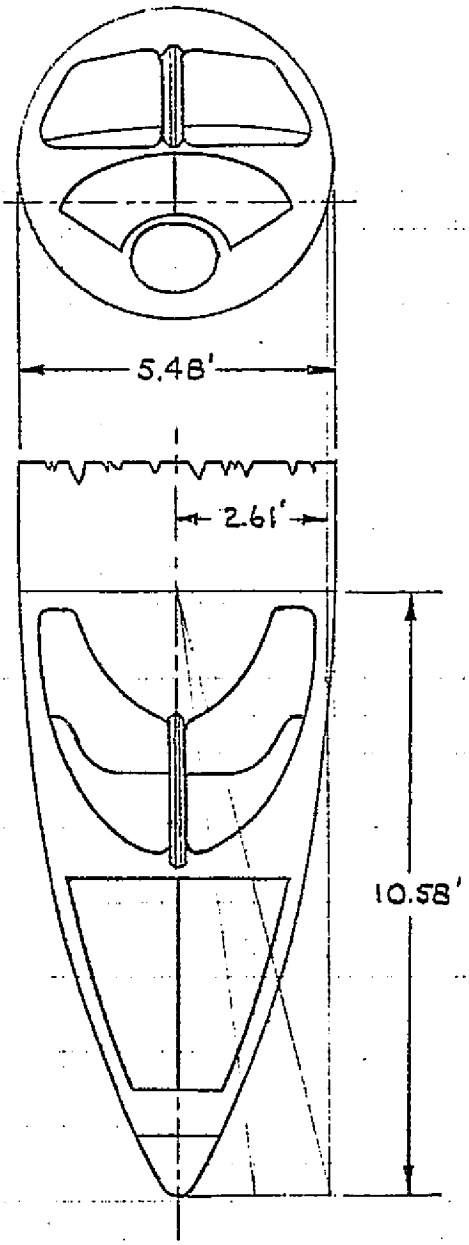

NOTE: SCALE: 1/40

NOSE SHAPE PARAMETERS

(TOP VIEW)

ℓ_{N1} = 10.58 ft.

W = 5.48 ft.

y_{N1} = 2.61 ft.

ϕ_{y1} = 0.644 ft.

ϕ_{y2} = 0.805 ft.

CALC	R.D.W.	28 MAR	REVISED	DATE	Figure C-2 Gates Learjet 35/36 Nose Shape Input Parameters (Top View).
CHECK					
APPD					
APPD					
					31 UNIVERSITY OF KANSAS PAGE

The values for the Cone N2 shape parameters, ϕ_{12} and ϕ_{22}, are easily calculated by constructing the box and diagonals of Figure A-4 around the windshield cone. This has been accomplished in Figure C-1. The values for these shape parameters are also presented in Figure C-1.

As Cone N1 is deformed and offset, the procedure becomes slightly more difficult. The first step is to fair the curve of the upper surface back to the base of the nose section. Again, in accomplishing this it should be remembered that the planform curves must be perpendicular to the cross-sectional plane at the base of the nose section. The centerline of the deformed cone is then constructed. By applying a parabolic curve fit routine the equation for z_0 is established. In this case a parabolic regression analysis was performed using a curve fit routine in the BASIC language. A listing of this program is provided in Appendix D. All offsets are referenced to the centerline of the fuselage.

The half-height of Cone N1, z_{N1}, measured as shown in Figure C-1. This will always be a positive value.

The shape parameters, ϕ_{11} and ϕ_{21}, cannot be properly determined from the deformed cone. Instead the cone is projected onto a straightened centerline of length, ℓ_{N1}, as shown. The shape parameters are then calculated by the rectangle and diagonals. The method for determining the geometry of a deformed elliptical cone may also be applied to the fuselage tail cone.

Figure C-2 pictures the top and front views of the nose section. The front view is used to determine what the maximum width of Cone N1 at the nose section base must be. To avoid discontinuities at the base of the nose section, y_{N1} should be no greater than the y-value of the cabin a distance z_{N1} above the bottom of the cabin. This has been demonstrated in Figure C-2. The shape parameters ϕ_{y1} and ϕ_{y2} are then calculated in the usual manner.

The cabin input parameters are relatively straightforward and should be easily determined. The length of the cabin is ℓ_u - or that part of the fuselage which may be simulated by a cylinder. The width of the cabin is W and the height is H. The tail cone shape parameters should be computed in a manner similar to that of the nose cones. The only differences are that the taper shape parameter, ϕ_{1C}, is calculated as the average of the top and side view taper shape parameters, and that the bluntness shape parameter, ϕ_{2C}, is the average of the top and side view bluntness shape parameters.

Table C-3 below provides a listing of the input data file for the Gates-Learjet 35/36.

Table C-3 Listing of the Data File for the Gates-Learjet 35/36

```
 3  7  7 15 10
GATES-LEARJET 35/36 -- 590 PANELS
10.58      5.63      10.34      25.83      5.48       5.48
0.651      0.825     0.598      0.749      0.602      0.772
0.644      0.805
 2.61       1.90     -1.90       0.195    -0.00834   0.00217   0.00238
1.         1.        1.         1.
1.         1.        1.         1.
```

C1.2 Design Mode Input Data

Design Mode data are input by an interactive question and answer sequence. The most effective way to describe this procedure is to follow the procedure for an example design. Such an example will be provided here. In this example underlined statements are those typed by the operator. The symbol "↑" will be used to indicate a carriage return. Note that all of the following questions and answers documented here occur after the program has been compiled and execution begun.

```
DESIGN OR SIMULATION MODE?
ENTER D OR S
=D ↑
PRINT DIMENSIONS? Y FOR YES, N FOR NO
=Y ↑
PRINT FUSELAGE COORDINATES? Y OR N
=Y ↑
PRINT TOTAL WETTED AREA? Y OR N
=Y ↑
PRINT PANEL AREAS AND RATIOS? Y OR N
=N ↑
PLOT FUSELAGE? Y OR N
=N ↑
BUSINESS JET OR PISTON COMMUTER?
ENTER J OR P
=P ↑
```

The questions about printing data and plotting the fuselage are asked for either the design or simulation mode. They are included here for the sake of coninuity but will be discussed in detail in Appendix C2. The question as to whether a jet or piston aircraft is to be designed determines which default values are to be used when needed. These values will be discussed later.

```
TITLE?
=CONFIGURATION -- 5; VARIED ROUND-OFFS ↑
NUMBER OF PANELS?
=60 ↑
NO. OF RADIAL DIV. EACH SIDE?
=10 ↑
ELLIPTICAL OR CIRCULAR CROSS-SECTIONS? Y OR N
=N ↑
CONE N1 ROUND-OFF RADII: TOP,BOTTOM
=.5,1. ↑
CONE N2 ROUND-OFF RADII: TOP,BOTTOM
=.6,.3 ↑
CABIN ROUND-OFF RADII: TOP,BOTTOM
=.6,.3
TAIL ROUND-OFF RADII: TOP,BOTTOM
=.6,.3 ↑
```

If the question, "ELLIPTICAL OR CIRCULAR CROSS-SECTION?", had been answered with yes, FUSE would have assumed that all round-off radii were equal to 1.0.

```
ENTER: PASSENGERS,SEATS ABREAST,PITCH
=25,3,30 ↑
SEAT WIDTH,AISLE WIDTH
=20,18 ↑
DESIRED INSIDE CABIN HEIGHT? (IN.)
=70 ↑
FUSELAGE WIDTH =  6.92 FT
SHOULD H=W ? Y OR N
=N ↑
INPUT H ? Y OR N
=N ↑

FUSELAGE HEIGHT =  6.44 FT

INSIDE CABIN HEIGHT = 70.00 IN.
```


If the operator had decided that H should equal W, then the desired inside cabin height is over-ridden. In this case the inside

cabin height is computed according to the McDonnell Douglas method documented in Chapter 2, and is output. Due to a programming oversight, if H is chosen to be input, the desired inside cabin height is output although this may no longer be valid.

```
BAGGAGE COMPARTMENT? Y OR N
=Y ↑
ENTER LLN,ZZN,ZN0
=,, ↑
ENTER PH11,PH21,PH12,PH22,PHY1,PHY2
=,,,,,↑
ENTER LED,LCD,ZZC
=,,↑
ENTER PHC1,PHC2
=, ↑
```

For this example a baggage compartment was chosen to be included. The baggage compartment is sized according to Section 2.4. The shape parameters were chosen to be default values in the example above. The use of commas alone implies values of zero for each parameter. A value of zero tells the program to select the appropriate default value. The parameters above are all defined in Table C-1.

With the data as input above the program will determine the aircraft size and compute the node coordinates.

The default values that have been mentioned are tabulated in Table C-4. These values have no statistical value. They were chosen during the programming stage rather arbitrarily. At that time it was felt that they did however generate designs which were representative of each of these two airplane types.

Table C-4 FUSE Default Values

Variable	Jet	Piston
LLN	2.5	2.5
ZZN	.75	.75
ZNØ	$Z\emptyset\|_{x=\ell_{N1}}$	$Z\emptyset\|_{x=\ell_{N1}}$
ϕ_H	.65	.65
ϕ_{21}	.825	.85
ϕ_{12}	.60	.60
ϕ_{22}	.75	.725
ϕ_{y1}	.64	.65
ϕ_{y2}	.825	.85
LBD	6.0	6.0
LCD	4.0	3.5
ZZC	.75	.75
ϕ_{1c}	.60	.60
ϕ_{2c}	.775	.80

C3 Program Operation

This program was written for the Honeywell 66/60 timesharing system. Consequently, many of the commands that will be described here will not be the same or perhaps even applicable on other systems. An attempt will be made to explain the reasons for each so that it will be possible for the reader to evaluate his own application.

C3.1 Program Initialization

As FUSE is written to be used with the Tektronix PLOT 10 graphics software package, and because it is sometimes necessary to read from, or write to, other disc files, it is necessary to link the program file with several others before compiling. This is accomplished as described in the following paragraphs.

Three files were required to operate the PLOT 10 package. The names for these on the University of Kansas system were ADEOUT, ADEIN, and OBJECT. To be linked with FUSE these files had to be placed on the Available File Table (AFT) for the KU-FRL project computer account. Each project account is identified by what is referred to as a Project Identifier (PI). To place a file in the AFT three things must be given: the PI under which the file is stored; the catalog name (if any) under which the file is stored; and the filename. Then the command is:

```
GET PI/CATALOG/FILENAME  ↑
```

If a logical unit number (L) is to be assigned to the file

when it is stored in the AFT, then the command becomes:

```
GET PI/CATALOG/FILENAME"L"  ↑
```

For the case of FUSE this might be accomplished as:

```
SYSTEM?  GET 7684WALLACE/PLOT10/ADEOUT  ↑
SYSTEM?  GET 7684WALLACE/PLOT10/ADEIN  ↑
SYSTEM?  GET 7684WALLACE/PLOT10/OBJECT  ↑
SYSTEM?  GET 7102DESIGN/LEARJET"03"  ↑
SYSTEM?  GET 7102DESIGN/LEARCOORD"07"  ↑
```

This would gather the PLOT10 files, and LEARJET and LEARCOORD onto the AFT. LEARJET would be assigned the logical unit number "03" (to be read from) and LEARCOORD, the logical unit number "07" (to be written to).

To load FUSE onto the AFT for use as a FORTRAN program the command was:

```
SYSTEM?  FORTRAN  ↑
OLD FILE OR NEW - OLD FUSE  ↑
```

And to compile and execute:

```
*  RUNH  *; ADEOUT; ADEIN; OBJECT  ↑
```

FUSE, in this case, is referred to as the star-level file; hence the * after the command RUNH. LEARJET and LEARCOORD are input/output files to be referred to by the program and therefore are not needed in the run command. Having completed these commands, the program is compiled and executed.

C2.2 Output Options

There are six output options available for both the design and simulation modes:

1) Print Dimensions

2) Print Coordinates

3) Print Total Wetted Area

4) Print Panel Areas and Ratios

5) Plot Fuselage

6) File Data

If dimensions are output, the result will appear either as in Table C-5a or as in Table C-5b, depending on whether the design or simulation mode is selected. Note that at the end of each printout, the operator is asked whether the data were satisfactory. If not, he is given the choice of resubmitting his input or terminating execution. When the dimensions are satisfactory, he may choose to file data.

If coordinates are output, the result will appear as in Table C-6. The I and J value locate the node longitudinally and radially, respectively; and the X, Y, and Z values provide the coordinates in feet.

Total wetted area of the fuselage appears as shown below:

```
**********************

TOTAL WETTED AREA =      769.52

**********************
```

Panel areas and ratios are output as shown in Table C-7. In this case, the I and J values locate the panels longitudinally and radially. The area of the panel is in ft^2. RATIO J is the ratio of the area of that panel to the (I,J-1) panel, and RATIO I is the ratio of the area of that panel to the (I-1,J) panel.

If a plot is requested, the fuselage is plotted on the graphics terminal similarly to the plots presented in Figures 2.43 and 2.44. The major difference is that the actual aircraft fuselage lines are not superimposed.

If it is requested that data be filed, the fuselage coordinates are filed in a manner compatible with the input data formats of the NCSU BODY program of Reference 20.

Table C-5a Dimension Printout for Design Mode

```
CONFIGURATION -- SJ VARIED POINT-CRFS

FUSE PROGRAM MODE -- D

DIVISIONS

   RADIAL (HALF FUSELAGE)                    10
   LENGTHWISE
     NOSE                                     7
     CABIN                                   12
     TAIL                                     9

CABIN CONFIGURATION

   NO. OF PASSENGERS                         25
   SEATS PER ROW                              3
   NO. OF ROWS                                9

FUSELAGE GEOMETRY

   NOSE CONE N1
     LENGTH                                10.96
     HALF HEIGHT                            2.42
     HALF WIDTH                             3.35
     SHAPE PARAMETERS
       PH11                                 0.650
       PH21                                 0.350
       PHY1                                 0.650
       PHY2                                 0.350

   NOSE CONE N2
     LENGTH                                 6.26
     SHAPE PARAMETERS
       PH12                                 0.600
       PH22                                 0.725

   CABIN
     LENGTH                                29.17
     HEIGHT                                 6.44
     WIDTH                                  6.92

   TAIL CONE
     LENGTH                                23.38
     SHAPE PARAMETERS
       PHC1                                 0.600
       PHC2                                 0.800

DATA SATISFACTORY? Y OR N
=Y
FILE FUSELAGE DATA? Y OR N
=N
```

Table C-5b Dimension Printout for Simulation Mode

```
   GATES-LEARJET 35/36 -- 500 PANELS

 FUSE PROGRAM MODE -- S

  DIVISIONS

     RADIAL (HALF FUSELAGE)                    10
     LENGTHWISE
       NOSE                                     7
       CABIN                                    7
       TAIL                                    15

  FUSELAGE GEOMETRY

     NOSE CONE N1
       LENGTH                                10.58
       HALF HEIGHT                            1.96
       HALF WIDTH                             2.61
       SHAPE PARAMETERS
         PH11                                 0.651
         PH21                                 0.825
         PHY1                                 0.644
         PHY2                                 0.885

     NOSE CONE N2
       LENGTH                                  5.63
       SHAPE PARAMETERS
         PH12                                 0.598
         PH22                                 0.749

     CABIN
       LENGTH                                10.34
       HEIGHT                                 5.48
       WIDTH                                  5.48

     TAIL CONE
       LENGTH                                25.83
       SHAPE PARAMETERS
         PHC1                                 0.602
         PHC2                                 0.773

DATA SATISFACTORY? Y OR N
=Y
FILE FUSELAGE DATA? Y OR N
=Y
```

Table C-6 Example Coordinate Printout

I	J	X	Y	Z
1	1	0.	0.	-0.964
1	2	0.	0.	-0.964
1	3	0.	0.	-0.964
1	4	0.	0.	-0.964
1	5	0.	0.	-0.964
1	6	0.	0.	-0.964
1	7	0.	0.	-0.964
1	8	0.	0.	-0.964
1	9	0.	0.	-0.964
1	10	0.	0.	-0.964
1	11	0.	0.	-0.964
2	1	1.812	0.	-2.261
2	2	1.812	0.458	-2.212
2	3	1.812	0.908	-2.054
2	4	1.812	1.320	-1.762
2	5	1.812	1.608	-1.326
2	6	1.812	1.662	-0.803
2	7	1.812	1.460	-0.329
2	8	1.812	1.113	0.005
2	9	1.812	0.731	0.203
2	10	1.812	0.359	0.303
2	11	1.812	0.	0.333
3	1	3.625	0.	-2.800
3	2	3.625	0.676	-2.724
3	3	3.625	1.336	-2.481
3	4	3.625	1.922	-2.039
3	5	3.625	2.305	-1.392
3	6	3.625	2.334	-0.643
3	7	3.625	2.009	0.010
3	8	3.625	1.508	0.453
3	9	3.625	0.981	0.707
3	10	3.625	0.480	0.834
3	11	3.625	0.	0.872
4	1	5.437	0.	-3.191
4	2	5.437	0.848	-3.092
4	3	5.437	1.668	-2.778
4	4	5.437	2.381	-2.212
4	5	5.437	2.819	-1.398
4	6	5.437	2.806	-0.482
4	7	5.437	2.375	0.290
4	8	5.437	1.760	0.796
4	9	5.437	1.136	1.081
4	10	5.437	0.553	1.221
4	11	5.437	0.	1.262
5	1	7.249	0.	-3.491
5	2	7.249	0.991	-3.372
5	3	7.249	1.942	-2.995
5	4	7.249	2.753	-2.321

Table C-7 Example of Panel Area and Ratio Output

(I,J) AREA RATIOJ RATIOI	(I,J) AREA RATIOJ RATIOI	(I,J) AREA RATIOJ RATIOI	(I,J) AREA RATIOJ RATIOI	(I,J) AREA RATIOJ RATIOI
1, 1	2, 1	3, 1	4, 1	5, 1
0.512E 00	0.108E 01	0.142E 01	0.170E 01	0.193E 01
0.10E 01	0.10E 01	0.10E 01	0.10E 01	0.10E 01
0.10E 01	0.21E 01	0.13E 01	0.12E 01	0.11E 01
1, 2	2, 2	3, 2	4, 2	5, 2
0.537E 00	0.112E 01	0.147E 01	0.175E 01	0.198E 01
0.10E 01	0.10E 01	0.10E 01	0.10E 01	0.10E 01
0.10E 01	0.21E 01	0.13E 01	0.12E 01	0.11E 01
1, 3	2, 3	3, 3	4, 3	5, 3
0.580E 00	0.118E 01	0.153E 01	0.181E 01	0.215E 01
0.11E 01	0.11E 01	0.10E 01	0.10E 01	0.11E 01
0.10E 01	0.20E 01	0.13E 01	0.12E 01	0.12E 01
1, 4	2, 4	3, 4	4, 4	5, 4
0.622E 00	0.123E 01	0.157E 01	0.184E 01	0.193E 01
0.11E 01	0.10E 01	0.10E 01	0.10E 01	0.90E 00
0.10E 01	0.20E 01	0.13E 01	0.12E 01	0.11E 01
1, 5	2, 5	3, 5	4, 5	5, 5
0.641E 00	0.123E 01	0.156E 01	0.182E 01	0.204E 01
0.10E 01	0.10E 01	0.10E 01	0.99E 00	0.11E 01
0.10E 01	0.19E 01	0.13E 01	0.12E 01	0.11E 01
1, 6	2, 6	3, 6	4, 6	5, 6
0.622E 00	0.120E 01	0.151E 01	0.174E 01	0.207E 01
0.97E 00	0.97E 00	0.97E 00	0.96E 00	0.10E 01
0.10E 01	0.19E 01	0.13E 01	0.12E 01	0.12E 01
1, 7	2, 7	3, 7	4, 7	5, 7
0.562E 00	0.110E 01	0.137E 01	0.153E 01	0.214E 01
0.90E 00	0.92E 00	0.90E 00	0.88E 00	0.10E 01
0.10E 01	0.20E 01	0.12E 01	0.11E 01	0.14E 01
1, 8	2, 8	3, 8	4, 8	5, 8
0.489E 00	0.964E 00	0.118E 01	0.144E 01	0.220E 01
0.87E 00	0.88E 00	0.86E 00	0.94E 00	0.10E 01
0.10E 01	0.20E 01	0.12E 01	0.12E 01	0.15E 01
1, 9	2, 9	3, 9	4, 9	5, 9
0.431E 00	0.854E 00	0.104E 01	0.147E 01	0.223E 01
0.88E 00	0.89E 00	0.88E 00	0.10E 01	0.10E 01
0.10E 01	0.20E 01	0.12E 01	0.14E 01	0.15E 01
1,10	2,10	3,10	4,10	5,10
0.401E 00	0.796E 00	0.960E 00	0.150E 01	0.225E 01
0.93E 00	0.93E 00	0.93E 00	0.10E 01	0.10E 01
0.10E 01	0.20E 01	0.12E 01	0.16E 01	0.15E 01

C3 FUSE Listing

This section provides a complete listing of the fuselage shape simulation program, FUSE.

```
      DIMENSION XFORX(3),SNOS1(20,30,3),SNOS2(20,30,3),SFUS(60,30,3),    00000010
     &NAMAX(2),ITITLE(18),DEFAULT(2,13),XX(1500),YY(1500),ZZ(1500),      00000020
     $ID(30,50),AQ(50,30),NWRITE(50),RATIOM(5,30),RATION(50,30)          00000030
      REAL LN1,LN2,LU,NN1,NN1,MN2,NN2,MC,NC,LC,LLN,LBD                   00000040
      REAL MY1,NY1,LCD                                                   00000050
      CHARACTER MODE,MODCK,TYPE,TYPCK,IOUT,OT                            00000060
      DATA MODE,TYPE,IOUT/1HS,1HP,1HY/                                   00000070
      DATA CON1,CON2,CON3/4.3333,2.1250,5.0/                             00000080
      DATA (DEFAULT(1,I),I=1,13)/1.75,.75,.65,.825,.6,.75,              00000090
     $.64,.825,5.C,.70,.6,.775,4.0/                                      00000100
      DATA (DEFAULT(2,I),I=1,13)/1.75,.75,.65,.85,.6,.725,              00000110
     $.65,.85,6.,.70,.6,.8,3.5/                                          00000120
      TAN(X)=SIN(X)/COS(X)                                               00000130
      CON(X,A,B,F,G) = G*((1.-(X/A)**B)**(1./G))                         00000140
   20 ITYP=1                                                             00000150
      IPL=0                                                              00000160
      IPR=0                                                              00000170
      ICO=0                                                              00000180
      IAREA=0                                                            00000190
      IPA=0                                                              00000200
      IFILE=0                                                            00000210
      PRINT:"DESIGN OR SIMULATION MODE?"                                 00000220
      PRINT:"ENTER D OR S"                                               00000230
      READ:MODCK                                                         00000240
      PRINT:"PRINT DIMENSIONS? Y FOR YES, N FOR NO"                      00000250
      READ:OT                                                            00000260
      IF(OT.EQ.IOUT)IPR=1                                                00000270
      PRINT:"PRINT FUSELAGE COORDINATES? Y OR N"                         00000280
      READ:OT                                                            00000290
      IF(OT.EQ.IOUT)ICO=1                                                00000300
      PRINT:"PRINT TOTAL WETTED AREA? Y OR N"                            00000310
      READ:OT                                                            00000320
      IF(OT.EQ.IOUT) IAREA=1                                             00000330
      PRINT:"PRINT PANEL AREAS AND RATIOS? Y OR N"                       00000340
      READ:OT                                                            00000350
      IF(OT.EQ.IOUT) IPA=1                                               00000360
      PRINT:"PLOT FUSELAGE? Y OR N"                                      00000370
      READ:OT                                                            00000380
      IF(OT.EQ.IOUT)IPL=1                                                00000390
      IF(MODCK.EQ.MODE) GO TO 90                                         00000400
      NFUS=3                                                             00000410
      PRINT:"BUSINESS JET OR PISTON COMMUTER?"                           00000420
      PRINT:"ENTER J OR P"                                               00000430
      READ:TYPCK                                                         00000440
      IF(TYPCK.EQ.TYPE) ITYP=2                                           00000450
      PRINT:"TITLE?"                                                     00000460
      READ(5,11)(ITITLE(I),I=1,18)                                       00000470
      PRINT:"NUMBER OF PANELS?"                                          00000480
      READ: PNL                                                          00000490
      PRINT:"NO. OF RADIAL DIV. EACH SIDE?"                              00000500
      READ:NRADX                                                         00000510
      IPNL=PNL                                                           00000520
      PRINT:"ELLIPTICAL OR CIRCULAR CROSS-SECTIONS? Y OR N"              00000530
      READ:OT                                                            00000540
      IF(OT.NE.IOUT)GO TO 25                                             00000550
      RT1=1.                                                             00000560
      RB1=1.                                                             00000570
      RT2=1.                                                             00000580
      RB2=1.                                                             00000590
```

```
      RTC=1.                                                          00000600
      RBC=1.                                                          00000610
      RTT=1.                                                          00000620
      RBT=1.                                                          00000630
      GO TO 30                                                        00000640
   25 PRINT:"CONE #1 ROUND-OFF RADII: TOP,BOTTOM"                     00000650
      READ:RT1,RB1                                                    00000660
      PRINT:"CONE #2 ROUND-OFF RADII: TOP,BOTTOM"                     00000670
      READ:RT2,RB2                                                    00000680
      PRINT:"CABIN ROUND-OFF RADII: TOP,BOTTOM"                       00000690
      READ:RTC,RBC                                                    00000700
      PRINT:"TAIL ROUND-OFF RADII: TOP,BOTTOM"                        00000710
      READ:RTT,RBT                                                    00000720
   30 PRINT:"ENTER: PASSENGERS,SEATS ABREAST,PITCH"                   00000730
      READ:IPAX,ISR,P                                                 00000740
      PRINT:"SEAT WIDTH,AISLE WIDTH"                                  00000750
      READ:WS,AS                                                      00000760
      PRINT:"DESIRED INSIDE CABIN HEIGHT? (IN.)"                      00000770
      READ:HC                                                         00000780
      IF(RTC.GT.0.3.AND.ISR.GT.2)GO TO 35                             00000790
      IF(RTC.GT.0.6.AND.ISR.LE.2)GO TO 35                             00000800
      GO TO 40                                                        00000810
   35 WC2=((ISR-1)*WS+AS)/2.                                          00000820
      A=49./2304.-1.                                                  00000830
      B=(-98./2304.)*(6.*WC2/7.-2219./14.)                            00000840
      C=(49./2304.)*((6.*WC2/7.-2219./14.)**2)+((WC2+6.)**2)          00000850
      S1=(SQRT(B*B-4.*A*C)-B)/(2.*A)                                  00000860
      S2=(SQRT(B*B-4.*A*C)+B)/(-2.*A)                                 00000870
      IF(S2.LT.1.)S2=S1                                               00000880
      W=S2/0.94/6.                                                    00000890
      HC=5.64*W*SQRT((5.64*W)**2-((((ISR-1)*WS+AS)/2.+6.)**2)         00000900
      GO TO 45                                                        00000910
   40 W=(ISR*WS+AS+5.)/12.                                            00000920
   45 WRITE(6,50)W                                                    00000930
   50 FORMAT("FUSELAGE WIDTH = ",F5.2," FT")                          00000940
      PRINT:"SHOULD H=W ? Y OR N"                                     00000950
      READ:OT                                                         00000960
      IF(OT.EQ.IOUT)H=W                                               00000970
      IF(OT.EQ.IOUT) GO TO 60                                         00000980
      PRINT:"INPUT H ? Y OR N"                                        00000990
      READ:OT                                                         00001000
      IF(OT.NE.IOUT)GO TO 55                                          00001010
      READ:H                                                          00001020
      GO TO 60                                                        00001030
   55 Q=SQRT(2.*(WS-12.)/(.94*RBC*3.14*12.)-((WS-12.)/(.94*RBC*W*12.))**2) 00001040
      H=(((P*3C/2.)*(1.-Q))/(1.-(RBC/2.)*(1.-Q))+1.)*HC/(.94*12.)     00001050
   60 WRITE(6,65)H,HC                                                 00001060
   65 FORMAT(1H //"FUSELAGE HEIGHT = ",F5.2," FT"//                   00001070
     &"INSIDE CABIN HEIGHT = ",F5.2," IN."//)                         00001080
      PL = 0.                                                         00001090
      PRINT:"BAGGAGE COMPARTMENT? Y OR N"                             00001100
      READ:OT                                                         00001110
      IF (OT.NE.IOUT)GO TO 70                                         00001120
      WF=((ISR-1)*WS+AS+12.)/2.                                       00001130
      WC=11.29*W                                                      00001140
      WBC=((ISR-1)*WS-0.5*AS+12.)/2.                                  00001150
      BL=(727.*IPAX)/(WBC*(2.*HC-5.64*W*(1.-RTC*SQRT(1.-              00001160
     &0.25*((WF-WC*WTC*WC)/(RTC*WC))**2))))                           00001170
   70 IROW=IPAX/ISR                                                   00001180
```

```
      IF((IROW*ISR).LT.IPAX)IROW=IROW+1                                  00001190
      LU=(IROW*P)/12.+9L                                                 00001200
      PRINT:"ENTER LLN,ZZN,ZN0"                                          00001210
      READ:LLN,ZZN,ZN0                                                   00001220
      IF(LLN.EQ.0.)LLN=DEFAULT(ITYP,1)                                   00001230
      IF(ZZN.EQ.0.)ZZN=DEFAULT(ITYP,2)                                   00001240
      PRINT:"ENTER PH11,PH21,PH12,PH22,PHY1,PHY2"                        00001250
      READ:PH11,PH21,PH12,PH22,PHY1,PHY2                                 00001260
      IF(PH11.EQ.0.)PH11=DEFAULT(ITYP,3)                                 00001270
      IF(PH21.EQ.0.)PH21=DEFAULT(ITYP,4)                                 00001280
      IF(PH12.EQ.0.)PH12=DEFAULT(ITYP,5)                                 00001290
      IF(PH22.EQ.0.)PH22=DEFAULT(ITYP,6)                                 00001300
      IF(PHY1.EQ.0.)PHY1=DEFAULT(ITYP,7)                                 00001310
      IF(PHY2.EQ.0.)PHY2=DEFAULT(ITYP,8)                                 00001320
      PRINT:"ENTER LAD,LCD,ZZC"                                          00001330
      READ:LAD,LCD,ZZC                                                   00001340
      IF(LAD.EQ.0.)LAD=DEFAULT(ITYP,9)                                   00001350
      IF(LCD.EQ.0.)LCD=DEFAULT(ITYP,10)                                  00001360
      IF(ZZC.EQ.0.)ZZC=DEFAULT(ITYP,11)                                  00001370
      PRINT:"ENTER PHC1,PHC2"                                            00001380
      READ:PHC1,PHC2                                                     00001390
      IF(PHC1.EQ.0.)PHC1=DEFAULT(ITYP,11)                                00001400
      IF(PHC2.EQ.0.)PHC2=DEFAULT(ITYP,12)                                00001410
      IF(ZN0.EQ.0.)ZN0=(ZZN-1.)*H/2.                                     00001420
      GO TO 95                                                           00001430
   80 CONTINUE                                                           00001440
      CBW=((WS+3.)-(1.-RT2)*(.94*W+12.))/12.                             00001450
      IF(CBW.GT.0.)GO TO 85                                              00001460
      CBZ=CBH1-.47*H                                                     00001470
      GO TO 86                                                           00001480
   85 CBZ=CBH1-0.47*RT2*H+SQRT(1.-((CBW/(.94*RT2*W))*((CBW/(.94*RT2*W))  00001490
     $-0.47*H*(1.-RT2)                                                   00001500
   86 YMC=ABS(CBH2-CBZ)                                                  00001505
      LN2=CBL1/((1.-((2.*YMC/(.94*H))**NN2))**(1./NN2))                  00001510
      LN1=LLN*LN2                                                        00001530
      ZN1=ZZN*H/2.                                                       00001540
      Z0X=ZN1-H/2.                                                       00001550
      QN2=(ZN0-Z0X)/(LN1+LN1)                                            00001560
      QN1=-2.*QN2*LN1                                                    00001570
      YH1=(W/2.)*SQRT(1.-(2.*Z0X/H)*(2.*Z0X/H))                          00001580
      LC=LAD*(W+H)/2.-LU-LN1                                             00001590
      D=(W+H)/2.                                                         00001600
      IF((LC/D).LT.LCD)LC=LCD*D                                          00001610
      QC1=0.                                                             00001620
      QC2=H*ZZC/(2.*LC*LC)                                               00001630
      NL=IPHL/2/NRADX                                                    00001640
      XNL=NL                                                             00001650
      X=(3.*LN1+2.*LU+1.5*LC)/(3.*XNL)                                   00001660
      NFORX(1)=LP1/X                                                     00001670
      NFORX(2)=LU/(1.5*X)                                                00001680
      NFORX(3)=NL-NFORX(1)-NFORX(2)                                      00001690
      GO TO 96                                                           00001700
   90 READ(3,1)NFUS,NFORX,NRADX                                          00001710
      READ(3,11)(TITLE(I),I=1,18)                                        00001720
      READ(3,2)LN1,LN2,LU,LC,W,H                                         00001730
      READ(3,2)PH11,PH21,PH12,PH22,PHC1,PHC2                             00001740
      READ(3,2)PHY1,PHY2                                                 00001750
      READ(3,2)YH1,ZN1,ZN0,QN1,QN2,QC1,QC2                               00001760
      READ(3,2)RT1,RH1,RT2,RH2                                           00001770
```

```
 95 CALL CONSHF(PH11,PH21,0.001,MN1,NN1)                          00001790
    CALL CONSHP(PH12,PH22,0.001,MN2,NN2)                          00001800
    CALL CONSHP(PHC1,PHC2,0.001,MC,NC)                            00001810
    CALL CONSHP(PHY1,PHY2,0.001,MY1,NY1)                          00001820
    IF(MODCK.NE.MODE) GO TO 90                                    00001830
 96 IF(IPR.EQ.0) GO TO 97                                         00001840
    WRITE(6,13)(TITLE(I),I=1,18)                                  00001850
    WRITE(6,14)MODCK                                              00001860
    WRITE(6,15)NRADX,(NFORX(I),I=1,3)                             00001870
    IF(MODCK.EQ.MODE) GO TO 1001                                  00001880
    WRITE(6,16)IPAX,ISF,IROW                                      00001890
1001 WRITE(6,17)LN1,ZN1,YN1,PH11,PH21,PHY1,PHY2                   00001900
    WRITE(6,18)LN2,PH12,PH22,LU,H,W,LC,PHC1,PHC2                  00001910
    PRINT:"DATA SATISFACTORY? Y OR N"                             00001920
    READ:OT                                                       00001930
    IF(OT.EQ.IOUT)GO TO 97                                        00001940
    PRINT:"RESUBMIT DATA? Y OR N"                                 00001950
    READ:OT                                                       00001960
    IF(OT.NE.IOUT)GO TO 3000                                      00001970
    GO TO 2C                                                      00001980
 97 PRINT:"FILE FUSELAGE DATA? Y OR N"                            00001990
    READ:OT                                                       00002000
    IF(OT.EQ.IOUT)IFILE=1                                         00002010
    I0=1                                                          00002020
    I2=0                                                          00002030
    PI=3.14159265                                                 00002040
    NRADX1=NRADX+1                                                00002050
    DO 1000 NF=1,NFUS                                             00002060
    I2=I2+NFORX(NF)                                               00002070
    IF(NF.EQ.NFUS) I2=I2+1                                        00002080
    DO900 I=I0,I2                                                 00002090
    NX=NFORX(NF)                                                  00002100
    IF(I-NF)600,500,100                                           00002110
100 X=LN1*(I-I0)/NX                                               00002120
    X1=LN1-X                                                      00002130
    IF(X.EQ.0.) GO TO 105                                         00002140
    IF(X.LE.(LN1-LN2)) GO TO 130                                  00002150
    GO TO 120                                                     00002160
105 DO 110 J=1,NRADX1                                             00002170
    SFUS(I,J,1)=X                                                 00002180
    SFUS(I,J,2)=0.                                                00002190
    SFUS(I,J,3)=ZN0                                               00002200
    SNOS1(I,J,1)=X                                                00002210
    SNOS1(I,J,2)=0.                                               00002220
    SNOS1(I,J,3)=ZN0                                              00002230
    SNOS2(I,J,1)=X                                                00002240
    SNOS2(I,J,2)=0.                                               00002250
    SNOS2(I,J,3)=0.                                               00002260
110  CONTINUE                                                     00002270
     GOTO 900                                                     00002280
120 YN2=CON(X1,LN2,(W/2.),NN2,MN2)                                00002290
    ZN2=CON(X1,LN2,(H/2.),NN2,MN2)                                00002300
130 YN1=CON(X1,LN1,YN1,PY1,NY1)                                   00002310
    ZN1=CON(X1,LN1,ZN1,MN1,PN1)                                   00002320
    ZN=ZN0+ZN1+X+ON2*X+X                                          00002330
    ZCL=ZN2-X+ZN/ZLN1                                             00002340
    DO 400 J=1,NRADX1                                             00002350
    SFUS(I,J,1)=X                                                 00002360
```

```
      SNOS1(I,J,1)=X                                                    00002370
      SNOS2(I,J,1)=X                                                    00002380
      IF(X.GT.(LN1-LN2)) GO TO 140                                      00002390
      SNOS2(I,J,2)=0.                                                   00002400
      SNOS2(I,J,3)=0.                                                   00002410
      GO TO 250                                                         00002420
  140 IF((J.EQ.1).OR.(J.EQ.NRADX1)) GO TO 245                           00002430
      B=TAN((J-1)*PI/NRADX-PI/2.)                                       00002440
      CALL CRSSEC(YN2,ZN2,RT2,RB2,ZCL,,3,YN,ZN,IERR)                    00002450
      IF(IERR.EQ.1) GO TO 200                                           00002460
      CALL CRSSEC(W/2.,H/2.,RTC,RBC,,,B,YC,ZC,)                         00002470
      IF((YC*YC+ZC*ZC).GE.(YN*YN+ZN*ZN))GO TO 150                       00002480
      YN=YC                                                             00002490
      ZN=ZC                                                             00002500
  150 SNOS2(I,J,2)=YN                                                   00002510
      SNOS2(I,J,3)=ZN                                                   00002520
      GO TO 250                                                         00002530
  200 SNOS2(I,J,2) = 0.                                                 00002540
      SNOS2(I,J,3) = 0.                                                 00002550
      GO TO 250                                                         00002560
  245 SNOS2(I,J,2)=0.                                                   00002570
      SNOS2(I,J,3)=(1-(2*(NRADX-J+1)/NRADX))*ZN2                        00002580
  246 SNOS1(I,J,2)=0.                                                   00002590
      SNOS1(I,J,3)=(1-(2*(NRADX-J+1)/NRADX))*ZN1+ZD                     00002600
      GO TO 550                                                         00002610
  250 IF((J.EQ.1).OR.(J.EQ.NRADX1)) GO TO 246                           00002620
      B=TAN((J-1)*PI/NRADX-PI/2.)                                       00002630
      CALL CRSSEC(YN1,ZN1,RT1,RB1,ZCL,ZD,B,YN,ZN,IERR)                  00002640
      IF(IERR.EQ.1) GO TO 350                                           00002650
      CALL CRSSEC(W/2.,H/2.,RTC,RBC,,,B,YC,ZC,)                         00002660
      IF((YC*YC+ZC*ZC).GE.(YN*YN+ZN*ZN))GO TO 300                       00002670
      YN=YC                                                             00002680
      ZN=ZC                                                             00002690
  300 SNOS1(I,J,2)=YN                                                   00002700
      SNOS1(I,J,3)=ZN                                                   00002710
      GO TO 550                                                         00002720
  350 WRITE(6,5)I,J                                                     00002730
      GO TO 3000                                                        00002740
  360 IF(X.LE.(LN1-LN2)) GO TO 350                                      00002750
      R1=SQRT(SNOS1(I,J,2)**2+(SNOS1(I,J,3)-ZCL)**2)                    00002760
      R2=SQRT(SNOS2(I,J,2)**2+(SNOS2(I,J,3)-ZCL)**2)                    00002770
      IF(R1-R2) 370,380,390                                             00002780
  370 SFUS(I,J,3)=SNOS2(I,J,3)                                          00002790
      SFUS(I,J,2)=SNOS2(I,J,2)                                          00002800
      GO TO 400                                                         00002810
  380 SFUS(I,J,2)=SNOS1(I,J,2)                                          00002820
      SFUS(I,J,3)=SNOS1(I,J,3)                                          00002830
  400 CONTINUE                                                          00002840
      GO TO 550                                                         00002850
  500 X=LO*(I-1)/NX+LN1                                                 00002860
      DO 550 J=1,NRADX1                                                 00002870
      SFUS(I,J,1)=X                                                     00002880
      IF((J.EQ.1).OR.(J.EQ.NRADX1)) GO TO 540                           00002890
      B=TAN((J-1)*PI/NRADX-PI/2.)                                       00002900
      CALL CRSSEC(W/2.,H/2.,RTC,RBC,,,B,SFUS(I,J,2),SFUS(I,J,3),)       00002910
      GO TO 550                                                         00002920
  540 SFUS(I,J,2)=0.                                                    00002930
      SFUS(I,J,3)=(1-(2*(NRADX-J+1)/NRADX))*(W/2.)                      00002940
  550 CONTINUE                                                          00002950
```

```
      GOTO 990                                                          00002960
  600 DX=LC/(NX+1)                                                      00002970
      X=(I-10)*DX                                                       00002980
      X1=X+LM1+LU                                                       00002990
      W2=W/2.                                                           00003000
      H2=H/2.                                                           00003010
      ZO=AC1*X+AC2*X*X                                                  00003020
      IF(I.LT.12) GO TO 610                                             00003030
      X1=LC+LM1+LU                                                      00003040
      DO 620 J=1,NRADX1                                                 00003050
      SFUS(I,J,1)=X1                                                    00003060
      SFUS(I,J,2)=0.                                                    00003070
      SFUS(I,J,3)=ZO                                                    00003080
  620  CONTINUE                                                         00003090
       GOTO 990                                                         00003100
  610 YMC=CON(X,LC,W2,HC,MC)                                            00003110
      ZMC=CON(X,LC,H2,HC,MC)                                            00003120
      DO 650 J=1,NRADX1                                                 00003130
      SFUS(I,J,1)=X1                                                    00003140
      IF((J.EQ.1).OR.(J.EQ.NRADX1)) GO TO 640                           00003150
      B=TAN((J-1)*PI/NRADX-PI/2.)                                       00003160
      CALL CRSSEC(YMC,ZMC,PYY,ROT,,ZO,B,SFUS(I,J,2),SFUS(I,J,3),)       00003170
      GO TO 650                                                         00003180
  640 SFUS(I,J,2)=0.                                                    00003190
      SFUS(I,J,3)=(1-(2*(NRADX-J+1)/NRADX))*ZMC+ZO                      00003200
  650 CONTINUE                                                          00003210
      SFUS(I,J,3)=(1-(2*(NRADX-J+1)/NRADX))*ZMC+ZJ                      00003220
  800 II=I                                                              00003230
  900 CONTINUE                                                          00003240
  950 IO=II+1                                                           00003250
 1000 CONTINUE                                                          00003260
      XORG=(SFUS(II,1,1)+SFUS(1,1,1))/2.                                00003270
      NS=1                                                              00003280
      DO 1010 I=1,50                                                    00003290
      DO 1010 J=1,30                                                    00003300
 1010 ID(J,I)=0                                                         00003310
      IF(IFILE.EQ.0)GO TO 1015                                          00003320
      WRITE (07,11) (TITLE(I),I=1,18)                                   00003330
 1015 LM=NFORX(1)+NFORX(2)+NFORX(3)                                     00003340
      NOE=LM*NRADX                                                      00003350
      IF(IFILE.EQ.0)GO TO 1020                                          00003360
      WRITE (07, 19) NOE                                                00003370
 1020 K=0                                                               00003380
      DO 1045 I=1,II                                                    00003390
      DO 1045 J=1,NRADX1                                                00003400
      K=K+1                                                             00003410
      XX(K)=XORG-SFUS(I,J,1)                                            00003420
      YY(K)=SFUS(I,J,2)                                                 00003430
      ZZ(K)=SFUS(I,J,3)                                                 00003440
      IF(IFILE.EQ.0) GO TO 1045                                         00003450
      WRITE (07, 21) XX(K),YY(K),ZZ(K),I,J,NS                           00003460
 1045 ID(J,I)=K                                                         00003470
      AMFT=0.                                                           00003480
      DO 1050 N=1,II                                                    00003490
      DO 1050 M=1,NRADX1                                                00003500
      P1=ID(M,N)                                                        00003510
      P2=ID(M+1,N)                                                      00003520
      P3=ID(M+1,N+1)                                                    00003530
      P4=ID(M,N+1)                                                      00003540
```

```
      II=ID(N,M)+ID(N+1,K)+ID(N+1,M+1)+ID(N,M+1)                        00003550
      IF (II.EQ.0) GO TO 1050                                           00003560
      X1=XX(P3)-XX(P1)                                                  00003570
      X2=XX(P4)-XX(P2)                                                  00003580
      Y1=YY(P3)-YY(P1)                                                  00003590
      Y2=YY(P4)-YY(P2)                                                  00003600
      Z1=ZZ(P3)-ZZ(P1)                                                  00003610
      Z2=ZZ(P4)-ZZ(P2)                                                  00003620
      XN=Y2*Z1-Y1*Z2                                                    00003630
      YN=X1*Z2-X2*Z1                                                    00003640
      ZN=X2*Y1-X1*Y2                                                    00003650
      R=SQ2(XN,YN,ZN)                                                   00003660
      AQ(N,M)=0.5*R                                                     00003670
 1050 AWET=AWET+2.*AQ(N,M)                                              00003680
      IF(AREA.EQ.1) GO TO 1051                                          00003690
      PRINT:"*********************"                                    00003700
      WRITE(6,91)AWET                                                   00003710
      PRINT:"*********************"                                    00003720
 1051 NDO=LN                                                            00003730
      MDO=MRABX                                                         00003740
      DO 1070 N=1,NDO                                                   00003750
      DO 1070 M=1,MDO                                                   00003760
      IF (N.EQ.1) GO TO 1055                                            00003770
      RATION(N,M)=AQ(N,M)/AQ(N-1,M)                                     00003780
      GO TO 1060                                                        00003790
 1055 RATION(N,M)=1.0                                                   00003800
 1060 IF (M.EQ.1) GO TO 1065                                            00003810
      RATION(N,M)=AQ(N,M)/AQ(N,M-1)                                     00003820
      GO TO 1070                                                        00003830
 1065 RATION(N,M)=1.0                                                   00003840
 1070 CONTINUE                                                          00003850
      IF(IPA.EQ.0) GO TO 2002                                           00003860
      WRITE (06,225)                                                    00003870
      WRITE (06, 22)                                                    00003880
      LINES=5                                                           00003890
      NCOUNT=5                                                          00003900
      NSTART=1                                                          00003910
 1075 NSTOP=MIN(NCOUNT,NDO)                                             00003920
      DO 1091 I=NSTART,NSTOP                                            00003930
 1090 WRITE(I)=I                                                        00003940
      DO 1095 I=1,MDO                                                   00003950
      WRITE (06, 23)(WRITE(J),I,J=NSTART,NSTOP)                         00003960
      WRITE (06, 24) (AQ(J,I),J=NSTART,NSTOP)                           00003970
      WRITE (06,26) (RATION(J,I),J=NSTART,NSTOP)                        00003980
 1095 WRITE (06, 27) (RATION(J,I),J=NSTART,NSTOP)                       00003990
      WRITE (06, 22)                                                    00004000
      IF (NSTOP.EQ.NDO) GO TO 1095                                      00004010
      NSTART=NSTART+5                                                   00004020
      NCOUNT=NCOUNT+5                                                   00004030
      LINES=LINES+NDO+5                                                 00004040
      IF (LINES.GT.50) GO TO 1090                                       00004050
      GO TO 1075                                                        00004060
 1095 WRITE (06,225)                                                    00004070
      LINES=5                                                           00004080
      GO TO 1075                                                        00004090
 1095 CONTINUE                                                          00004100
  225 FORMAT (1H1,1X,5(1X,5H(I,J),6X)//,1X,5(2X,6HAREA,6X)//,1X,5(2X,   00004110
     $6HRATIO),6X)//,1X,5(2X,6HRATIO),6X))                              00004120
      KODE=7                                                            00004130
```

```
      WRITE (6,25)                                                    00004140
 2032 IF(ICO.EQ.0) GO TO 2035                                         00004150
      WRITE(6,4)                                                      00004160
      WRITE(6,2)((((I,J,(SFUS(I,J,K),K=1,3)),J=1,NRADX1),I=1,11)      00004170
 2035 IF(IFL.NE.1) GO TO 3000                                         00004180
      CALL INDIT (300)                                                00004190
      CALL ANXODE                                                     00004200
      CALL MOVABS(130,260)                                            00004210
      WRITE(6,11)(TITLE(I),I=1,15)                                    00004220
      XMAX=SFUS(11,1,1)                                               00004230
      YMAX=(4./3.)*(1[illegible]./1023.)*XMAX                         00004240
      YMIN=-1.*YMAX                                                   00004250
      MINY=0                                                          00004260
      MAXY=250                                                        00004270
      DO 2501 K=2,3                                                   00004280
      K1=K-1                                                          00004290
      CALL DWINDO (0.,XMAX,YMIN,YMAX)                                 00004300
      MINY=(K-2)*260+MINY                                             00004310
      MAXY = MINY + 260                                               00004320
      CALL TWINDO (128.895,MINY,MAXY)                                 00004330
      DO 2203 I=1,11                                                  00004340
      DO 2100 J=1,NRADX1                                              00004350
      X=SFUS(I,J,1)                                                   00004360
      Y=SFUS(I,J,K)                                                   00004370
      IF((I.GT.1).AND.(J.GT.1)) GO TO 2010                            00004380
      CALL MOVEA (X,Y)                                                00004390
      GO TO 2020                                                      00004400
 2010 CALL DRAWA (X,Y)                                                00004410
 2020 IF(J.NE.NRADX1) GO TO 2100                                      00004420
 2050 INEXT=I+1                                                       00004430
      Y=   SFUS(INEXT,1,1)                                            00004440
      Y=   SFUS(INEXT,1,K)                                            00004450
      CALL MOVEA (X,Y)                                                00004460
 2100 CONTINUE                                                        00004470
 2200 CONTINUE                                                        00004480
      DO 2400 J=1,NRADX1                                              00004490
      DO 2300 I=1,11                                                  00004500
      X=SFUS(I,J,1)                                                   00004510
      Y=SFUS(I,J,K)                                                   00004520
      IF((I.GT.1).OR.(J.GT.1)) GO TO 2210                             00004530
      CALL MOVEA (X,Y)                                                00004540
      GO TO 2220                                                      00004550
 2210 CALL DRAWA (X,Y)                                                00004560
 2220 IF(I.NE.11) GO TO 2300                                          00004570
      JNEXT=J+1                                                       00004580
      X=   SFUS(1,JNEXT,1)                                            00004590
      Y=   SFUS(1,JNEXT,K)                                            00004600
      CALL MOVEA (X,Y)                                                00004610
 2300 CONTINUE                                                        00004620
 2400 CONTINUE                                                        00004630
 2500 CONTINUE                                                        00004640
      XMAX = XMAX/2                                                   00004650
      XMIN = -1.*XMAX                                                 00004660
      CALL DWINDO (XMIN,XMAX,YMIN,YMAX)                               00004670
      CALL TWINDO (128.895,525.780)                                   00004680
      I4=1                                                            00004690
      DO 2900 K=1,NFUS                                                00004700
      I3=I4                                                           00004710
      I4=NFORY(K)+I3                                                  00004720
```

```
      IF(K.EQ.2) GO TO 2930                                          00004730
      DO 2870 I=13,14                                                00004740
      DO 2775 J=1,NRADX1                                             00004750
      X=SFUS(I,J,2)                                                  00004760
      Y=SFUS(I,J,3)                                                  00004770
      IF(K.GT.2) X=-1.*X                                             00004780
      IF((I.EQ.13).AND.(J.EQ.1)) GO TO 2810                          00004790
      CALL DRAWA (X,Y)                                               00004800
      GO TO 2820                                                     00004810
 2810 CALL MOVEA (X,Y)                                               00004820
 2820 IF(J.NE.NRADX1) GO TO 2700                                     00004830
      JNEXT=J+1                                                      00004840
      X=SFUS(I,JNEXT,2)                                              00004850
      Y=SFUS(I,JNEXT,3)                                              00004860
      IF(K.GT.2) X=-1.*X                                             00004870
      CALL MOVEA (X,Y)                                               00004880
 2700 CONTINUE                                                       00004890
 2930 CONTINUE                                                       00004900
      DO 2980 J=1,NRADX1                                             00004910
      DO 2980 I=13,14                                                00004920
      X=SFUS(I,J,2)                                                  00004930
      Y=SFUS(I,J,3)                                                  00004940
      IF(K.GT.2) X=-1.*X                                             00004950
      IF((J.GT.1).OR.(I.GT.13)) GO TO 2810                           00004960
      CALL MOVEA (X,Y)                                               00004970
      GO TO 2820                                                     00004980
 2810 CALL DRAWA (X,Y)                                               00004990
 2820 IF(I.NE.14) GO TO 2860                                         00005000
      JNEXT=J+1                                                      00005010
      X=SFUS(13,JNEXT,2)                                             00005020
      Y=SFUS(13,JNEXT,3)                                             00005030
      IF(K.GT.2) X=-1.*X                                             00005040
      CALL MOVEA (X,Y)                                               00005050
 2860 CONTINUE                                                       00005060
 2890 CONTINUE                                                       00005070
 2900 CONTINUE                                                       00005080
      CALL FINITT (0,0)                                              00005090
 3000 PRINT:"NEW RUN? Y OR N"                                        00005100
      READ:QT                                                        00005110
      IF(QT.EQ.'OUT) GO TO 20                                        00005120
      STOP                                                           00005130
    1 FORMAT(513)                                                    00005140
    2 FORMAT(7F10.0)                                                 00005150
    3 FORMAT(1H ///10X,'****ERROR NO. 1 AT I=',I3,',J=',I3///)       00005160
    4 FORMAT(1H ///10X,'****ERROR NO. 2 AT I=',I3,',J=',I3///)       00005170
    5 FORMAT(1H ///10X,'****ERROR NO. 3 AT I=',I3,',J=',I3///)       00005180
    6 FORMAT(1H ///10X,'****ERROR NO. 4 AT I=',I3,',J=',I3///)       00005190
    8 FORMAT(1H ////11X,"I",5X,"J",7X,"(",9X,"Y",9X,"Z"////)         00005200
    9 FORMAT(1H ,2(I5,3X),3(F7.3,3X)))                               00005210
   10 FORMAT(13,F10.0)                                               00005220
   11 FORMAT(1234)                                                   00005230
   12 FORMAT(10X,14A4///)                                            00005240
   14 FORMAT(1H1,"FUSE PROGRAM MODE -- ",A1///)                      00005250
   15 FORMAT(10X,"DIVISIONS"//15X,"RADIAL (HALF FUSELAGE)",          00005260
     &I5,I7/15X,"LENGTHWISE"/15X,"NOSE",I5,I7/15X,"CABIN",          00005270
     &I5,I7/15X,"TAIL",I5,I7///)                                    00005280
   16 FORMAT(1H1,"CABIN CONFIGURATION"//13X,"NO. OF PASSEN",        00005290
     &"GERS",I5,I7/13X,"SEATS PER ROW",I5,I7/13X,"NO. OF",          00005300
     &" ROWS",I5,I7///)                                             00005310
```

```
      17 FORMAT(1H1,"FUSELAGE GEOMETRY"//15X,"NOSE CONE N1"/
     $15X,"LENGTH",T50,F7.2/15X,"HALF HEIGHT",T50,F7.2/
     $15X,"HALF WIDTH",T50,F7.2/15X,"SHAPE PARAMETERS"/
     $17X,"PH11",T50,F8.3/17X,"PH21",T50,F8.3/17X,"PHV1",
     $T50,F8.3/17X,"PHV2",T50,F8.3//)
      18 FORMAT(1H1,"NOSE CONE N2"//15X,"LENGTH",T50,F7.2/15X,
     $"SHAPE PARAMETERS"/17X,"PH12",T50,F8.3/17X,"PH22",T50,
     $F8.3//12X,"CABIN"/15X,"LENGTH",T50,F7.2/15X,"HEIGHT",
     $T50,F7.2/15X,"WIDTH",T50,F7.2//13X,"TAIL CONE"/15X,
     $"LENGTH",T50,F7.2/15X,"SHAPE PARAMETERS"/17X,"PHC1",
     $T50,F8.3/17X,"PHC2",T50,F8.3//)
      19 FORMAT (1X,13)
      21 FORMAT (1F12.7,5(2X,I2))
      22 FORMAT (1X,60(1H-))
      23 FORMAT (//,1X,5(2X,I2,1H,,I2,5X))
      24 FORMAT (1X,5(E10.3,2X))
      26 FORMAT (1X,5(1X,E9.2,2X))
      27 FORMAT (1X,5(1X,E9.2,2X),//)
      28 FORMAT (9I3)
      31 FORMAT(///" TOTAL WETTED AREA = ",F10.2//)
         END
         SUBROUTINE CONSHF(PHI1,PHI2,TOL,M,N)
         REAL M,N,M1,M2
         I=1
         J=1
         M=1.0
         DM2 = 10.0
      10 M1 = ALOG(1.0 -(PHI1**N))/ALOG(PHI1)
         M2 = ALOG(1.0 -(PHI2**N))/ALOG(PHI2/2.0)
         J = J+1
         IF(J.EQ.100)   GO TO 99
         DM1 = M1-M2
         IF(DM1.LE.0.) GO TO 30
         IF(DM1.GT.DM2) GO TO 50
      20 M = M+(0.25/I)
         DM2 = DM1
         GO TO 10
      30 IF(ABS(DM1).LT.TOL)GO TO 60
         I = I+5
      40 M = M - (0.25/I)
         M1 = ALOG(1.0 -(PHI1**N))/ALOG(PHI1)
         M2 = ALOG(1.0 -(PHI2**N))/ALOG(PHI2/2.0)
         J = J+1
         IF(J.EQ.100)   GO TO 80
         DM1 = M2-M1
         IF(DM1.LT.0.) GO TO 20
         IF(ABS(DM1).LT.TOL) GO TO 60
         GO TO 40
      50 WRITE(6,1)
         M = 1.0
         N = 1.0
         GO TO 70
      60 N = (M1 + M2)*0.5
      70 RETURN
      80 WRITE(6,4)
         GO TO 50
       1 FORMAT(1H0,"***ITERATION FOR M AND N DIVERGES***"/15X,"SET M=1.0
     $"/22X,"N=1.0"//)
       4 FORMAT(1H0,"***100 STEPS COMPLETE--DID NOT CONVERGE***"//)
```

```
      RETURN                                                            00005910
      END                                                               00005920
      FUNCTION SQ2(X,Y,Z)                                               00005950
C***  COMPUTE SQUARE ROOT OF X**2                                       00005940
      R=ABS(X)+ABS(Y)+ABS(Z)+.000000000001                              00005950
      RS=X**2+Y**2+Z**2                                                 00005960
      R=R+RS/R                                                          00005970
      R=0.25*R+RS/R                                                     00005980
      R=R+RS/R                                                          00005990
      SQ2=.25*R+RS/R                                                    00006000
      RETURN                                                            00006010
      END                                                               00006020
      SUBROUTINE CRSSEC(YM,ZM,RT,RH,ZCL,ZT,B,Y,Z,IERR)                  00006030
      QUAD1(A,B,C) = (SQRT(B*B-4.*A*C)-B)/(2.*A)                        00006040
      QUAD2(A,B,C) = -1.*(SQRT(B*B-4.*A*C)+B)/(2.*A)                    00006050
      IERR=0                                                            00006060
      Z=B*YM+ZCL                                                        00006070
      ZST=ZM*(1.-RT)+ZT                                                 00006080
      ZSH=ZM*(RH-1.)+ZT                                                 00006090
      IF((Z.LE.ZST).AND.(Z.GE.ZSH)) GO TO 60                            00006100
      YST=YM*(1.-RT)                                                    00006110
      YSH=YM*(1.-RH)                                                    00006120
      IF(B.EQ.0.)GO TO 5                                                00006130
      Y=ABS((ZM-ZCL)/B)                                                 00006140
      IF((B.LT.0.).AND.(Y.LE.YSH))GO TO 50                              00006150
      IF((B.GT.0.).AND.(Y.LE.YST))GO TO 50                              00006160
    5 Z1=ZST                                                            00006170
      Y1=YST                                                            00006180
      IF(B.LT.0.)Z1=ZSH                                                 00006190
      IF(B.LT.0.)Y1=YSH                                                 00006200
      A1=1.+(B*YM/ZM)*(B*YM/ZM)                                         00006210
      B1=-2.*Y1+2.*B*(ZCL-Z1)*(YM/ZM)*(YM/ZM)                           00006220
      C1=Y1*Y1+(((ZCL-Z1)/ZM)**2-1.)*YM*YM                              00006230
      IF((B1*B1-4.*A1*C1).LT.0.) IERR=1                                 00006240
      IF(IERR.EQ.1)RETURN                                               00006250
      YA=QUAD1(A1,B1,C1)                                                00006260
      YB=QUAD2(A1,B1,C1)                                                00006270
      IF((YA.LT.0.).AND.(YB.LT.0.)) GO TO 30                            00006280
      IF((YA.GT.0.).AND.(YB.GT.0.)) GO TO 40                            00006290
      IF((YA.LT.0.).AND.(YB.GT.0.)) GO TO 20                            00006300
   10 Y=YA                                                              00006310
   20 Y=YB                                                              00006320
      Z=B*YB+ZCL                                                        00006330
      GO TO 70                                                          00006340
   30 Y=0.                                                              00006350
      Z=0.                                                              00006360
      GO TO 70                                                          00006370
   40 IF(YA.GT.YB) GO TO 10                                             00006380
      GO TO 20                                                          00006390
   50 Z=SIGN(ZT,B)+Z                                                    00006400
      GO TO 70                                                          00006410
   60 Y=YM                                                              00006420
   70 RETURN                                                            00006430
      END                                                               00006440
```

APPENDIX D PARABOLIC LEAST-SQUARES CURVE-FIT ROUTINE

This appendix presents a listing for a time-sharing program in BASIC to compute the coefficients for a least-squares parabolic curve-fit of the general form:

$$Y = a_0 + a_1 x + a_2 x^2.$$

```
0010 DIM D(10,2),A(3,3),B(3),C(3)
0020 PRINT "NUMBER OF DATA POINTS?"
0030 INPUT N
0040 PRINT "INPUT DATA; X,Y"
0050 FOR I=1 TO N
0060 INPUT D(I,1),D(I,2)
0070 NEXT I
0080 FOR I=1 TO N
0090 PRINT D(I,1),D(I,2)
0100 NEXT I
0110 X1=0.
0120 X2=0.
0130 X3=0.
0140 X4=0.
0150 Y1=0.
0160 Y2=0.
0170 Y3=0.
0180 Y4=0.
0190 Y5=0.
0200 S1=0.
0210 S2=0.
0220 FOR I=1 TO N
0230 X1=X1+D(I,1)
0240 X2=X2+D(I,1)*D(I,1)
0250 X3=X3+D(I,1)*D(I,1)*D(I,1)
0260 X4=X4+D(I,1)↑4
0270 Y1=Y1+D(I,2)
0280 Y2=Y2+D(I,1)*D(I,2)
0290 Y3=Y3+D(I,1)*D(I,1)*D(I,2)
0300 Y5=Y5+D(I,2)*D(I,2)
0310 NEXT I
0320 Y4=Y1/N
0330 B(1)=Y1
0340 B(2)=Y2
0350 B(3)=Y3
0360 A(1,1)=N
0370 A(2,1)=X1
0380 A(1,2)=X1
0390 A(2,2)=X2
0400 A(1,3)=X2
0410 A(3,1)=X2
0420 A(2,3)=X3
0430 A(3,2)=X3
0440 A(3,3)=X4
0450 MAT A=INV(A)
0460 MAT C=A*B
```

```
0470 S2=(Y5-C(1)*Y1-C(2)*Y2-C(3)*Y3)/N
0480 S2=S2*S2
0490 FOR I=1 TO N
0500 Y=Y+(D(I,2,-Y4)↑2
0510 NEXT I
0520 S1=Y/N
0530 R2=1.-S2/S1
0540 PRINT "A0 =",C(1)
0550 PRINT "A1 =",C(2)
0560 PRINT "A2 =",C(3)
0570 PRINT "COEFF. OF DET.,R2 =",R2
0580 STOP
0590 END
```